

Genetics of Tissue Macrophage Development and Function

From zebrafish to human disease

Laura Esmee Kuil

The work presented in this thesis was financially supported by an Erasmus University Rotterdam Fellowship, a ZonMW VENI grant [VENI grant number 016.136.150], a Marie Curie Career Intergration Grant [Saving Dying Neurons, 322368] and an Alzheimer Nederland fellowship [grant number WE.15-2012-01].

The studies described in this thesis were performed at the department of Clinical Genetics in the Erasmus Medical Center, Rotterdam, The Netherlands.

Printing costs were supported by the Erasmus University Rotterdam, Tecniplast and Tecnilabs

ISBN: 978-94-6323-556-3

Author: Laura Kuil

Cover design & Layout: Laura Kuil

Printed by: Gildeprint, Enschede

Copyright © Laura Kuil, 2019. All rights reserved. No part of this thesis may be reproduced, stored in a retrieval system, or transmitted in any form by any means, without prior written permission from the author.

Genetics of Tissue Macrophage Development and Function

From zebrafish to human disease

Genetica van de ontwikkeling en functie van weefselmacrofagen

Van zebravis tot humane ziekte

Proefschrift

ter verkrijging van de graad van doctor aan de
Erasmus Universiteit Rotterdam
op gezag van de
rector magnificus

Prof.dr. R.C.M.E. Engels

en volgens besluit van het College voor Promoties.
De openbare verdediging zal plaatsvinden op

Dinsdag 23 april 2019 om 13:30 uur
door

Laura Esmee Kuil
geboren te Amsterdam

Promotiecommissie:

Promotor: Prof.dr. R. Willemsen

Overige leden: Prof.dr. A.H. Meijer
Prof.dr. G.J.V.M. van Osch
Prof.dr. S.A. Kushner

Copromotor: Dr. T.J. van Ham

Contents

Chapter 1	7
Introduction	
Chapter 2	23
Reverse genetic screen reveals that Il34 facilitates yolk sac macrophage distribution and seeding of the brain	
Chapter 3	55
Csf1r is dispensable for primitive and definitive myelopoiesis <i>in vivo</i> , but controls macrophage self-renewal and tissue macrophage properties	
Chapter 4	87
Homozygous mutations in <i>CSF1R</i> cause a pediatric onset leukoencephalopathy and can result in congenital absence of microglia	
Chapter 5	123
<i>In vivo</i> , colony-stimulating factor 1 receptor regulates microglia density and distribution, but not microglia differentiation	
Chapter 6	149
Hexb enzyme deficiency leads to lysosomal abnormalities in radial glia and microglia in zebrafish brain development	
Chapter 7	173
General discussion	
Appendix	191

Chapter 1

Introduction

The discovery of macrophages and their developmental origin

Macrophages are highly efficient phagocytes that clear debris, pathogens and foreign objects important to maintain tissue homeostasis. The process of phagocytosis was discovered in 1883, when Eli Metchnikoff observed that, after punching thorns into starfish larvae, cells started to surround the thorns to engulf debris and pathogens (1). He called these cells phagocytes, after the Greek word *phagein*, for “to eat”.

For many decades, macrophages were thought to be short-lived cells that are constantly replenished by monocytes from the bone marrow, which migrate into organs and tissues via the blood. This concept was based on seminal experiments by Ralph van Furth in 1968, when he studied the self-renewal capacity of macrophages. He showed that there was very little or no turnover of macrophages and their precursors in the blood, called monocytes. In contrast, precursors in the bone marrow, which he identified as the only adult source of mononuclear phagocytes, show very high turnover (2). Based on the work of van Furth it has for long been thought that all tissue macrophages derive from the bone marrow, called bone marrow derived macrophages (BMDMs). However, when genetic lineage tracing and parabiosis methods were more recently applied, it was discovered that many macrophages, in mice, were not BMDMs, but originated from embryonic macrophages (reviewed in: (3)). Analysis of very early embryonic precursors on the yolk sac revealed the presence of two distinct macrophage progenitors: yolk sac macrophages (YSMs) and erythroid myeloid progenitors (EMPs)(4). These progenitors are thought to differ based on their differentiation potential, as primitive YSMs are unipotent precursors, whereas EMPs are bipotent precursors (4-6). YSMs directly migrate into the embryo to colonize particularly the brain, and possibly other organs, to form macrophages resident to the tissue called tissue resident macrophages (TRMs)(5). EMPs are thought to seed the fetal liver, an embryonic hematopoietic site, to form a temporal source of embryonic definitive hematopoiesis. They seed several organs during embryonic development, such as the liver, lungs, spleen, and heart. At the time of birth, in mammals, the bone marrow generates hematopoietic stem and progenitor cells (HSPCs) that make up the adult definitive hematopoiesis (3, 7).

Genetic lineage tracing experiments are typically based on tamoxifen inducible recombinase activation of a fluorescent protein in cells expressing a transgenic reporter, after addition of tamoxifen, to label progenitor cells. Since YSMs and EMPs both appear on the embryonic yolk sac at around the same developmental stage, tamoxifen inducible genetic lineage tracing does not

offer the spatiotemporal resolution that is likely required to distinguish these two populations (4, 8). Therefore, YSMs and EMPs are most often referred to together as embryonic macrophages. In mammals, definitive myelopoiesis starts after birth, and the rate of replacement of embryonic derived TRM populations by HSPC derived macrophages from the bone marrow varies highly among organs. In some organs, such as the peritoneum, the TRMs are thought to be completely replaced by HSPC derived macrophages, whereas in other organs, primarily the brain, embryonic derived macrophages are maintained throughout life (Fig. 1)(9). However, the exact origin of TRMs, including microglia, remains highly debated (8, 10-12). This suggests that three myeloepoietic sources, contribute to TRMs at various proportions, depending on the organ of residence.

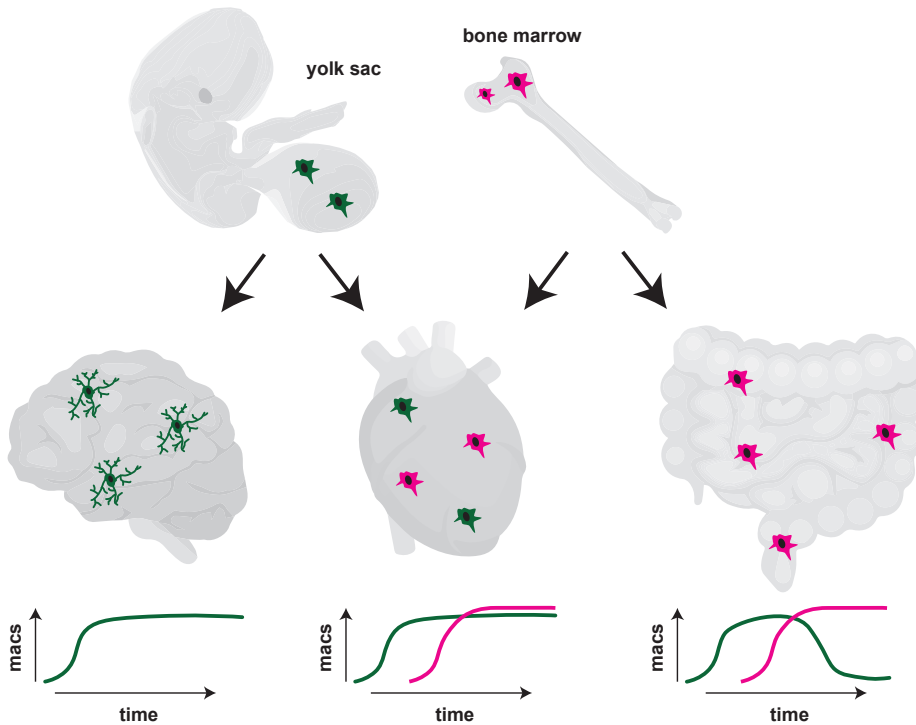


Figure 1. Tissue resident macrophages originate from multiple hematopoietic sources. Schematic representation of the different origins of tissue resident macrophages (TRMs). Unlike many other macrophages, microglia are not replenished by bone marrow derived macrophages (BMDMs) and are thought to be of embryonic origin only (13, 14). Macrophages in the heart are thought to be partially replenished and therefore are of mixed origin (15). Macrophages in the intestine are thought to be completely replenished by BMDMs (3, 9, 12, 16).

The tissue microenvironment induces unique properties of TRMs required for tissue specific functions

TRMs, which reside in almost all organs and tissues, exert a wide variety of specific functions influencing the development and homeostasis of their resident organ. Not surprisingly, they are thought to play a role in the pathogenesis of a large variety of diseases, including asthma, cancer and neurodegenerative disorders such as Alzheimer's disease, which makes modulating macrophage activity a good candidate for targeted therapy (17-19). For example, tumor associated macrophages can stimulate angiogenesis, and the growth and migration of tumors by producing growth factors, metalloproteinases, extracellular matrix remodeling molecules (reviewed in: (20)). These are trophic functions, which macrophages normally perform in virtually all tissues in the body, but in the case of tumor associated macrophages support malignant instead of normal healthy tissue. The main focus of this thesis is on the brain's TRMs, which are called microglia. In addition to more universal roles of TRMs, such as in vascular remodeling/maintenance, microglia have brain-specific roles since they are thought to remodel and prune synapses, and remodel myelin (21-28). To be able to manipulate the behavior, function or presence of TRMs in disease, in depth understanding of their emergence, differentiation, and functions *in vivo* is warranted.

Recently, transcriptomic experiments revealed both the general macrophage transcriptome and specific TRM gene expression profiles (29-35). The core macrophage signature includes genes involved in hematopoiesis, macrophage differentiation and typical macrophage functions important for all types of macrophages, including pathogen recognition, engulfment of apoptotic cells, and lysosomal degradation (30). During development, macrophages undergo step-wise gene expression changes correlating with changes in their microenvironment, and the transcription factor ZEB2 is essential for TRMs to gain and retain their identity (30, 31, 36). Macrophages are, regardless of their origin, highly plastic in acquiring or losing their TRM properties, which is likely regulated by factors in their microenvironment (29, 37-39). Importantly TRMs require inducing factors from the microenvironment continuously (32, 37, 39, 40). This TRM identity is most likely regulated at the transcriptional level. For several TRM populations transcription factors that induce TRM properties are identified. For example, locally produced retinoic acid induces the expression of the transcription factor GATA6 and other TRM genes specifically in peritoneal macrophages (41). Taken together, the microenvironment appears necessary

for the conversion of normal macrophages into their modified tissue resident counterparts, independent of their ontogeny. Therefore, to understand the genetic regulation and molecular pathways involved in the development and function of macrophages, it is important to gain insight *in vivo* while they reside in their native environment. Thereby the micro-environmental factors and genes involved in the induction of TRM properties could be elucidated.

Regulation of macrophage development by CSF1R

A key gene essential for macrophage development is colony-stimulating factor 1 receptor (*CSF1R*). *CSF1R* was originally discovered as the oncogene *c-fms*, homologous to the feline sarcoma virus (*v-fms*)(42). *CSF1R* is a tyrosine kinase, which regulates macrophage development. *CSF1R* dimerizes upon ligand binding and activates downstream signaling cascades, including BRAF/MAPK/ERK signaling (43-52). Two ligands for *CSF1R* exist, colony stimulating factor 1 (*CSF1*) and interleukin 34 (*IL34*), which show mostly non-overlapping expression patterns (53-56). *Csf1* mutant mice have mild microglia defects, but are also osteopetrotic, deaf and blind, whereas *Il34* deficient mice appear to primarily show reduced numbers of Langerhans cells and microglia (53, 54). Thus, *Csf1* and *Il34* knockout mice present with mostly non-overlapping aspects of the phenotype observed in *Csf1r* knockout mice. *In vitro* experiments have been fruitful in elucidating the molecular mechanisms of *CSF1R* signaling in macrophages. However, to generate or maintain macrophages *in vitro*, the addition of either of the two ligands for *CSF1R* is required, suggesting functional overlap of ligand function in macrophage differentiation, proliferation and survival (57). Interestingly, *CSF1R* signaling seems selectively essential for several TRM populations in brain, bone, and skin, known respectively as microglia, osteoclasts, and Langerhans cells. These populations are lacking in *Csf1r* mutant mice and rats, whereas other macrophage populations are reduced in numbers to a variable, but lesser extent (58-60). Many macrophages are still present in *Csf1r* knockout mice and rats, despite the lack of *CSF1R* signaling, this suggests that the role of *CSF1R in vivo* is more subtle than that *in vitro* and lowers the number of TRMs to different extent in several tissues and organs.

Thus, the precise role of *CSF1R in vivo*, particularly how *CSF1R* governs the generation of tissue specific macrophages, remains to be unraveled. Based on *Csf1r^{-/-} in vivo* phenotypes, loss of *CSF1R* appears to affect particularly TRMs. This is important to understand, since the neurodegenerative disorder, adult-onset leukoencephalopathy with axonal spheroids and pigmented glia (ALSP), is

caused by heterozygous loss of function mutations in *CSF1R* and it is unknown how microglia are affected by such mutations (61). Last, CSF1R inhibition provides an increasingly used therapeutic option in cancer, arthritis and possibly neurological disease, and better understanding which aspects of macrophage biology are precisely affected by CSF1R will therefore be important (62, 63).

Microglia in brain homeostasis and in neurodegenerative disease

In many brain disorders, including Alzheimer's disease, microglia are abundantly present, particularly in affected brain regions, suggesting their involvement in the pathogenesis. Alterations in the activation state of microglia during development, for example due to infection, are linked to neurodevelopmental disorders, including autism (23, 64). ALS is one of several neurodegenerative disorders that are caused by mutations in genes expressed selectively on microglia, called microgliopathies (61, 65-68). Thus, it seems that microglia do not only play a role in diseases related to aging but also in neurodevelopmental diseases and can be disease causing in for example microgliopathies.

Microglia fulfill functions in brain development by keeping close contact with neuronal synapses to support their growth, but also prune excessive synapses via complement components and clear apoptotic neurons, especially during development (21, 23, 69). In addition, in microglial absence (*Pu.1^{-/-}* and *Csf1^{op/op}* mice), blood vessels are less abundantly present in the brain, implying a role for microglia in the formation of blood vessels (70-74). Microglia also affect the presence of oligodendrocyte precursor cells, oligodendrocytes, as well as myelination and myelin remodeling (22, 26, 28). To understand the molecular mechanisms underlying ALS, and other diseases involving microglia, it is important to discover the functions affected by mutations in disease-causing microglia genes *in vivo*. In addition, by performing this type of studies we could learn how microglial dysfunction can lead to disease, and how microglia affect progression of neurodegenerative disorders.

The role of other highly microglia expressed genes in neurological disorders: the lysosomal storage disorder Sandhoff disease

Microglia have a specific gene expression signature compared to other macrophages or compared to other brain cells (32, 75-79). Several of these signature genes are linked to neurodegenerative disease including *TREM2*, in which homozygous mutations cause a severe white matter disorder and single variants contribute to dementia (80, 81). Another, much less studied microglia

signature gene, *HEXB*, causes a severe neurological, lysosomal storage disorder in humans when mutated, but its function in microglia is unclear. Lysosomal storage disorders (LSDs) comprise a group of ~ 55 disorders, which are caused by genetic variants in lysosomal enzymes leading to loss of protein function (82). LSDs frequently involve progressive neurodegeneration, and for most of them there is no treatment available yet. Sandhoff disease (SD), is caused by bi-allelic mutations in *HEXB*, leading to deficiencies in both β -Hexosaminidase A and β -Hexosaminidase B hydrolases, formed by *HEXA/B* or *HEXB/B* dimers, respectively (83, 84). β -Hexosaminidase plays a role in ganglioside metabolism and hydrolyzes GM2 gangliosides into smaller GM3 gangliosides in lysosomes. SD neuropathology involves GM2 accumulation, neuronal loss, hypomyelination in the infantile form, and the presence of increased numbers of activated microglia and astrocytes (85-89). In SD mice, GM2 storage is found in lysosomes of neurons, but also in lysosomes of astrocytes and microglia (90-92). In an SD mouse model, microglial activation was found to precede neurodegeneration (93). In addition, several studies showed that suppression of microglial or astrocytic inflammation could reduce SD pathology, suggesting both glial cells might be involved in SD pathogenesis (90, 93, 94). Based on pathology and gene expression data, it appears glia cell types contribute to the initiation and progression of disease. It is important to determine how *HEXB* deficiency affects glial function and whether gliosis is a consequence of neuronal problems caused by the loss of *HEXB*. Recently, it is becoming more clear that defects in glia cells –e.g. microglia, astrocytes or oligodendrocytes- often contribute or even cause neurological diseases. For brain diseases in general, it is therefore important to investigate them using a holistic approach, taking into account effects in various cell types in the brain.

Zebrafish as a model to study TRMs and glia *in vivo*

To study tissue-specific functions of TRMs, it is important to keep them in their native microenvironment, which is possible by using *in vivo* imaging. Zebrafish are small vertebrates that have several specific properties, which make them highly suitable to study macrophages in their native environment. For example, their offspring develops ex utero, transparently, and rapidly, as a complete embryo is present 24 hours after fertilization. In addition, zebrafish contain homologs of at least 70% of human genes (95). These properties make them highly suitable for forward genetics screens, which have been fruitful in identifying previously unknown processes that are essential for microglia development, for example

lysosomal function and suppression of inflammation (96-99). More recently, by using CRISPR/Cas9 to disrupt genes, it has now become possible to generate mutant alleles for target genes effectively and even reverse genetic screening is feasible (100). Many cell types and organ systems are highly conserved across evolution, and for example between mammals and zebrafish, including innate immunity and hematopoiesis, and findings from zebrafish research has proven to be relevant to understand human disease biology, including hematopoietic disorders and cancer (101-103). In addition, our recent work showed that many genes highly expressed specifically in mouse and human microglia are also highly expressed specifically in zebrafish microglia, suggesting that TRM properties are well conserved (76). The availability of transgenic reporter lines, using different fluorescent proteins, makes it possible to track, by *in vivo* imaging, the various cell types in the developing embryo, including macrophages and several glial cell types. Thereby zebrafish studies provided unprecedented insights in basic *in vivo* cellular mechanisms, ranging from phagocytosis and myelination to the discovery that microglia can tune neuronal activity (104-108). These properties facilitate functional genetic experiments *in vivo* to study macrophage and glial biology, which we can relate to human genetic diseases such as ALS.

Contents of this thesis

In this thesis we aimed to gain insight in the mechanisms and genetics regulating the embryonic development of macrophages, particularly microglia, and their role in disease. We therefore designed a reverse genetic screen to identify genes important for early microglia development in zebrafish larvae (**Chapter 2**). In this screen, we identified *il34* as a regulator of microglia development by attracting precursors towards the brain to form microglia. We used CRISPR/Cas9-based direct gene targeting to disrupt genes, followed by microglia visualization, using the vital dye neutral red, to quantify the number of microglia. To increase throughput, we developed automated image analysis software for quantification of microglia phenotypes. To further study the role of Csf1r-signaling in macrophage development *in vivo*, we generated zebrafish lacking both copies of the *Il34* receptor, *Csf1r*, which are described in **chapters 3, 4 and 5**. In **chapter 3**, we studied the role of *Csf1r* during embryonic and larval macrophage development and found that *Csf1r* mainly regulates macrophage proliferation, while differentiation to core-macrophages is *Csf1r*-independent. The defective macrophage proliferation in *csf1r* mutants results in large differences in macrophage numbers between *csf1r* mutants and controls. By following

macrophage development over time, up to 24 days post fertilization (dpf), we were able to detect the onset of definitive myelopoiesis both in controls and in *csf1r* mutants. In *csf1r* mutants macrophage numbers increased rapidly, but they failed to obtain a TRM phenotype based on *in vivo* imaging, and transcriptome analysis. In **chapter 4** we described a human patient with severe brain abnormalities who had homozygous loss of function mutations in *CSF1R*, and, as indicated by post mortem analysis, lacked microglia. We used the zebrafish to study how a lack of microglia affects brain development, in an attempt to identify a mechanism underlying the absence of major white matter tracts in the patient. We identified, both in zebrafish and in the human patient, reduced expression of the neuronal transcription factor CUX1, which is involved in the neuronal projections needed for generation of the corpus callosum. In **chapter 5** we used the zebrafish to study the role of *Csf1r* on embryonic and adult microglia. Hereby, we gained insight in the role of microglia in the rare neurodegenerative disorder and leukodystrophy ALSP, caused by heterozygous mutations in *CSF1R*. We showed that *CSF1R* regulates the distribution and density of microglia in the brains of zebrafish and in ALSP patients. Therefore, alterations in microglia distribution and reduced numbers may be an early event in the brain pathology observed in ALSP patients, which could contribute to white matter pathogenesis. Many other highly expressed microglia genes are involved in brain disease, including lysosomal genes, in which mutations cause lysosomal storage diseases (LSDs). Therefore, we investigated in **chapter 6** the role of the microglia signature gene *HEXB*, which causes Sandhoff disease when mutated. We generated *hexb* deficient zebrafish and discovered pathologies, both in microglia and in radial glia, during early embryonic brain development, suggesting a role for multiple glia in early Sandhoff disease pathogenesis. Hereby, we showed glial contribution to early pathologies in *hexb* mutant zebrafish, which could be relevant for Sandhoff disease. In **chapter 7** our findings are outlined and their significance is discussed in the context of current literature.

References

1. Metchnikoff E. Untersuchungen ueber die mesodermalen Phagocyten einiger Wirbeltiere. *Biologisches Centralblatt*. 1883;3:560-5.
2. van Furth R, Cohn ZA. The origin and kinetics of mononuclear phagocytes. *J Exp Med*. 1968;128(3):415-35.
3. Hoeffel G, Ginhoux F. Fetal monocytes and the origins of tissue-resident macrophages. *Cell Immunol*. 2018;330:5-15.
4. Bertrand JY, Jalil A, Klaine M, Jung S, Cumano A, Godin I. Three pathways to mature macrophages in the early mouse yolk sac. *Blood*. 2005;106(9):3004-11.
5. Stremmel C, Schuchert R, Wagner F, Thaler R, Weinberger T, Pick R, et al. Yolk sac macrophage progenitors traffic to the embryo during defined stages of development. *Nat Commun*. 2018;9(1):75.
6. McGrath KE, Frame JM, Fegan KH, Bowen JR, Conway SJ, Catherman SC, et al. Distinct Sources of Hematopoietic Progenitors Emerge before HSCs and Provide Functional Blood Cells in the Mammalian Embryo. *Cell Rep*. 2015;11(12):1892-904.
7. Hoeffel G, Chen J, Lavin Y, Low D, Almeida FF, See P, et al. C-Myb(+) erythro-myeloid progenitor-derived fetal monocytes give rise to adult tissue-resident macrophages. *Immunity*. 2015;42(4):665-78.
8. Xu J, Zhu L, He S, Wu Y, Jin W, Yu T, et al. Temporal-Spatial Resolution Fate Mapping Reveals Distinct Origins for Embryonic and Adult Microglia in Zebrafish. *Dev Cell*. 2015;34(6):632-41.
9. Williams M, Scott CL. Does niche competition determine the origin of tissue-resident macrophages? *Nat Rev Immunol*. 2017;17(7):451-60.
10. Ferrero G, Mahony CB, Dupuis E, Yvernogeu L, Di Ruggiero E, Miserocchi M, et al. Embryonic Microglia Derive from Primitive Macrophages and Are Replaced by cmyb-Dependent Definitive Microglia in Zebrafish. *Cell Rep*. 2018;24(1):130-41.
11. De S, Van Deren D, Peden E, Hockin M, Boulet A, Titen S, et al. Two distinct ontogenies confer heterogeneity to mouse brain microglia. *Development*. 2018;145(13).
12. Ginhoux F, Williams M. Tissue-Resident Macrophage Ontogeny and Homeostasis. *Immunity*. 2016;44(3):439-49.
13. Ginhoux F, Greter M, Leboeuf M, Nandi S, See P, Gokhan S, et al. Fate mapping analysis reveals that adult microglia derive from primitive macrophages. *Science*. 2010;330(6005):841-5.
14. Kierdorf K, Erny D, Goldmann T, Sander V, Schulz C, Perdiguero EG, et al. Microglia emerge from erythromyeloid precursors via Pu.1- and Irf8-dependent pathways. *Nat Neurosci*. 2013;16(3):273-80.
15. Epelman S, Lavine KJ, Beaudin AE, Sojka DK, Carrero JA, Calderon B, et al. Embryonic and adult-derived resident cardiac macrophages are maintained through distinct mechanisms at steady state and during inflammation. *Immunity*. 2014;40(1):91-104.
16. Bain CC, Schridde A. Origin, Differentiation, and Function of Intestinal Macrophages. *Front Immunol*. 2018;9:2733.
17. Fricker M, Gibson PG. Macrophage dysfunction in the pathogenesis and treatment of asthma. *Eur Respir J*. 2017;50(3).
18. Ostuni R, Kratochvill F, Murray PJ, Natoli G. Macrophages and cancer: from mechanisms to therapeutic implications. *Trends Immunol*. 2015;36(4):229-39.
19. Navarro V, Sanchez-Mejias E, Jimenez S, Munoz-Castro C, Sanchez-Varo R, Davila JC, et al. Microglia in Alzheimer's Disease: Activated, Dysfunctional or Degenerative. *Front Aging Neurosci*. 2018;10:140.
20. Zheng X, Turkowski K, Mora J, Brune B, Seeger W, Weigert A, et al. Redirecting tumor-associated macrophages to become tumoricidal effectors as a novel strategy for cancer therapy. *Oncotarget*. 2017;8(29):48436-52.
21. Schafer DP, Lehrman EK, Kautzman AG, Koyama R, Mardinly AR, Yamasaki R, et al. Microglia sculpt postnatal neural circuits in an activity and complement-dependent manner. *Neuron*. 2012;74(4):691-705.
22. Domingues HS, Portugal CC, Socodato R, Relvas JB. Oligodendrocyte, Astrocyte, and Microglia Crosstalk in Myelin Development, Damage, and Repair. *Front Cell Dev Biol*. 2016;4:71.
23. Miyamoto A, Wake H, Ishikawa AW, Eto K, Shibata K, Murakoshi H, et al. Microglia contact induces synapse formation in developing somatosensory cortex. *Nat Commun*. 2016;7:12540.
24. Parkhurst CN, Yang G, Ninan I, Savas JN, Yates JR, 3rd, Lafaille JJ, et al. Microglia promote learning-dependent synapse formation

- through brain-derived neurotrophic factor. *Cell*. 2013;155(7):1596-609.
25. Tremblay ME, Lowery RL, Majewska AK. Microglial interactions with synapses are modulated by visual experience. *PLoS Biol*. 2010;8(11):e1000527.
 26. Hagemeyer N, Hanft KM, Akriditou MA, Unger N, Park ES, Stanley ER, et al. Microglia contribute to normal myelinogenesis and to oligodendrocyte progenitor maintenance during adulthood. *Acta Neuropathol*. 2017;134(3):441-58.
 27. Safaiyan S, Kannaiyan N, Snaidero N, Brioschi S, Biber K, Yona S, et al. Age-related myelin degradation burdens the clearance function of microglia during aging. *Nat Neurosci*. 2016;19(8):995-8.
 28. Wlodarczyk A, Holtman IR, Krueger M, Yogev N, Bruttger J, Khoroshii R, et al. A novel microglial subset plays a key role in myelinogenesis in developing brain. *EMBO J*. 2017;36(22):3292-308.
 29. Lavin Y, Winter D, Blecher-Gonen R, David E, Keren-Shaul H, Merad M, et al. Tissue-resident macrophage enhancer landscapes are shaped by the local microenvironment. *Cell*. 2014;159(6):1312-26.
 30. Mass E, Ballesteros I, Farlik M, Halbritter F, Gunther P, Crozet L, et al. Specification of tissue-resident macrophages during organogenesis. *Science*. 2016;353(6304).
 31. Matcovitch-Natan O, Winter DR, Giladi A, Vargas Aguilar S, Spinrad A, Sarrazin S, et al. Microglia development follows a stepwise program to regulate brain homeostasis. *Science*. 2016;353(6301):aad8670.
 32. Butovsky O, Jedrychowski MP, Moore CS, Cialic R, Lanser AJ, Gabrieli G, et al. Identification of a unique TGF-beta-dependent molecular and functional signature in microglia. *Nat Neurosci*. 2014;17(1):131-43.
 33. Zhang Y, Chen K, Sloan SA, Bennett ML, Scholze AR, O'Keefe S, et al. An RNA-sequencing transcriptome and splicing database of glia, neurons, and vascular cells of the cerebral cortex. *J Neurosci*. 2014;34(36):11929-47.
 34. Reid DT, Reyes JL, McDonald BA, Vo T, Reimer RA, Eksteen B. Kupffer Cells Undergo Fundamental Changes during the Development of Experimental NASH and Are Critical in Initiating Liver Damage and Inflammation. *PLoS One*. 2016;11(7):e0159524.
 35. Hagemeyer N, Kierdorf K, Frenzel K, Xue J, Ringelhan M, Abdullah Z, et al. Transcriptome-based profiling of yolk sac-derived macrophages reveals a role for Irf8 in macrophage maturation. *EMBO J*. 2016;35(16):1730-44.
 36. Scott CL, T'Jonck W, Martens L, Todorov H, Sichien D, Soen B, et al. The Transcription Factor ZEB2 Is Required to Maintain the Tissue-Specific Identities of Macrophages. *Immunity*. 2018;49(2):312-25 e5.
 37. Gosselin D, Link VM, Romanoski CE, Fonseca GJ, Eichenfield DZ, Spann NJ, et al. Environment drives selection and function of enhancers controlling tissue-specific macrophage identities. *Cell*. 2014;159(6):1327-40.
 38. van de Laar L, Saelens W, De Prijck S, Martens L, Scott CL, Van Isterdael G, et al. Yolk Sac Macrophages, Fetal Liver, and Adult Monocytes Can Colonize an Empty Niche and Develop into Functional Tissue-Resident Macrophages. *Immunity*. 2016;44(4):755-68.
 39. Bohlen CJ, Bennett FC, Tucker AF, Collins HY, Mulinyawie SB, Barres BA. Diverse Requirements for Microglial Survival, Specification, and Function Revealed by Defined-Medium Cultures. *Neuron*. 2017;94(4):759-73 e8.
 40. Haynes SE, Hollopeter G, Yang G, Kurpius D, Dailey ME, Gan WB, et al. The P2Y12 receptor regulates microglial activation by extracellular nucleotides. *Nat Neurosci*. 2006;9(12):1512-9.
 41. Okabe Y, Medzhitov R. Tissue-specific signals control reversible program of localization and functional polarization of macrophages. *Cell*. 2014;157(4):832-44.
 42. Groffen J, Heisterkamp N, Spurr N, Dana S, Wasmuth JJ, Stephenson JR. Chromosomal localization of the human c-fms oncogene. *Nucleic Acids Res*. 1983;11(18):6331-9.
 43. Kelley TW, Graham MM, Doseff AI, Pomerantz RW, Lau SM, Ostrowski MC, et al. Macrophage colony-stimulating factor promotes cell survival through Akt/protein kinase B. *J Biol Chem*. 1999;274(37):26393-8.
 44. Murray JT, Craggs G, Wilson L, Kellie S. Mechanism of phosphatidylinositol 3-kinase-dependent increases in BAC1.2F5 macrophage-like cell density in response to M-CSF: phosphatidylinositol 3-kinase inhibitors increase the rate of apoptosis rather than inhibit DNA synthesis. *Inflamm Res*. 2000;49(11):610-8.
 45. Golden LH, Insogna KL. The expanding role of PI3-kinase in bone. *Bone*. 2004;34(1):3-12.
 46. Chang M, Hamilton JA, Scholz GM, Masendycz P, Macaulay SL, Elsegood CL. Phosphatidylinositol-3 kinase and phospholipase

- C enhance CSF-1-dependent macrophage survival by controlling glucose uptake. *Cell Signal*. 2009;21(9):1361-9.
47. Munugalavada V, Borneo J, Ingram DA, Kapur R. p85alpha subunit of class IA PI-3 kinase is crucial for macrophage growth and migration. *Blood*. 2005;106(1):103-9.
 48. Bourette RP, Myles GM, Carlberg K, Chen AR, Rohrschneider LR. Uncoupling of the proliferation and differentiation signals mediated by the murine macrophage colony-stimulating factor receptor expressed in myeloid FDC-P1 cells. *Cell Growth Differ*. 1995;6(6):631-45.
 49. Sampaio NG, Yu W, Cox D, Wyckoff J, Condeelis J, Stanley ER, et al. Phosphorylation of CSF-1R Y721 mediates its association with PI3K to regulate macrophage motility and enhancement of tumor cell invasion. *J Cell Sci*. 2011;124(Pt 12):2021-31.
 50. Mouchemore KA, Sampaio NG, Murrey MW, Stanley ER, Lannutti BJ, Pixley FJ. Specific inhibition of PI3K p110delta inhibits CSF-1-induced macrophage spreading and invasive capacity. *FEBS J*. 2013;280(21):5228-36.
 51. Cammer M, Gevrey JC, Lorenz M, Dovas A, Condeelis J, Cox D. The mechanism of CSF-1-induced Wiskott-Aldrich syndrome protein activation in vivo: a role for phosphatidylinositol 3-kinase and Cdc42. *J Biol Chem*. 2009;284(35):23302-11.
 52. Stanley ER, Chitu V. CSF-1 receptor signaling in myeloid cells. *Cold Spring Harb Perspect Biol*. 2014;6(6).
 53. Greter M, Lelios I, Pelczar P, Hoeffel G, Price J, Leboeuf M, et al. Stroma-derived interleukin-34 controls the development and maintenance of langerhans cells and the maintenance of microglia. *Immunity*. 2012;37(6):1050-60.
 54. Wang Y, Szretter KJ, Vermi W, Gilfillan S, Rossini C, Cella M, et al. IL-34 is a tissue-restricted ligand of CSF1R required for the development of Langerhans cells and microglia. *Nat Immunol*. 2012;13(8):753-60.
 55. Wei S, Nandi S, Chitu V, Yeung YG, Yu W, Huang M, et al. Functional overlap but differential expression of CSF-1 and IL-34 in their CSF-1 receptor-mediated regulation of myeloid cells. *J Leukoc Biol*. 2010;88(3):495-505.
 56. Nandi S, Gokhan S, Dai XM, Wei S, Enikolopov G, Lin H, et al. The CSF-1 receptor ligands IL-34 and CSF-1 exhibit distinct developmental brain expression patterns and regulate neural progenitor cell maintenance and maturation. *Dev Biol*. 2012;367(2):100-13.
 57. Brugger W, Kreutz M, Andreesen R. Macrophage colony-stimulating factor is required for human monocyte survival and acts as a cofactor for their terminal differentiation to macrophages in vitro. *J Leukoc Biol*. 1991;49(5):483-8.
 58. Dai XM, Ryan GR, Hapel AJ, Dominguez MG, Russell RG, Kapp S, et al. Targeted disruption of the mouse colony-stimulating factor 1 receptor gene results in osteopetrosis, mononuclear phagocyte deficiency, increased primitive progenitor cell frequencies, and reproductive defects. *Blood*. 2002;99(1):111-20.
 59. Erblisch B, Zhu L, Etgen AM, Dobrenis K, Pollard JW. Absence of colony stimulation factor-1 receptor results in loss of microglia, disrupted brain development and olfactory deficits. *PLoS One*. 2011;6(10):e26317.
 60. Pridans C, Raper A, Davis GM, Alves J, Sauter KA, Lefevre L, et al. Pleiotropic Impacts of Macrophage and Microglial Deficiency on Development in Rats with Targeted Mutation of the *Csf1r* Locus. *J Immunol*. 2018;201(9):2683-99.
 61. Rademakers R, Baker M, Nicholson AM, Rutherford NJ, Finch N, Soto-Ortolaza A, et al. Mutations in the colony stimulating factor 1 receptor (CSF1R) gene cause hereditary diffuse leukoencephalopathy with spheroids. *Nat Genet*. 2011;44(2):200-5.
 62. Cannarile MA, Weisser M, Jacob W, Jegg AM, Ries CH, Ruttinger D. Colony-stimulating factor 1 receptor (CSF1R) inhibitors in cancer therapy. *J Immunother Cancer*. 2017;5(1):53.
 63. Garcia S, Hartkamp LM, Malvar-Fernandez B, van Es IE, Lin H, Wong J, et al. Colony-stimulating factor (CSF) 1 receptor blockade reduces inflammation in human and murine models of rheumatoid arthritis. *Arthritis Res Ther*. 2016;18:75.
 64. Bilbo SD, Block CL, Bolton JL, Hanamsagar R, Tran PK. Beyond infection - Maternal immune activation by environmental factors, microglial development, and relevance for autism spectrum disorders. *Exp Neurol*. 2018;299(Pt A):241-51.
 65. Oyanagi K, Kinoshita M, Suzuki-Kouyama E, Inoue T, Nakahara A, Tokiwa M, et al. Adult onset leukoencephalopathy with axonal spheroids and pigmented glia (ALSP) and Nasu-Hakola disease: lesion staging and dynamic changes of axons and microglial subsets. *Brain Pathol*. 2017;27(6):748-69.
 66. Bianchin MM, Martin KC, de Souza AC, de

- Oliveira MA, Rieder CR. Nasu-Hakola disease and primary microglial dysfunction. *Nat Rev Neurol*. 2010;6(9):2 p following 523.
67. Goldmann T, Zeller N, Raasch J, Kierdorf K, Frenzel K, Ketscher L, et al. USP18 lack in microglia causes destructive interferonopathy of the mouse brain. *EMBO J*. 2015;34(12):1612-29.
 68. Sasaki A. Microglia and brain macrophages: An update. *Neuropathology*. 2017;37(5):452-64.
 69. Sierra A, Encinas JM, Deudero JJ, Chancey JH, Enikolopov G, Overstreet-Wadiche LS, et al. Microglia shape adult hippocampal neurogenesis through apoptosis-coupled phagocytosis. *Cell Stem Cell*. 2010;7(4):483-95.
 70. Checchin D, Sennlaub F, Levavasseur E, Leduc M, Chemtob S. Potential role of microglia in retinal blood vessel formation. *Invest Ophthalmol Vis Sci*. 2006;47(8):3595-602.
 71. Kubota Y, Takubo K, Shimizu T, Ohno H, Kishi K, Shibuya M, et al. M-CSF inhibition selectively targets pathological angiogenesis and lymphangiogenesis. *J Exp Med*. 2009;206(5):1089-102.
 72. Santos AM, Calvente R, Tassi M, Carrasco MC, Martin-Oliva D, Marin-Teva JL, et al. Embryonic and postnatal development of microglial cells in the mouse retina. *J Comp Neurol*. 2008;506(2):224-39.
 73. Fantin A, Vieira JM, Gestri G, Denti L, Schwarz Q, Prykhodzij S, et al. Tissue macrophages act as cellular chaperones for vascular anastomosis downstream of VEGF-mediated endothelial tip cell induction. *Blood*. 2010;116(5):829-40.
 74. Rigato C, Buckinx R, Le-Corronc H, Rigo JM, Legendre P. Pattern of invasion of the embryonic mouse spinal cord by microglial cells at the time of the onset of functional neuronal networks. *Glia*. 2011;59(4):675-95.
 75. Bennett FC, Bennett ML, Yaqoob F, Mulinyawe SB, Grant GA, Hayden Gephart M, et al. A Combination of Ontogeny and CNS Environment Establishes Microglial Identity. *Neuron*. 2018;98(6):1170-83 e8.
 76. Oosterhof N, Holtman IR, Kuil LE, van der Linde HC, Boddeke EW, Eggen BJ, et al. Identification of a conserved and acute neurodegeneration-specific microglial transcriptome in the zebrafish. *Glia*. 2017;65(1):138-49.
 77. Hickman SE, Kingery ND, Ohsumi TK, Borowsky ML, Wang LC, Means TK, et al. The microglial sensome revealed by direct RNA sequencing. *Nat Neurosci*. 2013;16(12):1896-905.
 78. Gosselin D, Skola D, Coufal NG, Holtman IR, Schlachetki JCM, Sajti E, et al. An environment-dependent transcriptional network specifies human microglia identity. *Science*. 2017;356(6344).
 79. Artegiani B, Lyubimova A, Muraro M, van Es JH, van Oudenaarden A, Clevers H. A Single-Cell RNA Sequencing Study Reveals Cellular and Molecular Dynamics of the Hippocampal Neurogenic Niche. *Cell Rep*. 2017;21(11):3271-84.
 80. Paloneva J, Kestila M, Wu J, Salminen A, Bohling T, Ruotsalainen V, et al. Loss-of-function mutations in TYROBP (DAP12) result in a presenile dementia with bone cysts. *Nat Genet*. 2000;25(3):357-61.
 81. Paloneva J, Manninen T, Christman G, Hovanes K, Mandelin J, Adolfsson R, et al. Mutations in two genes encoding different subunits of a receptor signaling complex result in an identical disease phenotype. *Am J Hum Genet*. 2002;71(3):656-62.
 82. Kielian T. Lysosomal storage disorders: Pathology within the lysosome and beyond. *J Neurochem*. 2019.
 83. Mahuran DJ. The biochemistry of HEXA and HEXB gene mutations causing GM2 gangliosidosis. *Biochim Biophys Acta*. 1991;1096(2):87-94.
 84. Utsumi K, Tsuji A, Kase R, Tanaka A, Tanaka T, Uyama E, et al. Western blotting analysis of the beta-hexosaminidase alpha- and beta-subunits in cultured fibroblasts from cases of various forms of GM2 gangliosidosis. *Acta Neurol Scand*. 2002;105(6):427-30.
 85. Jeyakumar M, Thomas R, Elliot-Smith E, Smith DA, van der Spoel AC, d'Azzo A, et al. Central nervous system inflammation is a hallmark of pathogenesis in mouse models of GM1 and GM2 gangliosidosis. *Brain*. 2003;126(Pt 4):974-87.
 86. Myerowitz R, Lawson D, Mizukami H, Mi Y, Tiff CJ, Proia RL. Molecular pathophysiology in Tay-Sachs and Sandhoff diseases as revealed by gene expression profiling. *Hum Mol Genet*. 2002;11(11):1343-50.
 87. Sargeant TJ, Drage DJ, Wang S, Apostolakis AA, Cox TM, Cachon-Gonzalez MB. Characterization of inducible models of Tay-Sachs and related disease. *PLoS Genet*. 2012;8(9):e1002943.
 88. Tavasoli AR, Parvaneh N, Ashrafi MR, Rezaei Z, Zschocke J, Rostami P. Clinical presentation and outcome in infantile Sandhoff disease: a case series of 25 patients from Iranian neurometabolic bioregistry with five novel mutations. *Orphanet J Rare Dis*. 2018;13(1):130.
 89. Steenweg ME, Vanderver A, Blaser S, Bizzi A, de Koning TJ, Mancini GM, et al. Magnetic resonance

- imaging pattern recognition in hypomyelinating disorders. *Brain*. 2010;133(10):2971-82.
90. Tsuji D, Kuroki A, Ishibashi Y, Itakura T, Kuwahara J, Yamanaka S, et al. Specific induction of macrophage inflammatory protein 1-alpha in glial cells of Sandhoff disease model mice associated with accumulation of N-acetylhexosaminyl glycoconjugates. *J Neurochem*. 2005;92(6):1497-507.
 91. Kawashima N, Tsuji D, Okuda T, Itoh K, Nakayama K. Mechanism of abnormal growth in astrocytes derived from a mouse model of GM2 gangliosidosis. *J Neurochem*. 2009;111(4):1031-41.
 92. Kyrkanides S, Brouxhon SM, Tallents RH, Miller JN, Olschowka JA, O'Banion MK. Conditional expression of human beta-hexosaminidase in the neurons of Sandhoff disease rescues mice from neurodegeneration but not neuroinflammation. *J Neuroinflammation*. 2012;9:186.
 93. Wada R, Tiffet CJ, Proia RL. Microglial activation precedes acute neurodegeneration in Sandhoff disease and is suppressed by bone marrow transplantation. *Proc Natl Acad Sci U S A*. 2000;97(20):10954-9.
 94. Wu YP, Proia RL. Deletion of macrophage-inflammatory protein 1 alpha retards neurodegeneration in Sandhoff disease mice. *Proc Natl Acad Sci U S A*. 2004;101(22):8425-30.
 95. Howe K, Clark MD, Torroja CF, Torrance J, Berthelot C, Muffato M, et al. The zebrafish reference genome sequence and its relationship to the human genome. *Nature*. 2013;496(7446):498-503.
 96. Shiao CE, Monk KR, Joo W, Talbot WS. An anti-inflammatory NOD-like receptor is required for microglia development. *Cell Rep*. 2013;5(5):1342-52.
 97. Meireles AM, Shiao CE, Guenther CA, Sidik H, Kingsley DM, Talbot WS. The Phosphate Exporter *xpr1b* Is Required for Differentiation of Tissue-Resident Macrophages. *Cell reports*. 2014;8(6):1659-67.
 98. Shen K, Sidik H, Talbot WS. The Rag-Ragulator Complex Regulates Lysosome Function and Phagocytic Flux in Microglia. *Cell Rep*. 2016;14(3):547-59.
 99. Rossi F, Casano AM, Henke K, Richter K, Peri F. The SLC7A7 Transporter Identifies Microglial Precursors prior to Entry into the Brain. *Cell reports*. 2015;11(7):1008-17.
 100. Shah AN, Davey CF, Whitebitch AC, Miller AC, Moens CB. Rapid reverse genetic screening using CRISPR in zebrafish. *Nat Methods*. 2015;12(6):535-40.
 101. Renshaw SA, Trede NS. A model 450 million years in the making: zebrafish and vertebrate immunity. *Dis Model Mech*. 2012;5(1):38-47.
 102. Gore AV, Pillay LM, Venero Galanternik M, Weinstein BM. The zebrafish: A fantastic model for hematopoietic development and disease. *Wiley Interdiscip Rev Dev Biol*. 2018;7(3):e312.
 103. Baeten JT, de Jong JLO. Genetic Models of Leukemia in Zebrafish. *Front Cell Dev Biol*. 2018;6:115.
 104. Li Y, Du XF, Liu CS, Wen ZL, Du JL. Reciprocal regulation between resting microglial dynamics and neuronal activity in vivo. *Dev Cell*. 2012;23(6):1189-202.
 105. Farrar MJ, Wise FW, Fetcho JR, Schaffer CB. In vivo imaging of myelin in the vertebrate central nervous system using third harmonic generation microscopy. *Biophys J*. 2011;100(5):1362-71.
 106. Auer F, Vagionitis S, Czopka T. Evidence for Myelin Sheath Remodeling in the CNS Revealed by In Vivo Imaging. *Curr Biol*. 2018;28(4):549-59 e3.
 107. Torraca V, Masud S, Spaink HP, Meijer AH. Macrophage-pathogen interactions in infectious diseases: new therapeutic insights from the zebrafish host model. *Dis Model Mech*. 2014;7(7):785-97.
 108. Colucci-Guyon E, Tinevez JY, Renshaw SA, Herbomel P. Strategies of professional phagocytes in vivo: unlike macrophages, neutrophils engulf only surface-associated microbes. *J Cell Sci*. 2011;124(Pt 18):3053-9.

Chapter 2

Reverse genetic screen reveals that Il34 facilitates yolk sac macrophage distribution and seeding of the brain

Laura E. Kuil^{1, #}, Nynke Oosterhof^{1, 2, #}, Samuël N. Geurts^{3, 4}, Herma C. van der Linde¹, Erik Meijering³, Tjakko J. van Ham^{1, *}

¹Department of Clinical Genetics, Erasmus University Medical Center, Wytemaweg 80, 3015 CN, Rotterdam, The Netherlands.

²European Research Institute for the Biology of Ageing, University Medical Center Groningen, Antonius Deusinglaan, 1, 9713 AV Groningen, The Netherlands.

³Biomedical Imaging Group Rotterdam, Departments of Medical Informatics and Radiology, Erasmus University Medical Center, Wytemaweg 80, 3015 CN, Rotterdam, The Netherlands.

⁴Quantitative Imaging, Faculty of Applied Sciences, Delft University of Technology, Lorentzweg 1, 2628 CJ, Delft, The Netherlands

#Equal contribution

Disease models and mechanisms, 2019

Abstract

Microglia are brain resident macrophages, which have specialized functions important in brain development and in disease. They colonize the brain in early embryonic stages, but few factors that drive the migration of yolk sac macrophages (YSMs) into the embryonic brain, or regulate their acquisition of specialized properties are currently known.

Here, we present a CRISPR/Cas9-based *in vivo* reverse genetic screening pipeline to identify new microglia regulators using zebrafish. Zebrafish larvae are particularly suitable due to their external development, transparency and conserved microglia features. We targeted putative microglia regulators, by Cas9/gRNA-complex injections, followed by neutral red-based visualization of microglia. Microglia were quantified automatically in 3-day-old larvae using a software tool we called SpotNGlia. We identified that loss of the zebrafish colony stimulating factor 1 receptor (CSF1R) ligand IL34, caused reduced microglia numbers. Previous studies on the role of the IL34 on microglia development *in vivo* were ambiguous. Our data, and a concurrent paper, show that in zebrafish, *il34* is required during the earliest seeding of the brain by microglia. Our data also indicate that IL34 is required for YSM distribution to other organs. Disruption of the other CSF1R ligand, *Csf1*, did not reduce microglia numbers in mutants, whereas overexpression increased the number of microglia. This shows *Csf1* can influence microglia numbers, but might not be essential for the early seeding of the brain. In all, we identified *il34* as a modifier of microglia colonization, by affecting distribution of YSMs to target organs, validating our reverse genetic screening pipeline in zebrafish.

Introduction

Tissue macrophages, in addition to their immunological roles, modulate organogenesis and exhibit organ-specific regulatory properties that are thought to affect virtually all organs in vertebrates (1, 2). Microglia are the brain's resident macrophages, which have roles in brain development and homeostasis. Described functions of microglia include the removal of dead cells and debris, modulation of neuronal connectivity by synaptic pruning and maintenance of myelin-producing cells (3-6). Defects in microglia function have been implicated in neurodevelopmental disorders such as autism spectrum disorder (ASD) (3). Pathogenic variants in genes thought to primarily affect microglia cause rare white matter disorders including Nasu-Hakola disease and adult onset leukoencephalopathy with axonal spheroids (ALSP), which may be caused by loss of microglia activity (7-10). In line with this, there is accumulating evidence that replenishing brain myeloid cells by hematopoietic cell transplantation (HCT) has powerful therapeutic potential in leukodystrophy and metabolic diseases affecting the brain, and better understanding the molecular regulation of brain colonization by microglia could lead to ways to facilitate this (11-13). However, the exact genes and mechanisms underlying the emergence of microglia in the brain and acquisition of their functional properties are still poorly understood.

Microglia originate from macrophage progenitors in the embryonic yolk sac, known as yolk sac macrophages (YSMs), which colonize the brain during early embryonic development (14, 15). Once they arrive in the brain, they acquire a highly ramified morphology, proliferate extensively and form a brain-wide network with non-overlapping territories (16). The transition from YSM to mature microglia or other tissue resident macrophages involves several differentiation stages characterized by distinct transcriptional profiles (17, 18). The progression through these transcriptional states is synchronised with, and most likely driven by, the different stages of brain development as microglia gene expression is highly sensitive to changes in the microenvironment and tissue macrophage identity is mostly determined by the host environment (17, 19-21). For the majority of the genes specifically expressed in microglia the function is still unknown, and as many of these genes are rapidly downregulated when they are taken out of the brain, it is difficult to study their functions *in vitro* (22, 23). In mammals, microglia development is relatively inaccessible to study, as YSMs emerge during development in utero. Despite progress in identifying methods to recreate microglia-like cells *in vitro*, improved understanding of their ontogeny is needed to guide *in vitro* efforts (24, 25). Therefore, identification of the functions

of genes affecting microglia development could provide valuable insights into regulation of microglia development and function *in vivo*.

Zebrafish embryos are relatively small, transparent, are relatively easy to manipulate genetically and develop ex-utero, which makes them highly suitable for *in vivo* genetic studies (26). We recently showed that microglia gene expression is well conserved between zebrafish and mammals and that, as shown in mice, loss of the two zebrafish homologs of the colony-stimulating factor 1 receptor (Csf1ra and Csf1rb) leads to absence of microglia (10, 27-29). Phenotype-driven, forward genetic screens in zebrafish have identified several microglia mutants with a defect in microglia development or function. Processes affected in these mutants include hematopoiesis, regulation of inflammation, phosphate transport and lysosomal regulation, which implies that these various processes are all critical for microglia development and function (30-34). However, such forward genetic screens are laborious and relatively low-throughput. A candidate-driven reverse genetic screening approach could lead to identification of additional genes important for microglia. The CRISPR/Cas9-system can be used to create insertions or deletions (indels) in target genes via the repair of Cas9-induced double strand breaks by error-prone non-homologous end joining (NHEJ) (35). Injection of gene specific guide RNAs (gRNAs) and Cas9 mRNA, can lead to gene disruption sufficiently effective to allow small-scale reverse genetic screening, for example to identify new genes involved in electrical synapse formation (36). Alternatively, active Cas9-gRNA ribonucleoprotein complexes injected into fertilized zebrafish oocytes can more efficiently induce indels in target genes and the resulting genetic mosaic zebrafish can phenocopy existing loss-of-function mutants (CRISPPants) (37, 38).

Here, we present a scalable CRISPR/Cas9-based reverse genetic screening pipeline in zebrafish to identify important genetic microglia regulators. In zebrafish larvae, microglia can be visualized by the vital dye neutral red, which shows a selective and pronounced staining in microglia over other macrophages and has been used as an effective readout for microglia numbers in forward genetic screens (15, 30-32). We developed an image quantification tool, SpotNGlia, to automatically detect the brain boundaries and count neutral red-positive (NR+) microglia. Out of the 20 putative microglia regulators we targeted by CRISPR/Cas9-mediated reverse genetics, disruption of *interleukin 34* (*il34*) showed the strongest reduction in microglia numbers in developing zebrafish larvae. In mammals, *Il34* is one of two ligands of the microglia regulator CSF1R. Further analysis in stable *il34* mutants revealed that *il34* is mainly important for the

recruitment of microglia to the brain, and likely other tissue resident macrophage populations, including Langerhans cells, to their target organs. Thus, we here present a scalable reverse genetic screening pipeline to identify additional new regulators important for microglia development and function.

Results

CRISPsants phenocopy existing mutants with microglia developmental defects

Loss of one of several key macrophage regulators, including *Spi1* (encoding PU.1), *Irf8* and *Csf1r*, and their zebrafish homologs *spi1b* (Pu.1), *csf1ra* and *csf1rb*, and *irf8*, leads to defects in microglia development (15, 28, 39-43). To investigate whether Cas9-gRNA ribonucleoprotein complexes (RNPs) targeting these regulators can be used to induce mutant microglia phenotypes directly, we injected zebrafish oocytes with RNPs targeting either *csf1ra* or *spi1b*. To assess whether CRISPR/Cas9-based targeting of those genes affects microglia development we determined microglia numbers by neutral red (NR) staining at 3 days post fertilization (dpf). At this time point, microglia have just colonized the optic tectum, are highly phagocytic and have low proliferative activity, which makes it an ideal time point to identify genes required for the earliest steps of microglia development (15, 44). We quantified NR+ microglia in *csf1ra* CRISPsants, in controls and in *csf1ra* loss-of-function mutants found in an ENU mutagenic screen (hereafter called *csf1ra*^{-/-}) (45). Similar to *csf1ra*^{-/-} mutants, *csf1ra* CRISPsants showed an 80% reduction in the number of NR+ microglia compared to controls suggesting highly effective targeting in F0 injected embryos (Fig 1A). To assess the targeting efficiency of the *csf1ra* gene we performed Sanger sequencing of the targeted locus of a small pool of *csf1ra* CRISPsants and calculated the spectrum and frequency of indels in the *csf1ra* gene using TIDE (tracking indels by decomposition) software (46). The mutagenic efficiency was >90%, showing efficient mutagenesis (Fig 1B). Similarly, *spi1b* CRISPsants showed a strong reduction in the number of microglia and 65-95% mutagenic efficiency (Fig 1C, D). This shows that CRISPR/Cas9-based mutagenesis can be used to reproduce mutant microglia phenotypes in Cas9-gRNA RNP injected zebrafish larvae.

SpotNGlia semi-automatically counts microglia numbers

Manual quantification of NR+ microglia, across z-stack images, is time-consuming and can be subjective. To standardize and speed up quantification, we developed

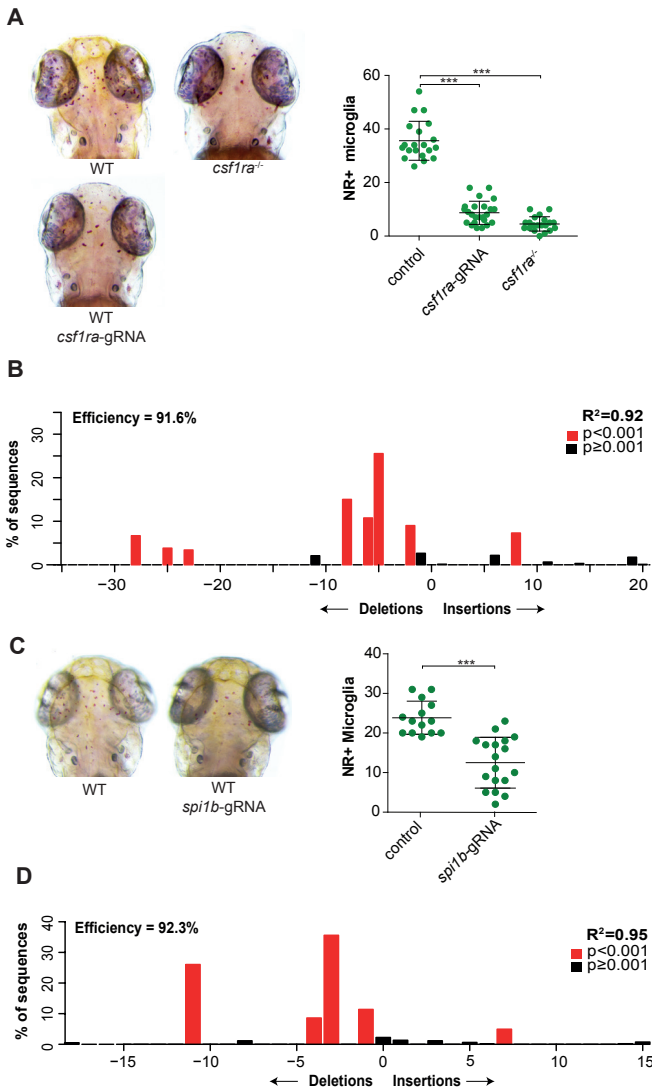


Fig 1. *csf1r* CRISPants phenocopy existing *csf1r* microglia mutants.

A Neutral red (NR⁺) images and quantification of WT, *csf1ra*^{-/-} and *csf1ra* CRISPant zebrafish larvae at 3 dpf. **B** Indel spectrum of a pool of *csf1ra* CRISPants calculated by tide. **C** Neutral red images and quantification of WT, and *spi1b* CRISPant zebrafish larvae at 3 dpf. **D** Indel spectrum of a representative individual *spi1b* CRISPant calculated by tide. R^2 value represents reliability of the de indelspectrum. *** $p < 0.001$. One-way anova and *t*-test. Each dot represents one larvae. Error bars represent s.d.

a software tool, SpotNGlia, that automatically counts NR⁺ microglia in the optic tectum where most microglia are located at 3 dpf. The SpotNGlia tool aligns stacked images of stained zebrafish larvae taken at different axial positions and blends the images into a single 2D image in which all NR⁺ cells are in focus (Fig 2A). Next, the images are segmented by using polar transformation and dynamic programming to identify the edges of the optic tectum. Finally, NR⁺ cells are detected and counted by a spot detection technique based on multiscale wavelet products (47). To test the SpotNGlia software tool, we created and manually annotated a dataset with representative z-stack images of 50 neutral red stained

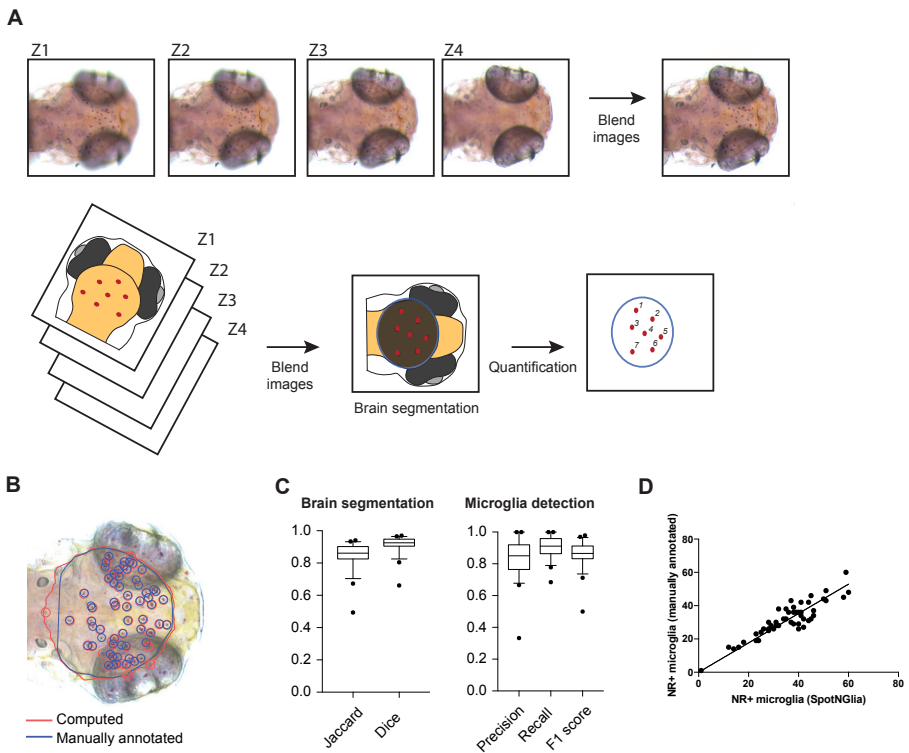


Fig 2. SpotNGlia semi-automatically counts microglia numbers. **A** Examples of z-stack images of NR stained larvae and a schematic representation of SpotNGlia analysis pipeline. **B** SpotNGlia output of test dataset with both manual (blue) and automated (red) brain segmentation and NR+ microglia annotation. **C** Boxplots showing Jaccard and Dice indices for accuracy of brain segmentation and F1, precision and recall scores for the accuracy of NR+ microglia annotation. **D** Correlation between manually and automated microglia quantification after manual correction for segmented brain area. Error bars represent s.d.

zebrafish larvae. To assess the accuracy of brain segmentation, Jaccard and Dice indices were determined, revealing indices of 0.86 (Jaccard) and 0.93 (Dice) (Fig 2B, C). To assess the accuracy of microglia detection we determined the precision, recall and F1 scores of the computed annotation, resulting in average scores of 0.85, 0.91 and 0.87, respectively (Fig 2B,C,D). These results indicate that SpotNGlia is able to automatically identify the boundaries of the midbrain region, and the microglia within that region, in the vast majority of cases. To correct manually for those instances where brain segmentation and microglia detection were not completely accurate -as determined by visual inspection, our tool offers the possibility of post-hoc correction. In our experiments we have found

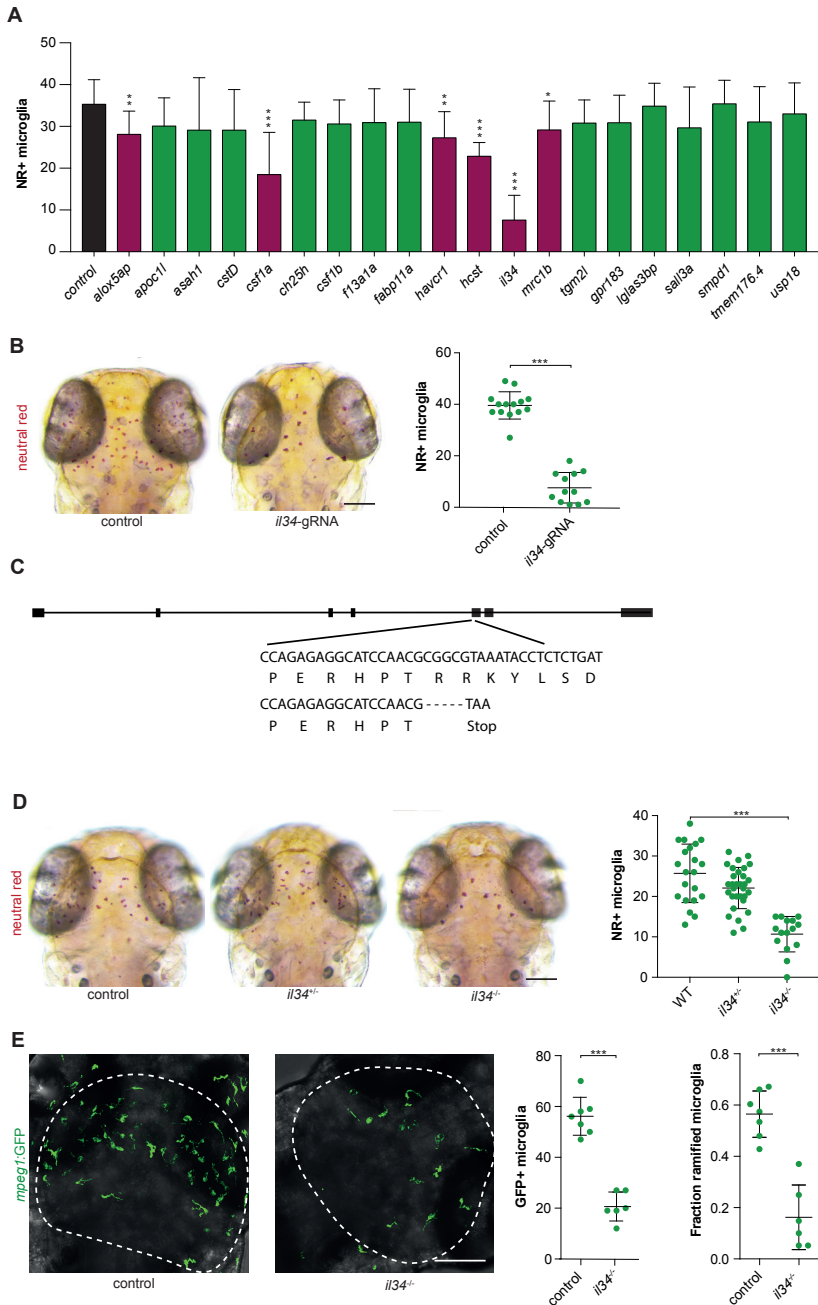


Fig 3. Reverse genetic screen reveals zebrafish *il34* as a regulator of microglia development.

A Accumulated data from all gRNA injections showing the number of NR+ microglia as quantified with SpotNGlia. Red bars represent genes which showed a significant reduction in microglia numbers upon CRISPR/Cas9-based targeting. **B** NR+ microglia numbers in 3 dpf zebrafish larvae injected

with gRNA-Cas9 RNPs targeting *il34*. Controls in **A** and **B** are non-injected wildtype larvae. **C** -5 bp deletion in exon 1 of *il34* directly introduces a stop codon **D** NR+ microglia numbers in *il34* mutants with a premature stop codon in exon 5 and their heterozygous and wildtype siblings at 3 dpf. **E** GFP+ microglia in the optic tecti (dotted line) of 3 dpf *il34* mutants and controls and quantification of their numbers and the fraction of microglia containing more than one protrusion (ramified microglia). Controls in **D** and **E** are wildtype (*il34^{+/+}*) larvae. * $p < 0.05$, ** $p < 0.01$, *** $p < 0.001$. One-way anova and t-test. Bonferroni correction for multiple testing. Scale bar represents 100 μm . Each dot represents one larvae. Error bars represent s.d.

that SpotNGlia results in about 80% reduction in the time it takes to quantify NR+ microglia numbers. In all, this indicates that SpotNGlia is a powerful tool for fast quantification of NR+ microglia numbers to assist in identifying novel genes important for generation of functional microglia.

Reverse genetic screen reveals zebrafish *IL34* as a regulator of microglia development

To identify new microglia regulators using direct CRISPR/Cas9-targeting and microglia phenotyping by SpotNGlia, we targeted 20 candidate genes individually. These genes were selected based on either our recently identified zebrafish microglia transcriptome (e.g. *slco2b1*, *hcst/dap10* and *mrc1b*), microglia expressed genes with a connection to brain disease (e.g. *usp18*), or genes which could affect microglia in a non-cell autonomous manner (CSF1R ligand encoding genes *il34*, *csf1a* and *csf1b*)(Fig 3A, Fig S1, Table S1)(27). Next, gRNAs were designed to effectively target these genes in one of their first exons. Cas9-gRNA RNPs targeting candidate genes were injected in fertilized oocytes, after which they were NR stained at 3 dpf, phenotyped and genotyped by Sanger sequencing followed by indel decomposition using TIDE (Table S1)(46). We did not observe obvious signs of developmental delay, morphological abnormalities or increased mortality upon Cas9-gRNA RNP injections, indicating that the observed microglia phenotypes were not due to Cas9-gRNA toxicity. The gRNAs for 6 of the targeted genes caused a significant reduction in the number of NR+ microglia (Fig 3A). The largest decrease in NR+ numbers was observed in embryos in which the zebrafish homolog of interleukin 34 (IL34) was targeted (Fig 3A, B)(48).

To validate our approach and confirm that this microglia phenotype is caused by loss of *il34* function, we generated a premature stop codon in exon 5 of the *il34* gene (Fig 2C). Neutral red labelling of homozygous *il34* mutants at 3 dpf revealed a ~60% reduction in NR+ microglia compared to wildtype siblings, suggesting this is a loss of function allele (Fig 3D). Similarly, live imaging of GFP

expressing microglia (GFP+), driven by the *mpeg1* promoter, in the optic tecti of *il34* mutants showed lowered microglia numbers compared to controls (Fig 3E). In mice, *Il34* knockout led to slightly different outcomes, causing, in one study, lowered microglia numbers already in early postnatal development that remained low into adulthood and, in another study, only reduced adult microglia numbers (49, 50). Therefore, the precise role of *Il34* in early microglia development remains ambiguous. In addition, the precise role of *Il34* in adult microglia has not been described yet (49, 50). Our results are consistent with an evolutionary conserved role for *Il34* in early microglia development (49). This is further supported by a concurrent study where, using another premature stop mutation in *il34*, the authors showed a similar reduction in microglia numbers at the same developmental stage (51). Interestingly, the receptor for *Il34*, colony stimulating factor 1 receptor (*Csf1r*), has two other ligands in zebrafish: *Csf1a* and *Csf1b*. To determine whether the other *Csf1r* ligands also affect early microglia development we generated stable frameshift mutants for *csf1a* and *csf1b* (Fig S3). However, individual *csf1a* and *csf1b* mutants did not show reduced microglia numbers (Fig S2A-B)(51). Surprisingly, larvae containing mutations in both zebrafish *csf1* homologs, *csf1a* and *csf1b* (*csf1a⁻b⁻*), also showed no reduction in microglia numbers (Fig S2C). As the mutants presented with the absence of yellow pigment cells, known as xanthophores, a phenotype also observed in *csf1ra⁻* mutants, this suggests that the *csf1a⁻b⁻* fish are loss of function mutants (45, 52-54). Many *in vitro* studies have shown that CSF1 can induce proliferation of myeloid cells (55, 56). Consistently, we find that overexpression of *Csf1a* (*Tg(hsp70l:csf1a-IRES-nlsCFP)*(52)) caused an increase in microglia numbers quantified (Fig S2D). This data suggests that increased *Csf1a* is capable of influencing microglia numbers, but *Csf1* is not essential for early microglia development. In all, the loss of *Il34*, but not *Csf1*, causes a reduction in microglia numbers in 3 dpf zebrafish.

***Il34* facilitates the distribution of macrophages, without affecting their proliferation**

In mice, tissue resident macrophages of the skin, known as Langerhans cells (LCs), are highly dependent on *Il34*/*CSF1R*-signaling for their maintenance and self-renewal (49, 50, 57). We therefore hypothesized that *Il34* in zebrafish might regulate the proliferative expansion of microglia, similar to LCs in mice, leading to the lower microglia numbers we observed. Microglia numbers increase sharply after 3 dpf, and to determine whether microglia numbers remained lower over time we quantified NR+ microglia also at 5 dpf (Fig 4A). Surprisingly, compared

to 3 dpf, microglia numbers in *il34*^{-/-} mutants were closer to those of controls at 5 dpf (~30% reduction 5 dpf vs ~60% reduction at 3dpf). To determine whether the increase in numbers was due to the continuation of seeding the brain or proliferative expansion we performed EdU pulse labelling between 3 and 4 dpf. EdU/L-plastin double labelling showed reduced microglia and reduced Edu+ microglia, but the fraction of EdU+ microglia did not differ between *il34* mutants and controls (Fig 4B Fig S4A). Thus, loss of *il34* does not change the proliferative fraction of microglia, therefore the decreased microglia numbers are unlikely explained by a defect in proliferation. Since the decrease in microglia numbers in *il34* mutants compared to controls was largest at 3 dpf, *Il34* likely affects YSMs, including microglia progenitors, preceding brain colonization. Indeed, Wu and colleagues showed that *Il34* deficiency causes impaired colonization by failing to attract YSMs to enter the brain in a *Csf1ra*-dependent mechanism (51). We used live-imaging to visualize *mpeg1*-GFP+ yolk sac macrophages (YSMs), which are the progenitors of microglia, but also of many other macrophages at this stage. At 2 dpf, YSM numbers and morphology were not different between *il34* mutants and controls (Fig 4C). Thus, reduced microglia numbers are likely not attributed to reduced YSM numbers. Therefore, impaired migration of *il34* deficient YSMs towards the brain could explain the lower microglia numbers. Imaging in the rostral/head region at 2 dpf showed an >80% decrease in the number of macrophages/microglia, suggesting that *il34* is indeed involved in the recruitment of YSMs to the brain (Fig 4D). To determine whether this effect is exclusive to microglia, we determined the fraction of total macrophages that was found in the head or in the trunk region at 3 dpf. This showed again an ~80% reduced infiltration of microglia in the brain in *il34* mutants compared to controls. Colonization of the trunk was also decreased in *il34* mutants compared to controls, but to a lesser extent (~25% reduction)(Fig 4E-F Movie S1). This was confirmed by time-lapse imaging of *il34* mutants and controls, which showed largely reduced colonization of all embryonic regions (Movie S1). In addition, we observed frequent proliferative events between 2-3 dpf, both in control but also in *il34* mutant larvae, and therefore proliferation of *il34* mutant YSMs caused an increase in the number of YSMs that had infiltrated the tissue (Movie S1). Analysis of entire larvae at 8 dpf revealed that total macrophage numbers were not reduced in *il34* mutants, suggesting normal macrophage development and expansion. However, whereas in control fish almost 60% of the total macrophages were found to have migrated away from the hematopoietic sites, into the embryonic tissues, in *il34* mutant fish only 40% of the macrophages colonized the embryo. Therefore, loss of *Il34*

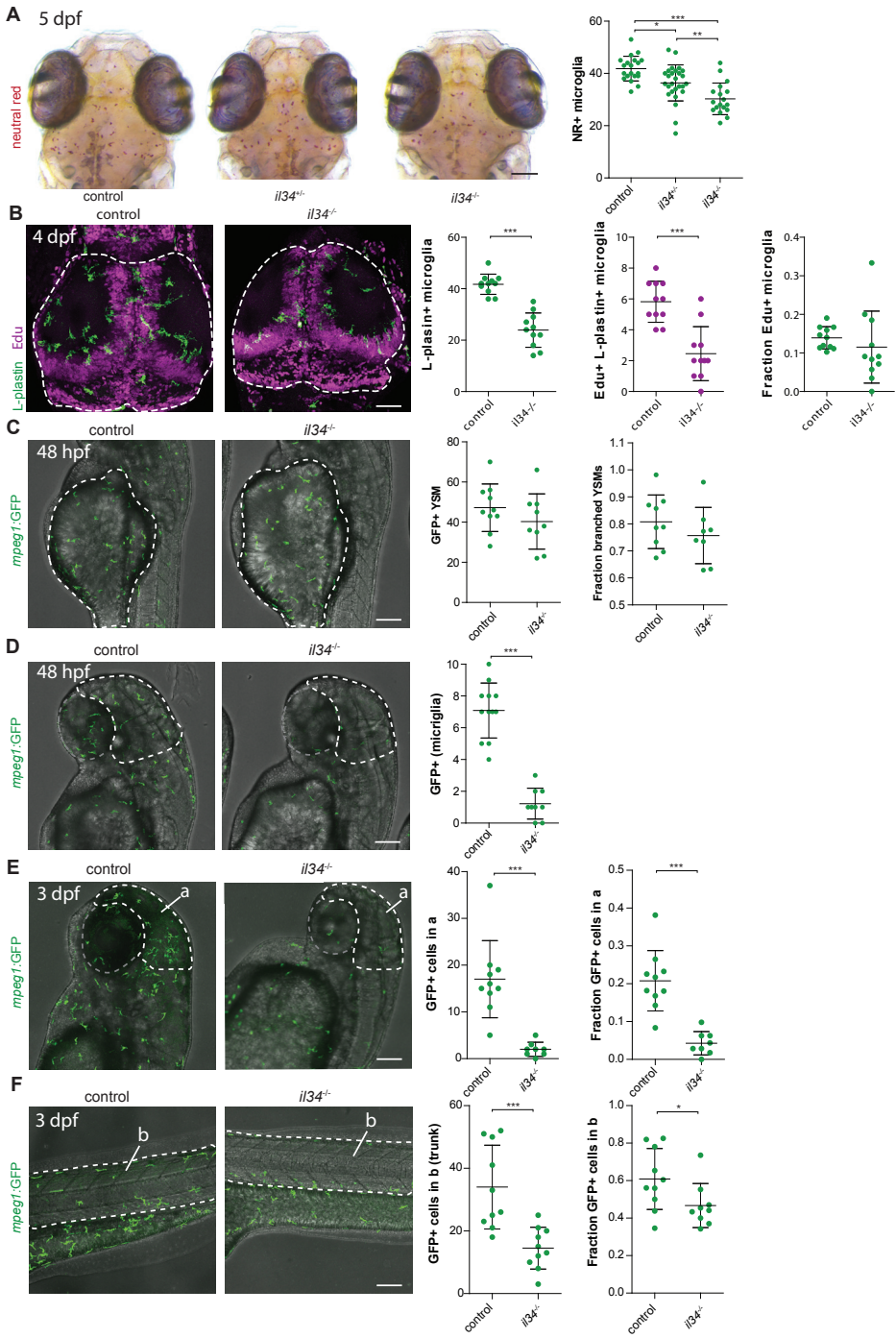


Fig 4. *Il34* does not affect proliferation but the distribution of YSMs to target organs. **A** NR+ microglia numbers in *il34* mutants and their heterozygous and wildtype siblings at 5 dpf. **B** EdU/Lplastin staining of microglia in the optic tecti (dotted line) of 4 dpf *il34* mutants and wildtype controls and quantification of microglia numbers, EdU+ microglia numbers and the fraction of EdU+ microglia among total numbers. **C** In vivo imaging of GFP+ macrophages located on the yolk sac (dotted line) in *il34* mutants and wildtype controls, transgenic for *mpeg1-GFP*, and quantification at 48 hpf. YSMs with more than 1 protrusion were counted as branched YSMs. **D** In vivo imaging of *mpeg1:GFP*+ macrophages located in the head region (dotted line) in *il34* mutants and wildtype controls and its quantification at 48 hpf. **E** In vivo imaging of GFP+ macrophages located in the head region (dotted line) in *il34* mutants and wildtype controls and its quantification at 3 dpf. **F** In vivo imaging of *mpeg1:GFP*+ macrophages located in the tail (dotted line) in *il34* mutants and wildtype controls and its quantification. Scale bar represents 100 μ m. * $p < 0.05$, ** $p < 0.01$, *** $p < 0.001$. One-way anova and t-test. Each dot represents one larvae. Error bars represent s.d.

affects the distribution of macrophages into various embryonic tissues including the brain, analogous to the effect of IL34 on the maintenance and development of LCs, as described in mice (49, 50, 57)(Fig 5).

Discussion

In this study, we developed a scalable CRISPR/Cas9-based reverse genetic screening pipeline using semi-automated image quantification to identify new regulators of microglia biology using zebrafish embryos. We showed that direct genetic targeting of known microglia regulators including *csf1ra* and *spi1b* by Cas9/gRNA injections in zebrafish embryos phenocopies previously identified microglia mutants. We next developed a software tool (SpotNGlia) that allows for automated phenotyping by quantification of neutral red positive microglia. As zebrafish are well suited for *in vivo* drug discovery, our strategy could potentially also be used to identify small molecules affecting microglia development (58). Using this pipeline, we here tested 20 candidate genes for a role in microglia development and found 6 genes significantly affecting microglia numbers when mutated. Loss of *il34* function caused the largest decrease in microglia numbers, which we confirmed by analysis of stable *il34* mutants. Furthermore, we uncovered IL34 as a regulator of distribution of tissue macrophages, needed to recruit YSMs to the brain and other embryonic tissues.

Even though we here examined 20 genes, there are several ways to increase the throughput of our screening strategy. First, mounting of the injected zebrafish larvae and subsequent image acquisition are the most time-consuming parts of our pipeline. Neutral red stained larvae were manually embedded in low melting point agarose before imaging, which restricts the number of animals that

can be screened per day. Automated imaging systems that can load zebrafish larvae from liquid medium in multi-well plates and image them in the orientation of interest in glass capillaries could overcome this hurdle (59). Together with the SpotNGlia tool this would permit a significantly increased screening throughput and efficiency. Additionally, we aimed to achieve maximal CRISPR/Cas9 mutagenic efficiency for individual genes of interest, and therefore targeted individual genes. Shah *et al.* previously reported a strategy where pools of up to 8 gRNAs are injected simultaneously to target multiple genes at once (60), which could lead to reduced targeting efficiency of the individual gRNAs. Although, a pooling strategy could significantly increase the number of genes that can be screened, we observed that, especially for genes with a relatively subtle microglia phenotype, a high mutagenic efficiency increases the chance of detecting the phenotype. Additionally, due to the clonal nature of hematopoietic progenitors, including yolk sac macrophages, a high targeting efficiency is likely required, because non-targeted cells could expand and compensate for mutated cells.

IL34 is one of two ligands of the colony stimulating factor 1 receptor (CSF1R), a main regulator of development of the macrophage lineage (55). Even though adult *Il34* deficient mice have fewer microglia, and no Langerhans cells, the precise role of IL34 in microglia development is unclear. Wang and colleagues, showed that neonatal *Il34*^{-/-} mice have lower microglia numbers, whereas Greter *et al* showed normal microglia numbers in *Il34*^{-/-} mice throughout embryonic development (49, 50). The exact function of IL34 in microglia development *in vivo*, and how this may differ from CSF1, remains therefore ambiguous. These discrepancies could be attributed to factors such as genetic background, or slightly different methods leading to different interpretations regarding the role of IL34 in embryonic and early postnatal microglia numbers (49, 50).

Our data revealed a ~60% reduction in microglia numbers in *il34* mutant larvae at 3 dpf, indicating that *il34* is required for early microglia development in zebrafish. We show that upon arrival in the brain, between 3 and 5 dpf, microglia numbers increase by proliferation in both controls and *il34* mutants, suggesting that the proliferative capacity of microglia is not affected by the loss of *il34* (Fig 5). In addition, YSM numbers were not affected by *il34* deficiency, indicating that there is a defect in the colonization of the embryonic brain, likely due to a failure to attract YSMs expressing *Csf1ra* and/or *Csf1rb*. Consistent with this, analysis of migration towards the brain at both 2 and 3 dpf showed much fewer microglia colonized the brains of *il34* deficient larvae. Our findings are consistent with a concurrent manuscript, where the authors show that nervous system expression

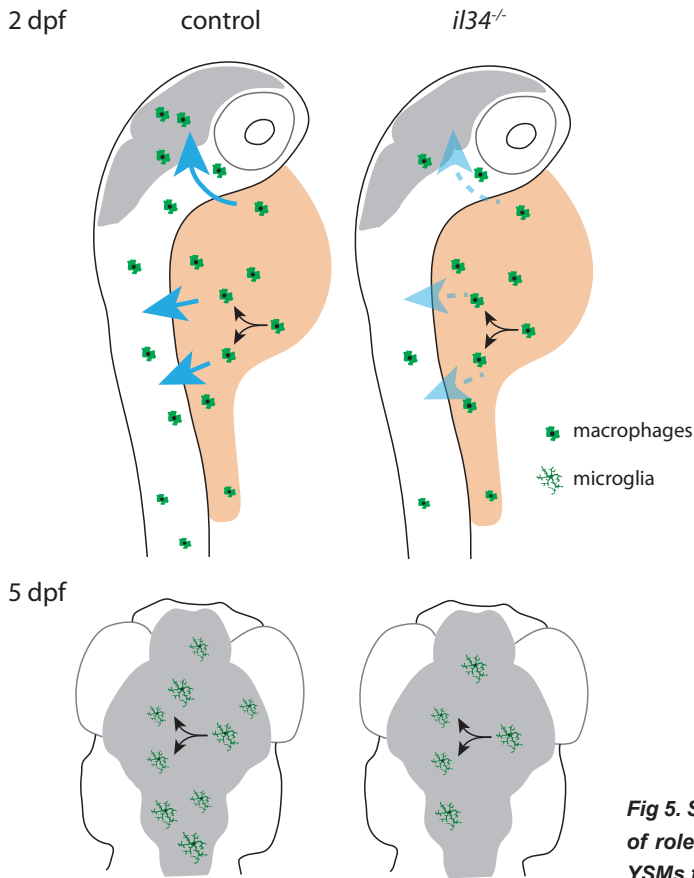


Fig 5. Schematic representation of role of *Il34* in distribution of YSMs to target organs.

of *Il34* can attract YSMs to migrate into the brain by the *Il34*/Csf1 receptor *Csf1ra* (51). However, we additionally found that distribution of *il34* mutant YSMs into trunk regions was reduced, indicating that the effect of *Il34* is not limited to microglia, but also affects the migration and colonization of other tissue resident macrophages. Consistent with this idea, recent single cell RNA seq studies show widespread expression of *il34* mRNA in early embryonic zebrafish (61). At 24 hpf, *il34* is already expressed in e.g. brain, but also in muscle, heart, pharyngeal arches, epidermis and neural crest (61). In mice *IL34* is also expressed in the brain during embryonic development (E11.5, and possibly earlier) and for example in the epidermis (50, 62). This early expression in brain and other cells supports our model that *Il34* attracts YSMs towards the brain and into other parts of the embryo, including the epidermis.

As we previously showed that mutants for both receptors, *Csf1ra* and *Csf1rb*, lack all microglia, in contrast to *Csf1ra* mutants, which have fewer

microglia only in early development, the expansion of microglia following colonization of the brain is likely regulated by other, possibly compensatory or redundant factors, including through CSF1 homologs *Csf1a* or *Csf1b* (10, 29). Although we repeatedly identified a decrease in microglia numbers in *csf1a* gRNA injected zebrafish, we did not identify a change in *csf1a* mutants, generated with the same gRNA. Our data is consistent with an already published *csf1a*^{-/-} line that also shows normal microglia numbers (51). Even when we combined *csf1a* and *csf1b* frameshift mutations, we did not find reduced microglia numbers. The pigmentation phenotype observed in *csf1a*^{-/-}*b*^{-/-} larvae, and not in the individual mutants, suggests that the mutations in *csf1a* and *csf1b* are likely loss of function and possibly compensate for each other. This suggests that genetic compensation, where alternative pathways are upregulated upon mutation of exonic regions, does not occur regarding the pigment phenotype (63, 64). Our *csf1* gRNA injections reduce microglia numbers, and overexpression of *csf1a* increases microglia numbers. Therefore, *csf1* in zebrafish seems capable of influencing microglia numbers. We cannot currently explain the discrepancy between results obtained with gRNA injections and stable mutants, and it is possible that genetic compensation for *csf1*, perhaps by other ligands, could occur in *csf1* mutants regarding microglia. This stresses the importance of using multiple independent approaches to detect false positive, but also false negative results (63-65).

Csf1 and *Il34* were both found to be expressed in the adult mouse brain, although in non-overlapping regions, however, during early embryonic development, *Il34* expression precedes *Csf1* expression in mice (49, 66). This corroborates our findings that *Il34* acts as a beacon for YSMs to migrate towards the brain, whereas loss of *Csf1* appears not to affect microglia numbers at this early developmental stage. In *il34* mutants, YSMs that arrive in the brain at 3 dpf, start to proliferate and reach 70% of control levels at 5 dpf. Time-lapse imaging showed frequent proliferative events in other tissues of *il34* mutants as well. Thus, we find that whereas *Csf1* appears able to influence microglia numbers, it seems not essential for the early embryonic microglia development. On the other hand, *il34* is a critical, non-cell autonomously regulator of seeding of the brain and other organs by YSMs, but does not appear to be required for their proliferation.

In conclusion, we here present a scalable reverse genetic screening method for the identification of novel regulators of microglia development and function. Microglia are key players in brain disease and there is strong evidence that microglia defects can be a primary cause of brain disease (7-10). Replenishing microglia, for example by hematopoietic stem cell transplantation (HCST) can

provide therapeutic benefit in human brain diseases. Better understanding of microglia development and acquisition of their specific cell fate *in vivo*, could lead to improved strategies to replace defective microglia. However, the mechanisms and genes regulating microglia development and function are still largely unknown. Therefore, better understanding of microglial gene functions could be a valuable step in the elucidation of mechanisms underlying microglial biology. As zebrafish larvae have proven their suitability for drug discovery, SpotNGlia automated analysis software in combination with automated imaging systems could also be used to screen for compounds affecting microglia (67). In all, we identified *il34* as a regulator of tissue resident macrophage distribution, primarily affecting macrophage colonization of the zebrafish embryonic brain by affecting the recruitment of YSMs to target organs including the brain. Our reverse genetic screening pipeline can be used to address genetic regulation of microglia development and function, and identify regulators essential to generate functional microglia *in vivo*.

Materials and methods

Fish care

For all experiments Tg(*mpeg1:EGFP*) fish expressing GFP under the control of the *mpeg1* promotor or Tg(*Neuro-GAL4, UAS:nsfB-mCherry, mpeg1:EGFP*) with neuronal specific nitroreductase expression, transgenic zebrafish lines were used (68). Zebrafish embryos were kept at 28°C on a 14h/10h light-dark cycle in HEPES-buffered E3 medium. At 24 hpf 0.003% 1-phenyl 2-thiourea (PTU) was added to prevent pigmentation. For overexpression of *Csf1a* we used Tg(*hsp70l:csf1a-IRES-nlsCFP*)^{wp.r.t4} fish kindly provided by David Parichy (University of Virginia) (52). Fish were heat-shocked twice at 37°C for 1 hour at 4 dpf, after heat-shock treatment fish were selected on CFP expression and divided in CFP- controls and CFP+ fish. In this manuscript we describe three new mutant fish lines *il34*^{re03/re03} containing a 5 bp deletion in exon 5 (Fig 2C), *csf1a*^{re05/re05} containing a 4 bp insertion in exon 2, and *csf1b*^{re06/re06} containing 4 bp deletion in exon 2, and a version in the *csf1a*^{re05/re05} background containing a -3bp deletion +28 insertion leading to a +25 bp insertion causing a frameshift in exon 2 (*csf1b*^{re07/re07})(Figure S4).

Ethics statement

Animal experiments were approved by the Animal Experimentation Committee at Erasmus MC, Rotterdam. Zebrafish embryos and larvae were anesthetized using tricaine and euthanized by ice-water.

sgRNA synthesis

To design sgRNAs the online program CRISPRscan (www.crisprscan.org) was used (69). The gRNAs were designed to target exons, except for exon 1, to be as close as possible to the transcription start site and to have no predicted off-target effects. The sgRNAs were generated from annealed primers, one containing a minimal T7 RNA polymerase promoter, the target sequence and a tail-primer target sequence and a generic tail-end primer (Vejnar et al., 2016). To generate primer-dimers the FastStart™ High Fidelity PCR System from Sigma was used. A solution was prepared containing 1 mM forward sgRNA oligo, 1 mM reverse oligo consisting of 20 nt overlap with sgRNA oligo and the Cas9-binding part, 0.8 mM dNTPS, 1x FastStart Buffer and 6.25 U / μ L FastStart Taq polymerase in 20 μ L total volume. Annealed DNA oligo dimers were generated by denaturation at 95°C for 5 minutes followed by annealing by reducing the temperature by 1°C per second during 20 seconds to 75°C and extension at 72°C for 10 minutes. The gRNAs were synthesized from annealed DNA oligo's, containing a minimal T7 RNA polymerase promoter, with the mMESSAGING mMACHINE™ T7 ULTRA Transcription Kit (Invitrogen) according to the manufacturer's instructions.

Cas9/gRNA complex injections into zebrafish larvae

The SP-Cas9 plasmid used for the production of Cas9 protein was a gift from Niels Geijsen (Addgene plasmid #62731) (70). Cas9 nuclease was synthesized as described (70). 600-900 ng of gRNA was mixed with 4 ng of Cas9 protein to form active gRNA-Cas9 RNPs. Next, 0.4 μ L of 0.5% Phenol red (Sigma) and the volume was adjusted with 300 mM KCl to a total volume of 6 μ L. Approximately 1 nL of the mix was injected in fertilized zebrafish oocytes. For the creation of the mutant lines CRISPRants were grown to adulthood and outcrossed to the AB background, and Sanger sequencing was used to identify mutations.

Neutral red staining and imaging

To label microglia, 3 or 5 dpf larvae were incubated in E3 medium containing neutral red (Sigma) (2.5 μ g/ml) for 2 hours at 28 °C, after which they were rinsed with E3 medium containing 0.003% PTU. Larvae were anaesthetized with 0.016% MS-222 and embedded in 1.8% low melting point agarose in E3 with the dorsal side facing upwards. Serial images (3-6) in the z-plane were acquired with a Leica M165 FC microscope using the 12x dry objective and a Leica DFC550 camera.

Larvae genotyping (Sanger sequencing)

Lysis Zebrafish larvae were euthanized and placed in single tubes containing 100 μ L lysis Buffer (0.3% 1M KCl, 1% 1M TrisHCl pH 9.0, 0.1% Triton, 0.15 mg/mL Proteinase K) per larva. The mix was incubated at 55 °C for 10 minutes and 95 °C for 10 minutes. The lysate was centrifuged for 5 to 10 minutes at 4000 rpm, and 1 μ L was used for PCR.

Sanger sequencing to determine CRISPR/Cas9 targeting efficiency For Sanger sequencing 500 bp long PCR products were obtained. For the sequencing reaction BigDye® Terminator v3.1 Cycle Sequencing Kit from Applied Biosystems was used. The product was placed on Sephadex® columns (Sigma) and centrifuged at 910 rcf for 5 minutes. The ABI 3130 genetic analyzer from Applied Biosystems was used for sanger sequencing. To assess the indel spectrum and frequencies at the target locus we used the program TIDE developed by the Netherlands Cancer Institute (NKI)(46)

SpotNGlia

The SpotNGlia software tool was developed in MATLAB (MathWorks, Natick, MA, USA). Its full source code and a technical description of how to use the tool is available from GitHub (<https://github.com/samuelgeurts/SpotNGlia>). The software is released under the GNU General Public License. A brief description of the three main steps (preprocessing, brain segmentation, and microglia detection) performed by the software is given below.

Preprocessing Images acquired from neutral red labelled larvae (n=50) were used to optimize the algorithm. For each larva, 3-6 images were taken at different depths of focus. Color channels were realigned by finding the translation that maximizes the correlation coefficient (71). To remove the background the triangle thresholding method was used (72). Next, we generated an all-in-focus image with extended depth of field (73).

Brain segmentation The orientation of the fish was determined by maximizing the correlation coefficient between the image and a mirrored version of itself, yielding the larvae's rotation angle. The translation parameters were found by directly correlating the image to a template image, which was established by averaging multiple aligned fish. Because of its near-circular shape, the optic tectum was segmented by performing a polar transformation after which the edges of the optic

tectum were found by using Dijkstra's algorithm (74, 75). The brain edge becomes an approximately straight line in polar coordinates if it is transformed with respect to the center of the optic tectum which we obtained from the template image. To make it applicable for the shortest path algorithm, the image was correlated with a small image, similar to the average appearance of the brain edge in the polar image. Also a priori information of the training set was used to exclude locations where the brain edge cannot be. After Dijkstra's algorithm was applied the found path was transformed back resulting in the brain edge coordinates.

Microglia detection To identify neutral red-positive (NR+) microglia a multiscale wavelets product was computed on the green channel of the image, which contains the highest contrast for the NR signal (47). Multiple smoothed images from a single fish image were produced with increasing spatial scale. Subtracting adjacent smoothed images resulted in subband images containing different scales of detail present in the image. A product of subband images in the range of the microglia spot size was performed to obtain an image with only high values at the location of the spots, i.e. the multiscale wavelet product. A threshold on the multiproduct image was applied to obtain a binary image to determine the spots. The identified spots were discriminated further on typical color and size obtained from the training set, resulting in accurate quantification of microglia numbers. All neutral red quantifications were performed using SpotNGlia, except for the 5 dpf larvae in Fig. 4A and S2D.

Immunofluorescence staining

Immunohistochemistry was performed as described (76, 77). Briefly, larvae were fixed in 4% PFA at 4°C overnight. Subsequently, dehydrated to 100% MeOH and stored at -20°C for at least 12 hours, and rehydrated to PBS. Followed by incubation for three hours in blocking buffer (10% goat serum, 1% Triton X-100 (Tx100), 1% BSA, 0.1% Tween-20 in PBS) at 4°C was followed by incubation in primary antibody buffer at 4°C overnight. Larvae were washed in 10% goat serum 1% Tx100 in PBS and PBS containing 1% TX100 for a few hours, followed by incubation in secondary antibody buffer at 4°C overnight. Primary antibody buffer: 1% goat serum, 0.8% Tx100, 1% BSA, 0.1% Tween-20 in PBS. Secondary antibody buffer: 0.8% goat serum, 1% BSA and PBS containing Hoechst. Primary antibody L-plastin (1:500, gift from Yi Feng, University of Edinburgh). Secondary antibody DyLight Alexa 488 (1:250).

EdU pulse-chase protocol

Larvae of 3 dpf were placed in a 12 wells plate in HEPES buffered (pH = 7.3) E3 containing 0.003% PTU and 0.5 mM EdU for 24 hours. Next, larvae were fixed in 4% PFA at 4°C overnight, dehydrated in 100% MeOH and stored at -20°C for at least 12 hours. Rehydrated to PBS in series and incubated in proteinase K (10 µg/ml in PBS) for an hour at room temperature. Followed by 15 minute post fixation in 4% PFA. Larvae were incubated in 1% DMSO in PBS containing 0.4% triton for 20 minutes. Thereafter 50µl Click-iTTM (Invitrogen) reaction cocktail was added for 3 hours at room temperature protected from light. Thereafter samples were subjected to immunolabelling using L-plastin antibody (see section on immunofluorescent labelling).

Confocal imaging

Intravital imaging was largely performed as previously described (76). Briefly, zebrafish larvae were mounted as described for neutral red staining. The imaging dish containing the embedded larva was filled with HEPES-buffered E3 containing 0.016% MS-222. Confocal imaging was performed using a Leica SP5 intravital imaging setup with a 20x/1.0 NA water-dipping lens. Imaging of GFP and L-plastin labelled with Alexa 488 was performed using the 488 nm laser, EdU labelled with Alexa 647 was performed using the 633 laser. Analysis of imaging data was performed using imageJ (Fiji) and LAS AF software (Leica). The sequence in which larvae were imaged (live-imaging) was randomized to avoid any adverse effects due to the anaesthetics or to mounting.

Statistical analysis

For image processing and quantitative analysis SpotNGlia, ImageJ and Prism (Graphpad) were used. Statistical significance was calculated using the one-way ANOVA with Bonferroni correction or Student's *t*-tests. Standard deviations (s.d.) are shown as error bars and $p < 0.05$ was considered significant. Exclusion criteria: fish showing signs of developmental delay, improper staining or incorrect mounting and/or annotation by SpotNGlia.

Acknowledgements

We thank Mike Broeders for synthesis of high quality Cas9 protein, Esther Hiemstra, Farzaneh Hosseinzadeh, Amber den Ouden, Lucas Verwegen, Ana Carreras Mascaró and Jordy Dekker for their assistance in the reverse genetics screen. We thank Yi Feng (Edinburgh) for the L-plastin antibody and David

Parichy (University of Virginia) for the *Tg(hsp70l:csf1a-IRES-nlsCFP)^{wp.r.t4}* fish. No competing interests declared. TVH is supported by an Erasmus University Rotterdam fellowship.

References

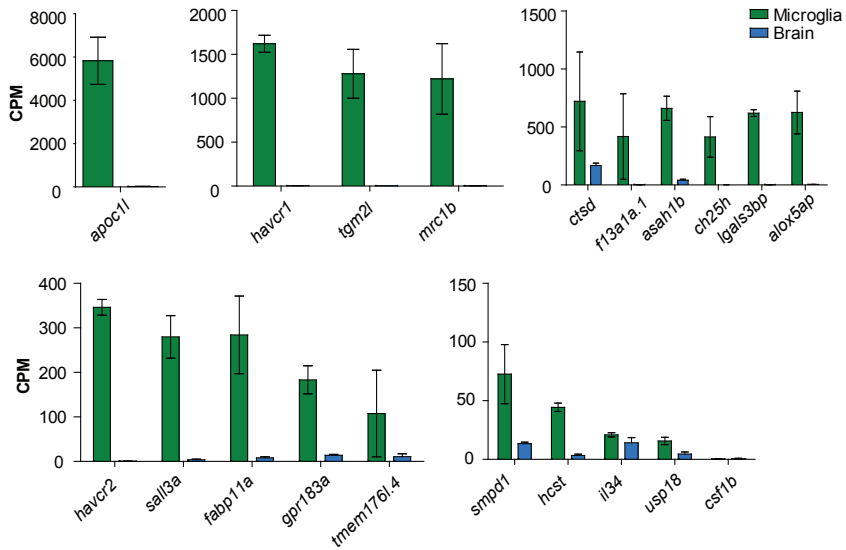
- Pollard JW. Trophic macrophages in development and disease. *Nat Rev Immunol.* 2009;9(4):259-70.
- Gordon S, Martinez-Pomares L. Physiological roles of macrophages. *Pflugers Arch.* 2017;469(3-4):365-74.
- Salter MW, Stevens B. Microglia emerge as central players in brain disease. *Nat Med.* 2017;23(9):1018-27.
- Hagemeyer N, Hanft KM, Akriditou MA, Unger N, Park ES, Stanley ER, et al. Microglia contribute to normal myelinogenesis and to oligodendrocyte progenitor maintenance during adulthood. *Acta Neuropathol.* 2017;134(3):441-58.
- Thion MS, Garel S. On place and time: microglia in embryonic and perinatal brain development. *Curr Opin Neurobiol.* 2017;47:121-30.
- Colonna M, Butovsky O. Microglia Function in the Central Nervous System During Health and Neurodegeneration. *Annu Rev Immunol.* 2017;35:441-68.
- Rademakers R, Baker M, Nicholson AM, Rutherford NJ, Finch N, Soto-Ortolaza A, et al. Mutations in the colony stimulating factor 1 receptor (CSF1R) gene cause hereditary diffuse leukoencephalopathy with spheroids. *Nat Genet.* 2011;44(2):200-5.
- Sundal C, Lash J, Aasly J, Oygarden S, Roeber S, Kretzschman H, et al. Hereditary diffuse leukoencephalopathy with axonal spheroids (HDLS): a misdiagnosed disease entity. *J Neurol Sci.* 2012;314(1-2):130-7.
- Paloneva J, Manninen T, Christman G, Hovanes K, Mandelin J, Adolfsson R, et al. Mutations in two genes encoding different subunits of a receptor signaling complex result in an identical disease phenotype. *Am J Hum Genet.* 2002;71(3):656-62.
- Oosterhof N, Kuil LE, van der Linde HC, Burm SM, Berdowski W, van Ijcken WFJ, et al. Colony-Stimulating Factor 1 Receptor (CSF1R) Regulates Microglia Density and Distribution, but Not Microglia Differentiation In Vivo. *Cell Rep.* 2018;24(5):1203-+.
- Stepien KM, Lum SH, Wraith JE, Hendriksz CJ, Church HJ, Priestman D, et al. Haematopoietic Stem Cell Transplantation Arrests the Progression of Neurodegenerative Disease in Late-Onset Tay-Sachs Disease. *JIMD Rep.* 2017.
- Eichler FS, Li J, Guo Y, Caruso PA, Bjonnes AC, Pan J, et al. CSF1R mosaicism in a family with hereditary diffuse leukoencephalopathy with spheroids. *Brain.* 2016;139(Pt 6):1666-72.
- van Rappard DF, Boelens JJ, van Egmond ME, Kuball J, van Hasselt PM, Oostrom KJ, et al. Efficacy of hematopoietic cell transplantation in metachromatic leukodystrophy: the Dutch experience. *Blood.* 2016;127(24):3098-101.
- Ginhoux F, Greter M, Leboeuf M, Nandi S, See P, Gokhan S, et al. Fate mapping analysis reveals that adult microglia derive from primitive macrophages. *Science.* 2010;330(6005):841-5.
- Herbomel P, Thisse B, Thisse C. Zebrafish early macrophages colonize cephalic mesenchyme and developing brain, retina, and epidermis through a M-CSF receptor-dependent invasive process. *Dev Biol.* 2001;238(2):274-88.
- Svahn AJ, Graeber MB, Ellett F, Lieschke GJ, Rinkwitz S, Bennett MR, et al. Development of ramified microglia from early macrophages in the zebrafish optic tectum. *Dev Neurobiol.* 2013;73(1):60-71.
- Matcovitch-Natan O, Winter DR, Giladi A, Vargas Aguilar S, Spinrad A, Sarrazin S, et al. Microglia development follows a stepwise program to regulate brain homeostasis. *Science.* 2016;353(6301):aad8670.
- Mass E, Ballesteros I, Farlik M, Halbritter F, Gunther P, Crozet L, et al. Specification of tissue-resident macrophages during organogenesis. *Science.* 2016;353(6304).
- Gosselin D, Link VM, Romanoski CE, Fonseca GJ, Eichenfield DZ, Spann NJ, et al. Environment drives selection and function of enhancers controlling tissue-specific macrophage identities. *Cell.* 2014;159(6):1327-40.
- Lavin Y, Winter D, Blecher-Gonen R, David E, Keren-Shaul H, Merad M, et al. Tissue-resident macrophage enhancer landscapes are shaped by the local microenvironment. *Cell.* 2014;159(6):1312-26.
- Thion MS, Low D, Silvin A, Chen J, Grisel P, Schulte-Schrepping J, et al. Microbiome Influences Prenatal and Adult Microglia in a Sex-Specific Manner. *Cell.* 2017.
- Gosselin D, Skola D, Coufal NG, Holtman IR, Schlachetzki JCM, Sajti E, et al. An environment-dependent transcriptional network specifies human microglia identity. *Science.* 2017;356(6344).
- Beutner C, Linnartz-Gerlach B, Schmidt SV, Beyer M, Mallmann MR, Staratschek-Jox A, et al. Unique transcriptome signature of mouse microglia. *Glia.* 2013;61(9):1429-42.

24. Lee CZW, Kozaki T, Ginhoux F. Studying tissue macrophages in vitro: are iPSC-derived cells the answer? *Nat Rev Immunol*. 2018.
25. Muffat J, Li Y, Yuan B, Mitalipova M, Omer A, Corcoran S, et al. Efficient derivation of microglia-like cells from human pluripotent stem cells. *Nat Med*. 2016;22(11):1358-67.
26. Oosterhof N, Boddeke E, van Ham TJ. Immune cell dynamics in the CNS: Learning from the zebrafish. *Glia*. 2015;63(5):719-35.
27. Oosterhof N, Holtman IR, Kuil LE, van der Linde HC, Boddeke EW, Eggen BJ, et al. Identification of a conserved and acute neurodegeneration-specific microglial transcriptome in the zebrafish. *Glia*. 2017;65(1):138-49.
28. Erblisch B, Zhu L, Etgen AM, Dobrenis K, Pollard JW. Absence of colony stimulation factor-1 receptor results in loss of microglia, disrupted brain development and olfactory deficits. *PLoS One*. 2011;6(10):e26317.
29. Dai XM, Ryan GR, Hapel AJ, Dominguez MG, Russell RG, Kapp S, et al. Targeted disruption of the mouse colony-stimulating factor 1 receptor gene results in osteopetrosis, mononuclear phagocyte deficiency, increased primitive progenitor cell frequencies, and reproductive defects. *Blood*. 2002;99(1):111-20.
30. Shiau CE, Monk KR, Joo W, Talbot WS. An anti-inflammatory NOD-like receptor is required for microglia development. *Cell Rep*. 2013;5(5):1342-52.
31. Meireles AM, Shiau CE, Guenther CA, Sidik H, Kingsley DM, Talbot WS. The phosphate exporter *xpr1b* is required for differentiation of tissue-resident macrophages. *Cell Rep*. 2014;8(6):1659-67.
32. Shen K, Sidik H, Talbot WS. The Rag-Ragulator Complex Regulates Lysosome Function and Phagocytic Flux in Microglia. *Cell Rep*. 2016;14(3):547-59.
33. Rossi F, Casano AM, Henke K, Richter K, Peri F. The *SLC7A7* Transporter Identifies Microglial Precursors prior to Entry into the Brain. *Cell Rep*. 2015;11(7):1008-17.
34. Demy DL, Tazuin M, Lancino M, Le Cabec V, Redd M, Murayama E, et al. *Trim33* is essential for macrophage and neutrophil mobilization to developmental or inflammatory cues. *J Cell Sci*. 2017;130(17):2797-807.
35. Cong L, Ran FA, Cox D, Lin S, Barretto R, Habib N, et al. Multiplex genome engineering using CRISPR/Cas systems. *Science*. 2013;339(6121):819-23.
36. Shah AN, Davey CF, Whitebitch AC, Miller AC, Moens CB. Rapid reverse genetic screening using CRISPR in zebrafish. *Nat Methods*. 2015;12(6):535-40.
37. Hwang WY, Fu Y, Reyon D, Maeder ML, Tsai SQ, Sander JD, et al. Efficient genome editing in zebrafish using a CRISPR-Cas system. *Nat Biotechnol*. 2013;31(3):227-9.
38. Burger A, Lindsay H, Felker A, Hess C, Anders C, Chiavacci E, et al. Maximizing mutagenesis with solubilized CRISPR-Cas9 ribonucleoprotein complexes. *Development*. 2016;143(11):2025-37.
39. Shiau CE, Kaufman Z, Meireles AM, Talbot WS. Differential requirement for *irf8* in formation of embryonic and adult macrophages in zebrafish. *PLoS One*. 2015;10(1):e0117513.
40. Horiuchi M, Wakayama K, Itoh A, Kawai K, Pleasure D, Ozato K, et al. Interferon regulatory factor 8/interferon consensus sequence binding protein is a critical transcription factor for the physiological phenotype of microglia. *J Neuroinflammation*. 2012;9:227.
41. Su F, Juarez MA, Cooke CL, Lapointe L, Shavit JA, Yamaoka JS, et al. Differential regulation of primitive myelopoiesis in the zebrafish by *Spi-1/Pu.1* and *C/ebp1*. *Zebrafish*. 2007;4(3):187-99.
42. Rhodes J, Hagen A, Hsu K, Deng M, Liu TX, Look AT, et al. Interplay of *pu.1* and *gata1* determines myelo-erythroid progenitor cell fate in zebrafish. *Dev Cell*. 2005;8(1):97-108.
43. Kierdorf K, Erny D, Goldmann T, Sander V, Schulz C, Perdiguero EG, et al. Microglia emerge from erythromyeloid precursors via *Pu.1*- and *Irf8*-dependent pathways. *Nat Neurosci*. 2013;16(3):273-80.
44. Xu J, Wang T, Wu Y, Jin W, Wen Z. Microglia Colonization of Developing Zebrafish Midbrain Is Promoted by Apoptotic Neuron and Lysophosphatidylcholine. *Dev Cell*. 2016;38(2):214-22.
45. Parichy DM, Ransom DG, Paw B, Zon LI, Johnson SL. An orthologue of the kit-related gene *fms* is required for development of neural crest-derived xanthophores and a subpopulation of adult melanocytes in the zebrafish, *Danio rerio*. *Development*. 2000;127(14):3031-44.
46. Brinkman EK, Chen T, Amendola M, van Steensel B. Easy quantitative assessment of genome editing by sequence trace decomposition. *Nucleic Acids Res*. 2014;42(22):e168.
47. Olivo-Marin J-C. Extraction of spots in biological images using multiscale products. *Pattern Recognition*. 2002;35(9):1989-96.

48. Wang T, Kono T, Monte MM, Kuse H, Costa MM, Korenaga H, et al. Identification of IL-34 in teleost fish: differential expression of rainbow trout IL-34, MCSF1 and MCSF2, ligands of the MCSF receptor. *Mol Immunol*. 2013;53(4):398-409.
49. Wang Y, Szretter KJ, Vermi W, Gilfillan S, Rossini C, Cella M, et al. IL-34 is a tissue-restricted ligand of CSF1R required for the development of Langerhans cells and microglia. *Nat Immunol*. 2012;13(8):753-60.
50. Greter M, Lelios I, Pelczar P, Hoeffel G, Price J, Leboeuf M, et al. Stroma-derived interleukin-34 controls the development and maintenance of langerhans cells and the maintenance of microglia. *Immunity*. 2012;37(6):1050-60.
51. Wu S, Xue R, Hassan S, Nguyen TML, Wang T, Pan H, et al. Il34-Csf1r Pathway Regulates the Migration and Colonization of Microglial Precursors. *Dev Cell*. 2018;46(5):552-63 e4.
52. Patterson LB, Parichy DM. Interactions with iridophores and the tissue environment required for patterning melanophores and xanthophores during zebrafish adult pigment stripe formation. *PLoS Genet*. 2013;9(5):e1003561.
53. Parichy DM, Turner JM. Temporal and cellular requirements for Fms signaling during zebrafish adult pigment pattern development. *Development*. 2003;130(5):817-33.
54. Patterson LB, Bain EJ, Parichy DM. Pigment cell interactions and differential xanthophore recruitment underlying zebrafish stripe reiteration and Danio pattern evolution. *Nat Commun*. 2014;5:5299.
55. Stanley ER, Chitu V. CSF-1 receptor signaling in myeloid cells. *Cold Spring Harb Perspect Biol*. 2014;6(6).
56. Tushinski RJ, Stanley ER. The regulation of mononuclear phagocyte entry into S phase by the colony stimulating factor CSF-1. *J Cell Physiol*. 1985;122(2):221-8.
57. Wang YM, Bugatti M, Ulland TK, Vermi W, Gilfillan S, Colonna M. Nonredundant roles of keratinocyte-derived IL-34 and neutrophil-derived CSF1 in Langerhans cell renewal in the steady state and during inflammation. *Eur J Immunol*. 2016;46(3):552-9.
58. Zon LI, Peterson R. The new age of chemical screening in zebrafish. *Zebrafish*. 2010;7(1):1.
59. Pardo-Martin C, Chang TY, Koo BK, Gilleland CL, Wasserman SC, Yanik MF. High-throughput in vivo vertebrate screening. *Nat Methods*. 2010;7(8):634-6.
60. Shah AN, Davey CF, Whitebitch AC, Miller AC, Moens CB. Rapid Reverse Genetic Screening Using CRISPR in Zebrafish. *Zebrafish*. 2016;13(2):152-3.
61. Wagner DE, Weinreb C, Collins ZM, Briggs JA, Megason SG, Klein AM. Single-cell mapping of gene expression landscapes and lineage in the zebrafish embryo. *Science*. 2018;360(6392):981-7.
62. Wei S, Nandi S, Chitu V, Yeung YG, Yu W, Huang M, et al. Functional overlap but differential expression of CSF-1 and IL-34 in their CSF-1 receptor-mediated regulation of myeloid cells. *J Leukoc Biol*. 2010;88(3):495-505.
63. El-Brolosy M, Rossi A, Kontarakis Z, Kuenne C, Guenther S, Fukuda N, et al. Genetic compensation is triggered by mutant mRNA degradation. *bioRxiv*. 2018:328153.
64. Rossi A, Kontarakis Z, Gerri C, Nolte H, Holper S, Kruger M, et al. Genetic compensation induced by deleterious mutations but not gene knockdowns. *Nature*. 2015;524(7564):230-3.
65. Kok FO, Shin M, Ni CW, Gupta A, Grosse AS, van Impel A, et al. Reverse genetic screening reveals poor correlation between morpholino-induced and mutant phenotypes in zebrafish. *Dev Cell*. 2015;32(1):97-108.
66. Nandi S, Gokhan S, Dai XM, Wei S, Enikolopov G, Lin H, et al. The CSF-1 receptor ligands IL-34 and CSF-1 exhibit distinct developmental brain expression patterns and regulate neural progenitor cell maintenance and maturation. *Dev Biol*. 2012;367(2):100-13.
67. MacRae CA, Peterson RT. Zebrafish as tools for drug discovery. *Nat Rev Drug Discov*. 2015;14(10):721-31.
68. Ellett F, Pase L, Hayman JW, Andrianopoulos A, Lieschke GJ. mpeg1 promoter transgenes direct macrophage-lineage expression in zebrafish. *Blood*. 2011;117(4):e49-56.
69. Moreno-Mateos, M.A., et al., CRISPRscan: designing highly efficient sgRNAs for CRISPR-Cas9 targeting in vivo. *Nat Methods*, 2015. 12(10): p. 982-8.
70. D'Astolfo DS, Pagliero RJ, Pras A, Karthaus WR, Clevers H, Prasad V, et al. Efficient intracellular delivery of native proteins. *Cell*. 2015;161(3):674-90.
71. Evangelidis GD, Psarakis EZ. Parametric Image Alignment Using Enhanced Correlation Coefficient Maximization. *IEEE Transactions on Pattern Analysis and Machine Intelligence*. 2008;30(10):1858-65.
72. Zack GW, Rogers WE, Latt SA. Automatic

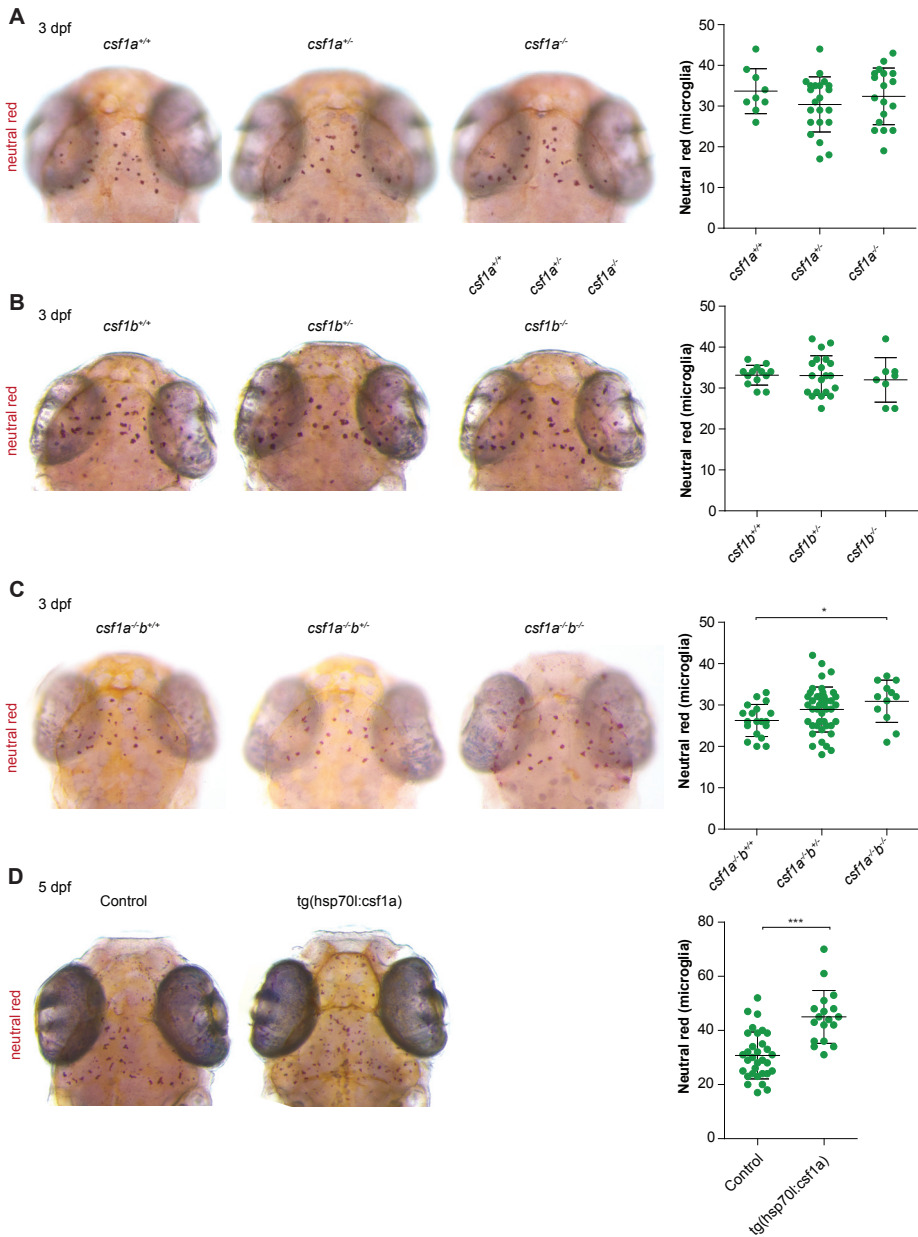
measurement of sister chromatid exchange frequency. *Journal of Histochemistry & Cytochemistry*. 1977;25(7):741-53.

73. Forster B, Van De Ville D, Berent J, Sage D, Unser M. Complex wavelets for extended depth-of-field: A new method for the fusion of multichannel microscopy images. *Microscopy Research and Technique*. 2004;65(1-2):33-42.
74. Dijkstra EW. A note on two problems in connexion with graphs. *Numer Math*. 1959;1(1):269-71.
75. Zinser G, Komitowski D. Segmentation of cell nuclei in tissue section analysis. *Journal of Histochemistry & Cytochemistry*. 1983;31(1):94-100.
76. van Ham TJ, Brady CA, Kalicharan RD, Oosterhof N, Kuipers J, Veenstra-Algra A, et al. Intravital correlated microscopy reveals differential macrophage and microglial dynamics during resolution of neuroinflammation. *Dis Model Mech*. 2014;7(7):857-69.
77. van Ham TJ, Kokel D, Peterson RT. Apoptotic cells are cleared by directional migration and elmo1- dependent macrophage engulfment. *Curr Biol*. 2012;22(9):830-6.

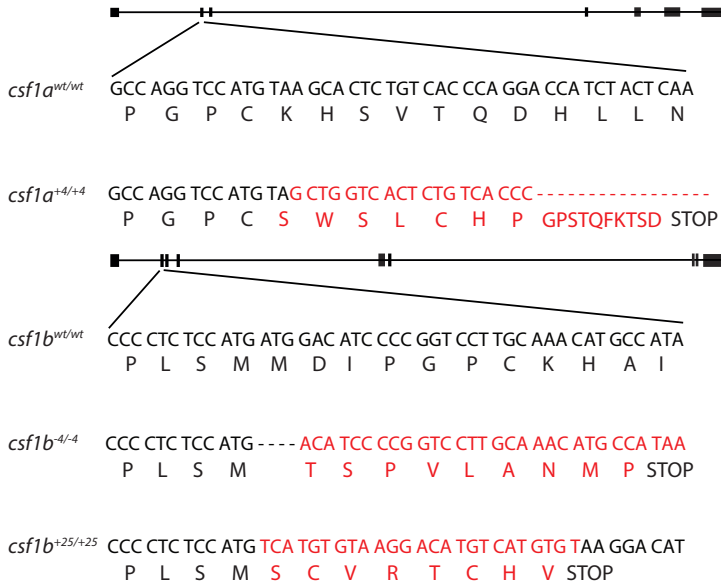


S Fig 1. Expression of putative regulators of microglia development in the zebrafish brain.

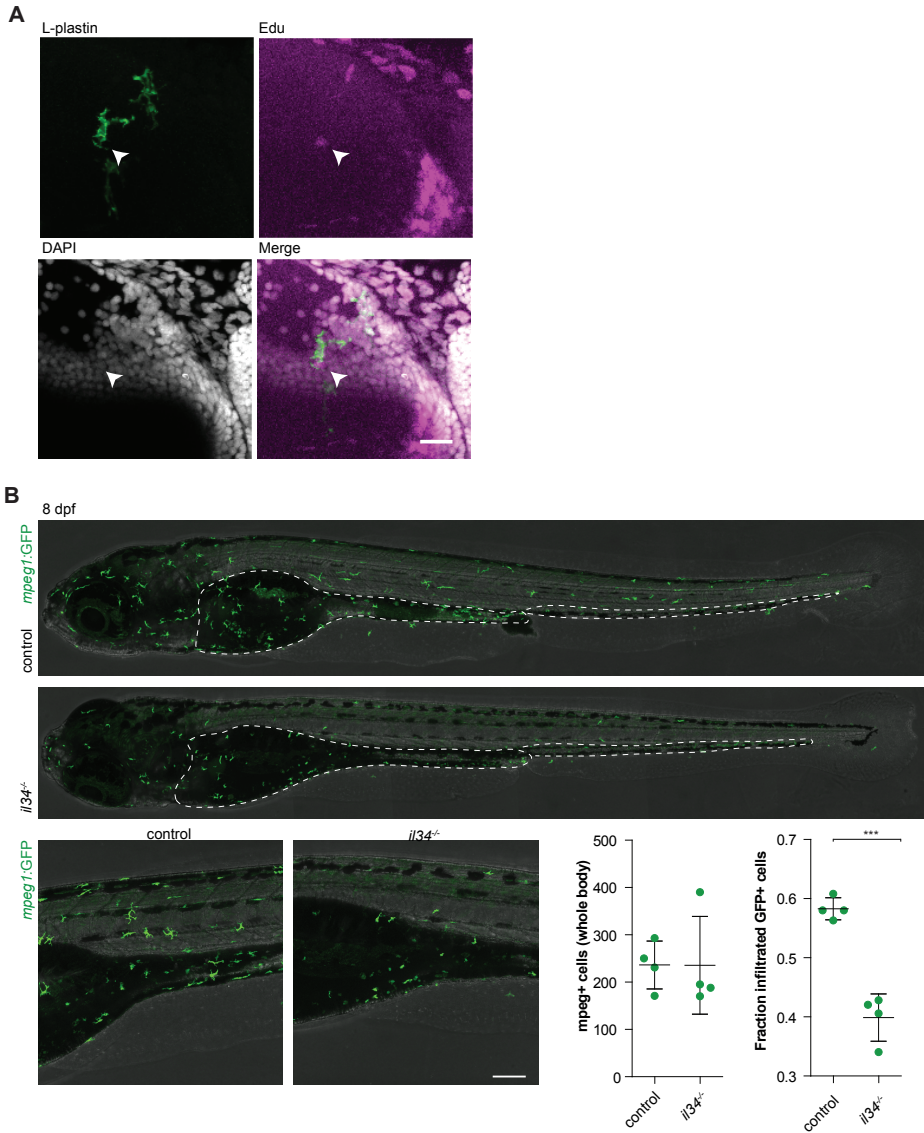
Bar graphs represent expression values of putative microglia regulators in microglia (green) and other brain cells (blue) observed in the microglia transcriptome (27). Error bars represent s.d.



S Fig 2. Mutations in *csf1* alleles do not affect microglia numbers at 3 dpf **A** *Csf1a* heterozygous cross shows similar numbers of microglia in *csf1a*^{wt/wt}, *csf1a*^{wt/+4}, and *csf1a*^{+4/+4} larvae at 3 dpf. **B** *Csf1b* heterozygous cross shows similar numbers of microglia in *csf1b*^{wt/wt}, *csf1b*^{wt/-4}, and *csf1b*^{-4/-4} larvae at 3 dpf. **C** Loss of *csf1b* in the *csf1a*^{+4/+4} background does not change the numbers of microglia at 3 dpf. *csf1a*^{+4/+4} and *csf1a*^{+4/+4}*csf1b*^{25/+25} show similar numbers of microglia. **D** Overexpression of *Csf1a* increases microglia numbers at 5 dpf. * $p < 0.05$, *** $p < 0.001$. One-way anova and t-test. Each dot represents one larvae. Error bars represent S.D.



S Fig 3. Schematic representation of out of frame mutations in *csf1a* and *csf1b*



S Fig 4. Loss of *Il34* reduces overall tissue colonization by macrophage progenitors

A Representative images of an individual *Lplastin*⁺/*Edu*⁺ microglia related to Fig. 4B. Arrowheads depict the *Lplastin*⁺/*Edu*⁺ microglia. Scale bar represents 20 μm **B** Representative images of 8 dpf wild-type control and *il34* mutant fish with in addition a magnified image of the trunk region. Quantification of total macrophage numbers, and the fraction that infiltrated the embryo (number of macrophages counted outside the area depicted by the dashed line divided by total macrophage count). Scale bar represents 100 μm , *** $p < 0.001$, t-test. Each dot represents one larvae. Error bars represent s.d.

Gene	gRNA sequence	Efficiency	R ²
<i>alox5ap</i>	GGATACGTACCCTACATTTTC	32%	0.98
<i>apoc1l</i>	GGCCCAGGAGGAGCCCACAC	84%	0.90
<i>asah1</i>	AGCTGGAGGATTGCAGAAAGT	52%	0.92
<i>cstD</i>	CGCGTCGGACGTGCAGAAAA	74%	0.90
<i>csf1a</i>	TGGGTGACAGAGTGCTTACA	91%	0.91
<i>ch25h</i>	GGTAGACTGTAATTGAGAAG	64%	0.89
<i>csf1b</i>	AGGACCGGGGATGTCCATCA	79%	0.79
<i>f13a1a</i>	GGTCAAACAAGATGTCGATG	30%	0.96
<i>fabp11a</i>	GGAGTCCACAATAGAGAGAG	-	-
<i>havcr1</i>	GGGAGCATATGATGGACTGA	85%	0.92
<i>hcst</i>	GGCTAGCGTACCAGTAGGTGG	49%	0.93
<i>il34</i>	CCATGGTCCAGTCCGAATGC	77%	0.8
<i>mrc1b</i>	GCGCACCACAGACGCTGGTC	83%	0.85
<i>tgm2l</i>	GGGTCTCTACAGCATGACTG	92%	0.92
<i>gpr183</i>	GACTCTGTACTCAGCCAACC	86%	0.94
<i>lgals3bp</i>	GGTCTACCATGATGGACAGT	84%	0.88
<i>sall3a</i>	GGAGTGGATGATTCAGACAG	79%	0.91
<i>smpd1</i>	CGACGGGGATGTAGAGACGG	83%	0.91
<i>tmem176.4</i>	GGGTCATCAATATTGCATTG	31%	0.94
<i>usp18</i>	TATGTCCAGCAGTTCAGTTG	11%	0.97

S Table 1. gRNAs and their mutagenic efficiencies.

S Movie 1. Timelapse imaging of a wildtype control (left) and *il34* mutant larva (right) between 2 and 3 dpf

Chapter 3

Csf1r is dispensable for primitive and definitive myelopoiesis *in vivo*, but controls macrophage self-renewal and tissue macrophage properties

Laura E. Kuil¹, Nynke Oosterhof¹, Herma C. van der Linde¹, Paulina M.H. van Strien², Eric M. J. Bindels², Tjakko J. van Ham¹

¹Department of Clinical Genetics, Erasmus MC, University Medical Center Rotterdam, Wytemaweg 80, 3015 CN Rotterdam, The Netherlands.

²Department of Hematology, Erasmus University Medical Center, Rotterdam, Wytemaweg 80, 3015 CN, The Netherlands.

Submitted

Abstract

Tissue resident macrophages (TRMs), are important for organogenesis and homeostasis, and reside in virtually all vertebrate tissues. Despite being terminally differentiated, they retain self-renewal capability. It is unknown precisely how these TRMs retain this ability and how they acquire their specific properties to meet their target organs' demands. Colony stimulating factor 1 receptor (CSF1R) is a key regulator of macrophages, but different populations TRMs are affected by loss of function at varying degree. To elucidate the role of CSF1R in macrophage development *in vivo*, we used zebrafish deficient in *csf1r*. Live imaging revealed that embryonic macrophages were present on the yolk sac (YSMs) in *csf1r* deficient fish. RNA sequencing analyses indicated that *csf1r* deficient YSMs and early macrophages had normal differentiation, but became cell cycle arrested from 2 days post fertilization (dpf), which we confirmed *in vivo*. Therefore, *csf1r* deficient fish that were older than 2 dpf contained fewer macrophages than controls did. We show that YSM development precedes subsequent waves of macrophage appearing between 12-22 dpf both in controls and in *csf1r* deficient fish. In addition, *csf1r* deficient fish lack the macrophages that contain a branched morphology in the skin, Langerhans cells (LCs), suggesting *csf1r* is essential for LC differentiation. To address this we analyzed fish mutant for *il34*, one of the two ligands for Csf1r, which according to mouse knockouts should also lack LCs, where we indeed found a similar phenotype. In all, Csf1r appears largely dispensable for core macrophage development, but is a critical regulator driving TRM expansion and tissue specific differentiation during embryogenesis and in juvenile stages. We speculate that macrophages need Csf1r signaling to become resident to several, but possibly all tissues and maintain their population by self-renewal.

Introduction

Tissue resident macrophages (TRMs) exert important functions in immune defense, but also actively contribute to organogenesis and tissue homeostasis of most, if not all, organs (1, 2). Each population of TRMs has to fulfil unique tissue specific functions encoded in specific transcriptomes (3-6). Microglia derive from embryonic macrophages emerging on the yolk sac at E7.25 (YSMs)(7-10). Most other TRMs are replaced by erythroid myeloid precursors (EMPs), which also emerge on the yolk sac (11, 12). During their colonization of the vertebrate embryo, embryonic macrophages gradually differentiate into TRMs, during which they acquire distinct, tissue specific gene expression profiles (6, 13). After birth, most TRM populations are (partly) replenished by hematopoietic stem and progenitor cell (HSPC) derived macrophages from the bone marrow (BMDMs) (14-16). The ontogeny of TRMs is determined by the availability and accessibility of the niche (reviewed in:(17)). Therefore, TRMs in tissues protected by barriers, e.g. microglia in the brain, are thought to remain of embryonic origin (8, 14, 18). The microenvironment seems to play a major role in determination of TRM morphology and function, regardless of ontogeny (5, 19, 20). Perturbations in TRM production or activity can have a broad range of detrimental consequences ranging from abnormal organ development to neurodegeneration and cancer (2, 21-23). However, the mechanisms involved in TRM colonization, and specification remain to be determined.

Colony stimulating factor 1 receptor (CSF1R) is a well-known conserved regulator of macrophage development and is controlled by two ligands; colony stimulating factor 1 (CSF1), and interleukin 34 (IL34). *In vitro*, CSF1R signaling, via either of its ligands, is essential to differentiate and maintain macrophages in culture (24). *In vivo*, the absence of *Csf1r* results in a complete lack of microglia, Langerhans cells, and osteoclasts whereas other subsets of TRMs are interestingly enough affected to a varying degree in mice (8, 25-29). Further analysis of this remarkable phenotype, should allow identification of specific and universal features of organism wide development of macrophages. Previously, Ginhoux and colleagues showed that, from E12.5 onwards, *Csf1r*^{-/-} mice show a large decrease in YSMs/EMPs on the yolk sac (8). However, already at ~E7.5, the first YSMs are generated, after which, at E10.5, they colonize the fetal liver (7, 8, 30). The presence of macrophages in *Csf1r*^{-/-} mice has not been addressed at these early developmental stages. It is therefore unknown, whether *Csf1r* is required for the development of early tissue macrophage precursors and it remains elusive why only specific TRMs are lacking in the absence of *Csf1r*.

Zebrafish are highly suitable to study immune cell development *in vivo* as they develop ex utero, are genetically tractable, and are transparent during early development (10, 31, 32). Macrophages emerge in embryonic zebrafish from yolk sac macrophages (YSMs)(22 hpf), and EMPs from the posterior blood island (PBI)(30-48 hpf)(10, 11, 33-35). Adult hematopoiesis takes place in the kidney marrow, the equivalent to mammalian bone marrow. Even though cmyb+ HSPCs appear in the pronephric tubules as early as 5 days post fertilization (dpf), production of macrophages from HSPCs has not been observed at before 14 dpf (36-38). The majority of genes found in mammals, including *CSF1R*, are present in the zebrafish (33). Here, we used *csf1ra*- and *csf1rb*-deficient zebrafish (*csf1r^{DM}*) to elucidate the role of Csf1r-signaling in TRM development. Adult *csf1r^{DM}* zebrafish have no microglia, but are viable, and other macrophages such as those in the skin and the intestine are still present (26). In addition, *csf1r^{DM}* zebrafish, similar to mice and humans, are osteopetrotic and likely lack osteoclasts (25, 26, 39).

In the present study we found that, in *csf1r^{DM}* zebrafish, early YSMs are morphologically indistinguishable from control YSMs. When control YSMs adopted a branched morphology and started to colonize the embryo, *csf1r^{DM}* YSMs stopped expanding and mostly remained located on the yolk sac. At the transcriptional level *csf1r^{DM}* yolk sac macrophages showed normal macrophage gene expression indicating their normal differentiation. In contrast, they showed reduced expression of genes involved in DNA replication involved in the cell cycle. Tracing larvae up to juvenile stages *in vivo* revealed the emergence of macrophages arising from definitive myelopoiesis ~15 dpf, both in control but strikingly also in *csf1r^{DM}* suggesting that again macrophages are formed independently of Csf1r signaling. Although macrophages are present in *csf1r^{DM}* fish, TRMs including at least microglia and LCs are absent, and remaining macrophages show altered morphology and migratory properties. Therefore, we also analyzed definitive macrophages by RNA-seq, revealing that TRM-specific gene-expression classes, including engulfment, are downregulated, whereas cell-cell adhesion genes are strongly upregulated, possibly explaining their abnormal tissue morphology and migration. Csf1r therefore appears to be primarily important to acquire tissue-resident macrophage properties, including self-renewal capacity, causing a failure to expand embryonic macrophages, but dispensable for primitive and definitive myelopoiesis.

Results

Zebrafish embryonic macrophages are formed independently of *csf1r*

To determine whether, in the absence of Csf1r signaling, YSMs or erythroid myeloid progenitors (EMPs), are still formed we analyzed previously generated *csf1ra* and *csf1rb* deficient mutants (referred to as *csf1r^{DM}*)(26). These zebrafish have almost no microglia and are osteopetrotic similar to mice, rats and humans deficient in CSF1R (25-27, 40). Zebrafish YSMs are present from 22 hour post fertilization (hpf) and EMPs are located at the posterior blood island (PBI) between 30 and 48 hpf (10, 41). *In vivo* imaging of GFP-expressing macrophages in Tg(*mpeg:GFP*) control embryos showed that, at 24 hpf, ~15 GFP positive (GFP+) YSMs were present in the yolk sac, and their numbers increased to ~45 at 42 hpf (Fig. 1A)(42). In *csf1r^{DM}* embryos, even though at 24 hpf YSM numbers were slightly lower, YSM numbers at 29 and 42 hpf did not significantly differ from those in controls (Fig. 1A). In the PBI or caudal hematopoietic tissue (CHT) GFP+ macrophages were present and their numbers did not differ between control and *csf1r^{DM}* zebrafish at 32 hpf (Fig. S1A). This indicates that Csf1r is largely dispensable for the development of the earliest embryonic macrophages.

As *csf1r^{DM}* larvae lack microglia at 5 dpf, we determined when macrophage development gets impaired in *csf1r^{DM}* animals. Whereas control YSMs from ~29hpf onwards, start to acquire a typical branched macrophage morphology with several protrusions, *csf1r^{DM}* YSMs appeared more rounded. Quantification of GFP+ YSMs with more than 1 protrusion showed significantly fewer YSMs with multiple protrusions in *csf1r^{DM}* compared to controls (Fig. 1C-D). Moreover, at 52 hpf nearly all control macrophages showed multiple protrusions, whereas *csf1r^{DM}* macrophages remained rounded and lacked protrusions. At this stage, macrophage numbers on the yolk and in the PBI/CHT, were significantly lower in *csf1r^{DM}* larvae compared to the number in controls (Fig. 1E-F, Fig. S1B). The morphological transition in YSMs correlated with the induction of migratory behavior, and colonization of the embryo and the brain, as half of the YSMs had migrated outside of the yolk sac epithelium in controls at 52 hpf (Fig. 1E-F)(33). In contrast, in *csf1r^{DM}* only 15% of the macrophages were found outside of the yolk sac. Migration trajectories of YSMs into the embryonic tissues, as shown by projections of images acquired over ~16 hours, were more widespread in controls, than those in *csf1r^{DM}*, and covered the entire embryo (Fig. 1G). Possibly, *csf1r^{DM}* macrophages have a general impairment of cell migration. However, time-lapse imaging showed directed migration of *csf1r^{DM}* macrophages, and, strikingly, even a few *csf1r^{DM}* macrophages ended up in the brain (data not shown). Thus,

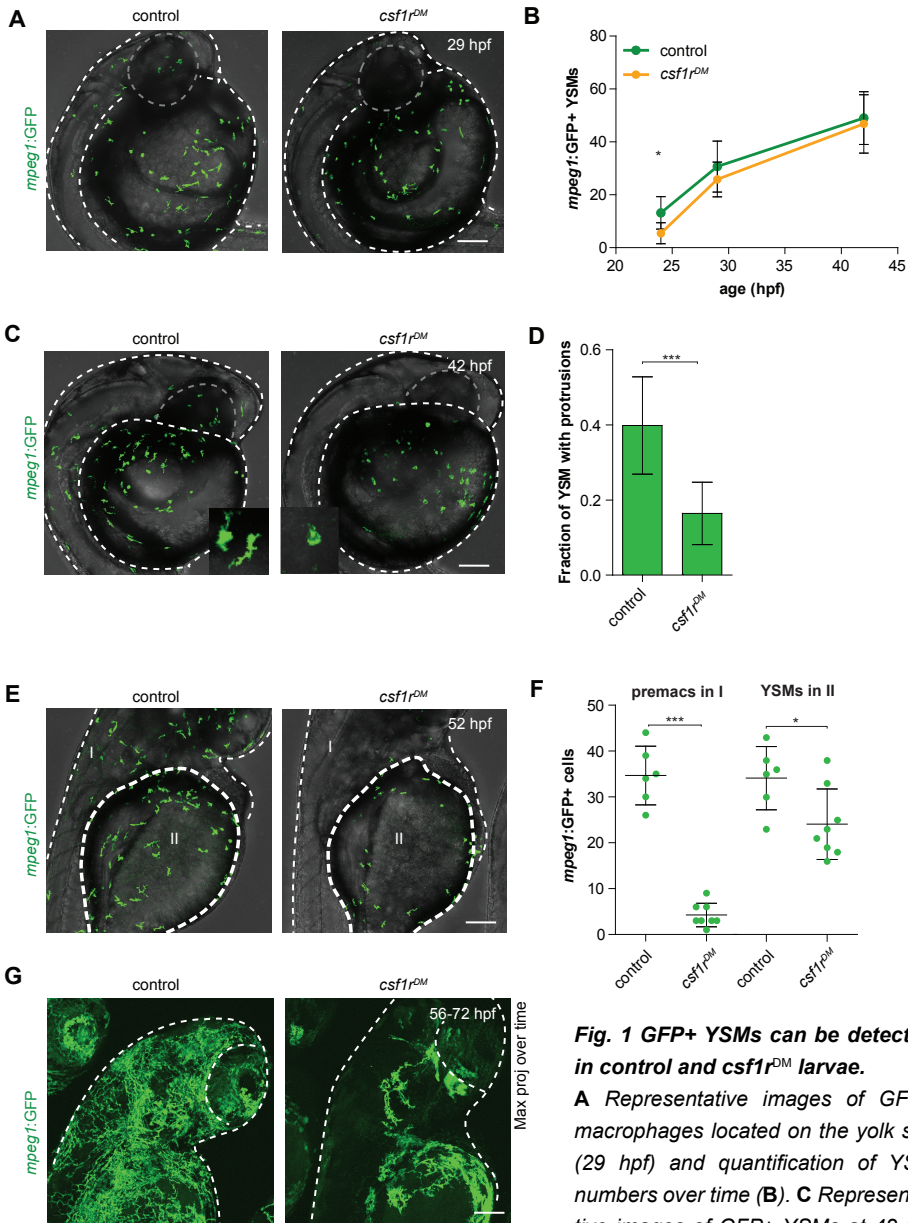


Fig. 1 GFP+ YSMs can be detected in control and *csf1r^{DM}* larvae.

A Representative images of GFP+ macrophages located on the yolk sac (29 hpf) and quantification of YSM numbers over time (**B**). **C** Representative images of GFP+ YSMs at 42 hpf used to quantify YSMs containing more than 1 protrusion (**D**). **E** Representative images of GFP+ positive YSMs at 52 hpf. The dotted line indicates the border between the embryonic tissue (I) and the yolk sac (II). **F** Quantification of GFP+ macrophages that colonized the tissue (I) and YSMs located on the yolk sac (II). **G** Representative maximum projection of long term time lapse imaging of control and *csf1r^{DM}* larvae showing migratory trajectories of GFP+ macrophages. Scale bars: 100 μ m. Error bars: SD. ANOVA or student's T-tests * < 0,05 ** < 0,01 *** < 0,001. GFP+ cells were quantified on one side of the embryo (right side). Each dot represents one fish.

although the generation of embryonic macrophages appears independent of *csf1r*, suddenly, after two days, macrophage numbers are reduced and their morphology and migration is abnormal suggesting their development is halted.

RNA sequencing of embryonic and early macrophages reveals *csf1r*-independent macrophage differentiation

To explore developmental and molecular processes affected by the loss of *csf1r*, we performed RNA-sequencing on macrophages FAC-sorted from 28 and 50 hpf *mpeg:GFP* animals. We chose these time points because at 28 hpf, *csf1r^{DM}* embryonic macrophages were morphologically, and in numbers, indistinguishable from controls, whereas at 50 hpf, *csf1r^{DM}* macrophage development diverged from that in controls (Fig. 2A). At 28 hpf, the isolated GFP+ macrophage population mainly consisted of YSMs and EMPs, whereas those isolated at 50 hpf contained migratory early macrophages colonizing the embryo, but also YSMs and EMPs.

Principal component analysis (PCA) of the macrophage gene expression data sets showed clustering of triplicate samples based on developmental stage (component 1) and genotype (component 2)(Fig. 2B). This suggests that, even though gene expression differed between control and *csf1r^{DM}* macrophages at both time points, the overall gene expression changes that occurred over time were comparable in *csf1r^{DM}* and control embryos (Fig. 2B,C). As CSF1R is needed for macrophage differentiation *in vitro*, the absence of CSF1R signaling *in vivo*, could result in impaired macrophage differentiation (43, 44). However, either at 28 or at 50 hpf, we did not observe major differences in expression of genes highly expressed in macrophages, including genes often used in zebrafish to label macrophages (e.g. *coro1a*, *lcp1*, *mfap4*), chemokine and pathogen recognition receptors (e.g. *marco*, *mrc1*, *tlr1*), and myeloid transcription factors (e.g. *irf8*, *spi1a*, *cebpb*, *zeb2a*)(logFC < 1)(Fig. 2D-E). To assess macrophage differentiation in *csf1r^{DM}* macrophages more systematically, we compared the gene expression profiles with a zebrafish macrophage single cell RNA-seq expression profile (45). We observed that, at both 28 and 50 hpf, more than 95% of 2031 macrophage-specific genes were not differentially expressed between control and *csf1r^{DM}* macrophages (Fig. 2F), suggesting *Csf1r* independent expression of the majority of these early macrophage-expressed genes. Together, *csf1r* deficient embryonic macrophages show a core macrophage gene expression profile similar to controls, further suggesting that *Csf1r* is dispensable for macrophage differentiation.

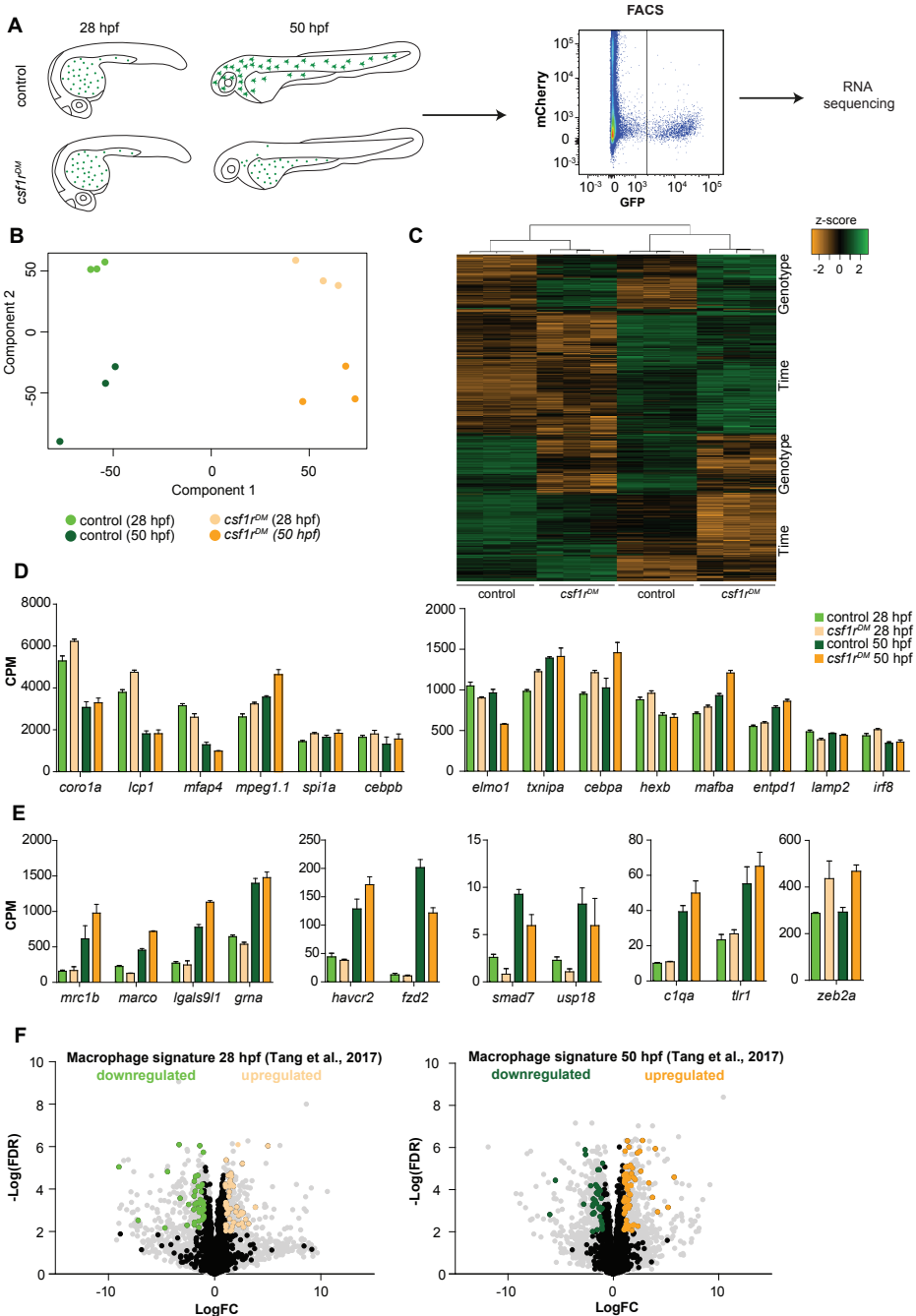


Fig. 2 RNA sequencing of YSMs at different developmental stages reveals normal macrophage gene expression in *csf1^{DM}* *mpeg+* cells **A** Schematic representation of the experimental set-up. GFP⁺ cells were isolated from both control and *csf1^{DM}* larvae at 28 hpf and 50 hpf using FACS. These cells were used for RNA sequencing. **B** PCA analysis shows clustering of triplicates and segregation

on genotype (component 1) and developmental stage (component 2). **C** Heat map showing all significantly differentially expressed genes ($\log_{2}FC > |1|$; $FDR < 0.01$). **D** CPM values of 'macrophage signature' genes show high expression in all groups. **E** CPM values of 'macrophage signature' genes induced over time in control and *csf1r^{DM}* macrophages. **F** Volcano plot showing genes expression changes between control and *csf1r^{DM}* at 28 hpf and 50 hpf respectively. Light grey: all reads, Black: Macrophage genes(45); Green: Macrophage genes significantly upregulated in control macrophages; Orange: Macrophage genes significantly upregulated in *csf1r^{DM}* macrophages ($\log_{2}FC > |1|$; $FDR < 0.01$). Only 4 and 5% of the macrophage genes were significantly differentially expressed between control and *csf1r^{DM}* macrophages at 28 and 50 hpf respectively.

Transcriptome analysis reveals that DNA replication in *csf1r^{DM}* macrophages is halted

Even though the expression of typical macrophage genes is not affected by loss of *Csf1r* signaling, there were extensive differences in gene expression profiles between control and *csf1r^{DM}* macrophages. At 28 hpf, 705 genes were differentially expressed between genotypes and at 50 hpf 890 genes were differentially expressed between genotypes ($\log_{2}FC > |1|$; $FDR < 0,01$). Gene set enrichment analysis (GSEA) revealed that, at both timepoints, *csf1r^{DM}* macrophages had lower expression of genes associated with RNA metabolism and DNA replication (Fig. 3A), and transcripts encoding all components of the replication complex were ~2-fold down regulated in *csf1r^{DM}* macrophages (Fig. S2A, 3C). Consistent with findings from GSEA, Gene ontology (GO) analysis showed that the *csf1r^{DM}* genes, which were downregulated at both time points, were associated with DNA replication ($\log_{2}FC < -1$; $FDR < 0,01$)(Fig. 3B). At 50 hpf, *csf1r^{DM}* macrophages showed also lower expression of genes in various other GO classes related to cell cycle (Fig. 3A, Fig. S2A). Thus, it appears that after 28 hpf DNA replication shuts down, followed by a decrease in general cell cycle related processes at 50 hpf. Together these analyses suggest that DNA replication is defective in *csf1r^{DM}* macrophages, possibly causing proliferative expansion of embryonic macrophages to cease.

Csf1r is required for proliferation of embryonic, early and tissue resident macrophages

To test whether macrophages deficient in *Csf1r* signaling stop dividing *in vivo*, we performed live imaging on YSMs and quantified cell divisions. Between ~32 and 48 hpf, the proliferative rates were not significantly different in control and in *csf1r^{DM}* embryos (Fig. 3D; Movie S1). However, whereas between ~56 and 72 hpf control macrophages (YSMs and early macrophages) still proliferated, *csf1r^{DM}* macrophages had completely stopped dividing (Fig. 3E). This suggests

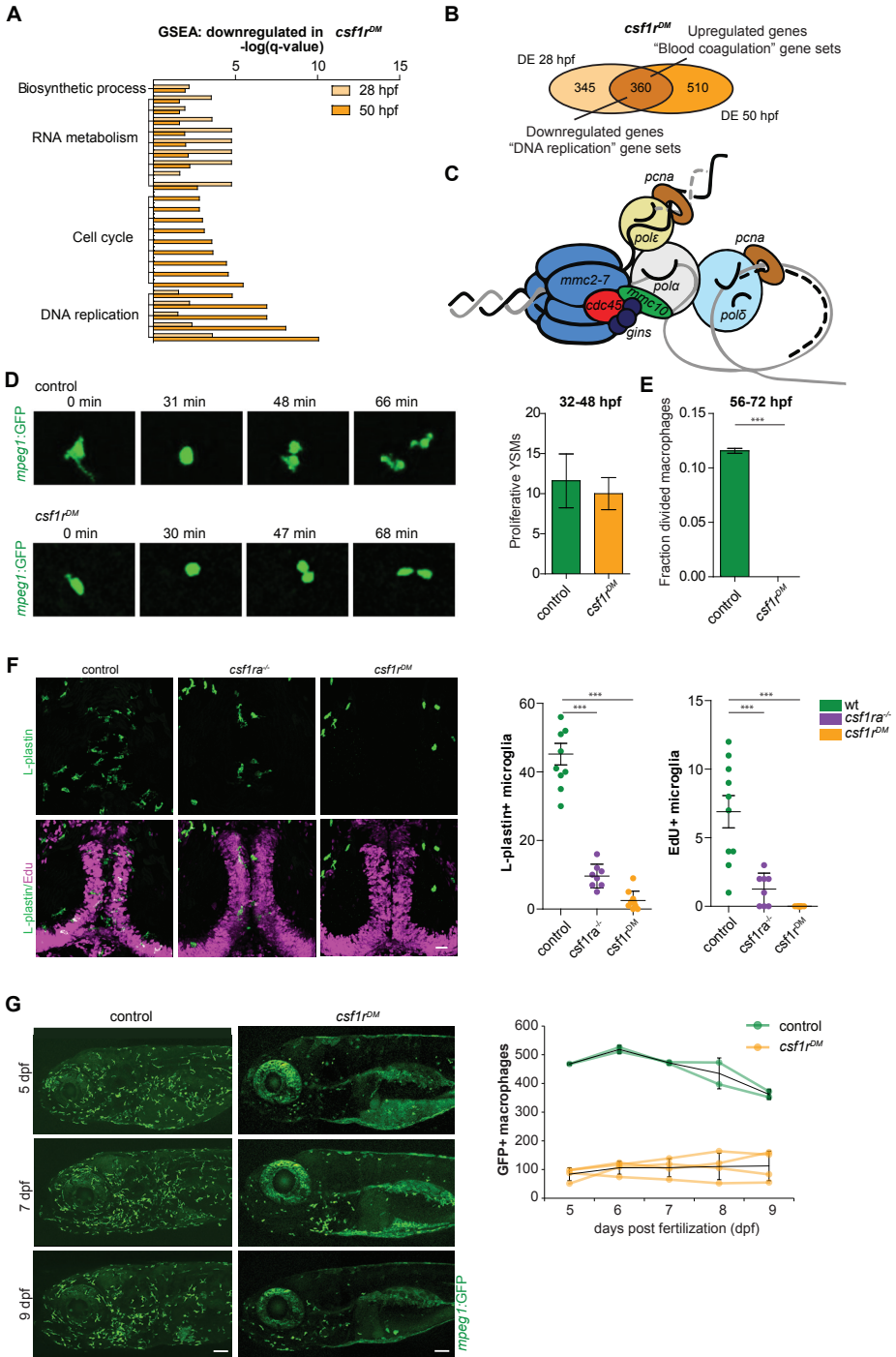


Fig. 3. *Csf1r* deficient macrophages show a proliferation defect after 2 days. **A** Bar graph showing the GO terms associated with enriched genes downregulated in *csf1r^{DM}* macrophages. **B** Venn diagram showing the amount of DE genes between control and *csf1r^{DM}* at 28 and 50 hpf and overlap between gene sets. **C** Cartoon representing the vertebrate DNA replication complex. **D** Snap shots from dividing GFP+ YSMs in control and *csf1r^{DM}* larvae (~36 hpf) and quantification of proliferative YSMs during 16 hour time lapse imaging (~32 hpf – 48 hpf). **E** Quantification of fraction proliferative YSMs during 16 hour time lapse imaging (~56 hpf – 72 hpf) in control and *csf1r^{DM}* larvae. **F** Representative images and quantification of L-plastin/Edu double positive microglia at 5 dpf. Scale bar represents 25 μ M. **G** Representative images of GFP+ macrophages in the anterior part of 5, 7 and 9 day old zebrafish and quantification of total number of macrophages at the imaged half of the total embryo and quantification. GFP+ cells were quantified on one side of the embryo (right side). Error bars: SD. ANOVA * < 0,05 ** < 0,01 *** < 0,001. Each dot represents one fish.

that YSMs and early macrophages undergo cell cycle arrest between 48 and 56 hpf. Thus, initially proliferation of emerging YSMs occurs independent of *csf1r*, whereas after 2 days, YSMs and early macrophages require Csf1r signaling to proliferate and likely to retain their self-renewal capacity.

Microglia are the first TRM population present during embryonic development, and microglia proliferate extensively upon their arrival in the brain (8, 33, 46, 47). Pcnal/L-plastin double immunostaining of early microglia in control embryos showed that both total microglia numbers increase between 2 and 4 dpf. At 2 dpf almost no microglia proliferated, whereas at 3 and 4 days, respectively ~7 and 20% of the microglia proliferated (Fig. S2A). Therefore, after early microglia arrive in the brain their proliferation becomes prominent from 3 dpf onwards in control zebrafish.

Next, we determined whether Csf1r signaling is involved in microglia proliferation. In *csf1r^{DM}* larvae occasionally a few microglia appeared in the brain, however none were Pcnal+ in almost all *csf1r^{DM}* larvae (Fig. S2A). This suggests that *csf1r* deficient microglia do not proliferate. We next used EdU pulse labeling, which marks all proliferative events within the pulsed time window. We found that, whereas all controls showed ~7 EdU+ microglia, EdU+ microglia were completely absent in all *csf1r^{DM}* larvae at 5 dpf, (Fig. 3F). Thus, proliferation is impaired both in *csf1r^{DM}* early YSMs and in early microglia.

Microglia, as well as osteoclasts, and the Langerhans cells of the skin, are largely absent in Csf1r deficient vertebrates (25-28). Nevertheless, although their numbers are generally reduced, many macrophages are still present. In addition to its effect on proliferation, Csf1r can influence survival and migration (48). Therefore, we assessed the presence of macrophages in developing *csf1r^{DM}* animals systemically. We live imaged individual whole larvae longitudinally for 4

days, starting at 5 dpf. Fish were imaged on each consecutive day, enabling us to determine absolute, individual changes in macrophage numbers over time. At 5 dpf, we visualized ~450 macrophages in control animals, and ~100 in *csf1r^{DM}* animals, indicating an > 4-fold reduction in macrophage numbers in *csf1r^{DM}* animals (Fig. 3G). Over the next 4 days, macrophage numbers in both groups did not show major changes (Fig. 3G). By analyzing time lapse imaging data of *csf1r^{DM}* larvae between 5 and 6 dpf we did not observe proliferative or newly appearing macrophages (Data not shown). This indicates that *csf1r^{DM}* macrophages are not compensating for their reduced numbers by proliferation, which therefore appears to remain impaired up to at least 9 dpf, or by supply of macrophages from an alternative source. Together these data show that, from the start of organ colonization onwards, the proliferative expansion of macrophages requires Csf1r signaling.

Macrophages are generated by definitive myelopoiesis independently of *csf1r*

Consecutive waves of myelopoiesis produce TRMs, the primitive myelopoiesis and the definitive myelopoiesis. Previously we showed that many Lplastin+ macrophages are present in the skin and intestine of adult *csf1r^{DM}* zebrafish (26). These cells could be derived from definitive myelopoiesis. We analyzed Lplastin+ macrophages in several other organs (e.g. spleen, intestine, gills, heart and skin) in 4.5-month-old adult zebrafish, which were abundantly present both in control and *csf1r^{DM}* animals (Fig. S3A). Nevertheless, whereas in controls the liver macrophages, likely Kupffer cells, were highly branched, *csf1r^{DM}* liver macrophages lacked a branched morphology (Fig. S3A). Similarly, in controls skin macrophages showed a branched morphology, whereas *csf1r^{DM}* macrophages in the skin were more rounded. In all other tissues both control and *csf1r^{DM}* macrophages showed a rounded morphology (Fig. S3A). Consistent with a loss of microglia from the CNS, the retina was largely devoid of microglia in *csf1r^{DM}* fish. This shows that, also in zebrafish, many macrophages are still present, suggesting that some populations of macrophages can be generated independently of Csf1r signaling. As embryonic *csf1r^{DM}* macrophage numbers were very low, and they failed to proliferate, the macrophages we observed in adult animals macrophages likely arise from definitive myelopoiesis. This would suggest that macrophages can be generated both from primitive and definitive myelopoiesis, independently of CSF1R.

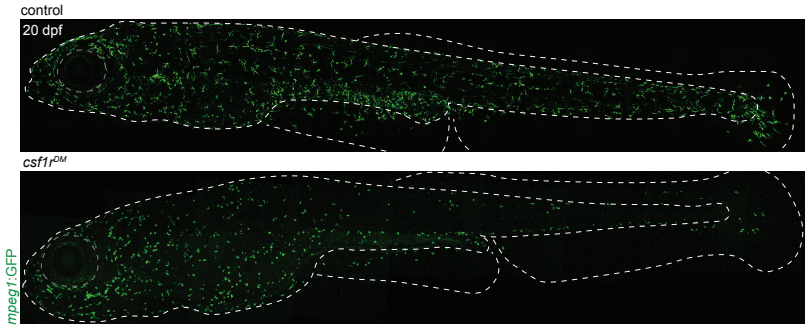
The zebrafish kidney marrow initiates definitive myelopoiesis likely

after 7 dpf, and consistently, lineage tracing studies have shown that definitive, likely HSPC-derived, macrophages, including microglia and Langerhans cells, are present around 20 dpf (36-38, 49-51). To determine whether and when new macrophages are generated in *csf1r^{DM}*, we live imaged entire zebrafish from 8 until 24 dpf (Fig. 4A). Between 10 and 13 dpf, control macrophages increased in numbers ~1.6 fold, whereas *csf1r^{DM}* macrophage numbers increased more than two-fold (2.4 fold), as a result of their lower macrophages numbers at the start of the experiment (Fig. 4B). Since *csf1r^{DM}* macrophages are cell cycle arrested, the increase in macrophage numbers can likely be attributed to definitive myelopoiesis. From 15-17 dpf onwards, macrophage numbers continue to increase almost exponentially, both in controls and in *csf1r^{DM}* fish. This increase coincides with the expected initiation of myelopoiesis in the kidney marrow (36, 38). We noticed large differences in the size of the fish, among controls and mutants, as they grew older, and therefore we plotted macrophages against fish size (Fig. 4B). Juvenile zebrafish rapidly grow in size, and their size often correlates better with developmental hallmarks than time in days (52). *csf1r^{DM}* fish smaller than 5 mm in length did not show an increase in macrophage numbers, whereas fish that were larger than 5 mm had an almost linear correlation with macrophage numbers, comparable to that in controls. Taken together, we show that beyond 15 dpf, or larger than 5 mm in size, macrophages numbers increase drastically, which correlates with the putative initiation of definitive kidney marrow myelopoiesis. In all, macrophages are generated by successive waves of primitive and definitive myelopoiesis, macrophages from progenitors including YSMs, EMPs and likely HSPCs, independently of Csf1r.

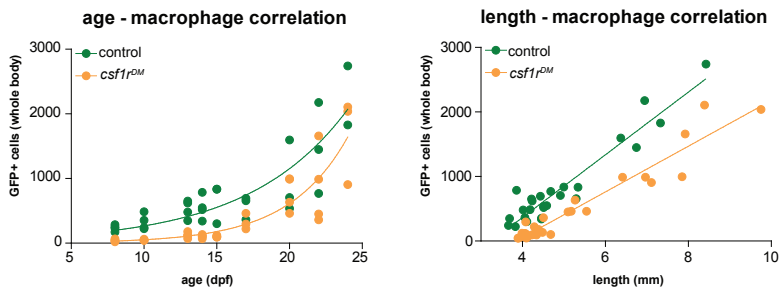
Csf1r deficient fish have abnormal Langerhans cells/skin macrophages

Despite the relatively large numbers of macrophages in the skin of *csf1r^{DM}* animals, we observed major morphological differences between control and *csf1r^{DM}* macrophages between 8 and 24 dpf. Since the animals size increases, and transparency decreases over time, it is likely that we mainly quantified macrophages located quite superficially (e.g. skin, intestine and retina) by *in vivo* imaging. Analyzing 24-day-old control zebrafish, we found that they contain roughly two macrophage morphologies: macrophages with thin and long protrusions, containing secondary and tertiary branches, and macrophages that appeared smaller and had only short, thick primary protrusions (Fig. 4C). Macrophages have been noted to exhibit two modes of migration including mesenchymal migration, which is dependent on proteolysis and cell-matrix

A



B



C

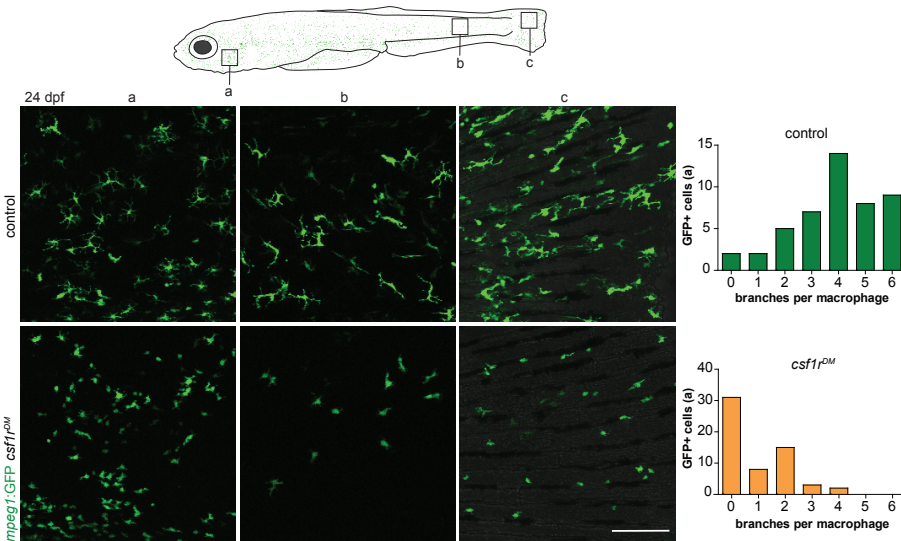


Fig. 4 Tracing larval fish to juvenile stages shows the emergence of a ‘second wave’ of macrophages **A** Representative images of a control and $csf1r^{DM}$ fish at 20 dpf. Dotted line represents the outline of the fish and its eye. **B** Quantification of the total number of macrophages in one side of the fish at different time points between 8 and 24 dpf. Plot showing the relationship between number of macrophages and fish size. Each dot represents one fish. **C** Representative images of GFP+ cells in different body regions at 24 dpf showing differences in morphology between controls and $csf1r^{DM}$ macrophages. GFP+ cells were quantified on one side of the embryo (right side).

adhesion and amoeboid migration, which is independent of cell adhesion (53). In contrast, *csf1r^{DM}* fish only contain the latter, amoeboid type of macrophages, suggesting that more mesenchymal macrophages fail to form. Time-lapse imaging showed that, both in controls and *csf1r^{DM}* fish, the smaller, amoeboid macrophages were very motile. In contrast, the branched macrophages found only in controls, even though they showed long, continuously extending and retracting protrusions, and showed a non-overlapping distribution, were largely confined to their location during 3-hour imaging periods (Movie S2). Many of these highly branched macrophages, which are absent in *csf1r^{DM}* fish, were located in the skin and based on their location, morphology and behavior, represent Langerhans cells (LCs)(50). This is consistent with the requirement of the Csf1r ligand, Il34, for LCs, as LCs are also absent in *Il34^{-/-}* mice (25, 50, 54-57). We therefore visualized highly branched macrophages in *Il34^{-/-}* zebrafish at 22 dpf, and found that hardly any were present, and they had a phenotype strikingly similar to *csf1r^{DM}* zebrafish, indicating that both mutants lack highly branched skin macrophages, LCs (Fig. 5B)(58). However, in contrast to *csf1r^{DM}*, which have much fewer macrophages, the total numbers of macrophages were not different in *Il34* mutants compared to total numbers in controls (Fig. 5A)(57, 58). These findings imply that Il34 hardly affects macrophage proliferation, as their numbers in skin did not differ from controls. Instead, it primarily regulates the acquisition of the highly branched macrophage morphology and their specific migratory behavior. This is consistent with our previous work, where we showed that Il34 has a role in microglia development which also relies on migration and not on regulation of proliferation (58). Thus, after largely Csf1r-independent generation of definitive macrophages, their further differentiation to highly branched TRMs, including the LCs and likely others such as Kupffer cells, is arrested in the absence of Csf1r signaling.

RNA sequencing of juvenile macrophages reveals reduced expression of genes involved in engulfment of apoptotic cells

Based on the aberrant morphology and migratory behavior of macrophages in the skin of *csf1r^{DM}* and *Il34* mutant juvenile fish, we hypothesized that Csf1r signaling is needed for the final differentiation of definitive macrophages into tissue resident macrophages, including LCs. To determine the molecular changes in these macrophages we collected *mpeg1-GFP* positive cells from 33 dpf and 1.5 mpf wildtype control, *csf1r^{DM}* and *Il34* mutant juvenile fish for RNA sequencing. Similar to what has been observed in mice and rats, overall *csf1r^{DM}* macrophages numbers

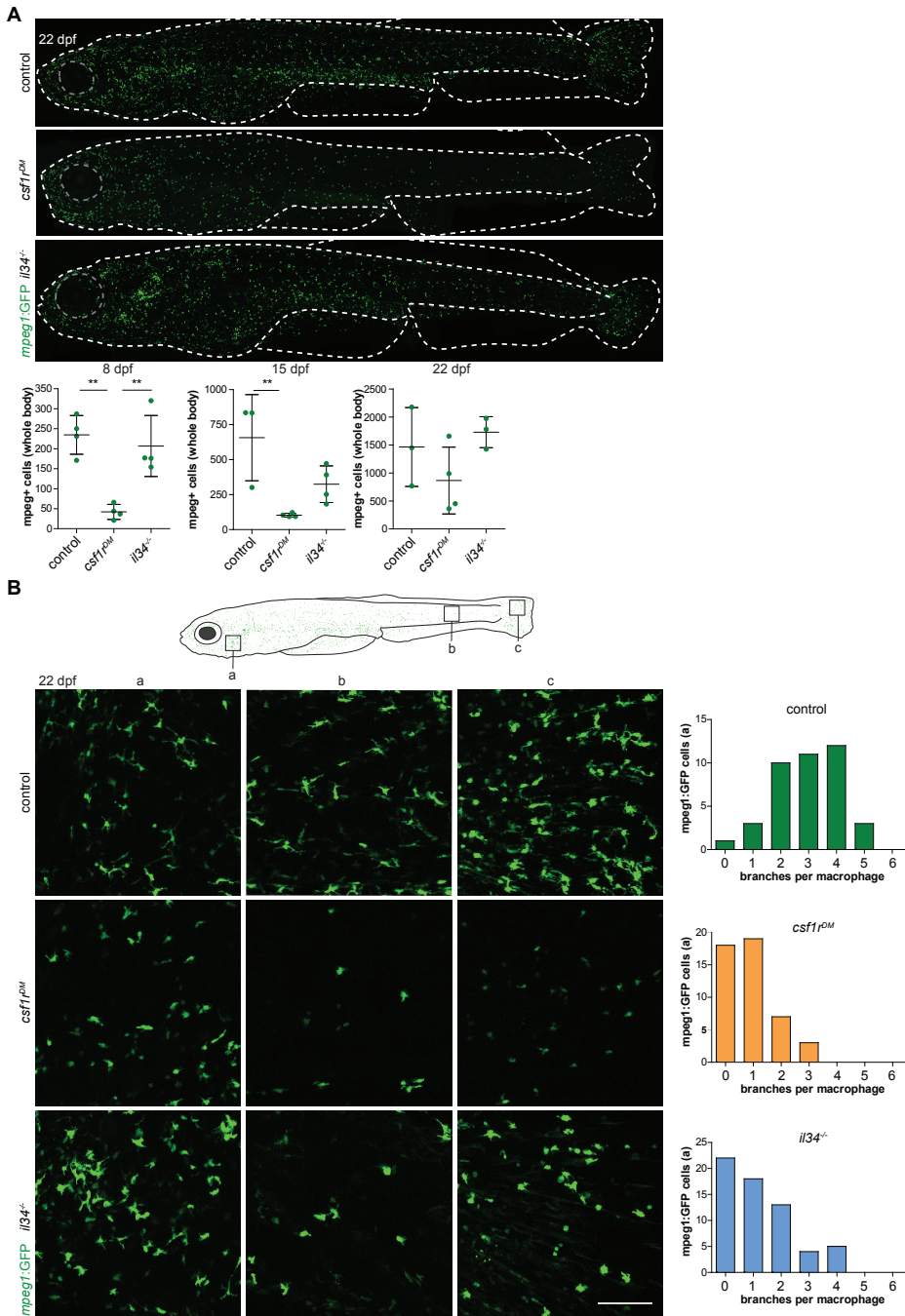


Fig. 5 Larval to juvenile *il34^{-/-}* fish show normal macrophage numbers but lack a branched population in the skin similar to *csf1^{rDM}* fish. **A Representative images of a control, *csf1^{rDM}* and *il34^{-/-}* fish at 22 dpf. Dotted line represents the outline of the fish and its eye. **B** Quantification of the**

total number of macrophages in one side of the fish at 8, 15 and 22 dpf. Each dot represents one fish. **C** Representative images of GFP+ cells in different body regions at 24 dpf showing differences in morphology between controls and *csf1^{DM}* and *il34^{-/-}* macrophages. GFP+ cells were quantified on one side of the embryo (right side). Statistical significance is calculated using ANOVA * < 0,05 ** < 0,01 *** < 0,001.

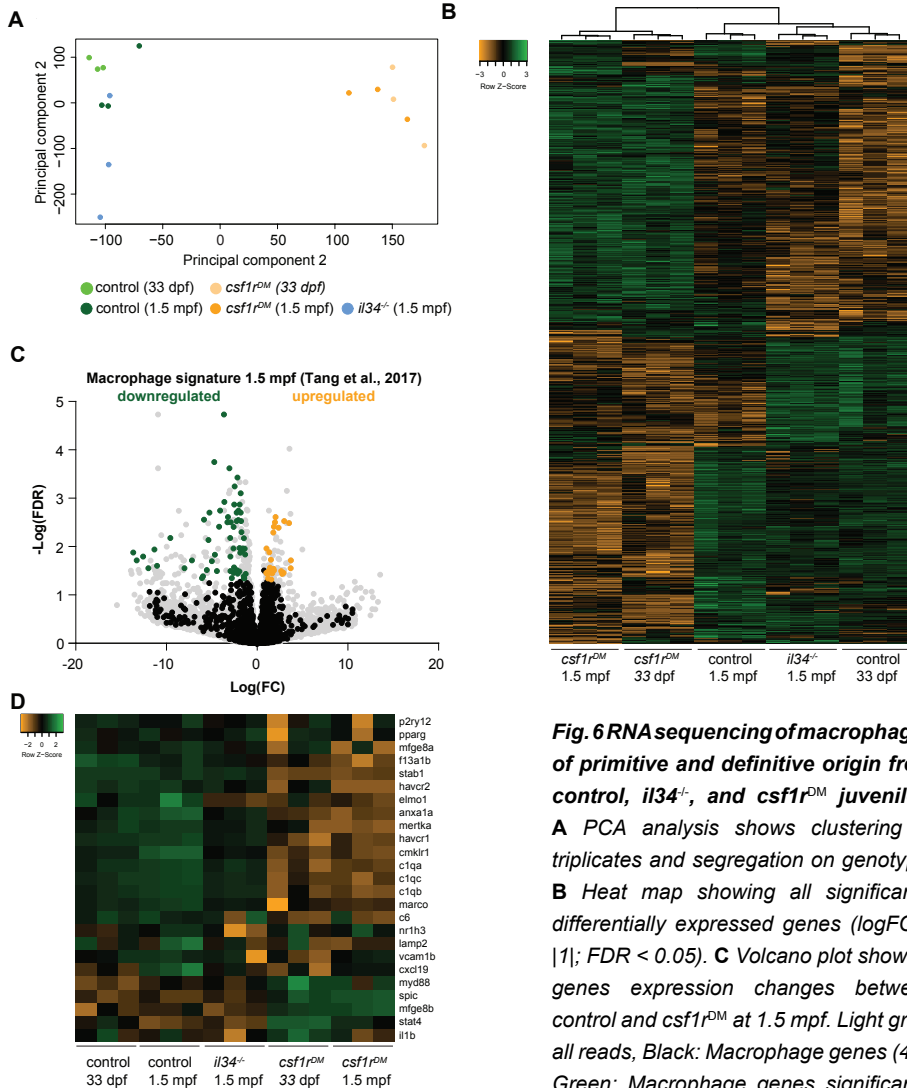


Fig. 6 RNA sequencing of macrophages of primitive and definitive origin from control, *il34^{-/-}*, and *csf1^{DM}* juveniles.

A PCA analysis shows clustering of triplicates and segregation on genotype.

B Heat map showing all significantly differentially expressed genes ($\log\text{FC} > |1|$; $\text{FDR} < 0.05$).

C Volcano plot showing genes expression changes between control and *csf1^{DM}* at 1.5 mpf. Light grey: all reads, Black: Macrophage genes (45), Green: Macrophage genes significantly upregulated in control macrophages; Orange: Macrophage genes significantly upregulated in *csf1^{DM}* macrophages ($\log\text{FC} > |1|$; $\text{FDR} < 0.05$). Only 4% of the macrophage genes were significantly differentially expressed between control and *csf1^{DM}* macrophages.

D Heat map showing genes involved in engulfment of apoptotic cells.

were largely reduced compared to those in control and *il34* mutants (Fig S4B) (25, 27). PCA analysis showed clustering of triplicates, and segregation based on genotype (component 2: *csf1r^{DM}* versus controls, component 1: *il34* mutants versus controls)(Fig. 6A). A heat map consisting of all differentially expressed genes shows that the majority of the differentially expressed genes are related to differences between *csf1r^{DM}* and controls ($\log_{2}FC > |1|$; $FDR < 0.05$)(Fig. 6B). To evaluate whether loss of *Csf1r* affects macrophage differentiation we compared our expression again to the macrophage signature determined by Tang and colleagues (45). We found, similar to our results in embryonic macrophages, that more than 95% of the 2039 macrophage genes were not differentially expressed between controls and *csf1r^{DM}* cells ($87/2039$, $\log_{2}FC > |1|$; $FDR < 0.05$)(Fig. 6C). The 5% macrophage genes that were differentially expressed included many genes involved in engulfment of apoptotic cells (e.g. *anxa1a*, *mertka*, *havcr1/2*, *c1qa/b/c*). Therefore, we analyzed a larger panel of “engulfment” genes and found the majority of these genes downregulated in *csf1r^{DM}* macrophages (e.g. *elmo1*, *stab1*, *pparg*)(Fig. 6D). This suggests that *csf1r^{DM}* macrophages have a reduced capability of, or activity in, engulfing apoptotic cells.

GO analysis on genes downregulated in *csf1r^{DM}* macrophages at 1.5 mpf ($\log_{2}FC > |1|$; $FDR < 0.05$) revealed downregulation of mainly classes involved in cell migration, immune response, translation and complement activation. In all, our data extend our observations that *Csf1r* does not affect core macrophage differentiation from primitive myelopoiesis to definitive myelopoiesis. Instead, *Csf1r* seems critical to acquire macrophage gene expression involved in engulfment of apoptotic cells and cell migration.

Discussion

Here, we investigated the developmental regulation of tissue macrophages in embryonic, juvenile and adult zebrafish by *Csf1r*. We showed that initially embryonic macrophages (YSMs and EMPs) emerge and proliferate independently of *csf1r*, and exhibit a normal macrophage morphology, behavior and gene expression profile. However, relatively normal embryonic *csf1r^{DM}* macrophages subsequently fail to distribute across the embryo and cease to expand in numbers. By tracing larval to juvenile fish *in vivo* we showed the emergence of a second wave of, likely definitive, macrophages, which occurred both in controls and in *csf1r* mutant fish. This revealed that around 15-17 dpf or in fish > 5 mm in size, a new set of macrophages is generated, likely from HSPCs that seeded the kidney marrow (36, 49, 50). Loss of *Il34-Csf1r* signaling results in the lack of highly branched

skin macrophages, known as LCs. This suggests the final differentiation of LCs is defective in the absence of *Csf1r* signaling. RNA seq on juvenile macrophages reveals normal “core” macrophage expression, but reduced expression of genes involved in engulfment of apoptotic cells in *csf1r^{DM}* macrophages. In all, *Csf1r* signaling is dispensable for the generation of primitive and definitive derived macrophages but required for the proliferation of late YSMs, early macrophages and TRMs, except for the earliest YSMs.

In the mouse, *Csf1r^{-/-}* embryonic yolk sac macrophages were reported to be largely absent at E12.5, but it is yet unknown if YSMs are present at a younger age (8). At E10.5 however, YSMs have already migrated to the fetal liver and to the embryonic organs (7), and this would, based on our findings, correspond to 2 - 2.5 dpf in zebrafish. At this stage we also found reduced macrophage numbers in *csf1r^{DM}* fish compared to controls, which therefore corresponds well with the *Csf1r^{-/-}* mouse model (8). Thus, it remains to be determined whether *Csf1r* signaling is essential for embryonic macrophage development in mice at earlier stages as well.

Although TRMs are terminally differentiated cells, they retain the ability to self-renew, which involves the relief of transcriptional suppression of proliferative enhancers by MAFB (61). Our findings suggest *Csf1r* also plays a central role in the maintenance of this proliferative capacity specifically in macrophages. Our embryonic macrophage transcriptome data revealed a twofold reduction of the majority of DNA replication genes in *csf1r^{DM}* embryos, pointing towards a *Csf1r*-dependent proliferation defect in the transition from G1 to S phase (DNA synthesis phase). *Csf1* can indeed rapidly stimulate S-phase entry and DNA replication of macrophages *in vitro* (62). The *Csf1r*-independent proliferation of the earliest YSMs, could be explained by signaling through others member of the type III receptor tyrosine kinase family, including *Flt3* or *C-kit*. Indeed, *Flt3* was found to be involved in the generation and proliferation of primitive macrophages and definitive hematopoietic stem cells in zebrafish (63). Zebrafish *C-kit* homolog *kitb* and its ligand was shown to regulate expansion of HSPCs (64). Furthermore, *C-kit* is essential for the proliferation of hematopoietic stem cells and down regulated upon differentiation, whereas *csf1r* is expressed rather low in HSPCs and is induced upon myeloid differentiation (18, 65-71). This could explain that initial proliferation of progenitors is not affected by *csf1r* deficiency, however upon *-csf1r* independent- differentiation, proliferation becomes dependent on *csf1r* signaling.

Even though CSF1R is considered essential for macrophage development,

particularly *in vitro*, nevertheless, macrophages are detected in most tissues of *Csf1r* deficient mice in numbers ranging between 10-50% of numbers found in controls (25, 44). Similar to mice, we find that macrophages are present in many adult *csf1r^{DM}* organs, except for microglia, LCs and likely osteoclasts (26). Our data suggests that *Csf1r* signaling is not essential for initial macrophage differentiation, regardless of their origin. The finding that *Csf1r*-deficient bi-potential granulocyte-macrophage precursors (GMPs) have a normal lineage potential corroborates our findings that *Csf1r* deficient primitive & definitive hematopoiesis produces macrophages (25, 72, 73). Although macrophages are present, in particular the TRMs are morphologically very different from control TRMs. For example, *csf1r^{DM}* macrophages are present in the liver, but lack the branched morphology observed in controls. Similarly, macrophages are present in skin, but lack the highly branched and migratory phenotype that Langerhans cells typically have. Recent data, from *Csf1r* deficient rats, showed that splenic macrophages fail to express splenic TRM specific genes, and instead show gene expression more similar to BMDMs (27). Transcriptome analysis of macrophages from juveniles revealed that in *csf1r^{DM}* macrophages genes involved in engulfment of apoptotic cells were downregulated. It was suggested that TRMs are locally primed to engulf apoptotic cells and that engulfment can also induce alterations in macrophage gene expression (74-76). We previously showed that *Il34* (most likely via *Csf1r* signaling) facilitates the tissue colonization by embryonic macrophages (58). Together this data would suggest *Csf1r* signaling is essential for acquisition of the tissue resident properties of macrophages, possibly by confining macrophages to their microenvironment, which was discovered to induce TRM properties (5, 19, 20).

In accordance to the 'niche' theory HSPC derived macrophages might only be able to seed the better accessible organs such as the liver and spleen but not organs protected by a barrier like the skin, bone, brain and lungs (15, 77, 78). We hypothesize that in *csf1r^{DM}* fish, instead of TRMs maintaining their population by proliferation, macrophages are continuously replaced by monocytes from the kidney marrow that differentiate into macrophages (79, 80). The absence of macrophages in selective organs could be attributed to the inaccessibility due to physical barriers, or the lack of migratory signals via *Il34*-*Csf1r* needed to attract macrophages to the organ and keep them there long enough to acquire TRM properties. Indeed, *Il34* has been shown to be involved in the final differentiation, maintenance and proliferation of LCs (57). Also, *Il34* is involved in seeding the brain with microglia precursors in zebrafish (58, 81). Therefore, *Csf1r* signaling

seems not only involved in the proliferative capacity of macrophages, but also regulates their final differentiation, maintenance and migration to several tissues, likely via Il34. Regardless of origin, the microenvironment induces TRM properties, suggesting macrophage precursors only need to enter the tissue and stay there long enough (3, 5, 6, 17, 19). Here we provide new insight in the function of *Csf1r* since loss of *Csf1r* signaling does not affect the generation of core macrophages during either primitive or definitive myelopoiesis. Our data shows that *Csf1r* is required for macrophage proliferation, proper tissue colonization and acquisition of TRM specific properties.

Materials and Methods

Animals

Csf1r mutants were created as described (26). *Tg(mpeg1:egfp, Neuro:Gal4, UAS:NTR-mCherry)* were used as control animals(82). Adult and larval fish were kept on a 14h/10h light–dark cycle at 28°C. Larvae were kept in HEPES-buffered E3 medium. Media was refreshed daily and at 24 hpf 0.003% 1-phenyl 2-thiourea (PTU) was added to prevent pigmentation. Animal experiments were approved by the Animal Experimentation Committee of the Erasmus MC.

Live imaging

Intravital imaging in zebrafish brains was largely performed as previously described (82). Briefly, zebrafish larvae were mounted in 1.8% low melting point agarose containing 0.016% MS-222 as sedative and anesthetic in HEPES-buffered E3. The imaging dish containing the embedded larva was filled with HEPES-buffered E3 containing 0.016% MS-222. For the experiment where larvae were followed over time between 5 and 9 dpf, larvae were removed from the low melting point agarose after imaging and put individually in wells of a 6 wells-plate containing HEPES-buffered E3 with PTU in which they were fed paramecia. For the experiment with juvenile fish between 8 and 24 dpf fish were kept in E3 medium until 5 dpf. From 5 dpf onwards they were raised under normal circumstances in the system and fed paramecia and dry food. From 13 dpf onwards they were fed brine shrimps, paramecia and dry food. Confocal imaging was performed using a Leica SP5 intravital imaging setup with a 20x/1.0 NA water-dipping lens. Imaging of *mpeg1*-GFP was performed using the 488 nm laser. Analysis of imaging data was performed using imageJ (FIJI) and LAS AF software (Leica).

Immunofluorescence staining

Immunohistochemistry was performed as described (82, 83). Briefly, larvae were fixed in 4% PFA at 4°C overnight. Subsequently, they were dehydrated with a 25%, 50%, 75%, 100% MeOH series and stored at -20°C for at least 12 hours, and rehydrated in series followed by incubation in 150 mM Tris-HCl (pH=9.0) for 15 minutes at 70°C. Samples were then washed in PBS containing 0.04% Triton (PBST) and incubated in acetone for 20 minutes at -20°C. After washing in PBST and ddH₂O larvae were incubated for three hours in blocking buffer (10% goat serum, 1% Triton X-100 (Tx100), 1% BSA, 0.1% Tween-20 in PBS) at 4°C, followed by incubation in primary antibody buffer at 4°C for three days. Larvae were washed in 10% goat serum 1% Tx100 in PBS and PBS containing 1% TX100 for a few hours, followed by incubation in secondary antibody buffer at 4°C for two and a half days. Hereafter the secondary antibody was washed away using PBS. Primary antibody buffer: 1% goat serum, 0.8% Tx100, 1% BSA, 0.1% Tween-20 in PBS. Secondary antibody buffer: 0.8% goat serum, 1% BSA and PBS containing Hoechst. Primary antibodies: PCNA (1:250, Dako), L-plastin (1:500, gift from Yi Feng, University of Edinburgh). Secondary antibodies used were DyLight Alexa 488 (1:250) and DyLight Alexa 647 (1:250). Samples were imaged as described above.

Immunohistochemistry to stain macrophages in adult zebrafish

Csf1r^{DM} and control zebrafish were euthanized in ice water at 4.5 months of age. Fish were fixated in 4% PFA over the weekend at 4°C. Bone was decalcified by putting the fish in 20% EDTA at room temperature for several weeks. Fish were embedded in paraffin to cut 10 µm sagittal sections that were deparaffinized and rehydrated to distilled water before staining. Sections were heated in 0.1 M sodium citrate pH = 6 for 13 minutes for antigen retrieval. After cooling down, endogenous peroxidase activity was blocked by 30 minute incubation in 0.6% H₂O₂, 1.5% sodium azide in PBS at room temperature. Slides were rinsed in PBS+ (0.5% protifar, 0.15% glycine) and stained with the L-plastin antibody (1:1000, thanks to Yi Feng, Edinburgh) overnight at 4°C in PBS+. Slides were rinsed with PBS+ before incubation with conjugated secondary antibody (anti-rabbit-HRP 1:100) for 60 minutes at room temperature. After washing steps slides were incubated in DAB-substrate (DAKO liquid DAB substrate-chromogen system). After washing with distilled water slices were counterstained with hematoxylin, dehydrated and mounted with Entellan (Merck). Images were acquired using an Olympus BX40 microscope with a 40x NA 0.65 objective and Olympus DP72

camera.

EdU pulse-chase protocol

Larvae of 4 dpf were placed in a 24 wells plate in HEPES buffered (pH = 7.3) E3 containing 0.003% PTU and 0.5 mM EdU for 24 hours. Next, larvae were fixed in 4% PFA for 3 hours at room temperature, dehydrated with a 25%, 50%, 75%, 100% MeOH series and stored at -20°C for at least 12 hours. Rehydrated in series followed by a proteinase K (10µg/ml in PBS) incubation for an hour. Followed by 15 minute post fixation in 4% PFA. Larvae were further permeabilized in 1% DMSO in PBS-T. Thereafter 50 µl Click-iT™ (Invitrogen) reaction cocktail was added for 3 hours at room temperature protected from light. After washing steps larvae were subjected to immunolabelling using L-plastin (see section immunofluorescent labelling). Samples were imaged as described above.

Isolation of mpeg1-GFP+ cells from zebrafish larvae

At 28 hpf, 35 larvae were collected in 0.16% MS-222 solution to euthanize them before adding 5x Trypsin-EDTA (0.25% Trypsin, 0.1% EDTA in PBS). For *csf1r^{DM}* cells, at 50 hpf, 70 larvae were used as these mutants had fewer mpeg1-GFP positive cells. Microcentrifuge tubes containing zebrafish embryos were incubated on ice on a shaking platform to dissociate the cells. At 33 dpf and 1.5 mpf, single fish were euthanized in ice water, an image was taken to measure their length, and they were cut in small pieces with a razor blade and incubated in 5x Trypsin-EDTA on ice for 1 hour to dissociate. Next, the cell suspension was transferred to FACS tubes by running it over a 35 µm cell strainer cap. PBS containing 10% fetal calf serum (FCS) was added over the strainer caps and the samples were centrifuges for 10 minutes 1000rpm at 4°C. The pellet was taken up in 300 µl PBS-10% FCS containing DAPI (1:1000). After analysis based on *mpeg1*-GFP expression, dapi signal and singlets, the cells were FAC-sorted and collected in Trizol, followed by RNA isolation (Fig. S2, S4).

RNA sequencing

cDNA was synthesized and amplified using SMART-seq® V4 Ultra® Low Input RNA kit for Sequencing (Takara Bio USA, Inc.) following the manufacturer's protocol. Amplified cDNA was further processed according to TruSeq Sample Preparation v.2 Guide (Illumina) and paired end-sequenced (2×75 bp) on the HiSeq 2500 (Illumina). Reads were mapped against the GRCz10 zebrafish genome. For differential gene expression analysis, GSEA and gene ontology we

used the Bioconductor packages edgeR, Gage, and goseq, respectively (84-87).

Statistical analysis For statistical analysis GraphPad was used to perform Student's *t* tests, ANOVAs, linear regression and non-linear regression analysis. Results were regarded significant at $p < 0.05$.

Acknowledgements

We acknowledge Remco M Hoogenboezem for assistance in RNA sequencing analysis and Michael Vermeulen for assistance in FACS.

References

1. T'Jonck W, Williams M, Bonnardel J. Niche signals and transcription factors involved in tissue-resident macrophage development. *Cell Immunol.* 2018;330:43-53.
2. Pollard JW. Trophic macrophages in development and disease. *Nat Rev Immunol.* 2009;9(4):259-70.
3. Gosselin D, Link VM, Romanoski CE, Fonseca GJ, Eichenfield DZ, Spann NJ, et al. Environment drives selection and function of enhancers controlling tissue-specific macrophage identities. *Cell.* 2014;159(6):1327-40.
4. Gosselin D, Skola D, Coufal NG, Holtman IR, Schlachetzki JCM, Sajti E, et al. An environment-dependent transcriptional network specifies human microglia identity. *Science.* 2017;356(6344).
5. Lavin Y, Winter D, Blecher-Gonen R, David E, Keren-Shaul H, Merad M, et al. Tissue-resident macrophage enhancer landscapes are shaped by the local microenvironment. *Cell.* 2014;159(6):1312-26.
6. Mass E, Ballesteros I, Farlik M, Halbritter F, Gunther P, Crozet L, et al. Specification of tissue-resident macrophages during organogenesis. *Science.* 2016;353(6304).
7. Stremmel C, Schuchert R, Wagner F, Thaler R, Weinberger T, Pick R, et al. Yolk sac macrophage progenitors traffic to the embryo during defined stages of development. *Nat Commun.* 2018;9(1):75.
8. Ginhoux F, Greter M, Leboeuf M, Nandi S, See P, Gokhan S, et al. Fate mapping analysis reveals that adult microglia derive from primitive macrophages. *Science.* 2010;330(6005):841-5.
9. Perdiguero EG, Geissmann F. The development and maintenance of resident macrophages. *Nat Immunol.* 2016;17(1):2-8.
10. Herbomel P, Thisse B, Thisse C. Ontogeny and behaviour of early macrophages in the zebrafish embryo. *Development.* 1999;126(17):3735-45.
11. Bertrand JY, Jalil A, Klaine M, Jung S, Cumano A, Godin I. Three pathways to mature macrophages in the early mouse yolk sac. *Blood.* 2005;106(9):3004-11.
12. McGrath KE, Frame JM, Palis J. Early hematopoiesis and macrophage development. *Semin Immunol.* 2015;27(6):379-87.
13. Matcovitch-Natan O, Winter DR, Giladi A, Vargas Aguilar S, Spinrad A, Sarrazin S, et al. Microglia development follows a stepwise program to regulate brain homeostasis. *Science.* 2016;353(6301):aad8670.
14. Hoeffel G, Chen J, Lavin Y, Low D, Almeida FF, See P, et al. C-Myb(+) erythro-myeloid progenitor-derived fetal monocytes give rise to adult tissue-resident macrophages. *Immunity.* 2015;42(4):665-78.
15. Scott CL, Zheng F, De Baetselier P, Martens L, Saeys Y, De Prijck S, et al. Bone marrow-derived monocytes give rise to self-renewing and fully differentiated Kupffer cells. *Nat Commun.* 2016;7:10321.
16. Epelman S, Lavine KJ, Randolph GJ. Origin and functions of tissue macrophages. *Immunity.* 2014;41(1):21-35.
17. Williams M, Scott CL. Does niche competition determine the origin of tissue-resident macrophages? *Nat Rev Immunol.* 2017;17(7):451-60.
18. Kierdorf K, Erny D, Goldmann T, Sander V, Schulz C, Perdiguero EG, et al. Microglia emerge from erythromyeloid precursors via Pu.1- and Irf8-dependent pathways. *Nat Neurosci.* 2013;16(3):273-80.
19. van de Laar L, Saels W, De Prijck S, Martens L, Scott CL, Van Isterdael G, et al. Yolk Sac Macrophages, Fetal Liver, and Adult Monocytes Can Colonize an Empty Niche and Develop into Functional Tissue-Resident Macrophages. *Immunity.* 2016;44(4):755-68.
20. Shemer A, Grozovski J, Leng Tay T, Tao J, Volaski A, Suess P, et al. Engrafted parenchymal brain macrophages differ from host microglia in transcriptome, epigenome and response to challenge. *bioRxiv.* 2018.
21. Goldmann T, Zeller N, Raasch J, Kierdorf K, Frenzel K, Ketscher L, et al. USP18 lack in microglia causes destructive interferonopathy of the mouse brain. *EMBO J.* 2015;34(12):1612-29.
22. Mass E, Jacome-Galarza CE, Blank T, Lazarov T, Durham BH, Ozkaya N, et al. A somatic mutation in erythro-myeloid progenitors causes neurodegenerative disease. *Nature.* 2017;549(7672):389-93.
23. Verheijen BM, Vermulst M, van Leeuwen FW. Somatic mutations in neurons during aging and neurodegeneration. *Acta Neuropathol.* 2018;135(6):811-26.
24. Stanley ER, Chitu V. CSF-1 receptor signaling in myeloid cells. *Cold Spring Harb Perspect Biol.* 2014;6(6).
25. Dai XM, Ryan GR, Hapel AJ, Dominguez MG,

- Russell RG, Kapp S, et al. Targeted disruption of the mouse colony-stimulating factor 1 receptor gene results in osteopetrosis, mononuclear phagocyte deficiency, increased primitive progenitor cell frequencies, and reproductive defects. *Blood*. 2002;99(1):111-20.
26. Oosterhof N, Kuil LE, van der Linde HC, Burm SM, Berdowski W, van Ijcken WFJ, et al. Colony-Stimulating Factor 1 Receptor (CSF1R) Regulates Microglia Density and Distribution, but Not Microglia Differentiation In Vivo. *Cell Rep*. 2018;24(5):1203-+.
 27. Pridans C, Raper A, Davis GM, Alves J, Sauter KA, Lefevre L, et al. Pleiotropic Impacts of Macrophage and Microglial Deficiency on Development in Rats with Targeted Mutation of the *Csf1r* Locus. *J Immunol*. 2018;201(9):2683-99.
 28. Erblisch B, Zhu L, Etgen AM, Dobrenis K, Pollard JW. Absence of colony stimulation factor-1 receptor results in loss of microglia, disrupted brain development and olfactory deficits. *PLoS One*. 2011;6(10):e26317.
 29. Cecchini MG, Dominguez MG, Mocci S, Wetterwald A, Felix R, Fleisch H, et al. Role of colony stimulating factor-1 in the establishment and regulation of tissue macrophages during postnatal development of the mouse. *Development*. 1994;120(6):1357-72.
 30. Gomez Perdiguero E, Geissmann F. Myb-independent macrophages: a family of cells that develops with their tissue of residence and is involved in its homeostasis. *Cold Spring Harb Symp Quant Biol*. 2013;78:91-100.
 31. Gore AV, Pillay LM, Venero Galanternik M, Weinstein BM. The zebrafish: A fantastic model for hematopoietic development and disease. *Wiley Interdiscip Rev Dev Biol*. 2018.
 32. Zhen F, Lan Y, Yan B, Zhang W, Wen Z. Hemogenic endothelium specification and hematopoietic stem cell maintenance employ distinct *Scl* isoforms. *Development*. 2013;140(19):3977-85.
 33. Herbolme P, Thisse B, Thisse C. Zebrafish early macrophages colonize cephalic mesenchyme and developing brain, retina, and epidermis through a M-CSF receptor-dependent invasive process. *Dev Biol*. 2001;238(2):274-88.
 34. Bertrand JY, Kim AD, Violette EP, Stachura DL, Cisson JL, Traver D. Definitive hematopoiesis initiates through a committed erythromyeloid progenitor in the zebrafish embryo. *Development*. 2007;134(23):4147-56.
 35. Bertrand JY, Cisson JL, Stachura DL, Traver D. Notch signaling distinguishes 2 waves of definitive hematopoiesis in the zebrafish embryo. *Blood*. 2010;115(14):2777-83.
 36. Willett CE, Cortes A, Zuasti A, Zapata AG. Early hematopoiesis and developing lymphoid organs in the zebrafish. *Dev Dyn*. 1999;214(4):323-36.
 37. Bertrand JY, Kim AD, Teng S, Traver D. CD41+ *cmyb*+ precursors colonize the zebrafish pronephros by a novel migration route to initiate adult hematopoiesis. *Development*. 2008;135(10):1853-62.
 38. Murayama E, Kissa K, Zapata A, Mordelet E, Briolat V, Lin HF, et al. Tracing hematopoietic precursor migration to successive hematopoietic organs during zebrafish development. *Immunity*. 2006;25(6):963-75.
 39. Meireles AM, Shiao CE, Guenther CA, Sidik H, Kingsley DM, Talbot WS. The Phosphate Exporter *xpr1b* Is Required for Differentiation of Tissue-Resident Macrophages. *Cell Rep*. 2014;8(6):1659-67.
 40. Monies D, Maddirevula S, Kurdi W, Alanazy MH, Alkhalidi H, Al-Owain M, et al. Autozygosity reveals recessive mutations and novel mechanisms in dominant genes: implications in variant interpretation. *Genet Med*. 2017;19(10):1144-50.
 41. Rossi F, Casano AM, Henke K, Richter K, Peri F. The SLC7A7 Transporter Identifies Microglial Precursors prior to Entry into the Brain. *Cell Rep*. 2015;11(7):1008-17.
 42. Ellett F, Pase L, Hayman JW, Andrianopoulos A, Lieschke GJ. *mpeg1* promoter transgenes direct macrophage-lineage expression in zebrafish. *Blood*. 2011;117(4):e49-56.
 43. Stanley ER. Action of the colony-stimulating factor, CSF-1. *Ciba Found Symp*. 1986;118:29-41.
 44. Pixley FJ, Stanley ER. CSF-1 regulation of the wandering macrophage: complexity in action. *Trends Cell Biol*. 2004;14(11):628-38.
 45. Tang Q, Iyer S, Lobbardi R, Moore JC, Chen H, Lareau C, et al. Dissecting hematopoietic and renal cell heterogeneity in adult zebrafish at single-cell resolution using RNA sequencing. *J Exp Med*. 2017;214(10):2875-87.
 46. Rossi F, Casano AM, Henke K, Richter K, Peri F. The SLC7A7 Transporter Identifies Microglial Precursors prior to Entry into the Brain. *Cell reports*. 2015;11(7):1008-17.
 47. Xu J, Wang T, Wu Y, Jin W, Wen Z. Microglia Colonization of Developing Zebrafish Midbrain Is Promoted by Apoptotic Neuron and Lysophosphatidylcholine. *Dev Cell*.

- 2016;38(2):214-22.
48. Elmore MR, Najafi AR, Koike MA, Dagher NN, Spangenberg EE, Rice RA, et al. Colony-stimulating factor 1 receptor signaling is necessary for microglia viability, unmasking a microglia progenitor cell in the adult brain. *Neuron*. 2014;82(2):380-97.
 49. Xu J, Zhu L, He S, Wu Y, Jin W, Yu T, et al. Temporal-Spatial Resolution Fate Mapping Reveals Distinct Origins for Embryonic and Adult Microglia in Zebrafish. *Dev Cell*. 2015;34(6):632-41.
 50. He S, Chen J, Jiang Y, Wu Y, Zhu L, Jin W, et al. Adult zebrafish Langerhans cells arise from hematopoietic stem/progenitor cells. *Elife*. 2018;7.
 51. Ferrero G, Mahony CB, Dupuis E, Yvernogeau L, Di Ruggiero E, Miserochi M, et al. Embryonic Microglia Derive from Primitive Macrophages and Are Replaced by cmyb-Dependent Definitive Microglia in Zebrafish. *Cell Rep*. 2018;24(1):130-41.
 52. Parichy DM, Elizondo MR, Mills MG, Gordon TN, Engeszer RE. Normal table of postembryonic zebrafish development: staging by externally visible anatomy of the living fish. *Dev Dyn*. 2009;238(12):2975-3015.
 53. Friedl P, Wolf K. Plasticity of cell migration: a multiscale tuning model. *J Cell Biol*. 2010;188(1):11-9.
 54. Greter M, Lelios I, Pelczar P, Hoeffel G, Price J, Leboeuf M, et al. Stroma-derived interleukin-34 controls the development and maintenance of langerhans cells and the maintenance of microglia. *Immunity*. 2012;37(6):1050-60.
 55. Wang T, Kono T, Monte MM, Kuse H, Costa MM, Korenaga H, et al. Identification of IL-34 in teleost fish: differential expression of rainbow trout IL-34, MCSF1 and MCSF2, ligands of the MCSF receptor. *Mol Immunol*. 2013;53(4):398-409.
 56. Wang Y, Szretter KJ, Vermi W, Gilfillan S, Rossini C, Cella M, et al. IL-34 is a tissue-restricted ligand of CSF1R required for the development of Langerhans cells and microglia. *Nat Immunol*. 2012;13(8):753-60.
 57. Wang YM, Bugatti M, Ulland TK, Vermi W, Gilfillan S, Colonna M. Nonredundant roles of keratinocyte-derived IL-34 and neutrophil-derived CSF1 in Langerhans cell renewal in the steady state and during inflammation. *Eur J Immunol*. 2016;46(3):552-9.
 58. Kuil LE, Oosterhof N, Geurts SN, van der Linde HC, Meijering E, van Ham TJ. Reverse genetic screen reveals that Il34 facilitates yolk sac macrophage distribution and seeding of the brain. *bioRxiv*. 2018.
 59. Park SY, Jung MY, Lee SJ, Kang KB, Gratchev A, Riabov V, et al. Stabilin-1 mediates phosphatidylserine-dependent clearance of cell corpses in alternatively activated macrophages. *J Cell Sci*. 2009;122(Pt 18):3365-73.
 60. Avellino R, Havermans M, Erpelinck C, Sanders MA, Hoogenboezem R, van de Werken HJ, et al. An autonomous CEBPA enhancer specific for myeloid-lineage priming and neutrophilic differentiation. *Blood*. 2016;127(24):2991-3003.
 61. Soucie EL, Weng Z, Geirsdottir L, Molawi K, Maurizio J, Fenouil R, et al. Lineage-specific enhancers activate self-renewal genes in macrophages and embryonic stem cells. *Science*. 2016;351(6274):aad5510.
 62. Tushinski RJ, Stanley ER. The regulation of mononuclear phagocyte entry into S phase by the colony stimulating factor CSF-1. *J Cell Physiol*. 1985;122(2):221-8.
 63. He BL, Shi X, Man CH, Ma AC, Ekker SC, Chow HC, et al. Functions of flt3 in zebrafish hematopoiesis and its relevance to human acute myeloid leukemia. *Blood*. 2014;123(16):2518-29.
 64. Mahony CB, Pasche C, Bertrand JY. Oncostatin M and Kit-Ligand Control Hematopoietic Stem Cell Fate during Zebrafish Embryogenesis. *Stem Cell Reports*. 2018;10(6):1920-34.
 65. Williams N, Bertoncello I, Kavnoudias H, Zsebo K, McNiece I. Recombinant rat stem cell factor stimulates the amplification and differentiation of fractionated mouse stem cell populations. *Blood*. 1992;79(1):58-64.
 66. Sarrazin S, Mossadegh-Keller N, Fukao T, Aziz A, Mourcin F, Vanhille L, et al. MafB restricts M-CSF-dependent myeloid commitment divisions of hematopoietic stem cells. *Cell*. 2009;138(2):300-13.
 67. Bartelmez SH, Bradley TR, Bertoncello I, Mochizuki DY, Tushinski RJ, Stanley ER, et al. Interleukin 1 plus interleukin 3 plus colony-stimulating factor 1 are essential for clonal proliferation of primitive myeloid bone marrow cells. *Exp Hematol*. 1989;17(3):240-5.
 68. Tushinski RJ, Stanley ER. The regulation of macrophage protein turnover by a colony stimulating factor (CSF-1). *J Cell Physiol*. 1983;116(1):67-75.
 69. Bartelmez SH, Stanley ER. Synergism between hemopoietic growth factors (HGFs) detected by their effects on cells bearing receptors for a lineage specific HGF: assay of hemopoietin-1. *J*

- Cell Physiol. 1985;122(3):370-8.
70. Kryszinska H, Hoogenkamp M, Ingram R, Wilson N, Tagoh H, Laslo P, et al. A two-step, PU.1-dependent mechanism for developmentally regulated chromatin remodeling and transcription of the *c-fms* gene. *Mol Cell Biol.* 2007;27(3):878-87.
 71. Walsh JC, DeKoter RP, Lee HJ, Smith ED, Lancki DW, Gurish MF, et al. Cooperative and antagonistic interplay between PU.1 and GATA-2 in the specification of myeloid cell fates. *Immunity.* 2002;17(5):665-76.
 72. Li J, Chen K, Zhu L, Pollard JW. Conditional deletion of the colony stimulating factor-1 receptor (*c-fms* proto-oncogene) in mice. *Genesis.* 2006;44(7):328-35.
 73. Endele M, Loeffler D, Kokkaliaris KD, Hilsenbeck O, Skylaki S, Hoppe PS, et al. CSF-1-induced Src signaling can instruct monocytic lineage choice. *Blood.* 2017;129(12):1691-701.
 74. Cummings RJ, Barbet G, Bongers G, Hartmann BM, Gettler K, Muniz L, et al. Different tissue phagocytes sample apoptotic cells to direct distinct homeostasis programs. *Nature.* 2016;539(7630):565-9.
 75. Roberts AW, Lee BL, Deguine J, John S, Shlomchik MJ, Barton GM. Tissue-Resident Macrophages Are Locally Programmed for Silent Clearance of Apoptotic Cells. *Immunity.* 2017;47(5):913-27 e6.
 76. N AG, Quintana JA, Garcia-Silva S, Mazariegos M, Gonzalez de la Aleja A, Nicolas-Avila JA, et al. Phagocytosis imprints heterogeneity in tissue-resident macrophages. *J Exp Med.* 2017;214(5):1281-96.
 77. Beattie L, Sawtell A, Mann J, Frame TCM, Teal B, de Labastida Rivera F, et al. Bone marrow-derived and resident liver macrophages display unique transcriptomic signatures but similar biological functions. *J Hepatol.* 2016;65(4):758-68.
 78. Bain CC, Hawley CA, Garner H, Scott CL, Schridde A, Steers NJ, et al. Long-lived self-renewing bone marrow-derived macrophages displace embryo-derived cells to inhabit adult serous cavities. *Nat Commun.* 2016;7:ncomms11852.
 79. Bain CC, Bravo-Blas A, Scott CL, Perdiguero EG, Geissmann F, Henri S, et al. Constant replenishment from circulating monocytes maintains the macrophage pool in the intestine of adult mice. *Nat Immunol.* 2014;15(10):929-37.
 80. Tamoutounour S, Henri S, Lelouard H, de Bovis B, de Haar C, van der Woude CJ, et al. CD64 distinguishes macrophages from dendritic cells in the gut and reveals the Th1-inducing role of mesenteric lymph node macrophages during colitis. *Eur J Immunol.* 2012;42(12):3150-66.
 81. Wu S, Xue R, Hassan S, Nguyen TML, Wang T, Pan H, et al. I134-Csf1r Pathway Regulates the Migration and Colonization of Microglial Precursors. *Dev Cell.* 2018;46(5):552-63 e4.
 82. van Ham TJ, Brady CA, Kalicharan RD, Oosterhof N, Kuipers J, Veenstra-Algra A, et al. Intravital correlated microscopy reveals differential macrophage and microglial dynamics during resolution of neuroinflammation. *Dis Model Mech.* 2014;7(7):857-69.
 83. van Ham TJ, Kokel D, Peterson RT. Apoptotic cells are cleared by directional migration and elmo1- dependent macrophage engulfment. *Curr Biol.* 2012;22(9):830-6.
 84. Robinson MD, McCarthy DJ, Smyth GK. edgeR: a Bioconductor package for differential expression analysis of digital gene expression data. *Bioinformatics.* 2010;26(1):139-40.
 85. Luo W, Friedman MS, Shedden K, Hankenson KD, Woolf PJ. GAGE: generally applicable gene set enrichment for pathway analysis. *BMC Bioinformatics.* 2009;10:161.
 86. Young MD, Wakefield MJ, Smyth GK, Oshlack A. Gene ontology analysis for RNA-seq: accounting for selection bias. *Genome Biol.* 2010;11(2):R14.
 87. Durinck S, Spellman PT, Birney E, Huber W. Mapping identifiers for the integration of genomic datasets with the R/Bioconductor package biomaRt. *Nat Protoc.* 2009;4(8):1184-91.

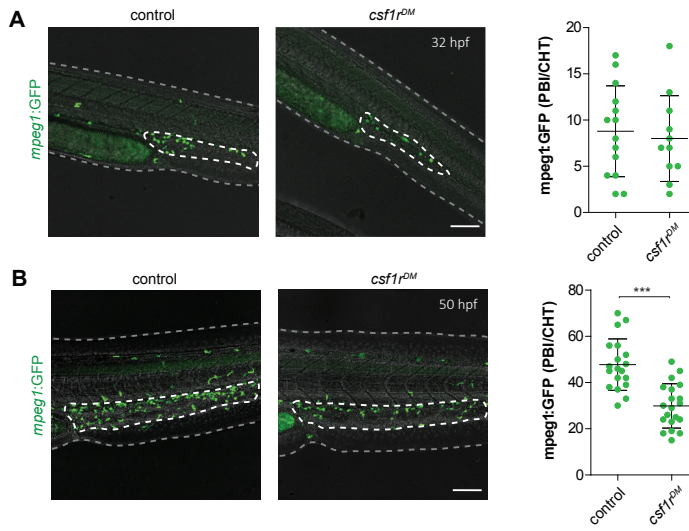


Fig. S1 GFP+ cells can be detected in the PBI/CHT of control and *csf1^{rDM}* larvae **A** Representative images of GFP+ myeloid progenitors located in the PBI/CHT at 32 hpf and quantification. **B** Representative images of GFP+ myeloid progenitors located in the PBI/CHY at 50 hpf and quantification. Scale bars represent 100 μ m. Error bars represent standard deviation. Statistical significance is calculated using student's T-tests *** < 0,001. GFP+ cells were quantified on one side of the embryo (right side). Each dot represents one fish.

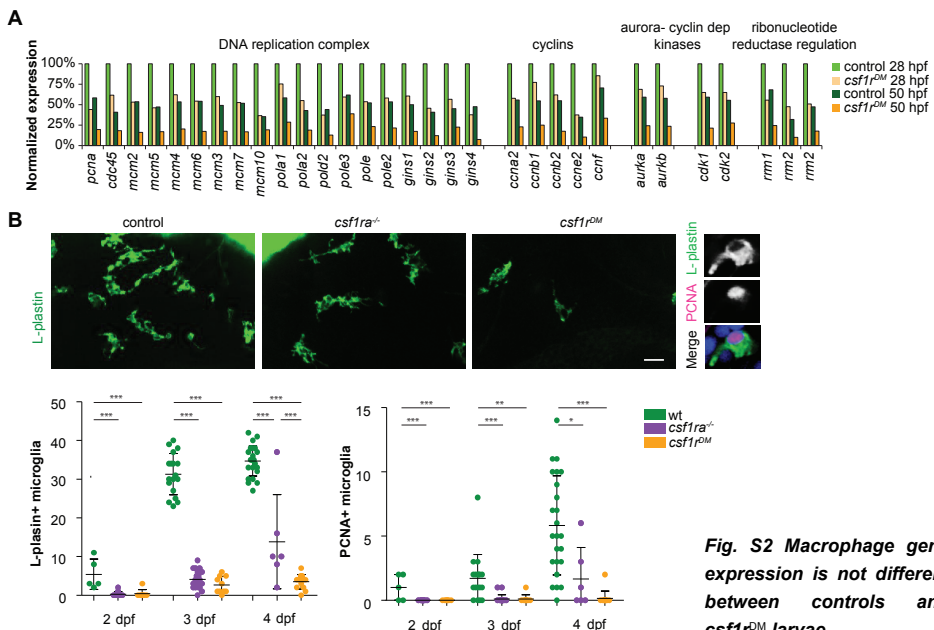


Fig. S2 Macrophage gene expression is not different between controls and *csf1^{rDM}* larvae.

A Normalized CPM values of genes involved in DNA replication/cell cycle. **B** Representative images of L-plastin immunohistochemistry of microglia in different *csf1^{rDM}* larvae at 4 dpf. Scale bar represents 20 μ m. Quantification of L-plastin+ microglia in control and different *csf1^r* mutants at 2, 3 and 4 dpf and quantification Pcn+ /L-plastin double positive microglia at 2, 3 and 4 dpf. Statistical significance is calculated using ANOVA * < 0,05 ** < 0,01 *** < 0,001. Each dot represents one fish.

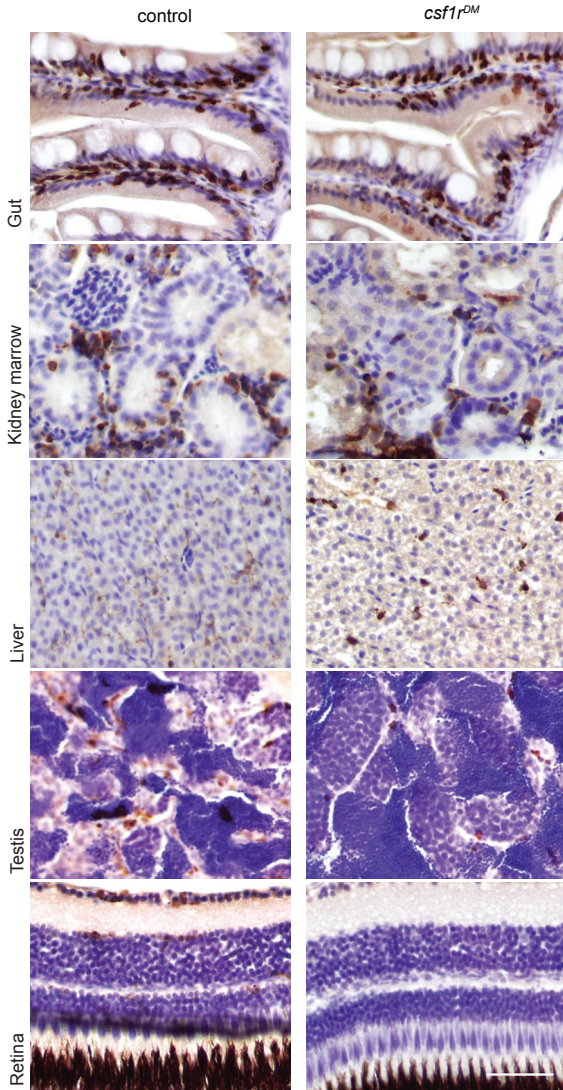


Fig. S3 *csf1r* deficient macrophages are present in several organs in adult zebrafish

A Representative images of L-plastin immunolabeling of macrophages in gut, kidney marrow, liver, testis and retina of 4.5 mpf old control and *csf1r^{DM}* fish. Scale bar represents 100 μ M.

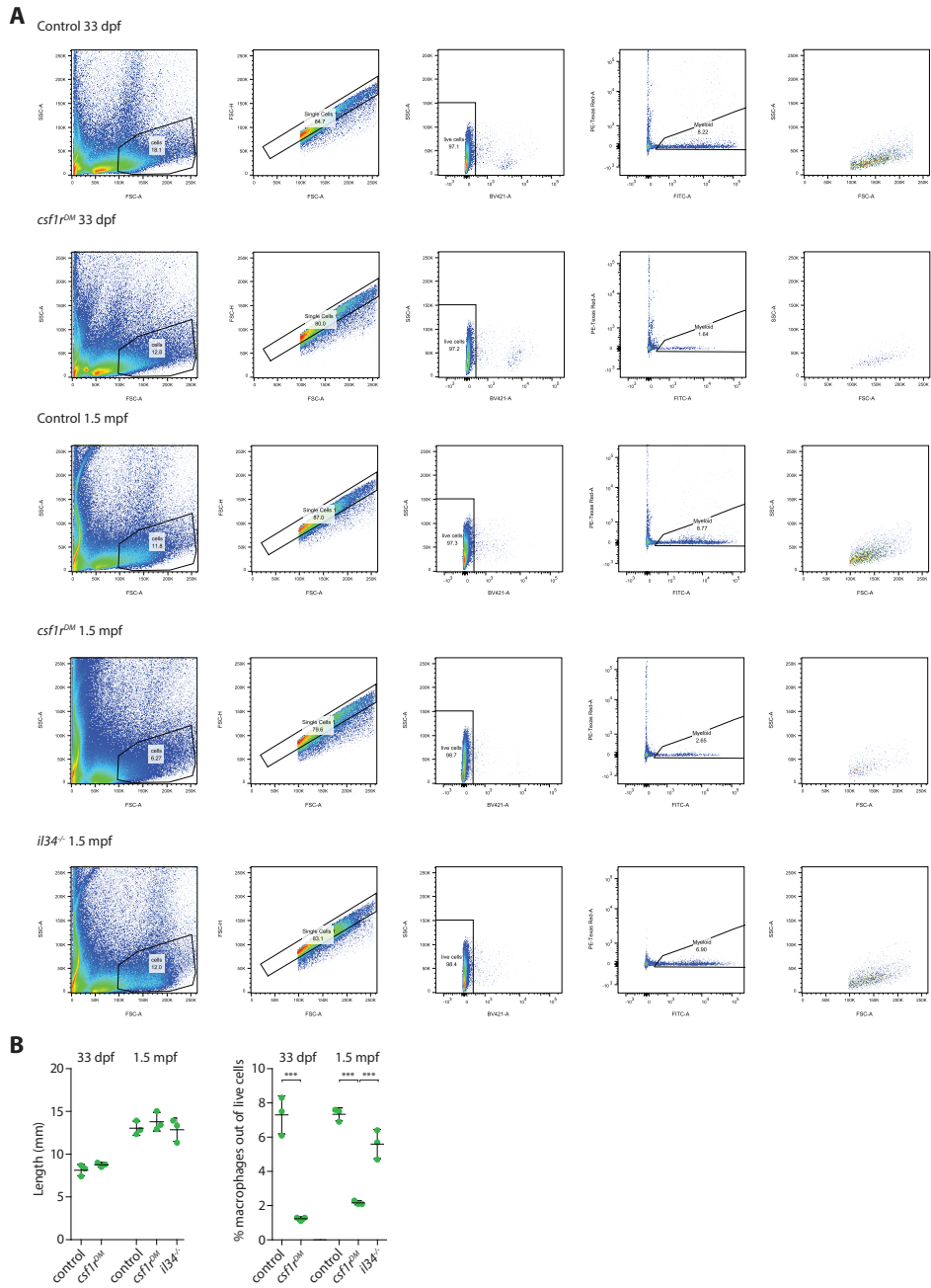


Fig. S4 FACS strategy for isolating mpeg+ macrophages from juveniles

A FACS sorting strategy showing one representative example for each genotype. **B** Quantification of the length of the fish and the percentage macrophages out of live cells *** < 0,001. Each dot represents one fish.

Chapter 4

Homozygous mutations in CSF1R cause a pediatric onset leukoencephalopathy and can result in congenital absence of microglia

Nynke Oosterhof,^{1,10} Irene J. Chang,^{2,10} Ehsan G. Karimini,^{3,10} Laura E. Kuil,¹ Dana M. Jensen,⁴ Ray Daza,⁵ Erica Young,⁵ Lee Astle,⁶ Herma C. van der Linde,¹ Jeroen Demmers,⁷ Caitlin S. Latimer,⁸ C. Dirk Keene,⁸ Emily Loter,⁹ Reza Maroofian,³ Tjakko J. van Ham,^{1,11} Robert F. Hevner,^{5,8,#,11} James T. Bennett^{2,4,9,11}

¹Department of Clinical Genetics, Erasmus MC, University Medical Center Rotterdam, Wytemaweg 80, 3015 CN, Rotterdam, the Netherlands.

²Department of Pediatrics, Division of Genetic Medicine, University of Washington School of Medicine, Seattle, WA, 98195 USA

³Genetics Research Centre, Molecular and Clinical Sciences Institute, St George's, University of London, Cranmer Terrace, London SW17 0RE, UK.

⁴Center for Developmental Biology and Regenerative Medicine, Seattle Children's Research Institute, Seattle, WA, 98101 USA

⁵Center for Integrative Brain Research, Seattle Children's Research Institute, Seattle, WA 98101 USA

⁶Department of Laboratory and Pathology, Alaska Native Medical Center, Anchorage, AK 99508 USA

⁷Proteomics Center, Erasmus University Medical Center, Wytemaweg 80, 3015 CN Rotterdam, the Netherlands

⁸Department of Pathology, University of Washington School of Medicine, Seattle WA 98195 USA

⁹Department of Laboratories, Seattle Children's Hospital, Seattle, WA 98105 USA

¹⁰Authors contributing equally to this work, ¹¹Authors contributing equally to this work

Present address: Department of Pathology, University of California, San Diego, La Jolla, CA 92093 USA

American Journal of Human Genetics, 2019

Abstract

Microglia are CNS-resident macrophages that scavenge debris and regulate immune responses. Proliferation and development of macrophages, including microglia, requires Colony Stimulating Factor 1 Receptor (*CSF1R*), a gene previously associated with a dominant adult-onset neurological condition (Adult-onset Leukoencephalopathy with axonal Spheroids and Pigmented glia). Here, we report two unrelated individuals with homozygous *CSF1R* mutations whose presentation was distinct from ALSP. Post-mortem examination of an individual with a homozygous splice mutation (c.1754-1G>C) demonstrated several structural brain anomalies, including agenesis of corpus callosum. Immunostaining demonstrated almost complete absence of microglia within this brain, suggesting that it developed in the absence of microglia. The second individual had a homozygous missense mutation (c.1929C>A, causing p.His643Gln), and presented with developmental delay and epilepsy in childhood. We analyzed a zebrafish model (*csf1r^{DM}*) lacking *Csf1r* function, and found that their brains also lacked microglia, and had reduced levels of *Cux1*, a neuronal transcription factor. *CUX1*⁺ neurons were also reduced in sections of homozygous *CSF1R* mutant human brain, identifying an evolutionarily conserved role for *CSF1R* signaling in production or maintenance of *CUX1*⁺ neurons. Since a large fraction of *CUX1*⁺ neurons project callosal axons, we speculate that microglia deficiency may contribute to agenesis of the corpus callosum via reduction in *CUX1*⁺ neurons. Our results suggest *CSF1R* is required for human brain development and establish the *csf1r^{DM}* fish as a model for microgliopathies. In addition, our results exemplify an under-recognized form of phenotypic expansion, in which genes associated with well recognized, dominant conditions produce different phenotypes when biallelically mutated.

Introduction

Microglia are tissue-resident macrophages of the brain that scavenge cellular debris and regulate CNS immune responses. Although research has focused on their role in age-related neurodegenerative disorders, more recently roles for microglia in normal nervous system development, both in the presence and absence of environmental stressors (prenatal inflammation, low birth weights) have emerged. For example, microglia remodel neuronal circuits, engulf neuronal progenitors, prune synapses and control axonal projections, and mice engineered to develop without microglia show structural brain abnormalities, including ventriculomegaly and agenesis of corpus callosum (ACC).¹⁻⁶ Microglia originate from macrophages within the embryonic yolk sac, and their development requires signaling through the colony stimulating factor 1 receptor (CSF1R).⁷⁻⁹ This receptor tyrosine kinase is expressed in macrophages and is thought to regulate their proliferation and development.¹⁰ In humans, heterozygous mutations in *CSF1R* cause Adult-onset Leukoencephalopathy with axonal Spheroids and Pigmented glia (ALSP [MIM: # 221820]), a fatal neurologic disorder that presents with progressive cognitive and motor impairment and seizures in the fourth to fifth decade of life.¹¹⁻¹⁶ Imaging shows diffuse signal changes and atrophy of the white matter, suggesting primary white matter disease.¹⁷ ALSP is a newer diagnostic term that includes both Hereditary Diffuse Leukoencephalopathy with axonal Spheroids (HDLS) and Pigmented Orthochromatic Leukodystrophy (POLD), now recognized as a single clinicopathological entity.¹³ ALSP is a prototypical “microgliopathy” because genetics point to microglial dysfunction as the primary disease mechanism.^{13; 18; 19}

Here, we describe two individuals with homozygous *CSF1R* mutations who presented with pediatric phenotypes distinct from ALSP. One individual had severe developmental delay in early childhood, developed epilepsy at 7 years of age, and was found to have severe leukodystrophy and periventricular calcifications at age 24. The other presented prenatally with structural brain malformations, including agenesis of the corpus callosum (ACC), and died before 1 year of age. Post-mortem analysis identified a complete absence of microglia within the brain, suggesting that it developed in the absence of microglia. To further investigate how absence of CSF1R signaling affects brain development, we generated *CSF1R*-deficient zebrafish.²⁰ These CSF1R deficient fish (*csf1r^{DM}*) also lacked microglia. Proteomics analysis (mass spectrometry) in *csf1r^{DM}* fish brain, in conjunction with immunostaining of human *CSF1R* mutant cortex, identified reduced levels of the neuronal transcription factor CUX1. Since

a large fraction of CUX1+ neurons project axons into the corpus callosum,²¹ we speculate that a deficiency of microglia numbers or function leads to decreased CUX1+ cells, possibly via reduced trophic support, contributing to an agenesis of corpus callosum phenotype. These results establish the *csf1r*^{DM} fish as a model for microgliopathy, and provide a starting point for unraveling the role of microglia in brain development.

Materials And Methods

Study Participants

Informed consent was obtained from subjects prior to enrollment in the study. Approval for research on human subjects was obtained from IRBs at Mashhad University of Medical Sciences and Seattle Children's Hospital.

Exome Sequencing

Exome sequencing (ES) was performed as part of clinical care on peripheral blood samples from probands and both biological parents, using the Agilent Clinical Research Exome kit. Targeted regions were sequenced simultaneously on an Illumina HiSeq with 100bp paired end reads. Bidirectional sequence was assembled and aligned to human reference genome build GRCh37/UCSC hg19. Data were analyzed for sequence variants as previously described.^{22; 23}

Zebrafish maintenance

For the experiments WT (TL), *csf1r*^{DM} and *csf1ra*^{-/-};*b*^{+/-} mutants were used. The *csf1r* mutants were described in detail elsewhere.²⁰ Briefly, *csf1ra*^{i4e1/j4e1} mutants have a p.Val614Met substitution in the first kinase domain.²⁴ The *csf1rb* deletion mutant was created by TALEN-mediated genome editing.²⁵ The TALEN arms targeted exon 3 of the *csf1rb* gene, resulting in a 4 bp deletion and premature stop codon. The zebrafish were kept at 28°C and fed brine shrimp twice a day. Animal experiments were approved by the Animal Experimentation Committee of the Erasmus MC, Rotterdam.

Zebrafish Histology and Immunostaining procedures

L-plastin antibody and neutral red staining performed as described previously.²⁶⁻²⁸

Human Cortical Sectioning and CUX1 Immunohistochemistry and Quantification

As a control for CUX1 immunohistochemistry in cerebral cortex, sections were taken from another autopsy case with similar age, sex, and tissue processing.

The control patient was a seven-month, two-week old male with 22q11 deletion syndrome who had died of aseptic shock. The post-mortem interval was 4 hours. Sections of cerebral cortex from three different brain lobes were obtained from patient and control brains, sectioned identically as described for other histological studies, deparaffinized, processed for CUX1 immunofluorescence using anti-CUX1 antibodies (ab54583, Abcam), and counterstained with DAPI, as described.²⁹ Fluorescence images were collected using the same exposure settings for all images. The number of CUX1+ cells was counted within segments of cerebral cortex extending from pia to white matter within a defined area, as described previously.³⁰ Using ImageJ, the areas of the rectangles were measured. Finally, the density of CUX1+ cells was calculated by dividing cell counts by area. Cell densities were compared statistically by t-test using each cortical sample as a separate count (n=3), with significance defined as $p < 0.05$.

Alizarin red staining

Size-matched adult zebrafish were eviscerated and incubated in 4% PFA at 4°C overnight. Next, they were rinsed in 80% EtOH for 1 h, after which they were washed in 70% MeOH for 5 min, and incubated in 70% MeOH at 4°C overnight. The fish were then washed in 50% MeOH for 5 min and 0.2% Triton X-100 for 5 min twice. Bleach (0.8% KOH, 0.9% H₂O₂, 0.2% Triton X-100) was used to remove the pigment. Bleaching was followed by two 5 min wash steps in 0.2% Triton X-100. The fish were neutralized in concentrated Borax for 15 min. Next, the fish were digested with 0.1% Trypsin, 0.6% Borax and 0.08% Triton X-100 for 4 hours). Then the fish were incubated in an alizarin red solution (0.05% Alizarin red, 25% glycerol, 100 mM Tris pH 7.5) at room temperature overnight. The fish were incubated in 0.5% KOH in 50% glycerol overnight, followed by incubation in 0.3% KOH in 70% glycerol for several weeks until sufficient staining is achieved as desired.

Mass spectrometry and proteomics analysis

Protein lysates were obtained from dissected brains from 6-8 month-old zebrafish (3 brains per sample, samples in triplicate) with the following genotypes: *csf1r*^{DM}, *csf1ra*^{-/-};*b*^{+/-}, and *csf1ra*^{+/+};*b*^{+/+} (aka wild type littermates). After endoproteinase and tryptic digestions, peptides were labelled with 10-plex tandem mass tag (TMT) reagents (Thermo Fisher Scientific) and subjected to orthogonal high-pH and reverse phase fractionation. Mass spectra were acquired on an Orbitrap Lumos (Thermo) coupled to an EASY-nLC 1200 system (Thermo), and peak

lists were automatically created using the Proteome Discoverer 2.1 (Thermo) software. Further analysis we used the R packages vsn and limma.^{31; 32} For complete proteomics methods, see Supplemental Methods.

Results

Clinical Findings and Exome Analysis

Trio-based exome sequencing (ES) identified homozygous variants (NM_005211.3:c.1754-1G>C) in the gene *CSF1R* (Figure 1) in a male infant (family CSF1R_01, individual II-1 in Figure 1) with multiple congenital anomalies. No other pathogenic variants were identified. Both parents and two grandparents carried this variant in the heterozygous state. All four of these individuals denied any neurologic symptoms; however they were all less than 40 years, the average age of symptom onset for ALSP. This infant presented with prenatal structural brain abnormalities, including ACC, ventriculomegaly, and pontocerebellar hypoplasia. These abnormalities were confirmed by postnatal brain MRI, which also demonstrated periventricular calcifications and Dandy-Walker malformation (Figure 2A-D). There was known shared ancestry, and a chromosomal microarray found 3.1 % of the autosomal genome to be homozygous. There was hypocalcemia requiring intravenous calcium supplementation, and x-rays showed generalized increased bone density (osteopetrosis) and irregular metaphyses (Figure 2L-N). His clinical course was complicated by respiratory failure, oromotor discoordination requiring gastrostomy feeding, and intractable epilepsy (Table 1). He died at ten months of age from streptococcal bacteremia, and a brain-only autopsy was performed (see below). A more complete clinical description can be found in Supplemental data.

The c.1754-1G>C variant disrupts a splice acceptor site, and is predicted to cause exon 13 skipping and production of an in-frame protein product (p.Gly585_Lys619delinsAla). Amino acids 585-619 are within the tyrosine kinase domain, like all but two of the previously reported pathogenic variants in this gene (Figure 1 and Table S1). We classified this variant as likely pathogenic using American College of Medical Genetics and Genomics (ACMG) guidelines: it is absent from the ExAC and gnomAD population databases (PM2), predicted to change the length of the protein (PM4) in a functional domain where pathogenic mutations have previously been reported (PM1).³³ In addition, a *de novo* heterozygous variant at the -2 position of the same splice acceptor site (c.1754-2A>G) has been previously reported

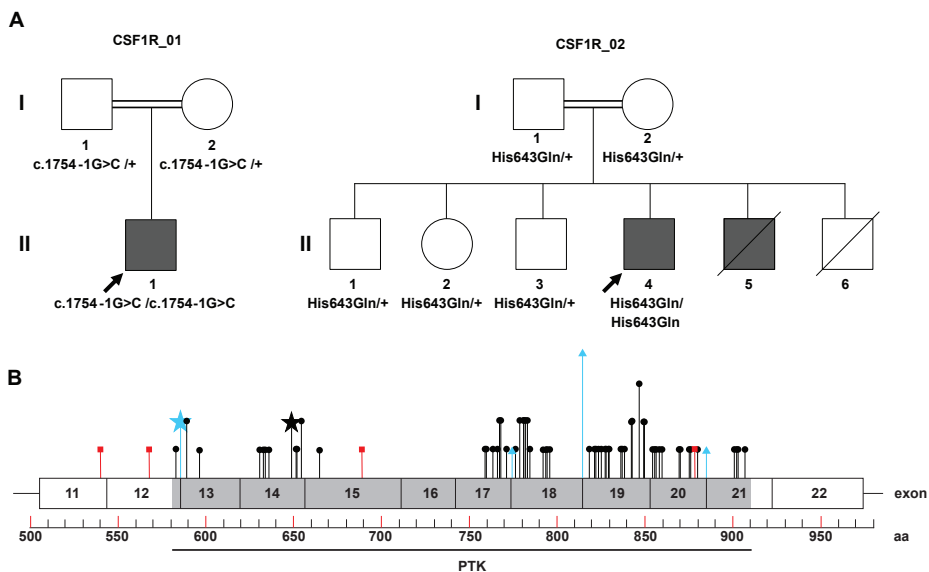


Figure 1: Pedigrees and distribution of CSF1R mutations. **A** Pedigrees of family CSF1R_01 and CSF1R_02 shown, with genotypes indicated. CSF1R sequencing was not performed for II-5, but this individual is shaded to reflect his leukodystrophy and periventricular calcifications **B** Exons 11-22 of the CSF1R protein (NP_005202.2) are shown. No mutations have been reported in the five immunoglobulin (Ig) domains and transmembrane domain upstream of exon 11, which are not shown. The intracellular protein tyrosine kinase (PTK) domain is indicated. The 65 previously reported pathogenic variants causative for ALSP are shown (truncating variants in red squares, missense and in-frame indel variants in black circles, splice variants in blue triangles). The novel splice site variant identified in family CSF1R_01 (NM_005211.3:c.1754-1G>C) is indicated by the blue star. The novel missense variant identified in family CSF1R_02 (NM_005211.3:c.1929C>A, p.His643Gln) is indicated by the black star. Amino acids containing multiple variants are specified by proportionally taller lines. A complete list of previously reported variants in supplemental table 1.

as pathogenic in ALSP.¹⁴ Our patient’s phenotype was distinct from ALSP, suggesting that biallelic variants in this gene cause a more severe, prenatal onset disorder. Additional support of pathogenicity comes from an independent report of siblings with a very similar phenotype whose parents both carried a heterozygous truncating mutation in CSF1R (c.620T>A, causing p.Tyr540*).³⁴ However, DNA was not available from the affected siblings for confirmation in this report.

To increase our confidence that homozygous mutations in CSF1R cause a phenotype distinct from ALSP, we used Genematcher to find an additional family (CSF1R_02) with homozygous CSF1R mutations (NM_005211.3:c.1929C>A, p.His643Gln), identified by trio exome sequencing. No other pathogenic variants

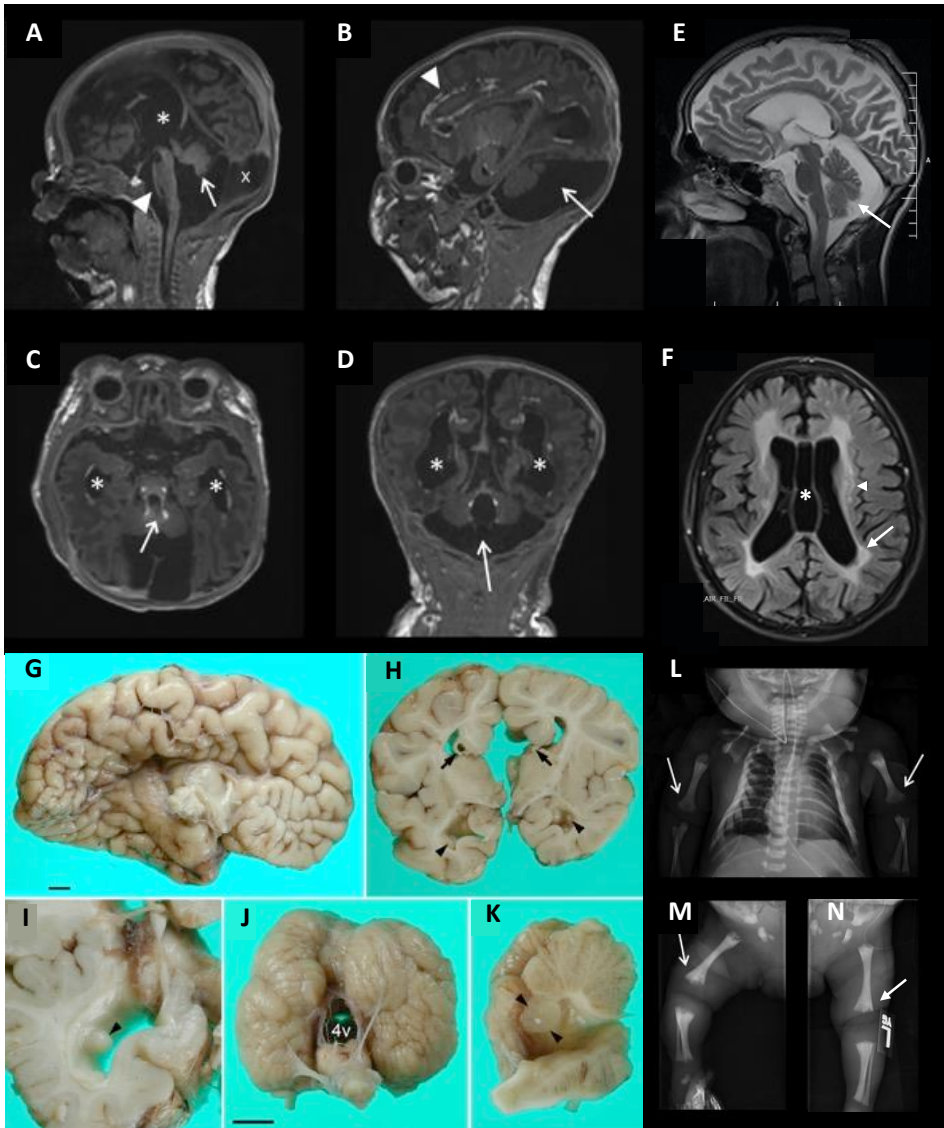


Figure 2: Macroscopic abnormalities of brain and bone in CSF1R deficiency.

A-D T1 weighted MRI without contrast of individual II-1 from family CSF1R_01. **A** Midsagittal section shows agenesis of corpus callosum (asterisk), pontocerebellar hypoplasia (arrowhead), and small and upwardly rotated cerebellar vermis (arrow) with large posterior fossa cyst ("X"). **B** Parasagittal section shows diffuse calcifications along lateral ventricles (arrowhead) and small cerebellum and posterior fossa cyst (arrow). **C** Horizontal section shows periventricular calcification around 3rd and lateral ventricles (arrow and asterisks, respectively). **D** Coronal section showing ventriculomegaly (asterisks), hypoplasia of cerebellar hemispheres and large posterior fossa cyst (arrow). **E-F** T2 Flair images of individual II-4 from family CSF1R_02. **E** Midsagittal section showing cerebellar vermis hypoplasia/atrophy (arrow) **F** Horizontal section shows leukodystrophy (arrow)

periventricular calcification (arrowhead), and cavum septum pellucidum (asterisk). **G-K** Gross neuropathology of individual II-1 from family CSFR1_01. **G** Medial view of left hemisphere. The corpus callosum and cingulate sulcus were absent. **H** Coronal slice of cerebrum at the level of the thalamus revealed small bilateral Probst bundles (arrows), reduced white/gray ratio, abnormally configured hippocampi, small basal ganglia, and periventricular heterotopia (arrowheads) protruding into the temporal horns of the lateral ventricles. **I** High magnification view of another periventricular heterotopia (arrowhead) in left temporal lobe. **J** Postero-inferior view of brainstem and cerebellum. The foramen of Magendie was dilated, revealing the fourth ventricle **4v**. The leptomeninges formed irregular adhesion-like connections between brainstem and cerebellum, which loosely covered the open foramen of Magendie but were disrupted after brain removal. **K** Medial view of left brainstem and cerebellum after sagittal bisection. A small arachnoidal cyst (arrowheads) displaced the posterior vermis superiorly. Scale bars: 1 cm for G, H; 1 cm for I-K. **L-M** X-rays of individual II-1 from family CSFR1_01 showing generalized increased bone density and metaphyseal dysplasia (arrows).

were identified. This 24-year old man (individual II-4 in Figure 1) presented with epilepsy and developmental regression at age 12 years (Table 1). MRI at age 24 years showed ventriculomegaly, severe leukodystrophy, periventricular calcifications, cerebellar vermis atrophy, cavum septum pellucidum, and mega cisterna magna (Figure 2E-F). Since the age of 12 he steadily lost developmental milestones and at the present time he is unable to walk, speak, read, or feed himself. His seizures were classified as generalized tonic-clonic and did not respond to multiple anti-epileptic drugs (AEDs); however he is currently seizure free and has not been taking AEDs for several years. His family history was notable for parental consanguinity and a brother (II-5) with a similar phenotype, died at age 21 (Figure 1). This individual (II-5) also had leukodystrophy, periventricular calcifications, developmental delay and epilepsy. Another sibling (II-6) died at age 4, but imaging and phenotypic details of this individual were not available. DNA was not available from either of these deceased individuals, but both parents (I-1 and I-2) and all three unaffected siblings (II-1, II-2 and II-3) were heterozygous for this variant (Figure S1). X-rays of individual II-4 at age 24 showed no evidence of osteopetrosis and there was no known history of hypocalcemia. There was no history of adult-onset neurologic disorder in the parents (ages 50 and 56 years) or the siblings (ages 18-34).

Using ACMGG guidelines³³ we classified this variant as likely pathogenic as follows: 1) it is absent from ExAC and gnomAD, as well as the Greater Middle East Variome and Iranome population databases (PM2); 2) it is located within the kinase domain, where the majority of pathogenic variation in this gene has been reported (PM1); 3) multiple *in silico* tools (polyphen,

SIFT) predict this variant to be damaging (PP3); and 4) segregation data is consistent (PP1). Together, our data suggest that homozygous *CSF1R* mutations cause a severe, pediatric onset neurodevelopmental condition that includes neuroimaging features that overlap with and are distinct from the adult onset condition caused by heterozygous *CSF1R* mutations.

Autopsy Findings

We were able to perform brain-only autopsy on the individual from family CSF1R_01 (II-1 in Figure 1). Gross examination identified ACC, ventriculomegaly, periventricular calcification and an expanded 4th ventricle with upward rotation of the cerebellar vermis (Dandy-Walker malformation), as detected by MRI (Figure 2G-K). Periventricular heterotopias of the lateral and 4th ventricles not recognized by MRI were detected at autopsy (Figure 2I). Histologic examination identified features also seen in ALS, including scattered foci of white matter atrophy, gliosis and dystrophic calcification, as well as abundant axonal spheroids in most white matter tracts, including corticospinal, dorsal column, and intracortical pathways (Figure 3A-H). In contrast to ALS, where microglia numbers are present but locally depleted,²⁰ we were unable to identify any microglia in the brain parenchyma (Figure 3I-T). We did identify a few CD68 and IBA1 positive cells, but these were clustered around small blood vessels and exhibited round rather than normal ramified morphology (Figure 3I-T; complete brain autopsy report found in Supplemental data). This data supports our conclusion that the homozygous c.1754-2A>G *CSF1R* mutations led to a brain that developed in the absence of normal numbers of microglia with numerous structural brain malformations.

We were unable to directly evaluate skeletal pathology in this patient, but hypothesize that a reduction in *CSF1R* signaling and developmental failure of yolk-sac derived tissue macrophages led to reduced numbers or function of osteoclasts. The presence of hypocalcemia and osteopetrosis is consistent with osteoclast failure (Table 1 and Figure 2L-N).

Model Organism Studies

To further explore mechanisms of brain development in the absence of microglia, we used recently developed zebrafish mutants.²⁰ Zebrafish have two *CSF1R* homologs, *csf1ra* and *csf1rb*. We engineered a 4 bp frameshifting deletion in exon 3 of *csf1rb* that results in a premature stop and crossed these fish to a previously generated missense mutation in *csf1ra*.²⁴ Microglia were not present

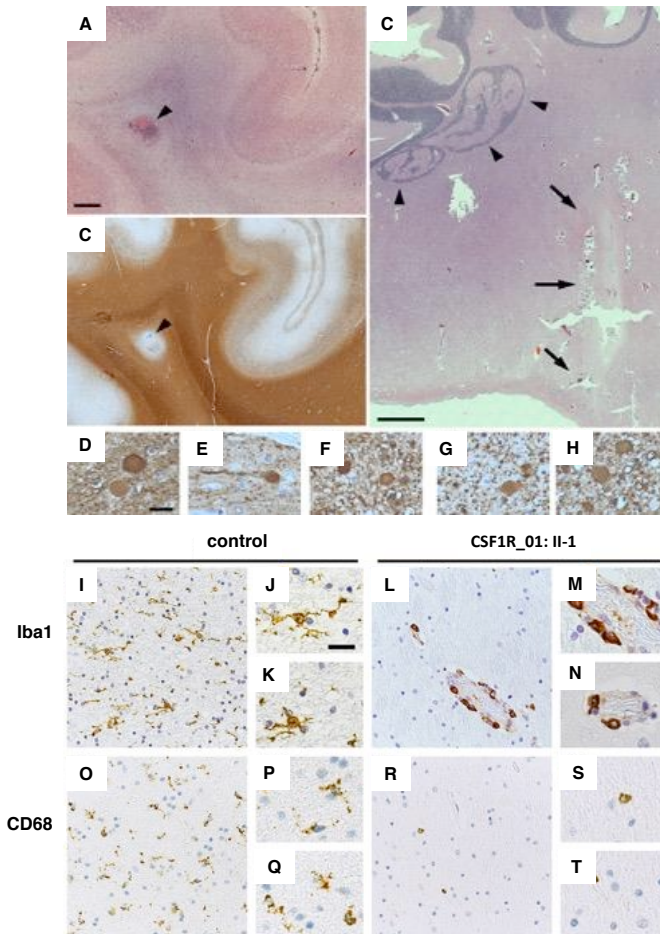


Figure 3: Microscopic brain abnormalities in CSF1R deficiency

A-H, L-N,R-T Sections from individual II-1 from family CSF1R_01; **I-K, O-Q** sections from control brain. **A,B** Adjacent sections through right frontal cortex, stained with H&E **A** and neurofilament protein immunohistochemistry **B**. The white matter contained a focus of calcification, necrosis, and axon loss (arrowheads). **C** Deep cerebellar white matter contained disorganized heterotopia (arrowheads) beneath the cerebellar cortex, and multiple periventricular foci of calcification and severe gliosis (arrows). Stained with H&E. **D-H** Neurofilament immunohistochemistry demonstrated axonal spheroids in many regions, such as right frontal white matter **D,E**, anterior **F** and lateral **G** corticospinal tracts, and nucleus cuneatus **H**. **I-K** Iba1 immunohistochemistry in control white matter labeled numerous microglia with long, ramified processes insinuating through brain tissue. **J** and **K** are enlarged two-fold relative to **I**. **L-N** Iba1 immunohistochemistry in white matter from individual II-1 revealed decreased numbers of microglia, with abnormal rounded morphology, located mainly in perivascular spaces. **M** and **N** are enlarged two-fold relative to **L**. **O-Q** CD68 immunohistochemistry in control white matter. **P** and **Q** are enlarged two-fold relative to **O**. **R-T** CD68 immunohistochemistry in white matter from individual II-1. **S** and **T** are enlarged two-fold relative to **R** Scale bars: **A** 1 cm for **A, B**. **C** 1 cm for **C** only. **D** 20 μm for **D-H**. 40 μm for **I, L, O, R**; 20 μm for **J, K, M, N, P, Q, S, T**.

4

in the brains of *csf1ra/csf1rb* double homozygous mutant (*csf1r^{DM}*) fish at five days post fertilization (Figure 4A-C). Similar to human *CSF1R* homozygous brain, we identified a few cells positive for zebrafish microglia marker L-plastin, which also lacked ramifications and were rounded (Figure 4C). To determine if *csf1r^{DM}* fish also showed evidence of osteopetrosis, similar to CSF1R_01, we

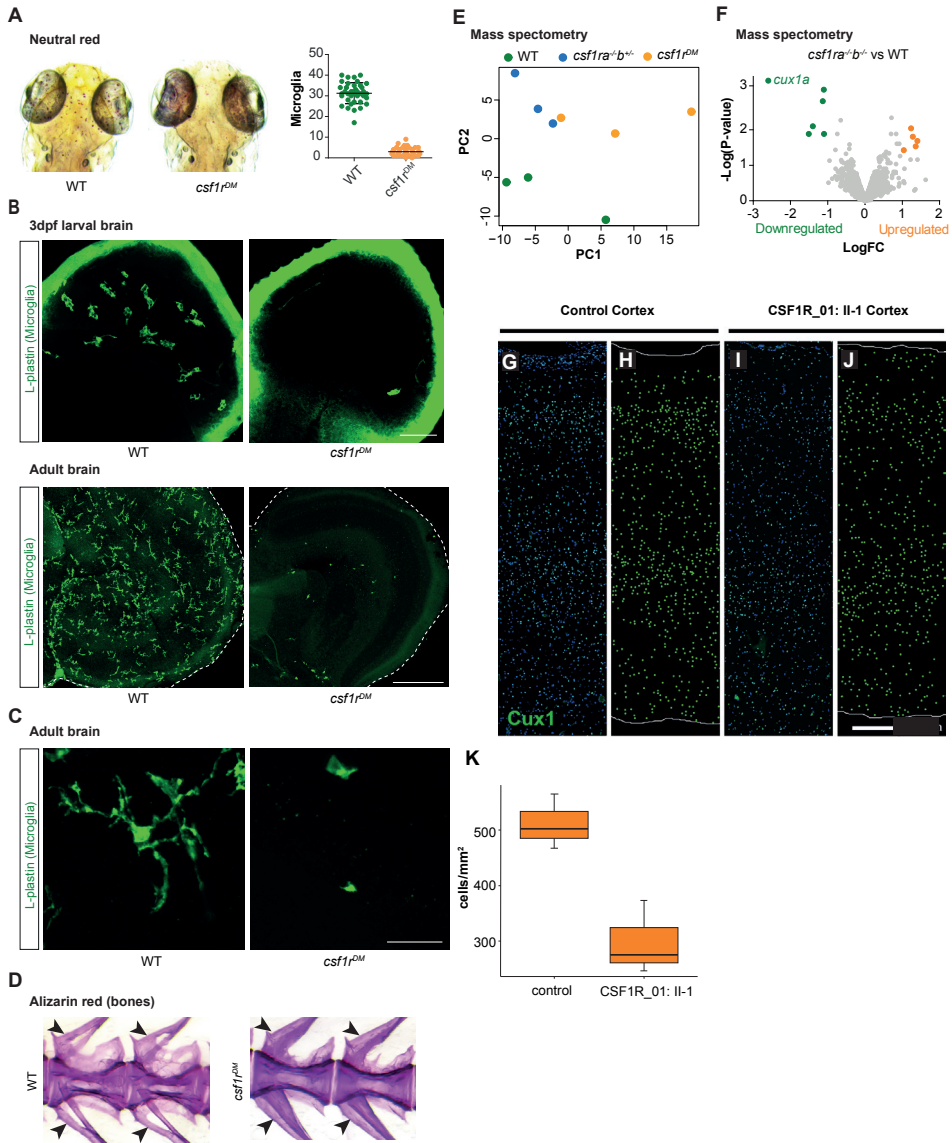


Figure 4: Analysis of *csf1r^{DM}* zebrafish and CSF1R deficient human cortex

A Neutral red staining and quantification of microglia in zebrafish larvae (5 days post fertilization). **B** Microglia immunostaining (L-plastin) in larval brains and adult brain sections of control and *csf1r^{DM}* zebrafish. **C** Microglia morphology in adult control and *csf1r^{DM}* zebrafish (L-plastin immunostaining). **D** Alizarin red staining of vertebrae and arches of adult control and *csf1r^{DM}* zebrafish (size-matched, age 6-8 months) Neural arch (upper arrow) and hemal arch (lower arrow) indicated **E** Principal component analysis (PCA) of mass spectrometry data of WT, *csf1ra^{-/-};b^{+/-}* and *csf1r^{DM}* adult zebrafish brains. *Csf1ra^{-/-};b^{+/-}* also have reduced microglia numbers. **F** Volcano plot showing differentially regulated proteins in *csf1r^{DM}* mutant brains as colored dots (FDR < 0.05,

LogFC > |1|). Volcano plot of *csf1ra*^{-/-}; *b*^{+/-} vs control brain is included as Figure S2. **G-L** CUX1+ cells were reduced in the cerebral cortex of CSF1R_01. CUX1 immunofluorescence (green) in control **G,H** and patient **I,J** lateral temporal neocortex. The images with DAPI (blue) counterstain are shown in **G,I**, and corresponding CUX1+ cell plots in **H,J**. **K** The density of CUX1+ cells was reduced in the cortex from three different areas of individual II-1, family CSF1R_01. Cortical regions in this analysis included left medial parietal, left lateral parietal, and left lateral temporal cortex (control) and left lateral temporal, right dorsolateral frontal, and right medial occipital cortex (CSF1R_01). Whiskers indicate 95% confidence interval, and difference between patient and control CUX1+ cell density was statistically significant ($p < 0.05$, one-sided t-test, and $p = 0.05$, one-sided exact Wilcoxon rank sums test). Scale bars: **B** 40 μm (larval brain), 100 μm (adult brain), **C** 20 μm , **G-I** 100 μm .

examined vertebral arches (Figure 4D). Vertebral arches that contain the spinal cord (neural) and dorsal aorta (hemal) were smaller in *csf1r*^{DM} fish compared to controls, as previously reported in osteopetrotic zebrafish mutants.³⁵ Therefore *csf1r*^{DM} fish display both deficiency in brain microglia as well as osteopetrosis, recapitulating some of the bone and brain phenotypes seen in the homozygous c.1754-2A>G CSF1R human patient.

Next, we performed proteomic analysis of *csf1r*^{DM} brains to explore underlying pathogenic mechanisms in human CSF1R mutant brains. Principal component analysis showed that the samples of the same genotype clustered together (Figure 4E), indicating consistent changes in protein levels among groups. The most highly downregulated protein was Cux1a (Figure 4F and see Table S2 for proteomic dataset), the zebrafish homologue of CUX1. CUX1 is a transcription factor present in subsets of neurons in all cortical layers, and is required for the formation of layer II/III callosal projections.²¹ We were intrigued by this finding, as it suggested a mechanism for the absence of corpus callosum seen in our patient that we could test by immunostaining cortical sections from CSF1R_01.

CUX1 cortical immunohistochemistry

Based on the zebrafish results, we hypothesized that CUX1+ neurons would also be decreased in CSF1R homozygous human brain. Sections of cerebral cortex from three different brain lobes from individual II-1 in family CSF1R_01 were processed and compared with sections from another age and sex matched autopsy case. The overall CUX1 laminar pattern was preserved, but immunoreactivity and density of CUX1+ cells was reduced (Figure 4G-L). Our data, together with the observation that CUX1 is also downregulated in

CSF1R deficient mice,³⁶ suggest an evolutionarily conserved role for CSF1R signaling in production or maintenance of CUX1+ neurons. We speculate that the decrease in the number of CUX1+ cells in the brains of our patient may have contributed to the ACC phenotype, as neurons from layers II-III contribute heavily to the corpus callosum.

Discussion

We report a detailed neuropathologic description of a human brain containing almost no microglia. Although scarce expression of *CSF1R* in neurons has recently been reported,^{36; 37} we believe the structural brain abnormalities are likely secondary to absence of myeloid cells, particularly microglia. Several observations support this claim. Brains of mice with neural lineage specific deletion of *Csf1r* (*Nestin^{cre/+};Csf1r^{fl/fl}*) do not exhibit ventriculomegaly, olfactory bulb atrophy, or ACC, all of which are seen in complete *Csf1r*-null mice.^{2; 36} Neonatal microglia have recently been shown to contribute to normal myelinogenesis in the developing mouse brain by secretion of trophic factors, including IGF1,^{3; 6} and oligodendrocyte differentiation from neuronal precursor cells (NPCs) is enhanced by soluble CSF1 ligand only in the presence of microglia in culture.^{36; 38} Microglia have also been reported to influence axonal outgrowth and positioning/migration of interneurons.⁵ In addition, a very recent study demonstrated transplanted bone-marrow derived cells could rescue the phenotypes of *Csf1r*-null mice.³⁹ Although a minor microglia-independent role for CSF1R cannot be completely ruled out,³⁸ these data suggest that the major neurodevelopmental defects caused by loss of CSF1R signaling are due to a lack of microglia. Although we do not precisely know how lack of microglia leads to the brain malformations seen in CSF1R_01 and _02, we speculate that their absence disrupts oligodendrocyte differentiation and myelinogenesis, as well as migration of interneurons, that could directly and indirectly lead to the widespread white matter abnormalities and heterotopias seen in these individuals. Further research is needed to address these questions.

More than 60 mutations in *CSF1R* have been reported in individuals with ALSP, the majority of which are missense or in-frame indels within the tyrosine kinase domain (Figure 1, Table S1). It has been suggested that these mutations produce disease via a dominant-negative mechanism, in which kinase-deficient CSF1R molecules dimerize with wild-type molecules, inactivating them.^{14; 40} Haploinsufficiency has also been proposed as a disease mechanism, with the adult onset of ALSP being caused by a steady decrease in

CSF1R levels, until it reaches a critical level.^{36; 41; 42} Our results provide genetic support that these mutations result in decreased CSF1R activity, possibly via both haploinsufficient or dominant negative mechanisms, depending on the mutation. Additional support for a loss-of-function disease mechanism comes from individuals with polycystic lipomembranous osteodysplasia with sclerosing leukoencephalopathy (PLOSL, aka Nasu-Hakola disease). Individuals with PLOSL develop progressive dementia and cognitive decline in their 4th decade of life, similar to ALSP; however, they also develop bony symptoms (bone cysts and pathological fractures) around the same time.^{18; 43-45} PLOSL is an autosomal recessive disease caused by loss of function mutations in components of the TREM2-TYROBP signaling complex, which interacts with CSF1R signaling, regulates osteoclast function, and is also present in microglia.⁴⁶⁻⁴⁸ Our patient's brain and bone features overlap somewhat with pathology observed in PLOSL, although with much earlier symptom onset. Together the evidence supports a loss-of-function mechanism for *CSF1R* mutations, both in ALSP and in individuals with homozygous *CSF1R* mutations.

There are at least two previous reports of individuals with similar features. In 1995 Rees *et al.* described two siblings with “infantile neuroaxonal dystrophy and osteopetrosis,” and, with great foresight, noted similarity to the spontaneously arising *osteopetrosis* mouse, now known to be due to mutations in *colony stimulating factor 1 (CSF1)*, the CSF1R ligand.⁴⁹ More recently, Monies *et al.* described two siblings with brain malformations and osteopetrosis, whose parents both carried the same heterozygous truncating *CSF1R* mutation, but DNA was unavailable from the siblings to confirm that they were both homozygous, and no pathologic data was available.³⁴ We summarized key phenotypic features of individuals with confirmed homozygous mutations (individual II-1 from family CSF1R_01 and individual II-4 from family CSF1R_02), likely homozygous mutations (Monies *et al.* sibs 1 and 2), and unsequenced individuals (Rees *et al.* sibs 1 and 2) in Table 1. Although the size of this cohort is insufficient to know the full phenotypic spectrum, agenesis of corpus callosum, periventricular calcifications, ventriculomegaly, osteopetrosis and hypocalcemia were seen in the majority, and axonal spheroids were seen in all individuals who underwent neuropathological examination.

Both individuals reported here had pediatric onset of disease, significantly earlier than been reported for ALSP. However, the phenotype of the individual from family CSF1R_01 (II-1) was significantly more severe than the individual from family CSF1R_02 (II-4), who remains alive at 24 years of

age, and whose brain MRI findings overlap with ALSP. We speculate that the p.H643Q single amino acid substitution is hypomorphic and results in relatively more CSF1R protein function than the exon 13 splice acceptor mutation (c.1754-1G>C) seen in CSF1R_01. Consistent with this hypothesis is the fact that the siblings reported by Monies *et al.*, who likely had a null mutation (c.620T>A, causing p.Tyr540*), demonstrated a perinatal lethal phenotype. Further studies of the impact of these mutations on CSF1R function are needed.

Several features of CSF1R_01's presentation -namely thrombocytopenia, transaminitis, intracranial calcifications, white matter loss, and failing the newborn hearing screen- are reminiscent of congenital infection. However, this individual presented with significant macrocephaly (+5 SD), whereas newborns with congenital infections are typically microcephalic. Aicardi-Goutieres syndrome (AGS) and the microcephaly-intracranial calcification syndrome (MICS, also known as pseudo-TORCH), also have overlapping presentations. Lumbar puncture was never performed in this individual, so we could not measure CSF cell counts or interferon-alpha levels. At the present we can only speculate as to the mechanism of the inflammatory like phenotype within the brain in the absence of microglia, the primary immune cells of the brain. Microglia, like other macrophages, have immune-regulatory roles as well, and it is possible that the lack of microglia leads to a failure to suppress immune responses. Alternatively, astrocytes have been shown to produce interferon-alpha, suggesting that cells other than microglia could also drive inflammation.⁵⁰

Significantly, there was no family history of adult onset neurodegenerative symptoms in either of the families we report, despite numerous individuals carrying heterozygous *CSF1R* mutations. Possible explanations include the age-related onset of symptoms, incomplete penetrance, or less deleterious variants in parents of children with pediatric-onset disease. This is similar to individuals with biallelic mutations in components of DNA mismatch repair proteins, who typically lack a family history of Lynch syndrome.⁵¹ The absence of a family history of ALSP cannot be used to rule out a possible diagnosis of biallelic *CSF1R* deficiency.

The zebrafish *csf1r^{DM}* model recapitulates both the bone and specific brain features of these disorders, making it an excellent new model to study microgliopathies and the consequences of microglia absence. As a demonstration of how this model can lead to new insights, we identified Cux1a as a protein whose levels were significantly decreased in *csf1r^{DM}* fish. We then

demonstrated that there is also a decrease in the density of CUX1+ neurons in human *CSF1R* brain sections. Further studies of *csf1r*-deficient zebrafish brain are needed to identify the precise cellular consequences of a lack of *Csf1r* signaling/depletion of microglia. Although our hypothesis- that a reduction in density of CUX1+ layer II/III neurons contributes to the ACC phenotype seen in our patient- remains speculative, it demonstrates the translational capacity of our new zebrafish microgliopathy model.

Lastly, our study exemplifies an under-recognized type of phenotypic expansion, in which genes associated with well-recognized, dominant phenotypes can produce different phenotypes when present in biallelic, recessive states. This is very important for interpretation and filtering of variants from genomic data, as candidate variants cannot be dismissed based on perceived poor phenotypic fit.³⁴

Declaration of Interests

The authors declare no competing interests.

Acknowledgements

We thank the patients and family for their consent and participation. I.J.C. is supported by the NIH T32GM007454. We also thank M. M. Formosa (University of Malta) for her help with the alizarin red staining. C.D.K. is supported by the Nancy and Buster Alvord Endowed Chair for Neuropathology. J.T.B. is supported by the Burroughs Wellcome Fund Career Award for Medical Scientists and the Arnold Lee Smith Endowed Professorship for Research Faculty Development. T.V.H. is supported by an Erasmus University Rotterdam fellowship.

Web Resources

www.omin.org, exac.broadinstitute.org, genome.ucsc.edu, www.genematcher.org, igm.ucsd.edu/gme, iranome.ir

	CSF1R_01: II-1	CSF1R_02: II-4	Monies et al. sib1	Monies et al. sib2	Rees et al. sib1	Rees et al. sib2
CSF1R Mutation (NM_005211.3)	c.1754-1G>C	c.1929C>A (p.His643Gln)	c.1620T>A (p.Tyr540*) ^a	c.1620T>A (p.Tyr540*) ^a	not sequenced	not sequenced
Symptom onset	Prenatal	<7y	Perinatal	Perinatal	Perinatal	Perinatal
Age at last evaluation	10m (death)	24y (living)	Perinatal (death)	Perinatal (death)	9m (death)	1m (death)
Consanguinity	+	+	+	+	-	-
More than 1 affected family member	-	+	+	+	+	+
Ethnicity	Native American	Arab	Arab	Arab	unk	unk
Gender	M	M	unk	unk	F	M
Developmental delay (onset)	+ (3m)	- (regression 12y)	unk	unk	unk	unk
Macrocephaly	present (+5SD)	absent	unk	unk	absent (10%)	"tower shaped"
Infantile hypotonia	+	unk	unk	unk	unk	unk
Spasticity	Mild	+ (spastic quad.)	unk	unk	unk	unk
Hyperreflexia	-	+	unk	unk	unk	unk
Epilepsy (onset)	Yes (8m)	Yes (12y)	unk	unk	unk	unk
Agenesis of corpus callosum	+	+ (hypoplastic)	+	+	+	+
Ventriculomegaly	+	+	+	+	+	+
Periventricular Calcification	+	+	+	+	unk	unk
Cerebellar hypoplasia/atrophy	+	+	+	+	unk	unk
Heterotopia	+	-	unk	unk	unk	unk
Leukodystrophy	+	+	unk	unk	+	unk
Mega Cisterna Magna	+	+	+	+	unk	unk
Upwardly rotated cerebellar vermis	+	-	+	+	unk	unk
Axonal spheroids	+	unk	unk	unk	+	unk
Osteopetrosis	+	-	+	+	+	+
Hypocalcemia	+	-	+	+	+	unk

Table 1: Phenotypes of 6 individuals with confirmed or possible biallelic *CSF1R* mutations
*mutation not confirmed but likely based on “linkage by exclusion”; “spastic quad.” = spastic quadriplegia; CSP = cavum septum pellucidum; unk = unknown because not reported in publication

References

1. Cunningham, C.L., Martinez-Cerdeno, V., and Noctor, S.C. (2013). Microglia regulate the number of neural precursor cells in the developing cerebral cortex. *J Neurosci* 33, 4216-4233.
2. Erblisch, B., Zhu, L., Etgen, A.M., Dobrenis, K., and Pollard, J.W. (2011). Absence of colony stimulation factor-1 receptor results in loss of microglia, disrupted brain development and olfactory deficits. In *PLoS ONE*. (Public Library of Science), p e26317.
3. Hagemeyer, N., Hanft, K.M., Akriditou, M.A., Unger, N., Park, E.S., Stanley, E.R., Staszewski, O., Dimou, L., and Prinz, M. (2017). Microglia contribute to normal myelinogenesis and to oligodendrocyte progenitor maintenance during adulthood. *Acta Neuropathol* 134, 441-458.
4. Paolicelli, R.C., Bolasco, G., Pagani, F., Maggi, L., Scianni, M., Panzanelli, P., Giustetto, M., Ferreira, T.A., Guiducci, E., Dumas, L., et al. (2011). Synaptic pruning by microglia is necessary for normal brain development. *Science* 333, 1456-1458.
5. Squarzoni, P., Oller, G., Hoeffel, G., Pont-Lezica, L., Rostaing, P., Low, D., Bessis, A., Ginhoux, F., and Garel, S. (2014). Microglia modulate wiring of the embryonic forebrain. *Cell Rep* 8, 1271-1279.
6. Wlodarczyk, A., Holtman, I.R., Krueger, M., Yogev, N., Bruttger, J., Khorooshi, R., Benmamar-Badel, A., de Boer-Bergsma, J.J., Martin, N.A., Karram, K., et al. (2017). A novel microglial subset plays a key role in myelinogenesis in developing brain. *EMBO J* 36, 3292-3308.
7. Chitu, V., and Stanley, E.R. (2006). Colony-stimulating factor-1 in immunity and inflammation. *Curr Opin Immunol* 18, 39-48.
8. Ginhoux, F., Greter, M., Leboeuf, M., Nandi, S., See, P., Gokhan, S., Mehler, M.F., Conway, S.J., Ng, L.G., Stanley, E.R., et al. (2010). Fate mapping analysis reveals that adult microglia derive from primitive macrophages. *Science* 330, 841-845.
9. Herbomel, P., Thisse, B., and Thisse, C. (2001). Zebrafish early macrophages colonize cephalic mesenchyme and developing brain, retina, and epidermis through a M-CSF receptor-dependent invasive process. *Dev Biol* 238, 274-288.
10. Stanley, E.R., Berg, K.L., Einstein, D.B., Lee, P.S., Pixture, F.J., Wang, Y., and Yeung, Y.G. (1997). Biology and action of colony-stimulating factor-1. *Mol Reprod Dev* 46, 4-10.
11. Baba, Y., Ghetti, B., Baker, M.C., Uitti, R.J., Hutton, M.L., Yamaguchi, K., Bird, T., Lin, W., DeLucia, M.W., Dickson, D.W., et al. (2006). Hereditary diffuse leukoencephalopathy with spheroids: clinical, pathologic and genetic studies of a new kindred. In *Acta Neuropathol*. pp 300-311.
12. Konno, T., Tada, M., Tada, M., Nishizawa, M., and Ikeuchi, T. (2014). [Hereditary diffuse leukoencephalopathy with spheroids (HDLS): a review of the literature on its clinical characteristics and mutations in the colony-stimulating factor-1 receptor gene]. In *Brain Nerve*. pp 581-590.
13. Nicholson, A.M., Baker, M.C., Finch, N.A., Rutherford, N.J., Wider, C., Graff-Radford, N.R., Nelson, P.T., Clark, H.B., Wszolek, Z.K., Dickson, D.W., et al. (2013). CSF1R mutations link POLD and HDLS as a single disease entity. In *Neurology*. (Lippincott Williams & Wilkins), pp 1033-1040.
14. Rademakers, R., Baker, M., Nicholson, A.M., Rutherford, N.J., Finch, N., Soto-Ortolaza, A., Lash, J., Wider, C., Wojtas, A., DeJesus-Hernandez, M., et al. (2012). Mutations in the colony stimulating factor 1 receptor (CSF1R) gene cause hereditary diffuse leukoencephalopathy with spheroids. In *Nat Genet*. pp 200-205.
15. Sundal, C., Baker, M., Karrenbauer, V., Gustavsen, M., Bedri, S., Glaser, A., Myhr, K.-M., Haugarvoll, K., Zetterberg, H., Harbo, H., et al. (2015). Hereditary diffuse leukoencephalopathy with spheroids with phenotype of primary progressive multiple sclerosis. In *Eur J Neurol*. pp 328-333.
16. Wider, C., and Wszolek, Z.K. (2014). Hereditary diffuse leukoencephalopathy with axonal spheroids: more than just a rare disease. In *Neurology*. (Lippincott Williams & Wilkins), pp 102-103.
17. van der Knaap, M.S., and Bugiani, M. (2017). Leukodystrophies: a proposed classification system based on pathological changes and pathogenetic mechanisms. *Acta Neuropathol* 134, 351-382.
18. Bianchin, M.M., Martin, K.C., de Souza, A.C., de Oliveira, M.A., and Rieder, C.R. (2010). Nasu-Hakola disease and primary microglial dysfunction. *Nat Rev Neurol* 6, 2 p following 523.
19. Prinz, M., and Priller, J. (2014). Microglia and brain macrophages in the molecular age: from origin to neuropsychiatric disease. *Nat Rev Neurosci* 15, 300-312.
20. Oosterhof, N., Kuil, L.E., van der Linde, H.C., Burm, S.M., Berdowski, W., van Ijcken, W.F.J., van Swieten, J.C., Hol, E.M., Verheijen, M.H.G., and

- van Ham, T.J. (2018). Colony-Stimulating Factor 1 Receptor (CSF1R) Regulates Microglia Density and Distribution, but Not Microglia Differentiation In Vivo. *Cell Rep* 24, 1203-1217 e1206.
21. Rodríguez-Tornos, F.M., Briz, C.G., Weiss, L.A., Sebastian-Serrano, A., Ares, S., Navarrete, M., Frangeul, L., Galazo, M., Jabaudon, D., Esteban, J.A., et al. (2016). Cux1 Enables Interhemispheric Connections of Layer II/III Neurons by Regulating Kv1-Dependent Firing. *Neuron* 89, 494-506.
 22. Makrythanasis, P., Maroofian, R., Stray-Pedersen, A., Musaev, D., Zaki, M.S., Mahmoud, I.G., Selim, L., Elbadawy, A., Jhangiani, S.N., Coban Akdemir, Z.H., et al. (2018). Biallelic variants in KIF14 cause intellectual disability with microcephaly. *Eur J Hum Genet* 26, 330-339.
 23. Retterer, K., Juusola, J., Cho, M.T., Vitazka, P., Millan, F., Gibellini, F., Vertino-Bell, A., Smaoui, N., Neidich, J., Monaghan, K.G., et al. (2016). Clinical application of whole-exome sequencing across clinical indications. *Genet Med* 18, 696-704.
 24. Parichy, D.M., Ransom, D.G., Paw, B., Zon, L.I., and Johnson, S.L. (2000). An orthologue of the kit-related gene *fms* is required for development of neural crest-derived xanthophores and a subpopulation of adult melanocytes in the zebrafish, *Danio rerio*. *Development* 127, 3031-3044.
 25. Liu, Y., Luo, D., Lei, Y., Hu, W., Zhao, H., and Cheng, C.H. (2014). A highly effective TALEN-mediated approach for targeted gene disruption in *Xenopus tropicalis* and zebrafish. *Methods* 69, 58-66.
 26. Herbomel, P., Thisse, B., and Thisse, C. (1999). Ontogeny and behaviour of early macrophages in the zebrafish embryo. *Development* 126, 3735-3745.
 27. Oosterhof, N., Kuil, L.E., and van Ham, T.J. (2017). Microglial Activation by Genetically Targeted Conditional Neuronal Ablation in the Zebrafish. *Methods Mol Biol* 1559, 377-390.
 28. van Ham, T.J., Brady, C.A., Kalicharan, R.D., Oosterhof, N., Kuipers, J., Veenstra-Algra, A., Sjollem, K.A., Peterson, R.T., Kampinga, H.H., and Giepmans, B.N. (2014). Intravital correlated microscopy reveals differential macrophage and microglial dynamics during resolution of neuroinflammation. *Dis Model Mech* 7, 857-869.
 29. Cipriani, S., Nardelli, J., Verney, C., Delezoid, A.L., Guimiot, F., Gressens, P., and Adle-Biassette, H. (2016). Dynamic Expression Patterns of Progenitor and Pyramidal Neuron Layer Markers in the Developing Human Hippocampus. *Cereb Cortex* 26, 1255-1271.
 30. Hevner, R.F., Daza, R.A., Englund, C., Kohtz, J., and Fink, A. (2004). Postnatal shifts of interneuron position in the neocortex of normal and reeler mice: evidence for inward radial migration. *Neuroscience* 124, 605-618.
 31. Huber, W., von Heydebreck, A., Sultmann, H., Poustka, A., and Vingron, M. (2002). Variance stabilization applied to microarray data calibration and to the quantification of differential expression. *Bioinformatics* 18 Suppl 1, S96-104.
 32. Ritchie, M.E., Phipson, B., Wu, D., Hu, Y., Law, C.W., Shi, W., and Smyth, G.K. (2015). limma powers differential expression analyses for RNA-sequencing and microarray studies. *Nucleic Acids Res* 43, e47.
 33. Richards, S., Aziz, N., Bale, S., Bick, D., Das, S., Gastier-Foster, J., Grody, W.W., Hegde, M., Lyon, E., Spector, E., et al. (2015). Standards and guidelines for the interpretation of sequence variants: a joint consensus recommendation of the American College of Medical Genetics and Genomics and the Association for Molecular Pathology. *Genet Med* 17, 405-424.
 34. Monies, D., Maddirevula, S., Kurdi, W., Alanazy, M.H., Alkhalidi, H., Al-Owain, M., Sulaiman, R.A., Faqeih, E., Goljan, E., Ibrahim, N., et al. (2017). Autozygosity reveals recessive mutations and novel mechanisms in dominant genes: implications in variant interpretation. *Genet Med* 19, 1144-1150.
 35. Meireles, A.M., Shiao, C.E., Guenther, C.A., Sidik, H., Kingsley, D.M., and Talbot, W.S. (2014). The phosphate exporter *xpr1b* is required for differentiation of tissue-resident macrophages. *Cell Rep* 8, 1659-1667.
 36. Nandi, S., Gokhan, S., Dai, X.M., Wei, S., Enikolopov, G., Lin, H., Mehler, M.F., and Stanley, E.R. (2012). The CSF-1 receptor ligands IL-34 and CSF-1 exhibit distinct developmental brain expression patterns and regulate neural progenitor cell maintenance and maturation. *Dev Biol* 367, 100-113.
 37. Luo, J., Elwood, F., Britschgi, M., Villeda, S., Zhang, H., Ding, Z., Zhu, L., Alabsi, H., Getachew, R., Narasimhan, R., et al. (2013). Colony-stimulating factor 1 receptor (CSF1R) signaling in injured neurons facilitates protection and survival. *J Exp Med* 210, 157-172.
 38. Chitu, V., and Stanley, E.R. (2017). Regulation of Embryonic and Postnatal Development by the CSF-1 Receptor. *Curr Top Dev Biol* 123, 229-275.

39. Bennett, F.C., Bennett, M.L., Yaqoob, F., Mulinyawe, S.B., Grant, G.A., Hayden Gephart, M., Plowey, E.D., and Barres, B.A. (2018). A Combination of Ontogeny and CNS Environment Establishes Microglial Identity. *Neuron*.
40. Pridans, C., Sauter, K.A., Baer, K., Kissel, H., and Hume, D.A. (2013). CSF1R mutations in hereditary diffuse leukoencephalopathy with spheroids are loss of function. In *Scientific Reports*. (Nature Publishing Group), p 3013.
41. Adams, S.J., Kirk, A., and Auer, R.N. (2018). Adult-onset leukoencephalopathy with axonal spheroids and pigmented glia (ALSP): Integrating the literature on hereditary diffuse leukoencephalopathy with spheroids (HDLS) and pigmentary orthochromatic leukodystrophy (POLD). *J Clin Neurosci* 48, 42-49.
42. Hoffmann, S., Murrell, J., Harms, L., Miller, K., Meisel, A., Brosch, T., Scheel, M., Ghetti, B., Goebel, H.H., and Stenzel, W. (2014). Enlarging the nosological spectrum of hereditary diffuse leukoencephalopathy with axonal spheroids (HDLS). *Brain Pathol* 24, 452-458.
43. Bianchin, M.M., Lima, J.E., Natel, J., and Sakamoto, A.C. (2006). The genetic causes of basal ganglia calcification, dementia, and bone cysts: DAP12 and TREM2. *Neurology* 66, 615-616; author reply 615-616.
44. Chouery, E., Delague, V., Bergougnoux, A., Koussa, S., Serre, J.L., and Megarbane, A. (2008). Mutations in TREM2 lead to pure early-onset dementia without bone cysts. *Hum Mutat* 29, E194-204.
45. Paloneva, J., Kestila, M., Wu, J., Salminen, A., Bohling, T., Ruotsalainen, V., Hakola, P., Bakker, A.B., Phillips, J.H., Pekkarinen, P., et al. (2000). Loss-of-function mutations in TYROBP (DAP12) result in a presenile dementia with bone cysts. *Nat Genet* 25, 357-361.
46. Kiialainen, A., Hovanes, K., Paloneva, J., Kopra, O., and Peltonen, L. (2005). Dap12 and Trem2, molecules involved in innate immunity and neurodegeneration, are co-expressed in the CNS. *Neurobiol Dis* 18, 314-322.
47. Otero, K., Turnbull, I.R., Poliani, P.L., Vermi, W., Cerutti, E., Aoshi, T., Tassi, I., Takai, T., Stanley, S.L., Miller, M., et al. (2009). Macrophage colony stimulating factor induces macrophage proliferation and survival through a pathway involving DAP12 and β -catenin. In *Nature Immunology*. (NIH Public Access), pp 734-743.
48. Paloneva, J., Mandelin, J., Kiialainen, A., Bohling, T., Prudlo, J., Hakola, P., Haltia, M., Kontinen, Y.T., and Peltonen, L. (2003). DAP12/TREM2 deficiency results in impaired osteoclast differentiation and osteoporotic features. *J Exp Med* 198, 669-675.
49. Rees, J.H., Vaughan, R.W., Kondeatis, E., and Hughes, R.A. (1995). HLA-class II alleles in Guillain-Barre syndrome and Miller Fisher syndrome and their association with preceding *Campylobacter jejuni* infection. *J Neuroimmunol* 62, 53-57.
50. Cuadrado, E., Jansen, M.H., Anink, J., De Filippis, L., Vescovi, A.L., Watts, C., Aronica, E., Hol, E.M., and Kuipers, T.W. (2013). Chronic exposure of astrocytes to interferon-alpha reveals molecular changes related to Aicardi-Goutieres syndrome. *Brain* 136, 245-258.
51. Wimmer, K., Kratz, C.P., Vasen, H.F., Caron, O., Colas, C., Entz-Werle, N., Gerdes, A.M., Goldberg, Y., Ilencikova, D., Muleris, M., et al. (2014). Diagnostic criteria for constitutional mismatch repair deficiency syndrome: suggestions of the European consortium 'care for CMMRD' (C4CMMRD). *J Med Genet* 51, 355-365.

Supplemental data

Supplemental Text 1: Complete Clinical Report for individual II-1, family CSF1R_01

This individual initially presented as a 1-day old, ex-35 week 4 day gestation male infant with macrocephaly, multiple congenital brain abnormalities including agenesis of the corpus callosum, ventriculomegaly, cerebellar hypoplasia, and skeletal anomalies. He had dysmorphic features including cranial asymmetry, flattened midface, depressed nasal bridge, deep palmar creases, and bony prominences in the bilateral parietal skull.

He was born via scheduled primary low cesarean section for multiple fetal anomalies to a primiparous mother of Native Alaskan ancestry with known consanguinity. There were no known antenatal infections or teratogenic exposures during pregnancy. Prenatal testing revealed elevated AFP (+8 MoM) on first trimester screen. Fetal MRIs repeatedly showed structural brain abnormalities including ventriculomegaly, pontocerebellar hypoplasia, agenesis of the corpus callosum, and small thorax/femur. Fetal echocardiogram was normal. Amniocentesis and microarray were performed, which did not show any pathogenic copy number variants but did reveal six regions of homozygosity totaling 89 Mb (3.1% of the autosomal genome). Birth weight was 4106 g (99th %tile, +3 SD) and head circumference was 40 cm (+5 SD). The macrocephaly was quite unusual, as most congenital infections (e.g TORCH) cause microcephaly. He was mechanically ventilated for respiratory failure shortly after birth and transferred to the NICU for higher level of care.

Postnatal brain MRI showed pontocerebellar hypoplasia, agenesis of the corpus callosum with colpocephaly, periventricular calcifications, and incomplete infolding of the perisylvian fissures (Figure 2). A retrocerebellar cyst and upturned roof of the 4th ventricle were also observed. Abdominal ultrasound showed borderline hepatomegaly but no splenomegaly, and grade 1 left pelviectasis. Skeletal survey showed generalized dense skeleton and irregular metaphyses (Figure 2). There was significant hypocalcemia but serum alkaline phosphatase levels were normal. Serum creatine kinase (CK) was elevated (6700 IU/L), all of which was MM isoenzyme by electrophoresis. He had mild but persistent transaminitis and thrombocytopenia. He failed BAER hearing screen. TORCH evaluation for congenital infections (toxoplasmosis IgG and IgM, urine CMV PCR) was negative. Ophthalmologic examination showed no evidence of chorioretinal lesions, cataracts, or coloboma. Urine organic acids and serum amino acids were non-diagnostic. CSF studies were not performed. Given the radiographic

and clinical findings suggestive of Raine syndrome, *FAM20C* was sequenced, but no pathogenic variants were found. Trio-based whole exome sequencing revealed biallelic homozygous pathogenic variants (NM_005211.3:c.1754-1G>C) in *CSF1R* (Figure 1).

Exome sequencing results demonstrated both parents (individuals I-1 and I-2) to possess the c.1754-1G>C *CSF1R* variant in heterozygous state. In light of this, the family history was extensively reviewed for any individuals with neurodegenerative condition or symptoms. There were no individuals in 4 generations who were described as having symptoms of neurodegeneration that could represent ALSP; however, the proband's parents were only 17 and 19 years of age, and all of the grandparents were in their mid to late 30's, so possibly too young to show symptoms of this age-related onset disorder.

His clinical course was complicated by progressive macrocephaly (+4.5 SD), hypercapnic respiratory failure, oromotor incoordination requiring gastrostomy feeding, intractable seizures starting at 8 months of age, and persistent hypocalcemia requiring IV calcium supplementation. He died at the age of 10 months in the setting of group A streptococcal bacteremia. The parents consented to a brain-only autopsy (see below).

Supplemental Text 2: Autopsy Report for individual II-1 from family CSF1R_01

A) GROSS NEUROPATHOLOGICAL EXAMINATION:

The whole brain fresh without dura weighed 1139 g, fixed 1041 g with ventricular fluid (without dura). The dura is normal without evidence of hemorrhage or mass lesions. The superior sagittal sinus is patent.

Externally the brain shows no evidence of herniations. The cerebral vasculature is unremarkable and the cranial nerves and olfactory bulbs are intact. The leptomeninges are normal over the cerebral convexities, but demonstrate thickening and redundancy over the posterior brainstem, forming a cystic cavity continuous with the fourth ventricle, resembling a Dandy-Walker cyst. There is no external evidence of cerebral cortical atrophy, asymmetry, or cerebral edema. The gyral configuration is unremarkable. The cerebellum is small but appropriately divided into vermis and hemispheres. The brainstem exhibits small pyramidal tracts in the medulla, and no definite decussation.

Coronal sections of the cerebral hemispheres reveal a normal gyral cerebral architecture with an even cortical ribbon distinctly separated from subcortical white matter. There is complete absence of the corpus callosum with

associated collapse of the fornix onto the thalamus inferiorly. The lateral ventricles are moderately enlarged, especially posteriorly (colpocephaly). The volume of hemispheric white matter relative to gray matter appears reduced, especially in periventricular zones (selective white matter atrophy). Multiple periventricular foci of discoloration and granular texture are observed, suspicious for calcifications. In the temporal lobes, multiple presumed periventricular heterotopia protrude into the lateral ventricles. The hippocampi appear malformed with anomalous gyrations. The deep grey nuclei, including the thalamus and neostriatum, appear unremarkable. The subcortical white matter displays scattered small foci of discoloration, possibly small calcifications.

There is a small cyst (~0.8 cm diameter) located within the enlarged fourth ventricle, attached to the ventricular surface of the left cerebellum. The cisterna magna is also enlarged and covered by thickened and redundant meninges, possibly representing a type of Dandy-Walker cyst. However, the vermis, although small and moderately rotated, appears well-formed with normal configuration of folia. Slices of the cerebellar hemispheres reveal small, irregular folia and indistinct deep nuclei. The cerebellum also has chalky calcifications within the periventricular white matter. Horizontal sections of the brainstem reveal small pyramidal tracts of the medulla, and no obvious decussation in the lower medulla.

C) MICROSCOPIC NEUROPATHOLOGICAL DESCRIPTION:

General observations: The brain shows numerous periventricular white matter calcifications with associated loss of axons and myelin. Numerous axonal spheroids are found throughout white matter (confirmed by neurofilament IHC). There is extensive moderate to severe reactive gliosis, involving white and gray matter, as seen by GFAP IHC. Multiple immunohistochemical stains for microglia, including CD11b, CD68, and IBA1, demonstrate a severe deficiency of immunoreactive cells. There are rare microglia, predominantly around blood vessels, characterized by abnormally round morphologies.

Cerebral cortex: Appropriately oriented sections of cerebral cortex exhibit normal laminar architecture with mild gliosis. Subcortical white matter demonstrates pallor with scattered calcifications, axonal spheroids, reactive astrocytes and Alzheimer's type II astrocytes. There is no significant inflammation or hypercellularity.

Ventricles and periventricular white matter: The lateral ventricles demonstrate multifocal loss of the ependymal lining with associated reactive gliotic surface.

Extending into the lateral ventricles are multiple exophytic heterotopia containing neurons and neuropil. The periventricular white matter exhibits scattered dystrophic calcifications, as well as focal small cystic and necrotic lesions.

Hippocampus: The hippocampus and adjacent temporal neocortex are abnormally convoluted. The dentate gyrus is small, wavy, and irregular but exhibits the usual trilaminar architecture. Reactive gliosis is demonstrated on GFAP IHC; however there is no evidence of selective loss of CA pyramidal neurons, or hypoxic-ischemic injury of the subiculum or hippocampus.

Brainstem and cerebellum: Axial sections of brainstem show large dystrophic calcifications scattered throughout. The cerebellar cortex is composed of attenuated and slightly distorted folia with intact external granule, molecular, Purkinje cell, and internal granule cell layers; however, there is patchy loss of Purkinje neurons. Cerebellar white matter tracts show scattered dystrophic calcifications and reactive gliosis. The fourth ventricular cyst is multiloculated with a gliotic lining that dissects up into the cerebellum, and is associated with atrophy of the cerebellar tissues. Adjacent to the cyst, within the cerebellum, there is also a focus of grey heterotopia. The meninges of the fourth ventricular cyst are largely fibrous, with an attenuated arachnoid lining.

D) NEUROPATHOLOGICAL DIAGNOSES

1. Severe microglia deficiency, consistent with genetic diagnosis of homozygous *CSF1R* mutation
2. Multiple brain malformations
 - a. Agenesis of corpus callosum
 - b. Periventricular heterotopia, temporal lobes, bilateral
 - c. Hippocampi with abnormal convolutions
 - d. Cerebellar heterotopia
 - e. Ventriculomegaly, moderate
 - f. Cystic fourth ventricle with non-dysplastic vermis (“mega cisterna magna”)
 - g. Subependymal cyst (0.8 cm), left cerebellum
 - h. Non-decussation of pyramidal tracts
3. Extensive axonal degeneration with numerous spheroids
4. Scattered intraparenchymal calcifications associated with brain tissue degeneration and gliosis, most abundant in white matter, especially periventricular regions

Supplemental Text 3: Detailed mass spectrometry and proteomics analysis

Dissected brains from 6-8 month-old zebrafish (3 brains per sample, samples in triplicate) were snap-frozen in liquid nitrogen. The brain tissue was cut and lysed in 1 ml 50 mM Tris/HCl pH 8.2, 0.5 % sodium deoxycholate (SDC) and MS-SAFE™ protease and phosphatase inhibitor using a Bioruptor ultasonicator (Diagenode). Protein concentrations were measured using the BCA assay (Thermo Scientific). Lysates were reduced with 5 mM DTT and cysteine residues were alkylated with 10 mM iodoacetamide. Protein was extracted by acetone precipitation at -20 °C overnight. Samples were centrifuged at 8,000 g for 10 min at 4 °C. The acetone was removed and the pellet was allowed to dry. The protein pellet (~4 mg protein) was dissolved in 1 ml 50 mM Tris/HCl pH 8.2, 0.5 % SDC and proteins were digested with LysC (1:200 enzyme:protein ratio) for 4 h at 37 °C. Next, trypsin was added (1:100 enzyme:protein ratio) and the digestion proceeded overnight at 30 °C. Digests were acidified with 50 µl 10 % formic acid (FA) and centrifuged at 8,000 g for 10 min at 4 °C to remove the precipitated SDC. The supernatant was transferred to a new centrifuge tube. The digests were purified with C18 solid phase extraction (Sep-Pak, Waters), lyophilized and stored at -20 °C.

Isobaric labeling of the enriched peptides was performed using the 10-plex tandem mass tag (TMT) reagents (Thermo Fisher Scientific) with some modifications to the method of Böhm *et al.*¹ Peptides were loaded onto 20 mg C18 cartridges prepared in-house. The C18 cartridges were washed once with 1 ml 0.1% TFA and two times with 1 mL of 50 mM KH₂PO₄ (pH 4.5). TMT reagents (0.8 mg) were dissolved in 10 µl of dry ACN and diluted with 200 µl 50 mM KH₂PO₄. This TMT solution was immediately loaded onto the column and labeling on column proceeded for 1 h at RT. Each of the 9 samples was labeled with a different TMT tag. After labeling columns were washed twice with 1 ml 2 % ACN / 0.2 % FA and the labeled peptides eluted with 1 ml 50 % ACN. TMT labeled samples were pooled and lyophilized.

TMT labeled peptides were subjected to offline orthogonal high-pH and reverse phase fractionation. TMT labeled peptides were solubilized in 0.1 % TFA and loaded onto a 20 mg PLRP-S cartridge made in-house. Cartridges were washed once with 1 ml 0.1 % TFA and three times with 1 ml milliQ water. Peptides were eluted step-wise from column with 5%, 10%, 15% and 50% ACN/ 10 mM ammonium formate (pH 10). The 4 fractions were dried by vacuum centrifugation and each fraction was reconstituted with 2 % ACN / 0.2 % FA for nLC-MS/MS analysis.

Mass spectra were acquired on an Oribtrap Lumos (Thermo) coupled to

an EASY-nLC 1200 system (Thermo). Peptides were separated on an in-house packed 75 μm inner diameter column containing 50 cm Waters CSH130 resin (3.5 μm , 130 \AA , Waters) with a gradient consisting of 2–20 % (ACN, 0.1 % FA) over 200 min at 300 nl/min. The column was kept at 50 $^{\circ}\text{C}$ in a NanoLC oven - MPI design (MS Wil GmbH). For all experiments, the instrument was operated in the data-dependent acquisition (DDA) mode. MS1 spectra were collected at a resolution of 120,000, with an automated gain control (AGC) target of 2E5 and a max injection time of 50 ms. The most intense ions were selected for MS/MS, top speed method 3 seconds cycle time. Precursors were filtered according to charge state (2-7), and monoisotopic peak assignment. Previously interrogated precursors were dynamically excluded for 70 seconds. Peptide precursors were isolated with a quadrupole mass filter set to a width of 1.2 Th. When applying the MS3 method, ion trap MS2 spectra were collected at an AGC of 5E4, max injection time of 50 ms and CID collision energy of 35 %. For Orbitrap MS3 spectra, the operation resolution was 60,000, with an AGC setting of 1E5 and a max injection time of 120 ms. The HCD collision energy was set to 65 % to ensure maximal TMT reporter ion yield. Synchronous precursor selection (SPS) was enabled at all times to include up to 5 MS2 fragment ions in the MS3 scan.

Peak lists were automatically created from raw data files using the Proteome Discoverer 2.1 (Thermo) software. The Mascot search algorithm (version 2.2, MatrixScience) was used for searching spectra against the Uniprot database (taxonomy: *Danio rerio*, version from December 2016). The peptide tolerance was set to 10 ppm and the fragment ion tolerance was set to 0.6 Da. A maximum number of 2 missed cleavages were allowed. TMT tags on peptide N termini/lysine residues (+229.162932 Da) and carbamidomethylation of cysteine residues (+57.02146 Da) were set as static modifications methionine oxidation (+15.99492 Da) was set as variable modification. The target false-discovery rate for both PSMs and peptides was set to 0.01. Only peptides marked 'high confidence' were taken into account for further analysis. Proteins were marked with 'high confidence' when they fulfilled the requirement for an FDR = 0.01. The co-isolation threshold was set to 75 % and the minimum signal-to-noise ratio to 10. For TMT quantification, a 0.01 Th window centered on the theoretical m/z value of each reporter ion was queried for the nearest signal intensity. Reporter ion intensities were adjusted to correct for the isotopic impurities of the different TMT reagents (according to the manufacturer's specifications). For further analysis we used the R packages vsn and limma^{2,3}.

Nucleotide (NM_005211.3)	Amino Acid Change	Reported by
c.620T>A	p.Tyr540*	Monies ⁴
c.699delA	p.Thr567Argfs*45	Guerreiro ⁵
c.1745T>C	p.Leu582Pro	Scuberth ⁶
c.1754-1G>C, c.1754-2A>G	p.Gly585_Lys619delinsAla	this paper , Rademakers ⁷
c.1765G>A	p.Gly589Arg	Konno ⁸
c.1766G>A	p.Gly589Glu	Rademakers ⁷
c.1786G>A	p.Val596Met	Lynch ⁹
c.1889T>G	p.Leu630Arg	Guerreiro ⁵
c.1897G>A	p.Glu633Lys	Rademakers, Lynch ^{7,9}
c.1901T>G	p.Leu634Arg	Lynch ⁹
c.1929C>A	p.His643Gln	this paper
c.1954G>C	p.Aal652Pro	Konno ⁸
c.1957T>C	p.Cys653Arg	Battisti ¹⁰
c.1958G>A	p.Cys653Tyr	Mitsui ¹¹
c.1990G>A	p.Glu664Lys	Eichler ¹²
c.2060dup	p.Ser688Glufs*13	Konno ⁸
c.2276C>T	p.Ser759Phe	Jin ¹³
c.2287G>C	p.Ala763Pro	Van Gerpen, Lynch ^{9,14}
c.2294G>A	p.Gly765Glu	Konno ⁸
c.2296A>G	p.Met766Val	Jin ¹³
c.2297T>C	p.Met766Thr	Rademakers ⁷
c.2308G>C	p.Aal770Pro	Rademakers ⁷
c.2320-2A>G	p.Cys774_Asn814del	Rademakers ⁷
c.2324T>A	p.Ile775Asn	Rademakers ⁷
c.2329C>T	p.Arg777Trp	Guerreiro ⁵
c.2330G>A	p.Arg777Gln	Mitsui ¹¹
c.2342C>T	p.Ala781Val	Karle ¹⁵
c.2342C>A	p.Ala781Glu	Konno ⁸
c.2344C>G	p.Arg782Gly	Foulds ¹⁶
c.2345G>A	p.Arg782His	Kinoshita ¹⁷
c.2350G>A	p.Val784Met	La Piana ¹⁸
c.2375C>A	p.Ala792Asp	Ueda ¹⁹
c.2378A>C	p.Lys793Thr	Kondo ²⁰
c.2381T>C	p.Ile794Thr	Rademakers, Guerreiro ^{5,7}
c.2442+1G>A,+1G>T, +2T>C,+5G>C	p.Cys774_Asn814delins- Gln...Gln	Saitoh, Konno, Kawakami, Rade- makers ^{7,8,21,22}
c.2450T>C	p.Leu817Pro	Guerreiro ⁵
c.2468C>T	p.Ala823Val	Terasawa ²³ (reported as c.2467C>T in paper)

c.2470C>T	p.Pro824Ser	Konno ⁸
c.2473G>A	p.Glu825Lys	Lynch ⁹
c.2480T>C	p.Ile827Thr	Guerreiro ⁵
c.2483T>C	p.Phe828Ser	Kleinfeld ²⁴
c.2498C>A	p.Thr833Lys	Codjia ²⁵
c.2509G>T	p.Asp837Tyr	Rademakers ⁷
c.2512G>C	p.Val838Leu	Karle ¹⁵
c.2522A>G	p.Tyr841Cys	Codjia ²⁵
c.2525G>T	p.Gly842Val	Codjia ²⁵
c.2527A>T	p.Ile843Phe	Battisti ¹⁰
c.2528T>A	p.Ile843Asn	Karle ¹⁵
c.2534T>C	p.Leu845Pro	Codjia ²⁵
c.2539G>A	p.Glu847Lys	Di Donato ²⁶
c.2540A>T	p.Glu847Val	Gore ²⁷
c.2541G>C	p.Glu847Asp	Guerreiro ⁵
c.2546_2548delTCT	p.Phe849del	Rademakers ⁷
c.2546T>C	p.Phe849Ser	Rademakers ⁷
c.2562T>A	p.Asn854Lys	Sundal ²⁸
c.2563C>A	p.Pro855Thr	Cheng ²⁹
c.2566T>C	p.Tyr856His	Guerreiro ⁵
c.2570C>T	p.Pro857Leu	Lynch ⁹
c.2603T>C	p.Leu868Pro	Rademakers ⁷
c.2624T>C	p.Met875Thr	Rademakers ⁷
c.2629C>T	p.Gln877*	Karle ¹⁵
c.2632C>A	p.Pro878Thr	Rademakers ⁷
c.2655-2A>G	p.Ile885Metfs*29	Guerreiro ⁵
c.2699G>A	p.Arg900Lys	Kortvelyessy ³⁰
c.2701C>T	p.Pro901Ser	Guerreiro ⁵
c.2717T>C	p.Ile906Thr	Battisti ¹⁰

Table S1: Complete list of all reported CSF1R variants used in Figure 1

Table S2 Differentially expressed proteins

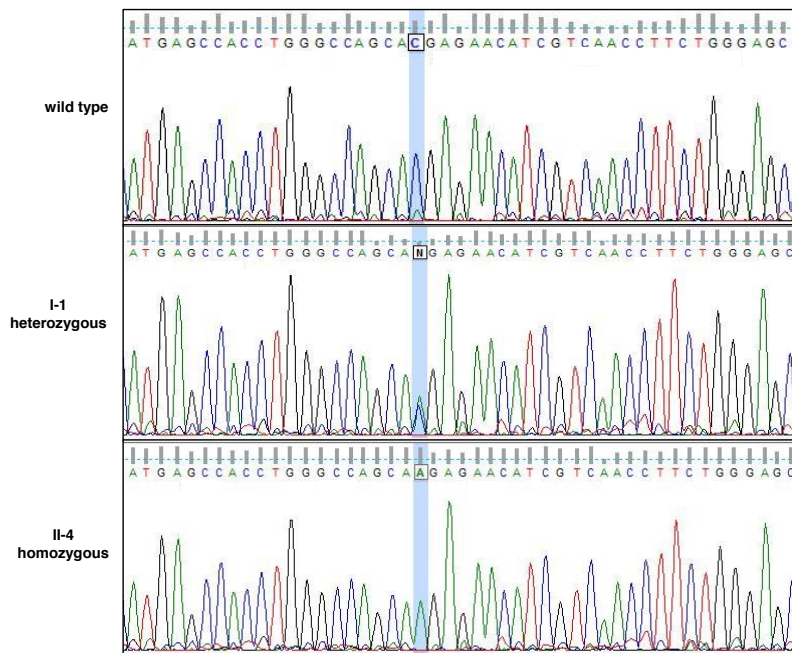


Figure S1: Sanger sequencing traces from family CSF1R_02: Location of the c.1929C>A (p.His643Gln) in CSF1R variant is highlighted in blue. Top is wild type control, middle is individual I-1 (father), and bottom is proband II-4.

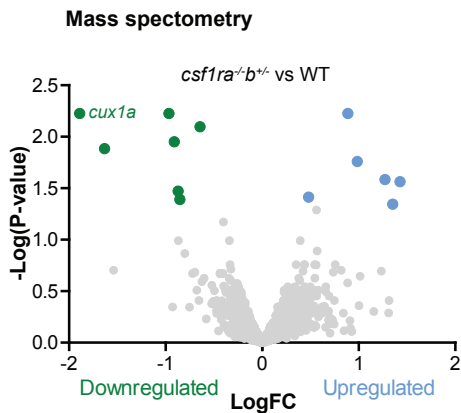
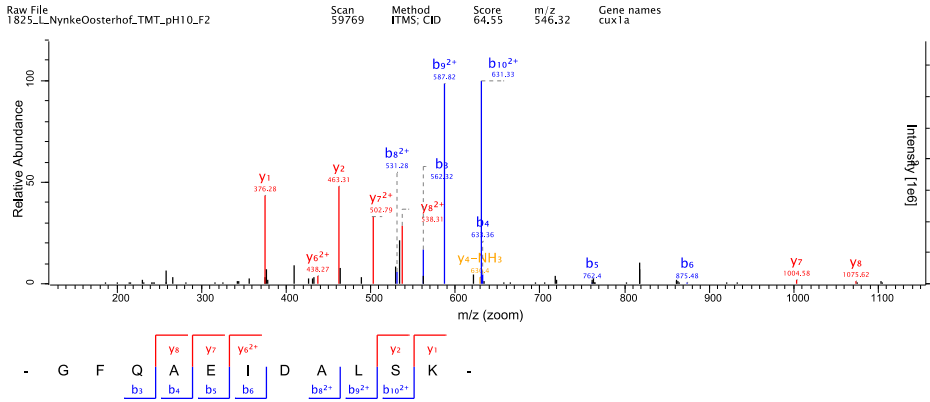


Figure S2 Volcano plot showing differentially expressed proteins in *csf1ra^{-/-};b^{+/-}* vs control brains.

The *csf1ra^{-/-};b^{+/-}* mutant zebrafish also have reduced microglia numbers.³¹ Significantly differentially expressed proteins are indicated in blue (upregulated) and green (downregulated). *Cux1a* is labeled in the upper left (green).



4

Figure S3 Cux1a peptide identified by mass spectrometry. Cux1a was the most highly downregulated protein. The tryptic peptide (GlyPheGlnAlaGlulleAspAlaLeuSerLys) analyzed to identify Cux1a is unique, and BLAST analysis across the zebrafish proteome indicated zebrafish Cux1a as the only perfect match. The next best hit was Cux1b, which did not possess a perfect match (SerPheGlnAlaGlulleAspAlaLeuSerLys), followed by proteins with poorly matching amino acid sequences. BLAST analysis of this tryptic peptide against all uniprot peptides identified only Cux1 homologs in other fish species, providing further evidence that this is a unique peptide.

Supplementary references

1. Bohm, G. et al. Low-pH Solid-Phase Amino Labeling of Complex Peptide Digests with TMTs Improves Peptide Identification Rates for Multiplexed Global Phosphopeptide Analysis. *J Proteome Res* 14, 2500-10 (2015).
2. Huber, W., von Heydebreck, A., Sultmann, H., Poustka, A. & Vingron, M. Variance stabilization applied to microarray data calibration and to the quantification of differential expression. *Bioinformatics* 18 Suppl 1, S96-104 (2002).
3. Ritchie, M.E. et al. limma powers differential expression analyses for RNA-sequencing and microarray studies. *Nucleic Acids Res* 43, e47 (2015).
4. Monies, D. et al. Autozygosity reveals recessive mutations and novel mechanisms in dominant genes: implications in variant interpretation. *Genet Med* 19, 1144-1150 (2017).
5. Guerreiro, R. et al. Genetic analysis of inherited leukodystrophies: genotype-phenotype correlations in the CSF1R gene. in *JAMA Neurol* Vol. 70 875-882 (American Medical Association, 2013).
6. Schubert, M. et al. [Hereditary diffuse leukoencephalopathy with spheroids: a microgliopathy due to CSF1 receptor impairment]. *Nervenarzt* 85, 465-70 (2014).
7. Rademakers, R. et al. Mutations in the colony stimulating factor 1 receptor (CSF1R) gene cause hereditary diffuse leukoencephalopathy with spheroids. in *Nat. Genet.* Vol. 44 200-205 (2012).
8. Konno, T., Tada, M., Tada, M., Nishizawa, M. & Ikeuchi, T. [Hereditary diffuse leukoencephalopathy with spheroids (HDLS): a review of the literature on its clinical characteristics and mutations in the colony-stimulating factor-1 receptor gene]. in *Brain Nerve* Vol. 66 581-590 (2014).
9. Lynch, D.S. et al. Hereditary leukoencephalopathy with axonal spheroids: a spectrum of phenotypes from CNS vasculitis to parkinsonism in an adult onset leukodystrophy series. in *J. Neurol. Neurosurg. Psychiatr.* Vol. 87 512-519 (BMJ Publishing Group Ltd, 2016).
10. Battisti, C. et al. Hereditary diffuse leukoencephalopathy with axonal spheroids: three patients with stroke-like presentation carrying new mutations in the CSF1R gene. in *J. Neurol.* Vol. 261 768-772 (Springer Berlin Heidelberg, 2014).
11. Mitsui, J. et al. CSF1R mutations identified in three families with autosomal dominantly inherited leukoencephalopathy. *Am J Med Genet B Neuropsychiatr Genet* 159B, 951-7 (2012).
12. Eichler, F.S. et al. CSF1R mosaicism in a family with hereditary diffuse leukoencephalopathy with spheroids. in *Brain* Vol. 139 1666-1672 (Oxford University Press, 2016).
13. Jin, C., Washimi, Y., Yoshida, K., Hashizume, Y. & Yazawa, I. Characterization of spheroids in hereditary diffuse leukoencephalopathy with axonal spheroids. in *J. Neurol. Sci.* Vol. 352 74-78 (Elsevier, 2015).
14. Van Gerpen, J.A. et al. Insights into the dynamics of hereditary diffuse leukoencephalopathy with axonal spheroids. in *Neurology* Vol. 71 925-929 (Lippincott Williams & Wilkins, 2008).
15. Karle, K.N. et al. De novo mutations in hereditary diffuse leukoencephalopathy with axonal spheroids (HDLS). in *Neurology* Vol. 81 2039-2044 (Lippincott Williams & Wilkins, 2013).
16. Foulds, N. et al. Adult-Onset Leukoencephalopathy with Axonal Spheroids and Pigmented Glia Caused by a Novel R782G Mutation in CSF1R. in *Scientific Reports* Vol. 5 10042 (Nature Publishing Group, 2015).
17. Kinoshita, M., Yoshida, K., Oyanagi, K., Hashimoto, T. & Ikeda, S. Hereditary diffuse leukoencephalopathy with axonal spheroids caused by R782H mutation in CSF1R: case report. *J Neurol Sci* 318, 115-8 (2012).
18. La Piana, R., Webber, A., Guiot, M.-C., Del Pilar Cortes, M. & Brais, B. A novel mutation in the CSF1R gene causes a variable leukoencephalopathy with spheroids. in *Neurogenetics* Vol. 15 289-294 (Springer Berlin Heidelberg, 2014).
19. Ueda, S. et al. A novel A792D mutation in the CSF1R gene causes hereditary diffuse leukoencephalopathy with axonal spheroids characterized by slow progression. *eNeurological Sci* 1, 7-9 (2015).
20. Kondo, Y., Kinoshita, M., Fukushima, K., Yoshida, K. & Ikeda, S. Early involvement of the corpus callosum in a patient with hereditary diffuse leukoencephalopathy with spheroids carrying the de novo K793T mutation of CSF1R. *Intern Med* 52, 503-6 (2013).
21. Kawakami, I. et al. A family with hereditary diffuse leukoencephalopathy with spheroids caused by a novel c.2442+2T>C mutation in the CSF1R gene. *J Neurol Sci* 367, 349-55 (2016).
22. Saitoh, B.Y. et al. A case of hereditary diffuse leukoencephalopathy with axonal spheroids

caused by a de novo mutation in CSF1R masquerading as primary progressive multiple sclerosis. *Mult Scler* 19, 1367-70 (2013).

23. Terasawa, Y. et al. Increasing and persistent DWI changes in a patient with hereditary diffuse leukoencephalopathy with spheroids. *J Neurol Sci* 335, 213-5 (2013).
24. Kleinfeld, K. et al. Adult-onset leukoencephalopathy with neuroaxonal spheroids and pigmented glia: report of five cases and a new mutation. in *J. Neurol.* Vol. 260 558-571 (Springer-Verlag, 2013).
25. Codjia, P. et al. Adult-Onset Leukoencephalopathy with Axonal Spheroids and Pigmented Glia: An MRI Study of 16 French Cases. *AJNR Am J Neuroradiol* 39, 1657-1661 (2018).
26. Di Donato, I. et al. A Novel CSF1R Mutation in a Patient with Clinical and Neuroradiological Features of Hereditary Diffuse Leukoencephalopathy with Axonal Spheroids. *J Alzheimers Dis* 47, 319-22 (2015).
27. Gore, E., Manley, A., Dees, D., Appleby, B.S. & Lerner, A.J. A young-onset frontal dementia with dramatic calcifications due to a novel CSF1R mutation. in *Neurocase* Vol. 22 257-262 (2016).
28. Sundal, C. et al. Parkinsonian features in hereditary diffuse leukoencephalopathy with spheroids (HDLS) and CSF1R mutations. in *Parkinsonism Relat. Disord.* Vol. 19 869-877 (Elsevier, 2013).
29. Cheng, X. et al. [Analysis of CSF1R gene mutation in a Chinese family with hereditary diffuse leukoencephalopathy with neuroaxonal spheroids]. *Zhonghua Yi Xue Yi Chuan Xue Za Zhi* 32, 208-12 (2015).
30. Kortvelyessy, P. et al. Hereditary diffuse leukoencephalopathy with spheroids (HDLS) with a novel CSF1R mutation and spinal cord involvement. *J Neurol Sci* 358, 515-7 (2015).
31. Oosterhof, N., Kuil, L.E., van der Linde, H.C., Burm, S.M., Berdowski, W., van Ijcken, W.F.J., van Swieten, J.C., Hol, E.M., Verheijen, M.H.G., and van Ham, T.J. (2018). Colony-Stimulating Factor 1 Receptor (CSF1R) Regulates Microglia Density and Distribution, but Not Microglia Differentiation In Vivo. *Cell Rep* 24, 1203-1217 e1206.

Chapter 5

***In vivo*, colony-stimulating factor 1 receptor regulates microglia density and distribution, but not microglia differentiation**

Nynke Oosterhof¹, Laura E. Kuil¹, Herma C. van der Linde¹, Saskia M. Burm², Woutje Berdowski¹, Wilfred F.J. van IJcken³, John C. van Swieten^{4,5}, Elly M. Hol^{2,6}, Mark H.G. Verheijen⁷, Tjakko J. van Ham¹

¹Department of Clinical Genetics, Erasmus University Medical Center, Rotterdam, Wytemaweg 80, 3015 CN, the Netherlands.

²Department of Translational Neuroscience, Brain Center Rudolf Magnus, University Medical Center Utrecht, Utrecht University, Utrecht, the Netherlands.

³Center for Biomics, Erasmus Medical Center, Wytemaweg 80, 3015 CN Rotterdam, the Netherlands.

⁴Department of Neurology, Erasmus Medical Center, Rotterdam, the Netherlands.

⁵Department of Clinical Genetics, VU Medical Center, Amsterdam, the Netherlands.

⁶Department of Neuroimmunology, Netherlands Institute for Neuroscience, an institute of the Royal Netherlands Academy of Arts and Sciences, the Netherlands.

⁷Department of Molecular and Cellular Neurobiology, CNCR, Amsterdam Neuroscience, VU University, Amsterdam, the Netherlands

Cell reports, 2018

Abstract

Microglia are brain resident macrophages with trophic and phagocytic functions. Dominant loss-of-function mutations in a key microglia regulator, colony-stimulating factor 1 receptor (CSF1R), cause adult onset leukoencephalopathy with axonal spheroids (ALSP), a progressive white matter disorder. As it remains unclear precisely how *CSF1R* mutations affect microglia, we generated an allelic series of *csf1r* mutants in zebrafish to identify *csf1r*-dependent microglia changes. We found that *csf1r* mutations led to aberrant microglia density and distribution, and regional loss of microglia. Remaining microglia still had a microglia-specific gene expression signature, indicating that they had differentiated normally. Strikingly, we also observed lower microglia numbers and widespread microglia depletion in post mortem brain tissue of ALSP patients. Both in zebrafish and in human disease, local microglia loss also presented in regions without obvious pathology. Together, this implies that CSF1R mainly regulates microglia density and that early loss of microglia may contribute to ALSP pathogenesis.

Introduction

Microglia are specialized brain macrophages whose functions in the brain include phagocytosis and provision of trophic support (1-5). Mutations in several genes that are highly expressed in microglia cause progressive white matter brain diseases (6-9). For example, dominant loss-of-function mutations in colony-stimulating factor 1 receptor (CSF1R) cause adult-onset leukoencephalopathy with axonal spheroids and pigmented glia (ALSP), also known as hereditary diffuse leukoencephalopathy with axonal spheroids (HDLS) (10, 11). Even though low expression of *Csf1r* has been reported in some neurons in the hippocampus, the expression of *CSF1R* is almost exclusive to microglia, suggesting that ALSP pathogenesis involves microglia dysfunction (12). But where one study showed reduced microglia numbers in cortical layers 3 and 4 in postmortem end-stage ALSP brain sections, another showed increased microglia numbers during earlier ALSP disease stages (13, 14). The mechanism whereby heterozygous *CSF1R* mutations affect microglia, and consequently brain homeostasis, is still unknown. Insight into ALSP pathogenesis will therefore contribute to our understanding of microglia function in the vertebrate brain and of microglia involvement in other brain diseases.

Even though CSF1R signal transduction has been studied extensively in macrophages, it is not entirely clear how defective CSF1R signaling affects microglia *in vivo*. Activation by one of the two CSF1R ligands, colony-stimulating factor 1 (CSF-1 or M-CSF) or interleukin 34 (IL-34) leads to auto-phosphorylation of the tyrosine kinase receptor. *In vitro*, downstream activation of signal transduction pathways regulates the production, survival, differentiation and function of macrophages (15-18). Genetic evidence for the consequences of CSF1R activation *in vivo* indicates that CSF1R primarily plays a homeostatic role in regulating the viability and proliferation of microglia (19, 20). Indeed, genetic deficiency of CSF1R signaling reduces protection against bacterial infection, mainly by limiting macrophage supply (15, 21-23). In contrast, by showing that *Csf1r*^{-/-} macrophage precursors have the same lineage potential as those in wildtype, differentiating efficiently into macrophages, but failing to form colonies, a recent study concluded that *Csf1r* deficiency has little effect on myeloid differentiation *in vivo* (24).

Loss of *Csf1r* in mice leads to an almost complete absence of microglia, and also to severe developmental abnormalities and a shorter lifespan (16-18). *Csf1r*^{-/-} brains show widened cerebral ventricles, which is also observed in ALSP patients. Mice lacking microglia also show cerebrovascular defects and

reduced numbers of oligodendrocyte lineage cells (18, 25, 26). In addition, postnatal pharmacological inhibition of CSF1R in mice reduces the number of oligodendrocytes and oligodendrocyte precursor cells (OPCs) in a region-dependent manner (25). The latter effect could predispose to myelination defects in later life.

To understand the effect of CSF1R haploinsufficiency on microglia we used the zebrafish as a model organism. Zebrafish are an upcoming genetic model organism to study brain diseases, including leukoencephalopathies (27). They are highly suitable for *in vivo* imaging, as they develop externally and are transparent at early stages (27-29). Previously, we identified the zebrafish microglia transcriptome, which shares high similarity with mouse and human microglia transcriptomes (30, 31). Zebrafish express two homologs of human *CSF1R*: *csf1ra* and *csf1rb*. We found that zebrafish *csf1ra* mutants show reduced microglia numbers only during development, thereby partially mimicking mouse mutants. This suggests that the cellular functions of CSF1R are highly conserved between species, but that zebrafish *csf1rb* and *csf1ra* are likely partially redundant. In the present study we therefore created an allelic series of zebrafish *csf1r* loss-of-function mutants in which we observed a local loss of microglia, a general reduction in microglia numbers, and an aberrant distribution of microglia. As we found that dysregulation of microglia density was a primary consequence of *csf1r* haploinsufficiency, we next investigated whether *CSF1R* haploinsufficiency also affects microglia density in postmortem brain tissue of ALS patients. This revealed widespread depletion of microglia and a general reduction in microglia density. In humans and zebrafish alike, changes in microglia density and distribution in the absence of obvious myelin pathology implied that loss of microglia may be an early event in ALS pathogenesis.

Results

Zebrafish *csf1ra* and *csf1rb* together are functionally homologous to mammalian CSF1R

To study how CSF1R mutations affect microglia and the brain, we exploited the fact that zebrafish have two homologs for human CSF1R: *Csf1ra* and *Csf1rb*. Both of these are highly expressed in adult zebrafish microglia (Fig. 1A)(30). Unlike *Csf1r* knock-out mice, which are almost completely devoid of microglia, zebrafish with homozygous loss-of-function mutations only in *csf1ra* (from here on: *csf1ra*^{-/-}), show reduced microglia numbers only during early development (32). This suggests that *csf1rb* and *csf1ra* share a role in microglia development.

To test this, we introduced a premature stop codon in exon 3 of the *csf1rb* gene by TALEN-mediated genome editing; and assessed microglia numbers by neutral red staining (Fig. 1B, S1A), which can be used to label microglia in zebrafish larvae *in vivo*. Whereas the microglia numbers in homozygous *csf1rb* mutants were a little lower than in wild type, mutants deficient in both *csf1ra* and *csf1rb* (from here on: *csf1r^{DM}*), were almost completely devoid of microglia (Fig. 1C,D). The absence of microglia in *csf1r^{DM}* mutants was confirmed in larval and adult zebrafish by immunostaining for L-plastin (Fig. 1E, 2A, B). Although microglia were almost completely absent in *csf1r^{DM}*, other macrophage populations were still present in adult organs, including the skin and the intestine (Fig. S1B). Adult *csf1r^{DM}* animals were viable, and, in-cross mating of *csf1r^{DM}* adult animals produced viable homozygous mutant offspring (data not shown). However, after around three months of age, mutant animals occasionally showed seizure-like behavior, and their survival rate was lower than that of wild type animals (data not shown). Some *csf1r^{DM}* brains displayed signs of cerebral hemorrhaging that were consistent with the hemorrhages previously reported in *Csf1r^{-/-}* mice (18). These data show that zebrafish *Csf1ra* and *Csf1rb* both regulate the development of the microglia population, and both are thus functionally homologous to mammalian CSF1R.

Csf1r regulates microglia density and distribution independently of brain pathology

Previous studies indicate that the density of tissue macrophages, including the microglia, is affected by reduced CSF1R signaling (33-36). To validate this in zebrafish, we used neutral red labeling and immunohistochemistry to assess microglia numbers in a series of *csf1r* mutant zebrafish larvae consisting of *csf1ra^{+/-}*, *csf1ra^{-/-}*, *csf1rb^{-/-}*, *csf1ra^{-/-};b^{+/-}* and *csf1r^{DM}* animals. In the larval stage, a gradual reduction in the number of *csf1r* alleles resulted in a corresponding decrease in microglia numbers (Fig. 1C,D,E). The greater reduction in microglia numbers in *csf1ra^{-/-}* mutants than in *csf1rb^{-/-}* mutants suggests that *csf1ra* is more important during early development. In adult zebrafish, however, microglia numbers in *csf1rb^{-/-}* mutants were strongly reduced, whereas in *csf1ra^{-/-}* mutants they were more comparable to those in wild type (Fig. 2F), suggesting differential requirements of *csf1ra* and *csf1rb* in microglia at different developmental stages. Surprisingly, in 5-month-old adult *csf1ra^{-/-};b^{+/-}* mutants, we observed that while microglia were absent in the dorsolateral side of the optic tectum, they appeared to accumulate in the underlying deep brain regions (Fig. 2G).

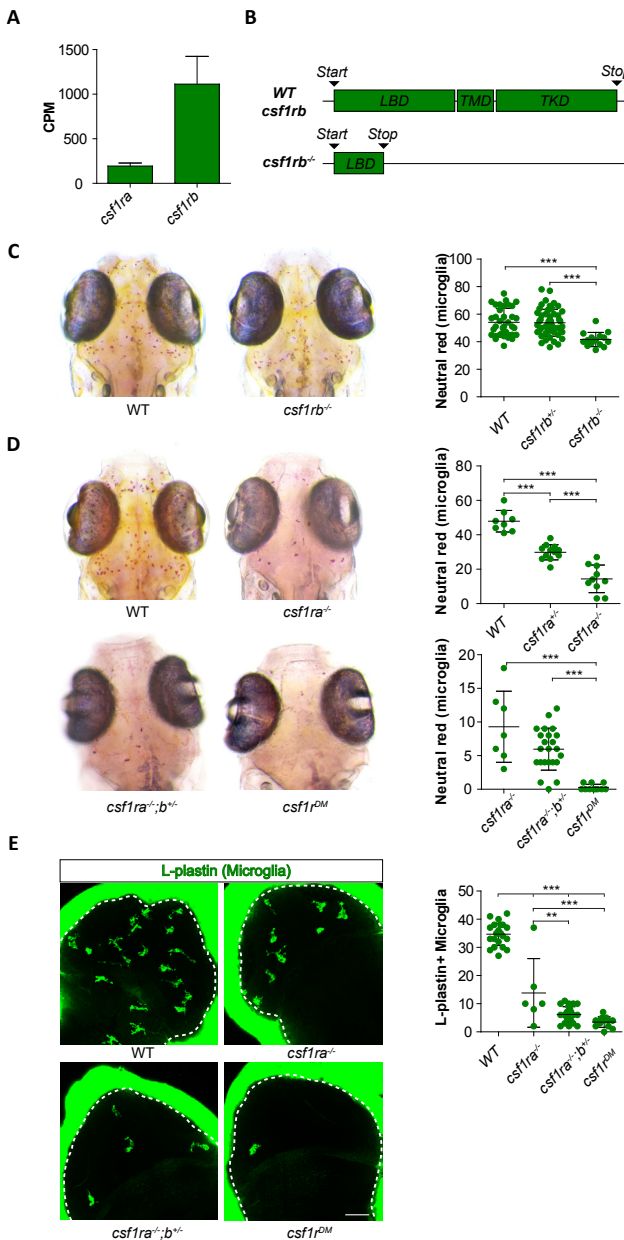
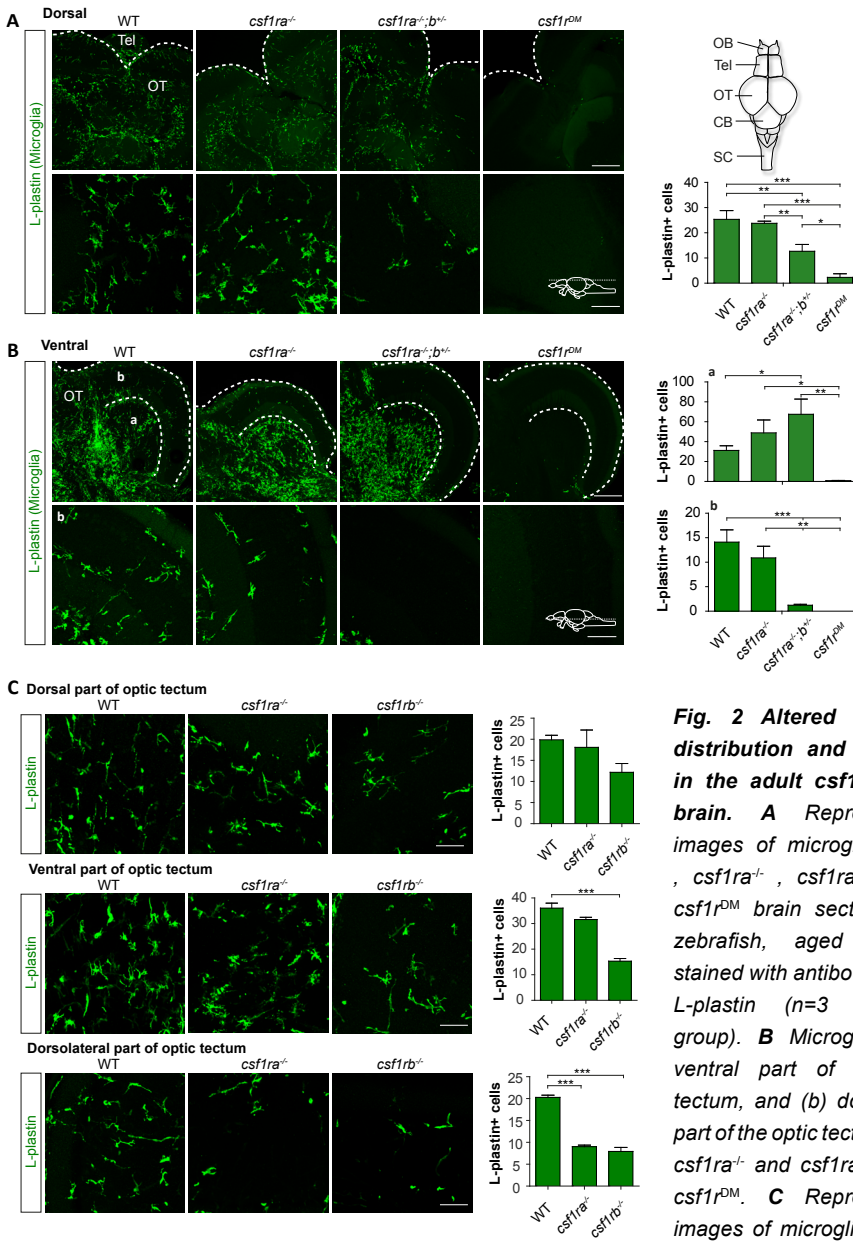


Fig. 1 Microglia numbers during development are *csf1r* dosage dependent.

A CPM expression values of *csf1ra* and *csf1rb* from our previous RNA sequencing study in adult zebrafish microglia (30). **B** Schematic representation of the *csf1rb* mutation introduced with TALEN-mediated genome editing. **C,D** At 5 dpf WT, *csf1ra*^{-/-}, *csf1rb*^{-/-}, *csf1ra*^{-/-}; *b*^{+/-}, *csf1ra*^{DM} and larvae were treated with neutral red for 2.5 h. Images were acquired with a stereomicroscope and microglia numbers were determined by counting the number of neutral red dots. **E** 4 dpf WT, *csf1ra*^{-/-}, *csf1ra*^{-/-}; *b*^{+/-} and *csf1ra*^{DM} were labeled with an antibody against L-plastin (69), and L-plastin-positive cells were quantified in the optic tecti. CPM = counts per million, LBD = Ligand-binding domain, TMD = Transmembrane domain, TKD = Tyrosine kinase domain, dpf = days post fertilization. Error bars represent the standard deviation. ** $p < 0.01$, *** $p < 0.001$ (one-way ANOVA, Bonferroni multiple testing correction). Scale bar = 40 μ m.

To investigate whether any pathological hallmarks of ALSP are also present in *csf1r* mutant zebrafish, we assessed tissue and white matter integrity in adult *csf1ra*^{-/-}, *csf1ra*^{-/-}; *b*^{+/-} and *csf1ra*^{DM} mutants. Hematoxylin and eosin labeling did not reveal signs of brain pathology (data not shown). Neither did immunolabeling



for Claudin K (Cldnk) — which labels myelin tracts throughout the zebrafish brain — reveal major loss of myelin, even in *csf1r*^{DM} mutants (Fig. S2A)(37). To determine whether *csf1r* mutants display more subtle myelin abnormalities, such as degeneration, hypomyelination, or hypermyelination, we analyzed their white matter by electron microscopy (EM). We observed highly myelinated regions in the midbrain containing multilayered myelin sheets, which resembled those in mammals, but no apparent abnormalities in the multilayered myelin sheets in *csf1r* mutants (Fig. S2B, C). Immunolabeling for Sox10 also indicated normal numbers of oligodendrocyte lineage cells in *csf1r* mutants (Fig. S2D). Together, this indicates that *csf1r* deficiency in zebrafish does not result in overt myelin degeneration at this adult stage.

To establish whether loss of *csf1r* causes more subtle pathological changes, we performed RNA sequencing on brains of adult *csf1r*-mutant zebrafish that were ~8 month old (Fig. 3A). Multidimensional scaling of gene expression data showed clustering of the samples based on the *csf1r* mutation status (WT, *csf1ra*^{-/-}, *csf1ra*^{-/-};*b*^{+/-}, *csf1r*^{DM}), indicating *csf1r*-dependent changes in gene expression (Fig. 3B). Differential gene expression analysis between wild type and *csf1r*^{DM} mutant brains revealed 154 differentially expressed genes, 85 of which (e.g. *spi1b*, *irf8*, *csf1ra* and *csf1rb*) we had previously identified as part of the zebrafish microglial transcriptome (Fig. 3C,D,E, Table S2)(30). Hierarchical clustering of the samples on the basis of 154 differentially expressed genes revealed that *csf1ra*^{-/-};*b*^{+/-} mutants clustered with *csf1r*^{DM} mutants, whereas *csf1ra*^{-/-} mutants clustered with wild type (Fig. 3D). This suggests that loss of *csf1r* leads mainly to reduced expression of microglia-specific genes, which indicates that loss of *csf1r* in zebrafish predominantly affects microglia. The downregulated genes that were not specifically expressed in microglia included the cysteine-glutamine exchanger *slc7a11* and *growth hormone 1*, as well as many poorly annotated genes (Table S2). This indicates that *csf1r* deficiency and thus loss of microglia causes very few molecular changes and no obvious myelin-related pathology in ~ 8 month old adult zebrafish.

***Csf1r* deficient microglia increase expression of genes involved in chemotaxis and migration**

To assess in more detail how *csf1r* deficiency affects microglia independently of brain pathology, we performed RNA sequencing on microglia that were FACS-sorted from wild type, *csf1ra*^{-/-} and *csf1ra*^{-/-};*b*^{+/-} mutant brains that were dissected from ~9 month old zebrafish (Fig. 4A). Multidimensional scaling revealed clustering

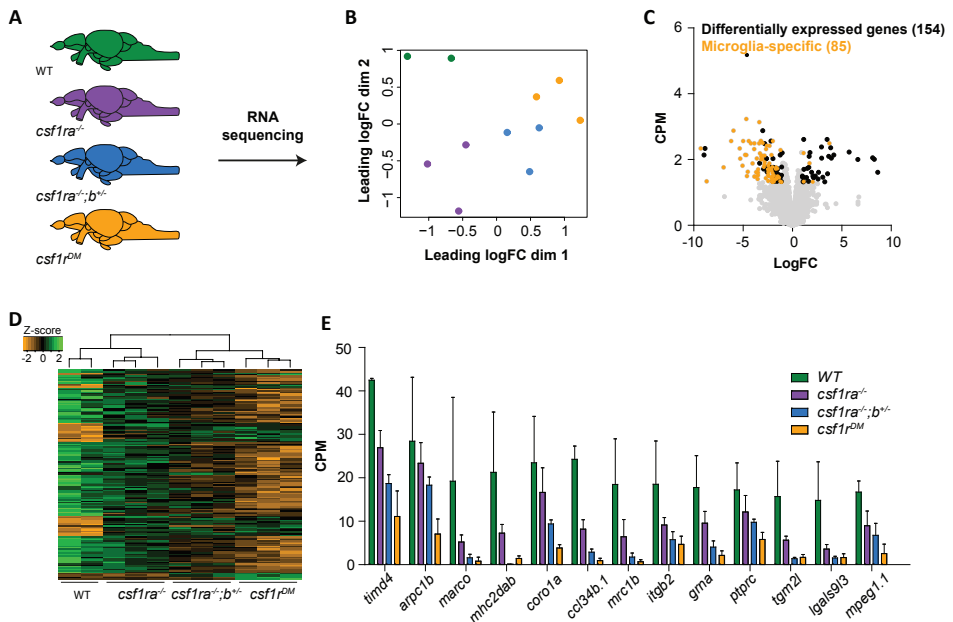


Fig. 3 RNA sequencing reveals no signs of brain pathology in *csf1r* mutant zebrafish.

A Schematic representation of whole brain RNA sequencing experiment. RNA was isolated from whole brains of WT, *csf1ra*^{-/-}, *csf1ra*^{-/-};*b*^{+/-} and *csf1r*^{DM} fish (3 brains per sample, 2-3 samples per genotype). **B** Multidimensional scaling plot. **C** Volcano plot with genes differentially expressed between *csf1r*^{DM} and WT fish. Yellow dots represent genes that are part of the zebrafish microglia transcriptome (30). Black dots represent the other differentially expressed genes. Gray dots are all detected genes. **D** Heat map with genes differentially expressed between *csf1r*^{DM} and WT fish genes. **E** Expression values of differentially expressed microglia-specific genes. Genes were differentially expressed with FDR < 0.05 and LogFC > |1|. FDR = false discovery rate, LogFC = Log fold change.

of the samples on the basis of *csf1r* mutation status, indicating *csf1r*-dependent changes in microglial gene expression (Fig. 3B). Based on our microglia density measurements, and the importance of *csf1rb* for adult microglia, we reasoned that *csf1ra*^{-/-};*b*^{+/-} mutant microglia could mimic CSF1R haploinsufficiency that occurs in ALS patient microglia, and compared microglia gene expression of these mutants with that of controls. We identified 1466 genes that were differentially expressed between *csf1ra*^{-/-};*b*^{+/-} mutant and wildtype microglia (Fig. 4C, Table S3). Interestingly, the normalized expression values of 750 out of the 1466 differentially expressed genes in *csf1ra*^{-/-} mutant microglia lay in between those of *csf1ra*^{-/-};*b*^{+/-} and wild-type microglia (Fig. 4C,D, Table S3). As more than half of the genes differentially expressed between wildtype and *csf1ra*^{-/-};*b*^{+/-} show *csf1r*-dependent changes in expression, this indicates that these genes

are regulated by *Csf1r*-signaling and their altered expression could be a primary consequence of *csf1r* deficiency. Gene ontology analysis on genes that showed *csf1r*-dependent changes in expression revealed that downregulated genes were associated with brain and nervous system development, and with regulation of neuronal differentiation (Fig. 4E). Upregulated genes were mainly associated with immune response, immune system process, and leukocyte chemotaxis (Fig. 4F). The differentially expressed genes in the gene ontology classes associated with the upregulated genes were mainly chemokines and chemokine receptors (e.g. *cxcl12a*, *ccl25b*, *ccl19a.1*, *cxcr4b*) (Fig. 4G). In fact, the expression of most chemokines and chemokine receptors in zebrafish microglia was higher in *csf1ra*^{-/-};*b*^{+/-} mutants than in wild types (Fig. 4G), which may explain the aberrant microglia distribution in *csf1ra*^{-/-};*b*^{+/-} mutants.

To test whether the expressional changes observed in *csf1ra*^{-/-};*b*^{+/-} microglia and brain indicated a general microglia differentiation defect, we investigated whether adult *csf1r*-mutants showed a loss of microglia-specific gene expression or a gain in gene expression associated with immature microglia or macrophages (Figs 4 and 5). Only 8 of the 300 most microglia-specific genes in zebrafish (many of which are also included in the mouse and human homeostatic microglia signature e.g. *slco2b1*, *pdgfra*, *scn4bb*) were significantly downregulated in *csf1ra*^{-/-};*b*^{+/-} microglia, suggesting that there is no loss of a homeostatic microglia signature (Fig. 5A,D,E)(30, 31, 38, 39).

Next, we analyzed the expression of 378 zebrafish orthologs for genes that are strongly downregulated during microglia differentiation in the mouse brain to assess whether *csf1r* mutant microglia fail to downregulate genes specific to immature microglia (40). Expression of only 10 of these 378 genes was increased in *csf1ra*^{-/-};*b*^{+/-} mutant microglia when compared to the expression in wild type microglia (Fig. 5B,F). We also found no evidence for increased expression of genes that discern microglia and macrophages (Fig. 5C)(41). Additionally, *csf1ra*^{-/-};*b*^{+/-} microglia were still highly ramified and showed no signs of activation (Fig. 5G). This suggests that the *csf1r*-dependent changes in microglial gene expression are largely independent of differentiation status. Together, these data imply that the changes in the expression of genes involved in chemotaxis and cell migration in *csf1r* mutants are a specific consequence of *csf1r* deficiency and not of a global differentiation defect.

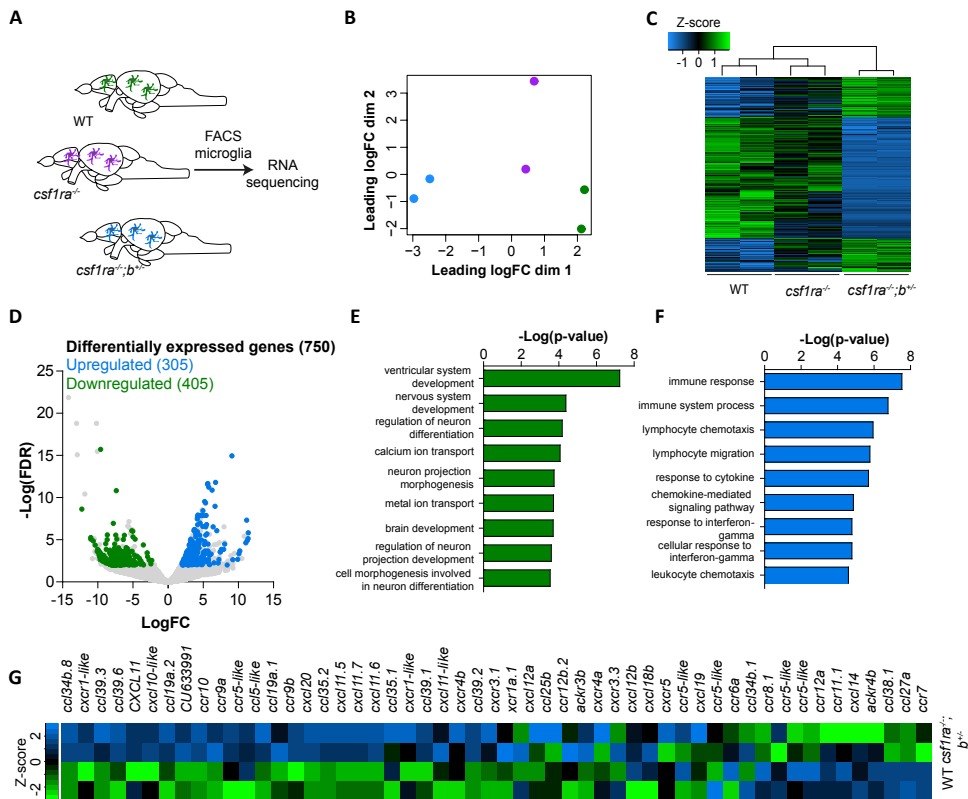


Fig. 4 RNA sequencing reveals increased expression of genes associated with chemotaxis in *csf1ra*^{-/-};*b*^{+/-} mutant microglia. **A** Schematic representation of RNA sequencing experiment. Microglia were FACS-sorted from dissected brains from WT (4 brains per sample, 2 samples); *csf1ra*^{-/-} (4 brains per sample, 2 samples); and *csf1ra*^{-/-};*b*^{+/-} (4-5 brains per sample, 2 samples) zebrafish. **B** Multidimensional scaling plot. **C** Heat map of differentially expressed genes between *csf1ra*^{-/-};*b*^{+/-} and WT microglia. **D** Volcano plot of differentially expressed genes (*csf1ra*^{-/-};*b*^{+/-} vs WT), whose expression values in *csf1ra*^{-/-} mutants lay between those of WT and *csf1ra*^{-/-};*b*^{+/-} mutants. **E**, **F** Gene ontology analysis was performed on the genes that showed a *csf1r*-dependent decrease in expression (**E**) and increase in expression (**F**). **G** Heat map with expression z-scores for all chemokines and chemokine receptors that are expressed in zebrafish microglia. Genes were differentially expressed with FDR < 0.01 and LogFC > |2|. Adult zebrafish used were between 9-12 months old.

The damage-induced proliferative response of *csf1r* mutant microglia is delayed

Microglia respond quickly to damage by migration and proliferation, and CSF1R has been linked to this proliferative response of microglia (42). Therefore, to assess whether proliferation defects could be linked to aberrant microglia localization,

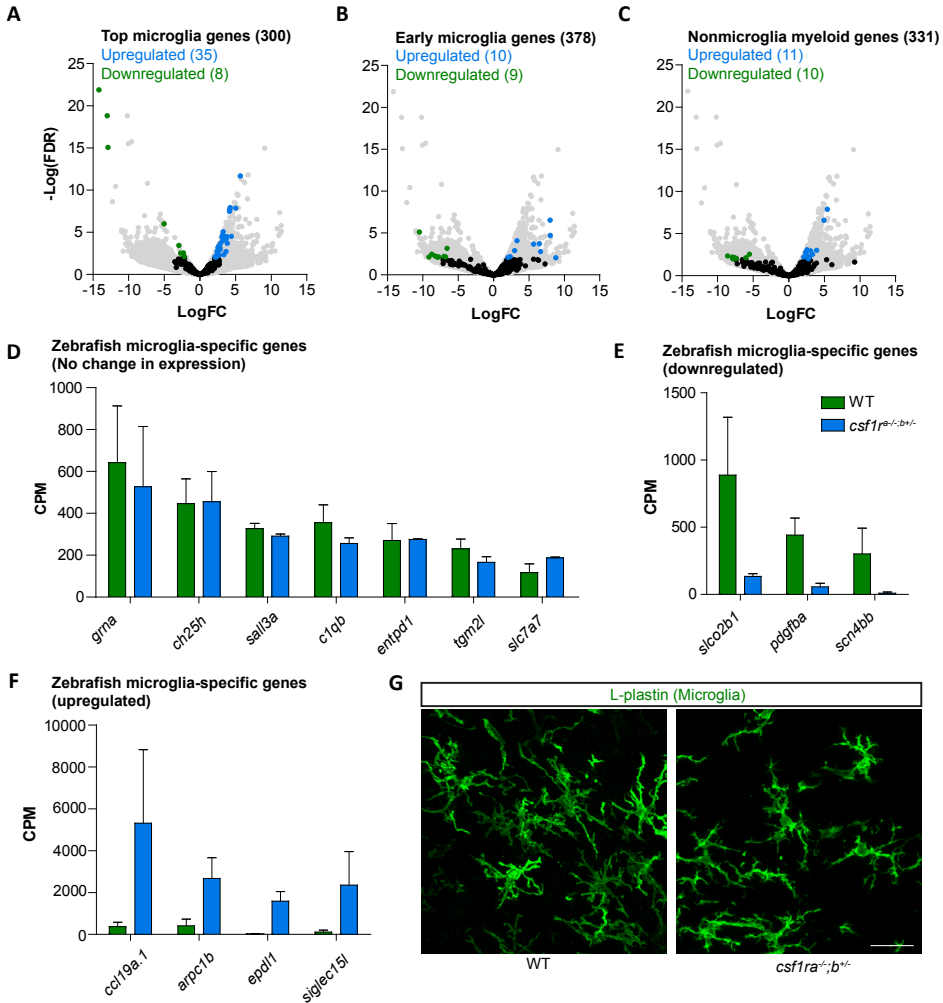


Fig. 5 Differential gene expression of *csf1r*-deficient microglia shows normal microglia differentiation. **A** Volcano plot showing expressional changes of the 300 most highly expressed microglia-specific genes in *csf1ra^{-/-};b^{+/-}* mutant microglia (30). **B** Volcano plot showing the expressional changes in *csf1ra^{-/-};b^{+/-}* mutant microglia of normally downregulated genes during differentiation (40) and of genes normally expressed in other macrophages in the CNS (41). **C** Volcano plot showing the expression changes of non-microglia myeloid genes. **D** Expression values of zebrafish microglia-specific genes. **E** Expression values of downregulated microglia-specific genes. **F** Expression values of upregulated microglia-specific genes. **G** Representative images of microglia (5-month-old fish) in the ventral part of the optic tectum labeled with an antibody against L-plastin. CPM = Counts per Million. Scale bar = 20 μ m.

and possibly to microglia migration, we used our previously established neuronal ablation model. In this model, metronidazole (MTZ) treatment in zebrafish with brain-specific transgenic expression of nitroreductase (NTR) results in neuronal cell death (4, 43). We have shown previously that increasing the local demand for microglia by inducing neuronal cell death causes a strong local proliferative response by microglia (30). To investigate whether microglia proliferation depends on *csf1r* dosage, we used Pcn^a as a cell-proliferation marker to assess microglia proliferation upon induction of neuronal ablation. One day after treatment, control NTR transgenic larvae showed that the microglia numbers had increased from 25 to 32 locally, with a corresponding increase in the fraction of Pcn^a+ microglia (Fig. 6A). In contrast, *csf1r* mutant microglia, upon MTZ treatment, showed a much larger increase in microglia numbers, respectively from 5 to 24 and from 2 to ~12, but had not yet increased significantly in the fraction of Pcn^a+ microglia (Fig. 6A). Therefore the increased microglia numbers in treated *csf1r* mutants cannot be explained by the fraction of dividing microglia relative to control. Based on the much stronger increase in L-plastin⁺ cells in either of the mutants however, one would expect a much higher fraction of Pcn^a+ cells in MTZ-treated vs controls, if the increase is due to proliferation alone. Intriguingly, at 2 days post treatment, the fractions of Pcn^a+ microglia were increased to similar levels in control and in *csf1r* mutants (Fig. 6B). This showed that although *csf1ra*^{-/-} and *csf1ra*^{-/-};*b*^{+/-} mutant microglia were able to mount a proliferative response, the proliferative response was delayed. Nevertheless, as numbers still increased it seems that potential initial proliferation deficiencies were compensated through microglia recruitment. Therefore, the aberrant distribution of microglia upon *csf1r* deficiency may be a compensatory mechanism intended to meet the brain's local demand for microglia.

Severe microglia depletion in gray and white matter of postmortem ALSP patient brains

It has been reported that degenerated white matter in the brains of ALSP patients contains many CD68⁺ myeloid cells and reduced numbers of IBA1-positive microglia (44) (13, 14). We wanted to investigate whether altered microglia density and distribution, as we identified in the zebrafish, would recur in the non-degenerated brain tissue of ALSP patients. By immunohistochemistry, we therefore analyzed microglia morphology, distribution and density in gray matter, normal-appearing white matter (NAWM) (occipital lobe), and degenerated white matter (middle frontal gyrus and cingulate gyrus) of two ALSP patients and

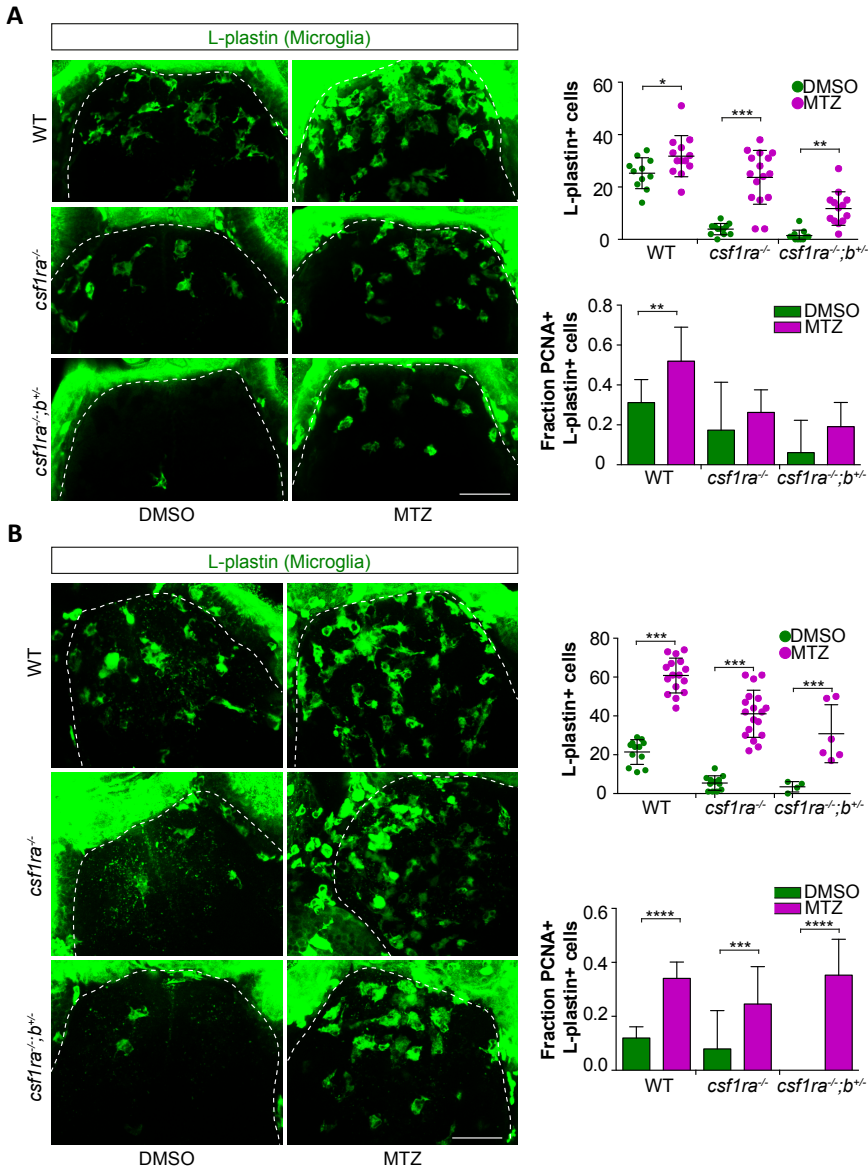


Fig. 6 Response to neuronal cell death of *csf1r* mutant microglia depends more on recruitment than on proliferation. We used our previously described conditional neuronal ablation model (4, 43), in which treatment with metronidazole (MTZ) leads to selective ablation of neurons with transgenic expression of nitroreductase (the *nsfB* gene encoding nitroreductase, NTR). WT, *csf1ra*^{-/-} and *csf1ra*^{-/-}; *b*^{-/-} larvae were treated with MTZ at 5 dpf for 16 hours and fixed for immunohistochemistry (whole mount) at 6 dpf (A) and 7 dpf (B). Immunostaining was performed for dividing (PCNA+) microglia (L-plastin+), and the entire forebrain was imaged and quantified. Scale bar = 40 μ m (A, B). Group sizes were at least $n = 10$ zebrafish larvae. dpf = days post fertilization. Error bars indicate the standard deviation. * $p < 0.05$, ** $p < 0.01$, *** $p < 0.001$ (one-way ANOVA, Bonferroni multiple testing correction).

age-matched controls (Fig. 7; Fig. S4A). As in previous studies, we observed numerous HLA-DR⁺ cells and large, rounded CD68⁺ cells in degenerated white matter, whereas, apart from a few IBA1/CD68 double positive cells, IBA1⁺ cells were almost completely absent (Fig. 7A, S3A,B,C). As we also observed a few CD68⁺ cells with a low level of IBA1 staining, this suggests that highly CD68⁺ cells lose IBA1 expression (Fig. S3D).

Most IBA1⁺ microglia still present in the degenerated white matter appeared in clusters of ~10-100 cells (Fig. 7B). Interestingly, with the exception of sparse microglia clusters, microglia in the NAWM and gray matter were also severely depleted (Fig. 7B,C; Fig. S3B,C). Many of these IBA1⁺ microglia clusters were located at the border between the gray and the white matter (Fig. 7B). Whereas the few IBA1⁺ cells present in the white matter looked like foam cells, microglia in the gray matter and NAWM either looked activated or had a normal ramified morphology (Fig. 7B). In all the brain areas examined we also observed areas of gray matter in which IBA1⁺ microglia had a normal distribution and a ramified morphology. However, the density of these microglia was ~50 % lower in ALSP patient brain sections than in controls (Fig 7D). This is reminiscent of the findings in our zebrafish experiments, where we also observed regional differences in microglia density in unaffected brain tissue (Fig 2 and 7B,D). The loss of IBA1⁺ microglia, the aberrant microglia distribution and altered morphology in microglia clusters — not only in the gray matter, but also in NAWM — indicates that microglial changes could precede white matter degeneration.

Discussion

Although mutations in genes that are particularly important for the microglia can cause severe brain disorders, it is still unclear whether pathogenesis involves a gain or loss of specific microglia activities. Here, we used the zebrafish to investigate the impact of a gradual reduction in functional *csf1r* alleles on microglia numbers, microglia differentiation status and their response to tissue damage. We found that *Csf1r* haploinsufficiency was correlated with a lower density of microglia in the dorsal part of the optic tectum. Additionally, we observed altered microglia distribution and local microglia depletion in the ventral and dorsolateral part of the optic tectum, respectively. Loss of three *csf1r* alleles did not severely impede the proliferative capacity of microglia to dying neurons, nor did it affect the homeostatic microglia signature. Instead, in response to increased phagocytic demand, *csf1r* mutant microglia initially increased their numbers locally through recruitment rather than proliferation. Accordingly, the expression of migration and

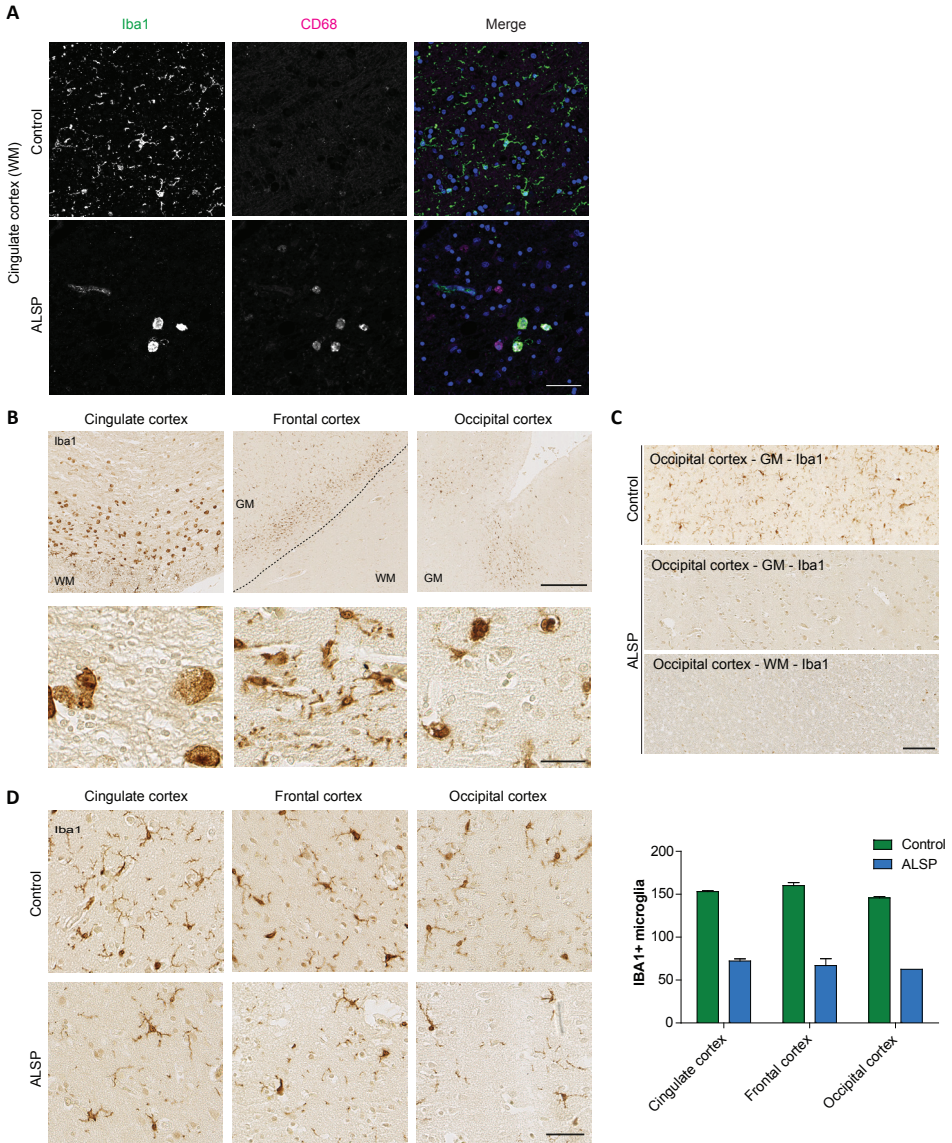


Fig. 7 ALSP patient brains show widespread microglia depletion. Representative images of IBA1 and CD68 staining of microglia in white and gray matter of post mortem brain tissue of two ALSP patients and two age-matched control donors. **A** IBA1 and CD68 double labeling in the white matter of the cingulate gyrus of ALSP patient and control tissue. **B** Clusters of IBA1+ microglia are apparent at the borders between the gray matter and the white matter. **C** Severe depletion of IBA1+ microglia in the gray and white matter of the occipital cortex. **D** The ramified morphology of microglia in gray matter areas of ALSP patients was similar to that in controls. Quantification of microglia numbers in gray matter areas of the cingulate cortex, frontal cortex, and occipital cortex which showed a homogeneous distribution of ramified microglia (5 gray matter areas, 1.5 mm² in size, per brain region per patient). **D** Scale bar = 50 μ m (A), 500 μ m (B, low magnification), 30 μ m (B, high magnification), 100 μ m (C), 50 μ m (D). WM = white matter, GM = gray matter.

chemotaxis genes in *csf1r* mutants was also increased. We also showed that, in the absence of extensive white matter degeneration in the occipital lobe of the cortex, CSF1R haploinsufficiency results in widespread depletion and aberrant distribution of IBA1+ microglia in humans. These findings support the presence of a disease mechanism in which CSF1R haploinsufficiency reduces microglia density, causes microglial relocation, and results in depletion of functional microglia. This indicates that loss of microglia may be an early pathogenic event in ALSP patients.

Although the focus of this study is on brain microglia, CSF1R haploinsufficiency could potentially affect other macrophages, such as those in the gut, or even neurons, as low level of *Csf1r* expression was reported in few scattered neurons in the mouse hippocampus (12). As the composition of the gut microbiome, or perturbed barrier function of the gut, has major effects on microglia and on the CNS (45, 46) it is possible that, in ALSP patients, defects in other macrophage populations, such as those in the intestine, play a role in pathogenesis. Nevertheless, gastrointestinal symptoms related to perturbed gut barrier function were not reported in ALSP patients (11). Additionally, our zebrafish data do not imply an increased inflammatory response or response to microbial infection. Given that a potentially protective role of *Csf1r* has been described in neurons, it is possible that these protective effects are reduced due to CSF1R deficiency and could be a contributing factor in disease. As neuronal loss is not obvious in ALSP patients, however, we speculate that this is unlikely to play a major part.

CSF1R coding sequence and function are well conserved across species. CSF1R-deficient zebrafish, rodents and most likely humans lack microglia, are osteopetrotic and occasionally show cerebral hemorrhages (data not shown) (16-18, 47). Our data indicate that *csf1r* haploinsufficiency leads to a local loss of microglia, possibly through the maldistribution of microglia. This is similar to the aberrant distribution of microglia and widespread loss of microglia we observed in the NAWM and gray matter of post mortem ALSP patient brains. Interestingly, based on neuropathological analysis of different ALSP stages, in the early stages, microglia numbers were predicted to be higher than in controls and microglia appear activated in specific brain regions (13). This is reminiscent of the increased microglia density we observed in deep brain regions of *csf1ra*^{-/-}; *b*^{+/-} haploinsufficient zebrafish (13). Similarly, microglia numbers are also higher in some brain regions in heterozygous *Csf1r* mutant mice than in control animals, but it is unclear whether microglia density is reduced in other areas or at later

stages in the mouse (48). Between them, these observations indicate that *CSF1R* haploinsufficiency causes aberrant microglia distribution, where some regions become devoid of microglia.

Although microglia are efficient phagocytes that clear dead cells, dysfunctional synapses and myelin (5, 49, 50), the accumulation of myelin debris in microglia can compromise their phagocytic capacity and can also lead to microglial senescence (5, 51, 52). Based on the size and morphology of large numbers of CD68+ cells in degenerated white matter, the accumulation of debris could have preceded their presence. We cannot exclude that CD68+ cells include infiltrated macrophages, as other macrophage and microglia markers, including IBA1 and P2RY12, appear lost or very low in these cells (14). Regardless, accumulation of myelin debris, as occurs during normal aging, may contribute to the progressive loss of functional IBA1+ microglia over the course of the disease. In fact, it was shown in a tuberculosis infection model that, due to reduced *csf1r* signaling, the loss of macrophages was driven by a failure to meet phagocytic demand (22). Consistent with this idea, the morphology of microglia among clusters in ALSP patients ranged from ramified to completely round and foamy in appearance, due most likely to the accumulation of phagocytized myelin debris in microglia (51). Simultaneously, it is possible that one functional *CSF1R* copy is not sufficient to sustain both normal microglia survival and proliferation, as microglia turn over in humans in adulthood (53, 54). Together, this indicates that *CSF1R*-dependent loss of microglia in ALSP patients may be progressive.

The absence of overt neuropathology or myelin pathology in *csf1r* mutant zebrafish may be related their relatively young age, to the fact that the central nervous system of the zebrafish is smaller and less complex than that of humans, or to the time needed for the pathology to develop in humans. The pathological hallmarks of ALSP are observed mainly in the neocortex, which is unique to mammals and has expanded immensely during evolution, particularly in primates and humans (55, 56). As the neocortex is rich in white matter, it may be more susceptible to pathology than the zebrafish brain, in which there is relatively little white matter (57). Consistent with this, mutations that result in a relatively mild pathology in mice can lead to severe leukodystrophy in humans (58). Additionally, it takes about 30-40 years before ALSP becomes symptomatic, whereas mice and zebrafish live only a few years (11). Even though the *csf1r* mutant zebrafish brain is relatively unaffected, the direct effects of *csf1r* mutations on microglia as described here were very similar to those in humans.

Although it is still unknown how long-term depletion of microglia in

adulthood would affect brain homeostasis, and how it might cause pathology, white matter degeneration is a hallmark of several other brain disorders classified as microgliopathies. For example, mutations in microglia genes *TREM2* and *TYROBP* both cause Nasu-Hakola disease (NHD), which is also characterized by white matter pathology. Even though the precise pathogenic mechanisms remain elusive, these disorders support the idea that microglia are critical to the maintenance of myelin in adulthood. In fact, it was recently shown in the adult brain that lower microglia numbers lead to a reduction in the numbers of oligodendrocytes or oligodendrocyte precursors (OPCs) in many brain regions (25). We anticipate that a progressive depletion of microglia occurs in ALSP, which could lead to a lower number of myelinating cells in adulthood, and could thereby contribute to ALSP pathogenesis.

Like tissue macrophages, the microglia influence the development and repair of organs by secreting trophic factors including insulin-like growth factor 1 (IGF1), and by mediating signaling between cells (65-67). Local depletion of microglia could lead to a failure to provide such trophic factors, which could contribute to ALSP pathogenesis, for example, by affecting the capacity to form new oligodendrocytes.

In conclusion, the greatest effect of CSF1R haploinsufficiency seems to be a general reduction in microglia density in addition to large areas completely devoid of microglia. The partial or complete lack of microglia occurs in normal appearing gray and white matter, which suggests that loss of microglia may eventually result in ALSP pathology. Our gene expression data in an allelic series of *csf1r*-deficient microglia and brains therefore provide an opportunity to further delineate not only the function of *csf1r* in microglia, but also the consequences for the brain. Elucidating these is crucial to a more comprehensive understanding of the physiological functions of microglia and microglia-dependent disease mechanisms. Several studies have shown that pharmacological inhibition of CSF1R causes microglia depletion and, in mouse models, that it ameliorates neurodegenerative disease-like symptoms by depleting microglia or diminishing their proliferation and activation (68-70). As microglia depletion may underlie and contribute to the development and progression of ALSP, this raises the question of whether long-term inhibition of CSF1R in neurodegenerative diseases like Alzheimer's disease is a viable treatment option (69, 70). This warrants further studies to determine how the brain is affected by loss of microglia interactions and microglia-derived factors, and to devise ways of promoting the supply of functional microglia.

Materials and methods

Animals

The following transgenic zebrafish lines were used: Wild type AB, Tg(*mpeg1:EGFP*) fish expressing GFP under the control of the *mpeg1* promoter (71), Tg(*Neuro-Gal4, uas:nsfB-mCherry, mpeg1:EGFP*) with neuronal specific *nsfB* expression encoding nitroreductase (NTR)(43), *csf1ra*^{*j4e1/j4e1*} with a V614M substitution in the first kinase domain (72). *Csf1ra* mutants were also crossed in with the transgenic lines specified above. The *csf1rb* deletion mutant was created by TALEN-mediated genome editing (73). The TALEN arms targeted exon 3 (Fig. S1) of the *csf1rb* gene, resulting in a 4 bp deletion and premature stop codon. Animal experiments were approved by the Animal Experimentation Committee at Erasmus MC, Rotterdam.

Vital dye labeling

Neutral red labeling was performed as described previously (32). Neutral red images were acquired by using a Leica M165FC stereo microscope.

Induction neuronal cell death

For neuronal ablation, neuro-NTR transgenic zebrafish were used as described previously (43).

Immunofluorescence staining

Whole mount larvae This was usually done as described previously (74).

Adult brain sections Immunostaining on adult brain slices was performed largely as described previously (30).

Paraffin sections human brain Paraffin sections seven μm in thickness were collected on Superfrost Plus glass slides (VWR international, Leuven, Belgium) and dried at 37°C. Tissue sections were characterized for the presence of microglia by staining for IBA1 and CD68 as previously described (75).

RNAseq library synthesis and bioinformatics analysis

Microglia Microglia were FAC-sorted, lysed and processed for RNAseq largely as described (30). RNA was reverse transcribed using an oligo(dT) primer, and cDNA was pre-amplified followed by tagmentation with Tn5. The tagmented library was extended with Illumina adaptor sequences. The resulting sequencing library was sequenced according to the Illumina TruSeq v3 protocol on the HiSeq2500, and mapped against the GRCz10 zebrafish genome followed by differential gene

expression analysed using the Bioconductor package edgeR and goseq for gene ontology.

Brain Brains were dissected as described previously (30) and snap frozen in liquid nitrogen. Brains were homogenized followed by total RNA isolation using Trizol. RNA samples were processed for RNA sequencing and analysis largely as described for microglia.

Electron microscopy

Electron microscopy was performed largely as described previously (43). For each myelinated axon present the g-ratio was calculated.

Human brain tissue

Human brain tissue samples were obtained from the Netherlands Brain Bank (www.brainbank.nl). All patients and controls, or their next of kin, had given informed consent for autopsy and the use of brain tissue for research purposes. Relevant clinical information was retrieved from the medical records and is summarized in Table S1. We obtained paraffin-embedded post mortem tissue blocks of cingulate gyrus, frontal cortex and occipital lobe from 2 ALSP patients and 2 age-matched controls without neurological disease.

Author contributions

Conceptualization, N.O. and T.v.H., Methodology, N.O., H.v.d.L., and L.E.K., Investigation, N.O., L.E.K., S.B., W.B. H.v.d.L., M.H.G.V., Formal Analysis, N.O., Resources, W.v.IJ., E.M.H. and J.v.S., Writing – Original Draft, N.O. and T.v.H., Writing – Review & Editing, N.O., L.E.K., S.B., E.M.H., M.H.V., W.v.IJ. and T.v.H., Supervision, T.v.H., Funding acquisition, T.v.H.

Acknowledgements/Funding

This work was sponsored by an Erasmus University Rotterdam fellowship, a ZonMW VENI grant, a Marie Curie Career Integration Grant and an Alzheimer Nederland fellowship to T.v.H., and a MKMD ZonMW grant to EMH. We thank Dr. B. Giepmans and A. Wolters (UMC Groningen) for advice on Electron Microscopy; T. van Gestel and Dr. G. Schaaf (Erasmus MC) for help with flow cytometry; and the Netherlands Brain Bank for human brain tissue (NBB; coordinator Dr. I. Huitinga, Amsterdam, the Netherlands); and J. Wortel (VUMC) for her contribution to electron microscopy preparations.

References

1. Paolicelli RC, Bolasco G, Pagani F, Maggi L, Scianni M, Panzanelli P, et al. Synaptic pruning by microglia is necessary for normal brain development. *Science*. 2011;333(6048):1456-8.
2. Tremblay ME, Lowery RL, Majewska AK. Microglial interactions with synapses are modulated by visual experience. *PLoS Biol*. 2010;8(11):e1000527.
3. Stevens B, Allen NJ, Vazquez LE, Howell GR, Christopherson KS, Nouri N, et al. The classical complement cascade mediates CNS synapse elimination. *Cell*. 2007;131(6):1164-78.
4. van Ham TJ, Kokel D, Peterson RT. Apoptotic cells are cleared by directional migration and elmo1- dependent macrophage engulfment. *Curr Biol*. 2012;22(9):830-6.
5. Safaiyan S, Kannaiyan N, Snaidero N, Brioschi S, Biber K, Yona S, et al. Age-related myelin degradation burdens the clearance function of microglia during aging. *Nat Neurosci*. 2016;19(8):995-8.
6. Rademakers R, Baker M, Nicholson AM, Rutherford NJ, Finch N, Soto-Ortolaza A, et al. Mutations in the colony stimulating factor 1 receptor (CSF1R) gene cause hereditary diffuse leukoencephalopathy with spheroids. *Nat Genet*. 2012;44(2):200-5.
7. Paloneva J, Manninen T, Christman G, Hovanes K, Mandelin J, Adolfsson R, et al. Mutations in two genes encoding different subunits of a receptor signaling complex result in an identical disease phenotype. *Am J Hum Genet*. 2002;71(3):656-62.
8. Prinz M, Priller J. Microglia and brain macrophages in the molecular age: from origin to neuropsychiatric disease. *Nat Rev Neurosci*. 2014;15(5):300-12.
9. Meuwissen ME, Schot R, Buta S, Oudesluijs G, Tinschert S, Speer SD, et al. Human USP18 deficiency underlies type 1 interferonopathy leading to severe pseudo-TORCH syndrome. *J Exp Med*. 2016;213(7):1163-74.
10. Wider C, Van Gerpen JA, DeArmond S, Shuster EA, Dickson DW, Wszolek ZK. Leukoencephalopathy with spheroids (HDLs) and pigmentary leukodystrophy (POLD): a single entity? *Neurology*. 2009;72(22):1953-9.
11. Konno T, Yoshida K, Mizuno T, Kawarai T, Tada M, Nozaki H, et al. Clinical and genetic characterization of adult-onset leukoencephalopathy with axonal spheroids and pigmented glia associated with CSF1R mutation. *Eur J Neurol*. 2017;24(1):37-45.
12. Luo J, Elwood F, Britschgi M, Villeda S, Zhang H, Ding Z, et al. Colony-stimulating factor 1 receptor (CSF1R) signaling in injured neurons facilitates protection and survival. *J Exp Med*. 2013;210(1):157-72.
13. Oyanagi K, Kinoshita M, Suzuki-Kouyama E, Inoue T, Nakahara A, Tokiwai M, et al. Adult onset leukoencephalopathy with axonal spheroids and pigmented glia (ALSP) and Nasu-Hakola disease: lesion staging and dynamic changes of axons and microglial subsets. *Brain Pathol*. 2016.
14. Tada M, Konno T, Tada M, Tezuka T, Miura T, Mezaki N, et al. Characteristic microglial features in patients with hereditary diffuse leukoencephalopathy with spheroids. *Ann Neurol*. 2016;80(4):554-65.
15. Wang Y, Szretter KJ, Vermi W, Gilfillan S, Rossini C, Cella M, et al. IL-34 is a tissue-restricted ligand of CSF1R required for the development of Langerhans cells and microglia. *Nat Immunol*. 2012;13(8):753-60.
16. Dai XM, Ryan GR, Hapel AJ, Dominguez MG, Russell RG, Kapp S, et al. Targeted disruption of the mouse colony-stimulating factor 1 receptor gene results in osteopetrosis, mononuclear phagocyte deficiency, increased primitive progenitor cell frequencies, and reproductive defects. *Blood*. 2002;99(1):111-20.
17. Ginhoux F, Greter M, Leboeuf M, Nandi S, See P, Gokhan S, et al. Fate mapping analysis reveals that adult microglia derive from primitive macrophages. *Science*. 2010;330(6005):841-5.
18. Erlich B, Zhu L, Etgen AM, Dobrenis K, Pollard JW. Absence of colony stimulation factor-1 receptor results in loss of microglia, disrupted brain development and olfactory deficits. *Plos One*. 2011;6(10):e26317.
19. Jenkins SJ, Ruckerl D, Thomas GD, Hewitson JP, Duncan S, Brombacher F, et al. IL-4 directly signals tissue-resident macrophages to proliferate beyond homeostatic levels controlled by CSF-1. *J Exp Med*. 2013;210(11):2477-91.
20. Cecchini MG, Dominguez MG, Mocci S, Wetterwald A, Felix R, Fleisch H, et al. Role of colony stimulating factor-1 in the establishment and regulation of tissue macrophages during postnatal development of the mouse. *Development*. 1994;120(6):1357-72.
21. Teitelbaum R, Schubert W, Gunther L, Kress

- Y, Macaluso F, Pollard JW, et al. The M cell as a portal of entry to the lung for the bacterial pathogen *Mycobacterium tuberculosis*. *Immunity*. 1999;10(6):641-50.
22. Pagan AJ, Yang CT, Cameron J, Swaim LE, Ellett F, Lieschke GJ, et al. Myeloid Growth Factors Promote Resistance to Mycobacterial Infection by Curtailing Granuloma Necrosis through Macrophage Replenishment. *Cell Host Microbe*. 2015;18(1):15-26.
 23. Cheers C, Hill M, Haigh AM, Stanley ER. Stimulation of macrophage phagocytic but not bactericidal activity by colony-stimulating factor 1. *Infect Immun*. 1989;57(5):1512-6.
 24. Endele M, Loeffler D, Kokkalis KD, Hilsenbeck O, Skylaki S, Hoppe PS, et al. CSF-1-induced Src signaling can instruct monocytic lineage choice. *Blood*. 2017;129(12):1691-701.
 25. Hagemeyer N, Hanft KM, Akriditou MA, Unger N, Park ES, Stanley ER, et al. Microglia contribute to normal myelinogenesis and to oligodendrocyte progenitor maintenance during adulthood. *Acta Neuropathol*. 2017.
 26. Nandi S, Gokhan S, Dai XM, Wei S, Enikolopov G, Lin H, et al. The CSF-1 receptor ligands IL-34 and CSF-1 exhibit distinct developmental brain expression patterns and regulate neural progenitor cell maintenance and maturation. *Dev Biol*. 2012;367(2):100-13.
 27. Zhang J, Lachance V, Schaffner A, Li X, Fedick A, Kaye LE, et al. A Founder Mutation in VPS11 Causes an Autosomal Recessive Leukoencephalopathy Linked to Autophagic Defects. *PLoS Genet*. 2016;12(4):e1005848.
 28. Haud N, Kara F, Diekmann S, Henneke M, Willer JR, Hillwig MS, et al. maset2 mutant zebrafish model familial cystic leukoencephalopathy and reveal a role for RNase T2 in degrading ribosomal RNA. *Proc Natl Acad Sci U S A*. 2011;108(3):1099-103.
 29. Oosterhof N, Boddeke E, van Ham TJ. Immune cell dynamics in the CNS: Learning from the zebrafish. *Glia*. 2015;63(5):719-35.
 30. Oosterhof N, Holtman IR, Kuil LE, van der Linde HC, Boddeke EW, Eggen BJ, et al. Identification of a conserved and acute neurodegeneration-specific microglial transcriptome in the zebrafish. *Glia*. 2017;65(1):138-49.
 31. Gosselin D, Skola D, Coufal NG, Holtman IR, Schlachetzki JCM, Sajti E, et al. An environment-dependent transcriptional network specifies human microglia identity. *Science*. 2017;356(6344).
 32. Herbomel P, Thisse B, Thisse C. Zebrafish early macrophages colonize cephalic mesenchyme and developing brain, retina, and epidermis through a M-CSF receptor-dependent invasive process. *Dev Biol*. 2001;238(2):274-88.
 33. Naito M, Hayashi S, Yoshida H, Nishikawa S, Shultz LD, Takahashi K. Abnormal differentiation of tissue macrophage populations in 'osteopetrosis' (op) mice defective in the production of macrophage colony-stimulating factor. *Am J Pathol*. 1991;139(3):657-67.
 34. Umeda S, Takahashi K, Naito M, Shultz LD, Takagi K. Neonatal changes of osteoclasts in osteopetrosis (op/op) mice defective in production of functional macrophage colony-stimulating factor (M-CSF) protein and effects of M-CSF on osteoclast development and differentiation. *J Submicrosc Cytol Pathol*. 1996;28(1):13-26.
 35. Wegiel J, Wisniewski HM, Dziewiatkowski J, Tarnawski M, Kozielski R, Trenkner E, et al. Reduced number and altered morphology of microglial cells in colony stimulating factor-1-deficient osteopetrotic op/op mice. *Brain Res*. 1998;804(1):135-9.
 36. Sasaki A, Yokoo H, Naito M, Kaizu C, Shultz LD, Nakazato Y. Effects of macrophage-colony-stimulating factor deficiency on the maturation of microglia and brain macrophages and on their expression of scavenger receptor. *Neuropathology*. 2000;20(2):134-42.
 37. Munzel EJ, Schaefer K, Obirei B, Kremmer E, Burton EA, Kuscha V, et al. Claudin k is specifically expressed in cells that form myelin during development of the nervous system and regeneration of the optic nerve in adult zebrafish. *Glia*. 2012;60(2):253-70.
 38. Zhang Y, Chen K, Sloan SA, Bennett ML, Scholze AR, O'Keefe S, et al. An RNA-sequencing transcriptome and splicing database of glia, neurons, and vascular cells of the cerebral cortex. *J Neurosci*. 2014;34(36):11929-47.
 39. Butovsky O, Jedrychowski MP, Moore CS, Cialic R, Lanser AJ, Gabriely G, et al. Identification of a unique TGF-beta-dependent molecular and functional signature in microglia. *Nat Neurosci*. 2014;17(1):131-43.
 40. Matcovitch-Natan O, Winter DR, Giladi A, Vargas Aguilar S, Spinrad A, Sarrazin S, et al. Microglia development follows a stepwise

- program to regulate brain homeostasis. *Science*. 2016;353(6301):aad8670.
41. Bennett ML, Bennett FC, Liddel SA, Ajami B, Zamanian JL, Fernhoff NB, et al. New tools for studying microglia in the mouse and human CNS. *Proc Natl Acad Sci U S A*. 2016;113(12):E1738-46.
 42. Gomez-Nicola D, Franssen NL, Suzzi S, Perry VH. Regulation of microglial proliferation during chronic neurodegeneration. *J Neurosci*. 2013;33(6):2481-93.
 43. van Ham TJ, Brady CA, Kalicharan RD, Oosterhof N, Kuipers J, Veenstra-Algra A, et al. Intravital correlated microscopy reveals differential macrophage and microglial dynamics during resolution of neuroinflammation. *Dis Model Mech*. 2014;7(7):857-69.
 44. Konno T, Tada M, Tada M, Koyama A, Nozaki H, Harigaya Y, et al. Haploinsufficiency of CSF-1R and clinicopathologic characterization in patients with HDLS. *Neurology*. 2014;82(2):139-48.
 45. Erny D, Hrabé de Angelis AL, Jaitin D, Wieghofer P, Staszewski O, David E, et al. Host microbiota constantly control maturation and function of microglia in the CNS. *Nat Neurosci*. 2015;18(7):965-77.
 46. Sampson TR, Debelius JW, Thron T, Janssen S, Shastri GG, Ilhan ZE, et al. Gut Microbiota Regulate Motor Deficits and Neuroinflammation in a Model of Parkinson's Disease. *Cell*. 2016;167(6):1469-80 e12.
 47. Monies D, Maddirevula S, Kurdi W, Alanazy MH, Alkhalidi H, Al-Owain M, et al. Autozygosity reveals recessive mutations and novel mechanisms in dominant genes: implications in variant interpretation. *Genet Med*. 2017;19(10):1144-50.
 48. Chitu V, Gokhan S, Gulino M, Branch CA, Patil M, Basu R, et al. Phenotypic characterization of a *Csf1r* haploinsufficient mouse model of adult-onset leukodystrophy with axonal spheroids and pigmented glia (ALSP). *Neurobiol Dis*. 2015;74:219-28.
 49. Sierra A, Encinas JM, Deudero JJ, Chancey JH, Enikolopov G, Overstreet-Wadiche LS, et al. Microglia shape adult hippocampal neurogenesis through apoptosis-coupled phagocytosis. *Cell Stem Cell*. 2010;7(4):483-95.
 50. Ling EA. Transformation of monocytes into amoeboid microglia in the corpus callosum of postnatal rats, as shown by labelling monocytes by carbon particles. *J Anat*. 1979;128(Pt 4):847-58.
 51. Boven LA, Van Meurs M, Van Zwam M, Wierenga-Wolf A, Hintzen RQ, Boot RG, et al. Myelin-laden macrophages are anti-inflammatory, consistent with foam cells in multiple sclerosis. *Brain*. 2006;129(Pt 2):517-26.
 52. Neumann H, Kotter MR, Franklin RJ. Debris clearance by microglia: an essential link between degeneration and regeneration. *Brain*. 2009;132(Pt 2):288-95.
 53. Reu P, Khosravi A, Bernard S, Mold JE, Salehpour M, Alkass K, et al. The Lifespan and Turnover of Microglia in the Human Brain. *Cell Rep*. 2017;20(4):779-84.
 54. Askew K, Li K, Olmos-Alonso A, Garcia-Moreno F, Liang Y, Richardson P, et al. Coupled Proliferation and Apoptosis Maintain the Rapid Turnover of Microglia in the Adult Brain. *Cell Rep*. 2017;18(2):391-405.
 55. Florio M, Huttner WB. Neural progenitors, neurogenesis and the evolution of the neocortex. *Development*. 2014;141(11):2182-94.
 56. Hofman MA. Evolution of the human brain: when bigger is better. *Front Neuroanat*. 2014;8:15.
 57. Merrifield GD, Mullin J, Gallagher L, Tucker C, Jansen MA, Denvir M, et al. Rapid and recoverable in vivo magnetic resonance imaging of the adult zebrafish at 7T. *Magn Reson Imaging*. 2017;37:9-15.
 58. Choquet K, Yang S, Moir RD, Forget D, Larivière R, Bouchard A, et al. Absence of neurological abnormalities in mice homozygous for the *Polr3a* G672E hypomyelinating leukodystrophy mutation. *Mol Brain*. 2017;10(1):13.
 59. Terada S, Ishizu H, Yokota O, Ishihara T, Nakashima H, Kugo A, et al. An autopsy case of hereditary diffuse leukoencephalopathy with spheroids, clinically suspected of Alzheimer's disease. *Acta Neuropathol*. 2004;108(6):538-45.
 60. Kleinberger G, Brendel M, Mracsko E, Wefers B, Groeneweg L, Xiang X, et al. The FTD-like syndrome causing *TREM2* T66M mutation impairs microglia function, brain perfusion, and glucose metabolism. *EMBO J*. 2017;36(13):1837-53.
 61. Kisler K, Nelson AR, Rege SV, Ramanathan A, Wang Y, Ahuja A, et al. Pericyte degeneration leads to neurovascular uncoupling and limits oxygen supply to brain. *Nat Neurosci*. 2017;20(3):406-16.
 62. Yamazaki T, Nalbandian A, Uchida Y, Li W, Arnold TD, Kubota Y, et al. Tissue Myeloid Progenitors

- Differentiate into Pericytes through TGF-beta Signaling in Developing Skin Vasculature. *Cell Rep.* 2017;18(12):2991-3004.
63. Arnold T, Betsholtz C. The importance of microglia in the development of the vasculature in the central nervous system. *Vasc Cell.* 2013;5(1):4.
 64. Montagne A, Nikolakopoulou AM, Zhao Z, Sagare AP, Si G, Lazic D, et al. Pericyte degeneration causes white matter dysfunction in the mouse central nervous system. *Nat Med.* 2018.
 65. Eom DS, Parichy DM. A macrophage relay for long-distance signaling during postembryonic tissue remodeling. *Science.* 2017;355(6331):1317-20.
 66. Wynn TA, Chawla A, Pollard JW. Macrophage biology in development, homeostasis and disease. *Nature.* 2013;496(7446):445-55.
 67. Wlodarczyk A, Holtman IR, Krueger M, Yogev N, Bruttger J, Khorooshi R, et al. A novel microglial subset plays a key role in myelinogenesis in developing brain. *EMBO J.* 2017;36(22):3292-308.
 68. Elmore MR, Najafi AR, Koike MA, Dagher NN, Spangenberg EE, Rice RA, et al. Colony-stimulating factor 1 receptor signaling is necessary for microglia viability, unmasking a microglia progenitor cell in the adult brain. *Neuron.* 2014;82(2):380-97.
 69. Spangenberg EE, Lee RJ, Najafi AR, Rice RA, Elmore MR, Blurton-Jones M, et al. Eliminating microglia in Alzheimer's mice prevents neuronal loss without modulating amyloid-beta pathology. *Brain.* 2016;139(Pt 4):1265-81.
 70. Olmos-Alonso A, Schettters ST, Sri S, Askew K, Mancuso R, Vargas-Caballero M, et al. Pharmacological targeting of CSF1R inhibits microglial proliferation and prevents the progression of Alzheimer's-like pathology. *Brain.* 2016;139(Pt 3):891-907.
 71. Ellett F, Pase L, Hayman JW, Andrianopoulos A, Lieschke GJ. *mpeg1* promoter transgenes direct macrophage-lineage expression in zebrafish. *Blood.* 2011;117(4):e49-56.
 72. Parichy ^{PM}, Ransom DG, Paw B, Zon LI, Johnson SL. An orthologue of the kit-related gene *fms* is required for development of neural crest-derived xanthophores and a subpopulation of adult melanocytes in the zebrafish, *Danio rerio*. *Development.* 2000;127(14):3031-44.
 73. Liu Y, Luo D, Lei Y, Hu W, Zhao H, Cheng CH. A highly effective TALEN-mediated approach for targeted gene disruption in *Xenopus tropicalis* and zebrafish. *Methods.* 2014;69(1):58-66.
 74. Inoue D, Wittbrodt J. One for all--a highly efficient and versatile method for fluorescent immunostaining in fish embryos. *PLoS One.* 2011;6(5):e19713.
 75. Hovens IB, Nyakas C, Schoemaker RG. A novel method for evaluating microglial activation using ionized calcium-binding adaptor protein-1 staining: cell body to cell size ratio. *Neuroimmunology and Neuroinflammation.* 2014;1(2):82-8.

Chapter 6

Hexb enzyme deficiency leads to lysosomal abnormalities in radial glia and microglia in zebrafish brain development

Laura E. Kuil¹, Anna López Martí^{1, #}, Ana Carreras Mascaró^{1, #}, Paul van den Berg¹, Herma C. van der Linde¹, Kees C. Schoonderwoerd¹ and Tjakko J. van Ham¹

¹Department of Clinical Genetics, Erasmus MC, University Medical Center Rotterdam, Wytemaweg 80, 3015 CN Rotterdam, The Netherlands.

Equal contribution

In revision, Glia

Abstract

Sphingolipidoses are severe, mostly infantile lysosomal storage disorders (LSDs) caused by defective glycosphingolipid degradation. Two of these sphingolipidoses, Tay Sachs and Sandhoff diseases, are caused by β -Hexosaminidase (HEXB) enzyme deficiency, resulting in ganglioside (GM2) accumulation and neuronal loss. The precise sequence of cellular events preceding and leading to neuropathology remain unclear, but likely involve inflammation and lysosomal accumulation of GM2 in multiple cell types. We aimed to elucidate, by mutating *hexb* in zebrafish, how loss of Hexb activity causes cellular pathology in the developing brain. Hexb deficient zebrafish (*hexb*^{-/-}) showed lysosomal abnormalities already early in development both in radial glia, which are the neuronal and glial progenitors, and in microglia. Additionally, at 5 days post-fertilization, *hexb*^{-/-} zebrafish showed reduced locomotor activity and increased apoptosis in the brain. Lysosomal alterations in glia, cell death in the brain and reduced locomotor activity occur simultaneously, suggesting that glial abnormalities could precede neuronal loss. In all, we identified cellular consequences of loss of Hexb enzyme activity during embryonic brain development, showing early effects on glia, which possibly underlie the subsequent neurodegeneration and behavioral aberrations. Hereby, we identified clues into the contribution of non-neuronal lysosomal abnormalities in LSDs affecting the brain and provide a tool to further study the consequences of Hexb deficiency *in vivo*.

Introduction

Lysosomal storage disorders (LSDs) comprise a group of at least 55 disorders, which are caused by genetic variants in lysosomal enzymes leading to loss of protein function. LSDs frequently involve progressive neurodegeneration, and for most of them there is no treatment available yet. How lysosomal dysfunction leads to neurodegeneration in LSDs is not completely understood. One LSD, Sandhoff disease, is caused by mutations in *HEXB*, leading to deficiencies in both β -Hexosaminidase A and β -Hexosaminidase B hydrolases, formed by HEXA/B or HEXB/B dimers, respectively. Recessive mutations in *HEXA* cause Tay-Sachs disease, which presents with identical clinical pathology to SD. β -Hexosaminidase plays a role in ganglioside metabolism and hydrolyzes GM2 gangliosides into GM3 gangliosides in lysosomes. Loss of either *HEXA* or *HEXB* results in accumulation of the ganglioside GM2, and therefore these disorders are clustered as GM2 gangliosidoses. GM2 accumulation is mainly found in brain cells, including neurons and glia. It is unknown however what molecular and cellular events precede pathology and cause SD.

In the most common and severe form of SD, symptoms appear during infancy. At about 3 to 6 months after birth, after an initially normal post-natal development, development slows down and skeletal muscles weaken, causing loss of acquired motor abilities such as turning over, sitting upright and crawling (1). Most symptoms are neurological and include an exaggerated startle response to loud noises, seizures, vision and hearing loss, intellectual disability, and paralysis. There is no treatment available and infantile Sandhoff patients typically do not live longer than 5 years (1). Due to the very early onset and rapid disease progression, the initial cellular events leading to neuronal loss remain obscure.

SD neuropathology involves neuronal loss, the presence of increased numbers of activated microglia -the brain's macrophages- and astrocytes (2-4). Expansion of both microglia and astrocyte numbers are in fact found in many brain disorders including epilepsy, other LSDs, multiple sclerosis, and neurodegenerative disorders, and likely play a role in pathogenesis (5-11). In SD mice, GM2 storage is found in lysosomes of neurons, but also in lysosomes of astrocytes and microglia (12-14). Based on pathology and gene expression data, it is still unclear which cell types are responsible for the initiation and progression of the pathology. In SD mice microglial activation was found to precede neurodegeneration (15). In microglia, *HEXB* is remarkably highly expressed compared to expression in other brain cell types and even considered to be a microglial signature gene (16-21). Given that microglia are highly phagocytic,

lysosomal function is critical for processing ingested material and HEXB could also be important for microglial function. Several studies showed that suppression of microglial or astrocytic inflammation could reduce SD pathology, suggesting both glial cells might be involved in SD pathogenesis (12, 15, 22). It is important to determine if, and to what extent, HEXB deficiency also affects glial function or if gliosis is a consequence of neuronal problems directly caused by the loss of HEXB. Analysis of *Hexb*^{-/-} mouse fetal neuronal stem cells (NSCs), also called radial glia, revealed a more frequent differentiation towards the astrocyte lineage rather than neurons, indicating abnormal differentiation of brain cells (23). SD patient IPS cell-derived organoids also showed aberrant neuronal differentiation (24). These studies suggest that *HEXB* deficiency could intrinsically affect neuronal differentiation and induce increased astrocyte numbers, which could be an initiating event in the pathogenesis of SD.

Potential therapeutic options for SD include gene therapy, immune suppression and bone marrow transplantation. Gene therapy in SD mouse models, applied by intravenous viral transduction from postnatal day 1 and 2, prevented pathology (25). However, the subclinical disease process preceding the onset of symptoms makes early intervention using gene therapy difficult to implement. Immune suppression or bone marrow transplantations improve neurological function in SD mice, likely by reducing gliosis (15, 26-29). Although these therapies seem very promising, it is important to understand to what extent such approaches are targeting the cause, rather than inhibiting the symptoms. Therefore, understanding the early cellular pathogenic processes will facilitate the development of an effective treatment for SD.

Remarkably, natural occurring *HEXB* or *HEXA* variants leading to gangliosidoses, have been observed in various domesticated as well as wild vertebrate species including dogs, cats, sheep, Muntjak deer and flamingos (30-36). The disease course in these animals is similar to that in humans, showing the conserved importance of proper processing of gangliosides. To understand SD pathogenesis, we aimed to visualize the earliest lysosomal abnormalities to discern the affected cell types during brain development *in vivo*. We used the zebrafish as a model since their offspring develop ex utero allowing the visualization of pathology *in vivo* using live imaging, they have a relative small size and are transparent, and have previously been used to study lysosomal (dys) function (37-42). Moreover, zebrafish harbor a single *HEXB* homolog, *hexb*, and transgenic reporter lines are available to label different cell types. We generated an SD zebrafish model in which we investigated the earliest emergence of cell-

type specific lysosomal abnormalities in the developing brain. Already in the first days of brain development, we identified increased lysosomal volume in radial glia and altered lysosomal morphology in microglia. With the present study we identified some of the cellular consequences of loss of Hexb enzyme activity during embryonic brain development, showing early effects on glia, which possibly underlie the subsequent neurodegeneration and behavioral aberrations.

Results

Direct mutagenesis causes Hexb enzyme deficiency and glial lysosomal abnormalities

Zebrafish Hexb has a ~64% sequence identity with the human protein, and is encoded by a single *hexb* gene. We targeted *hexb* by injecting fertilized zebrafish oocytes at the one-cell stage with Cas9 protein/gRNA complex targeting exon 1 of *hexb*. To determine the efficiency of targeting the zebrafish *hexb* locus, the generation of insertions and deletions (InDels) was determined by Sanger sequencing genomic DNA from individual 4 dpf larvae (n=24). This was followed by sequence decomposition using TIDE showing that, on average, 94% of the alleles harbor InDels (i.e. mutagenesis efficiency)(Fig 1A)(43). We refer to the F0 generation of larvae that are directly injected with Cas9 protein/gRNA complex as crispants. HEXA and HEXB enzyme activity are both affected in SD patients. Therefore, we analyzed β -Hexosaminidase (Hexa and Hexb) enzyme activity in dissected heads of control and *hexb* crispants. Tail genomic DNA of these larvae showed highly efficient (97-100%) InDel generation, and, consistent with loss of Hexb activity, *hexb* crispants showed >95% detectable reduction in substrate conversion by β -Hexosaminidase A+B (Fig. 1B).

HEXB is a microglial signature gene, and is one of the highest expressed lysosomal enzymes in microglia (17, 19, 20, 44). SD neuropathology includes microglial activation, and therefore we hypothesized that Hexb deficiency would affect microglial lysosomes. To visualize lysosomes *in vivo* we used lysotracker (LT) staining, which labels all acidic organelles including lysosomes, and to visualize microglia we used transgenic zebrafish in which GFP expression is driven by the *mpeg1*-promotor (37, 39, 45). At 4 dpf, although there were no major differences in microglial numbers, lysosomal compartments of *hexb* deficient microglia were found to be enlarged compared to those in controls, suggesting that Hexb deficiency results in lysosomal abnormalities in microglia (Fig 1C-D). Unexpectedly, however, we also observed numerous LT+ speckles outside microglia that were more prominently present in *hexb* crispants (Supplemental movie 1). These speckles are most likely

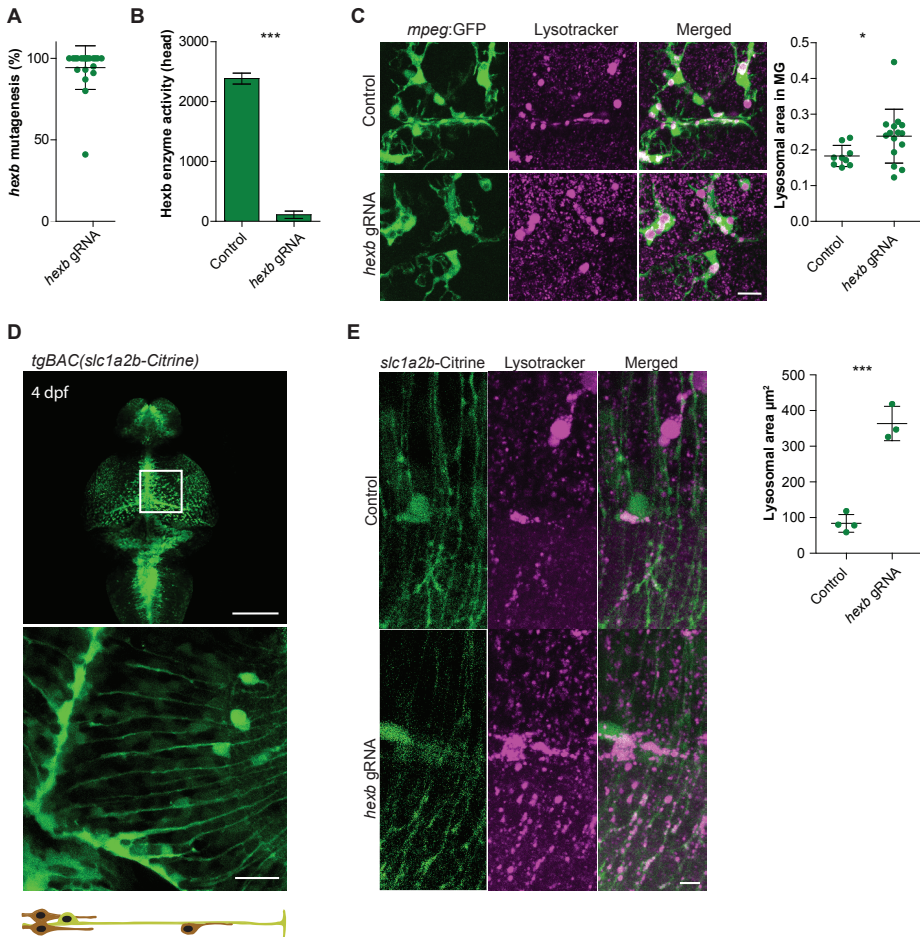


Fig 1. Efficient mutagenesis in *hexb* crispants shows abnormal lysosomes in microglia and radial glia **A** Graph shows mutagenesis efficiency for 24 injected fish at 4 dpf. **B** *hexb* crispants show almost no enzymatic conversion of substrate by β -Hexosaminidase A+B at 4 dpf. **C** Representative images of microglia in 8 dpf larvae imaged in the depicted area. Scale bar represents 20 μm . Quantification of relative lysotracker (LT+) area within microglia of 8 dpf larvae. **D** Expression pattern of the tgBAC(*slcl1a2b:Citrine*) transgenic line at 4 dpf with magnification showing the radial fibers in the optic tectum, and a schematic showing radial glia orientation and direction of neurogenic migration along the radial fibers. Scale bars represent 100 and 20 μm , respectively **E** Representative images of radial glia at 4 dpf in controls and in *hexb* crispants with quantification of relative LT+ signal per measured area. Scale bars represent 10 μm . Error bars represent SD. **A**, **C**, **E** each dot represents 1 larva.

lysosomes of another cell type that is not fluorescently labelled in the *mpeg1* reporter line.

Astrocytes have been shown to accumulate gangliosides GM2 and GA2

in postnatal *Hexb*^{-/-} mice, and showed increased proliferation (13). In zebrafish, radial glia have both astrocytic and radial glia/neural stem cell properties (reviewed in: (46)). For example, homologs of two mammalian astrocytes genes, *Slc1a2*, encoding the glutamate transporter GLT-1, and *Gfap*, are expressed in radial glia in zebrafish (*slc1a2b* and *gfap*)(47). Similarly, astrocyte endfeet in mammals express tight junction proteins, which in zebrafish are also expressed particularly in radial glia (48, 49). We hypothesized that the lysosomal puncta observed outside microglia in *hexb* crispants may reside in radial glia (RG). We used bacterial artificial chromosome (BAC)-recombineering to generate an *slc1a2b* fluorescent reporter line, TgBAC(*slc1a2b:Citrine*), expressing Citrine in the cytoplasm of RG (Fig 1D + S1)(50). In *slc1a2b:Citrine* zebrafish, the fluorescent expression pattern appeared highly similar to that observed by *slc1a2b* mRNA in situ hybridization, showing cell bodies lining the ventricle and radial fibers extending throughout the brain (Fig. 1D + S1)(47). We next visualized lysosomes in RG of control and *hexb* crispants. The majority of LT+ speckles, both in control and in *hexb* crispant larvae, showed co-localization with the radial fibers of *slc1a2b*+ RG (Supplementary movie 2; Fig S2). Quantification of the lysosomal area in the imaged regions, which contain RG fibers and cell bodies, showed more abundant lysosomes present in *hexb* crispants (Fig. 1E). Together, loss of Hexb enzyme activity results in abnormal lysosomal phenotypes in both microglia and RG.

Early abnormal lysosomal phenotypes both in microglia and RG of *hexb*^{-/-} larvae

To validate and further investigate the Hexb deficient phenotype, which we observed in *hexb* crispants, we generated stable mutants containing a 14 bp frame-shifting deletion in the first exon of *hexb*, leading to 19 out of frame amino acids followed by a premature stop codon (Fig 2A). To test whether this causes β -Hexosaminidase (Hexa + Hexb) deficiency, we measured β -Hexosaminidase A+B activity in lysates from control and *hexb*^{-/-} larval heads, and also in adult brain and internal organs, which showed that activity was reduced by > 99% (Fig 2B). Surprisingly, adult *hexb*^{-/-} zebrafish were viable and do not show obvious motility defects.

We wanted to further explore the consequences of Hexb-deficiency on brain function and development, and determined by LT staining when lysosomal aberrations in microglia first appeared. We first quantified LT-stained surface in control and *hexb*^{-/-} microglia in 5 dpf larvae, which in contrast to the increased lysosomal volume that we observed in 8 dpf *hexb* crispants, showed

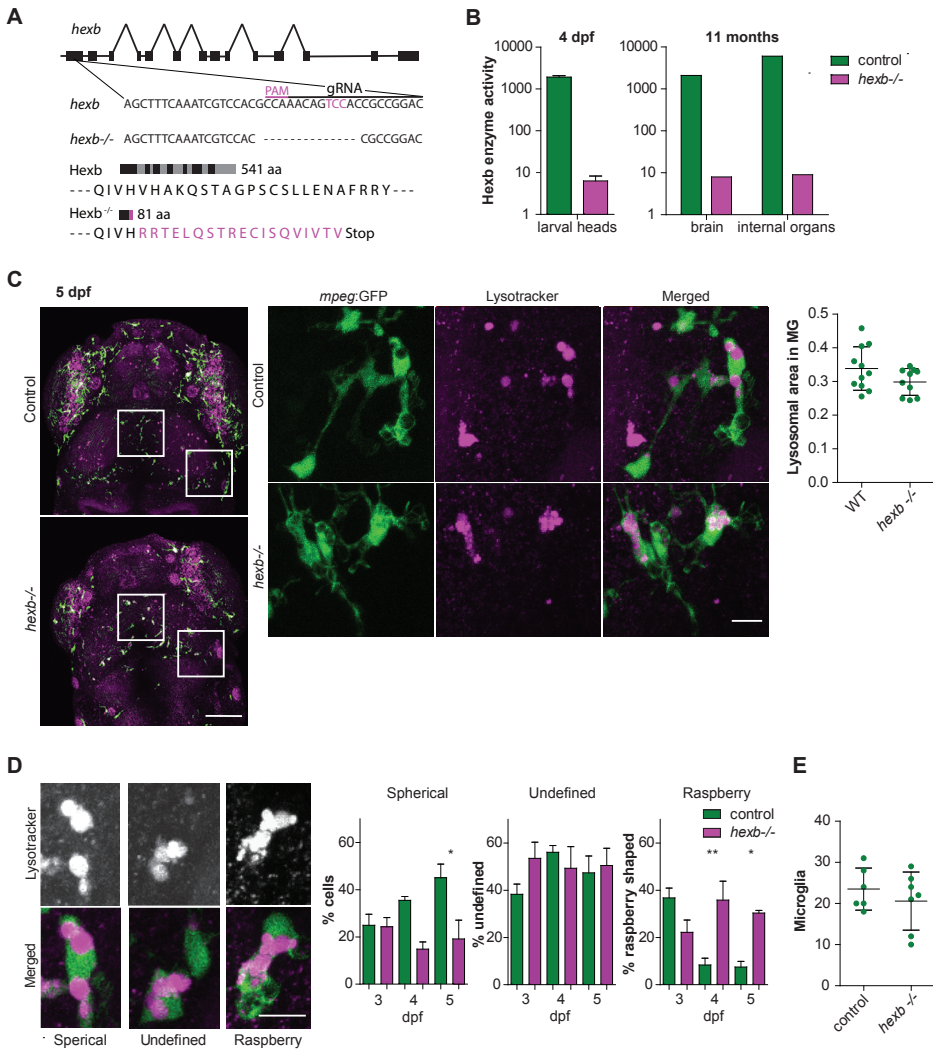


Fig 2. Stable *hexb*^{-/-} fish show impaired Hexb enzyme function and lysosomal abnormalities in microglia. **A** Schematic representation of the *hexb* gene and the 18 bp gRNA and PAM motif. The *hexb*^{-/-} fish show a 14 bp out of frame deletion disrupting part of the gRNA target sequence and PAM motif, resulting in 19 out of frame amino acids (magenta) followed by a premature stop codon. **B** Enzymatic substrate conversion by β -Hexosaminidase A+B in larval heads and adult brain and internal organs. **C** Representative images of microglia in LT-stained larvae at 5 dpf, scale bar represents 100 μ m. Quantifications were performed on detailed images of depicted regions, scale bar represents 10 μ m. Quantification of relative lysotracker area within microglia. **D** Classification of lysosomal morphology in microglia with their quantification at 3, 4 and 5 dpf. $n = 4$ to 6 larvae per group. Scale bars represent 10 μ m. **E** Quantification of total microglia in the imaged regions. Error bars represent SD. Each dot represents 1 larva.

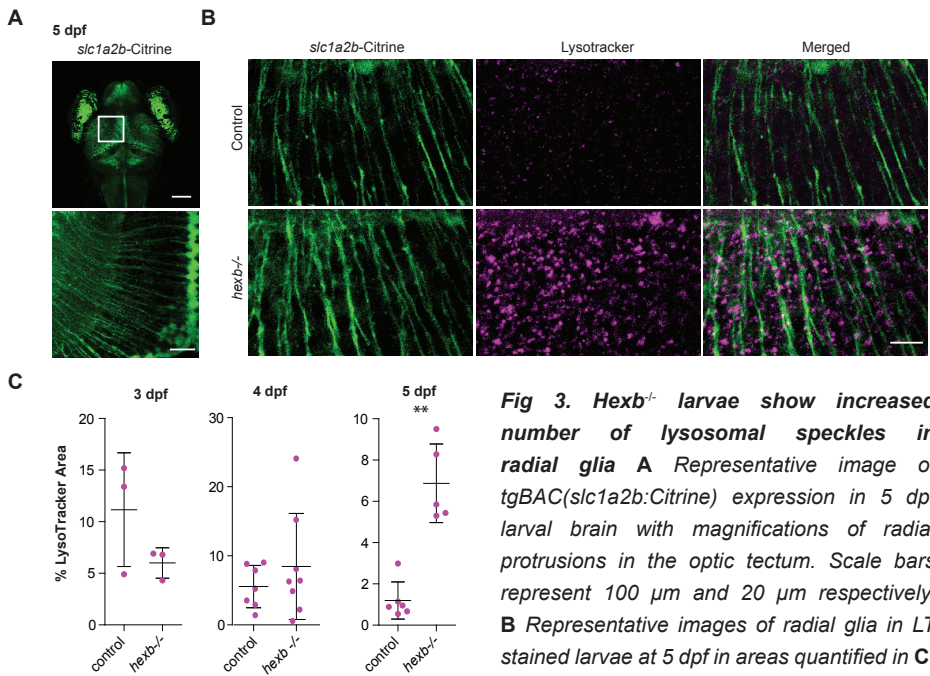


Fig 3. Hexb^{-/-} larvae show increased number of lysosomal speckles in radial glia **A** Representative image of tgBAC(slcl1a2b:Citrine) expression in 5 dpf larval brain with magnifications of radial protrusions in the optic tectum. Scale bars represent 100 μm and 20 μm respectively. **B** Representative images of radial glia in LT stained larvae at 5 dpf in areas quantified in **C**. Scale bar represents 10 μm. The brightness of the control LT image was enhanced to indicate the presence of some LT+ speckles. **C** Quantification of LT coverage, in percentage, within quantified areas. Each dot represents one larva. Error bars represent SD.

no changes (Fig 2C). However, detailed inspection of lysosomes in *hexb*^{-/-} and control microglia showed changes in lysosomal morphology. *hexb*^{-/-} microglia showed fewer lysosomes consisting of a single round compartment, but more lysosomes that seemed to consist of clustered small lysosomes. To quantify this, we defined three lysosomal categories: spherical (lysosomes that consist of a large, single round compartment), raspberry (lysosomes consisting of clustered smaller compartments) and undefined (lysosomes with intermediate morphology between those categories)(Fig 2D). At 3 dpf, lysosomal morphologies did not differ between controls and *hexb*^{-/-} brains, with the majority of lysosomes being raspberry shaped (Fig 2D). In control microglia the fraction of raspberry-shaped lysosomes decreased over time between 3 and 5 dpf, whereas *hexb*^{-/-} microglia contained relatively more raspberry shaped lysosomes, and fewer spherical shaped lysosomes (Fig 2D). This could indicate that small lysosomal vacuoles in *hexb*^{-/-} microglia fail to fuse and fail to form a larger spherical vacuole, which can possibly be explained by reduced phagocytic flux or reduced autophagosome fusion. Alternatively, lower numbers of microglia could result in increased

phagocytic demand for the residual microglia, which could lead to altered lysosomal morphologies. To evaluate this possibility, we quantified microglia numbers. Loss of *Hexb* activity did not affect microglial numbers (Fig 2E), and therefore the changes in lysosomal morphology are likely not caused by lower microglial numbers.

To determine when the abnormal lysosomes in RG first appeared, we imaged RG lysosomes in control and *hexb*^{-/-} zebrafish, and quantified lysosomal volume by measuring LT fluorescence in selected areas (Fig 3A). At 3 dpf LT+ lysosomal speckles were abundantly present in control and *hexb*^{-/-} radial fibers (Fig 3C). Over time however, LT+ speckles became undetectable in control RG, whereas LT+ speckles in the *hexb*^{-/-} radial fibers became more abundant. At 5 dpf *hexb*^{-/-} RG showed significantly more LT+ speckles than controls did (Fig 3B-C). These LT+ speckles in the radial fibers were highly motile, showing rapid and bidirectional trafficking inside the radial glial fibers, in both controls and *hexb*^{-/-} larvae. In all, we show that loss of *Hexb* activity early in embryonic development results in the persistence of enlarged lysosomal speckles in RG fibers.

***hexb*^{-/-} deficiency causes reduced locomotor activity and increased apoptosis in the brain**

The earliest symptoms that present in *SD* patients are loss of muscle strength and reduced motor function, both of which are likely caused by atrophy of the innervating lower and/or upper motor neurons. Therefore, we also measured locomotor activity under light and dark conditions in control and *hexb*^{-/-} fish. Zebrafish show stereotypical locomotor responses to shifts in light/dark conditions as early as 24 hpf (51-53). Locomotor activity over repeated light-dark cycles was recorded by infrared imaging and measured by automated tracking. Although control and *hexb*^{-/-} larvae both responded to light/dark switches, *hexb*^{-/-} larvae showed reduced locomotor activity, which was consistently detected at 4, 5 and 6 dpf (n=24 per group, per experiment)(Fig. 4A). This test mainly focuses on the behavioral response to shifts in light intensity, whereas we were mainly interested in general locomotor activity. Therefore, we developed a locomotor assay consisting of gradually increasing and decreasing light intensities, mimicking more physiological relevant changes regulating circadian behavior. *Hexb*^{-/-} larvae show >50% less locomotor activity during the light periods in this dusk/dawn cycle assay (Fig 4B). These findings indicate that reduced locomotor activity of *hexb*^{-/-} larvae is not due to a defect in the behavioral response to light/dark changes, but due to overall reduced locomotor activity compared to controls. Thus, *hexb*^{-/-}

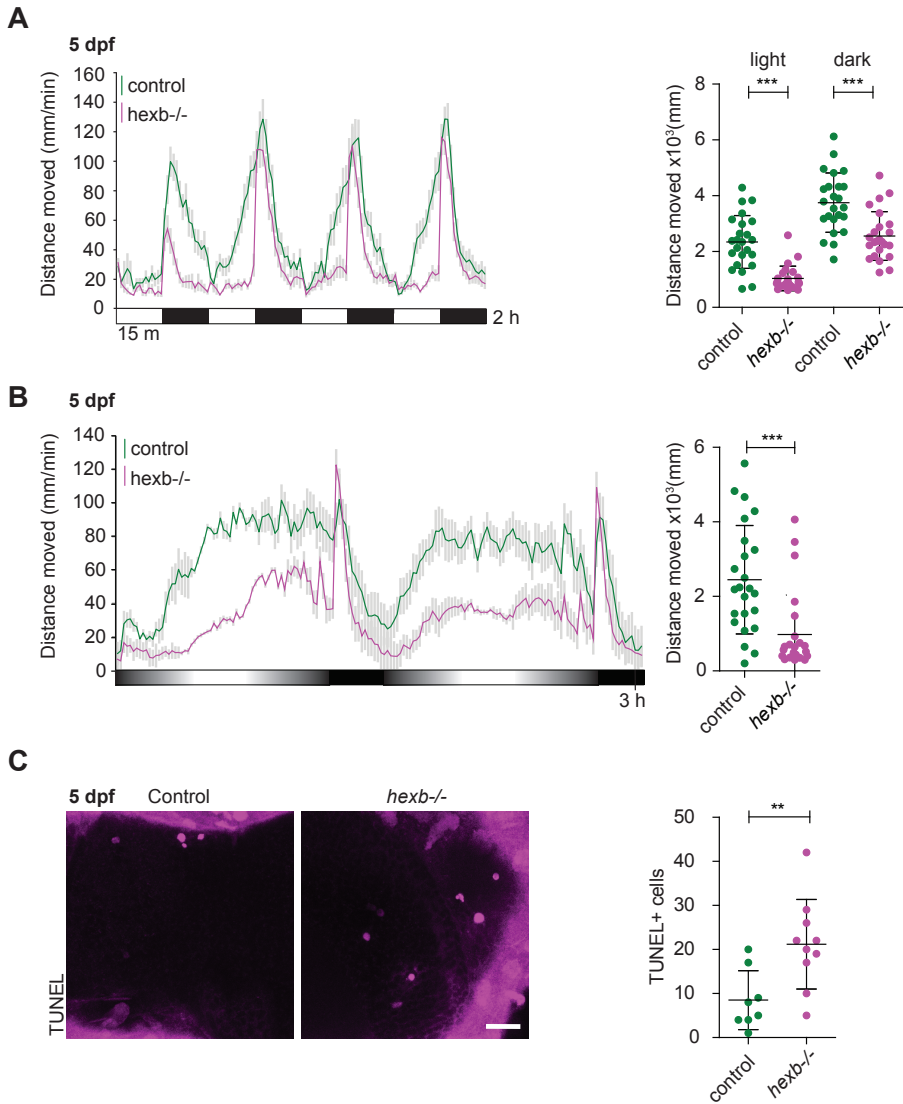


Fig 4. Locomotor activity assay shows abnormal locomotor activity in $hexb^{-/-}$ larvae

A Representative graph showing the locomotor responses of larvae to alternating light and dark periods indicated by white and black squares. Grey bars represent SEM. The dot plot shows the quantification of the sum distance moved during all the light and all the dark periods. **B** Representative graph showing the total distance travelled by larvae during the dusk-dawn routine (total time: 3 h 12 min). Quantification of the total distance moved throughout the experiment excluding the dark period. **A**, **B**, $n = 24$ larvae per genotype. Grey shading shows the standard error of the mean. **C** Representative images of TUNEL staining at 5 dpf with quantifications. Each dot represents one larva. Scale bar represents $20 \mu\text{m}$. Error bars represent SD unless stated otherwise.

larvae show abnormally low locomotor activity, which coincides with the timing of appearance of glial lysosomal abnormalities in the brain.

SD pathology is characterized by extensive loss of neurons. We performed TUNEL labelling at 5 dpf to test whether loss of brain cells occurs in *hexb*^{-/-} zebrafish. During normal vertebrate brain development extensive apoptosis occurs, and in zebrafish developmental apoptosis in brain development is particularly high at 3 and 4 dpf (54-58). In 5 day-old *hexb*^{-/-} brains we observed an ~2-fold increase in the number of apoptotic cells, consistent with increased loss of brain cells (Fig 4C). Taken together, Hexb deficiency in zebrafish leads to reduced locomotor activity and increased cell death in the brain, reminiscent of the pathology and symptoms observed in SD patients and β -Hexosaminidase deficiency in other vertebrate species. However, in zebrafish pathological signs are already visible at a very early stage within 4 days post fertilization.

Discussion

Here we generated *hexb*^{-/-} zebrafish, which are β -Hexosaminidase enzyme-deficient, and their pathology mimics molecular, cellular and behavioral phenotypes that are also observed in *HEXB*-deficient Sandhoff disease patients. Already within 5 days of development, *hexb*^{-/-} larvae presented with abnormal lysosomes in microglia and in radial glia. The appearance of abnormal lysosomes in glia coincided with increased apoptosis in the brain and reduced locomotor activity. These phenotypes were observed both in Cas9/*hexb* gRNA injected and in *hexb*^{-/-} larvae, which indicates that crispants are a very suitable method to rapidly screen for pathologic phenotypes, also for other lysosomal or metabolic diseases. In all, we demonstrated that loss of Hexb function causes abnormal lysosome accumulation in microglia and in RG as early as 96 hours post fertilization, concomitant with a decrease in locomotor activity and increased apoptosis in the brain. Therefore, based on our zebrafish model, the early presentation of abnormal lysosomes in glial cells implies that pathogenesis, including neuronal loss, might be characterized by dysfunctional glial cells in the first stages of SD.

Both in controls and *hexb*^{-/-} RG, we observed abundant lysosomal speckles in the radial fibers, at 3 and 4 dpf. In controls, the lysosomal speckles were undetectable by 5 dpf, whereas in *hexb*^{-/-} fish these abundant RG lysosomes persisted or remained enlarged. Enlarged lysosomal compartments are a characteristic of LSDs. This suggests that, to resolve lysosomes in RG, β -Hexosaminidase enzyme activity is required, and could imply that extensive processing of sphingolipids such as GM2 occurs at this stage of brain

development. Importantly, RG in vertebrates are neuronal stem cells, and are thought to produce most neurons, but also astrocytes and oligodendrocytes (59). This process requires extensive membrane remodeling involving synthesis and degradation of membrane lipids, including glycolipids, in which lysosomes play a key role (60-62). Consistent with this idea, differentiation of RG into astrocytes in mice was accompanied by an increase in lysosomes and autophagosomes (63). Furthermore, differentiation of SD-patient iPSC-derived RG to neurons and astrocytes was skewed towards astrocyte development (23). Based on these findings, the persistence or enlargement of lysosomal speckles that we observed in *hexb*^{-/-} RG *in vivo*, could be the result of impaired glycolipid metabolism, essential for membrane remodeling, and this could influence differentiation towards neurons and glia.

Lysosomes are typically thought to reside in the neuronal cell body, but trafficking of lysosomes has recently been reported in neuronal axons (64, 65). We found that lysosomes followed a continuous and rapid bidirectional trafficking within the radial glial fibers via live imaging. In addition, lysosomal transport in the axonal fibers is impaired in Alzheimer's disease and could be directly involved in the progression of the disease (66, 67). This suggests that lysosomal transport plays a role in brain diseases. Therefore, in case of Hexb deficiency, abnormal lysosomal transport in RG could perhaps alter the generation of neurons and glia cells early in larval development.

The *hexb* mutant locomotor phenotype is likely the consequence of alterations in the brain, as we did not observe obvious alterations in peripheral motoneurons and neuromuscular junctions (data not shown), whereas aberrant lysosomes in glia are already detected at these early stages. The reduced locomotor activity could be the result of lysosomal dysfunction in either microglia or RG. Microglia have essential functions for brain hemostasis, including clearance of apoptotic cells, myelin remodeling and synaptic pruning (58, 68-72). Defects in such processes could perhaps contribute to defects in locomotor control in the hindbrain leading to locomotor aberrations (73, 74). RG on the other hand produce neurons in the brain and alterations in neurogenesis during early development likely affects brain circuitry formation, which could also explain the reduced locomotor activity.

Gangliosidoses due to *HEXA* or *HEXB* mutations are associated with severe neurological symptoms that often precede early lethality. These diseases have been described in several mammalian species, including dogs, cats, and Muntjak deer, and even in birds as Hexa deficiency has been observed

in Flamingo's (30-36)(Rahman et al. 2012; Kolicheski et al. 2017; Martin et al. 2004; Kanae et al. 2007; Zeng et al. 2008). *hexb* deficient zebrafish seem to recapitulate early disease stages. On the other hand, adult homozygous *hexb*^{-/-} zebrafish, even though they lack Hexb activity, are viable and do not show obvious behavioral symptoms. To our knowledge, zebrafish are the first vertebrate species tested that do not succumb to pathology caused by loss of Hexb activity. Mice deficient in *Hexa* do not have a severe phenotype as they can bypass the need for HEXBA heterodimer activity by an alternative pathway requiring a sialidase, NEU3, to degrade gangliosides (75). Although the Hexb substrate conversion assay showed almost no activity in adult *hexb*^{-/-} zebrafish brain, it is possible that there is an alternative metabolic conversion route of GM2 preventing disease in zebrafish. Another explanation could be that zebrafish, in contrast to mammalian species, can regenerate brain tissue and produce new neurons throughout life (76-79). Zebrafish thereby could have the capacity to compensate for neuronal loss by regenerating neurons and might thereby be resistant to loss of Hexb activity.

In conclusion, *hexb*^{-/-} zebrafish show loss of enzyme activity, lysosomal abnormalities in glia, loss of brain cells and reduced locomotor activity, reminiscent of the molecular, cellular, neuropathological and motility aspects of Sandhoff disease. The very early accumulation of lysosomes, which rapidly traffic in radial processes of RG or seem to have a fusion defect in microglia, may represent that changes in glia are an early event in pathogenesis. These Hexb deficient zebrafish could be used to further dissect cellular mechanisms leading to disease and to identify small molecules that suppress the earliest emergence of cellular pathogenic features.

Material and methods

Zebrafish larvae husbandry

Zebrafish embryos and larvae were kept at 28°C on a 14–10-hour light-dark cycle in 1 M HEPES buffered (pH 7.2) E3 medium (34.8 g NaCl, 1.6 g KCl, 5.8 g CaCl₂ · 2H₂O, 9.78 g MgCl₂ · 6 H₂O). The medium was changed at 1 dpf to E3 + 0.003% 1-phenyl 2-thiourea (PTU) to prevent pigmentation. Larvae used for swimming assays were kept in media without PTU. Transgenic lines used were Tg(*mpeg1:GFP*)(45)(Lieschke Laboratory, Clayton, Australia) and TgBAC(*slc1a2b:Citrine*)^{re01tg}, generated in our lab with an TL background. Animal experiments were approved by the Animal Experimentation Committee at Erasmus MC, Rotterdam.

Generation of the tgBAC(*slc1a2b*:*Citrine*) reporter line

To generate the tgBAC(*slc1a2b*:*Citrine*)^{re01tg} reporter line we used the following clone DKEY-49F8 (HUKGB735F0849Q) in the pIndigoBAC-536 vector. To perform recombination to insert *tol2* sites and the cytoplasmic *Citrine*, the BAC recombineering protocol developed by Bussmann et al. (2011) was used (50). Primers are described in table 1.

Table 1. Primers used for BAC recombineering

Primer name	Primer sequence
pIndigoBAC_HA1_iTol2_fw	5'-ttctctgtttttgtccgtggaatgaacaatggaagtcgagctcatcgctCCCTGCTCGAGCC-GGGCCCAAGTG-3'
pIndigoBAC_HA2_iTol2_rev	5'-agccccgacaccgccaacaccgctgacgcgaaccttgccgcccgcattATATGATCCTCTAGATCAGATC-3'
pTarBAC_HA1_control_fw	5'-CTGTCAAACATGAGAATTGGTC-3'
amp_HA1_control_rev	5'-ACATTTCCTCCGAAAAGTGG-3'
amp_HA2_control_fw	5'-CTGAGATAGGTGCCTCACTG-3'
pIndigoBAC_HA2_control_rev	5'-TGGTGCACCTCTCAGTACAATC-3'
<i>Citrine</i> _HA1_control_rev	5'-GGACACGCTGAACCTTGTGG-3'
kanR_HA2_control_fw	5'-TCCTCGTGCTTTACGGTATC-3'
<i>slc1a2b</i> HA1 GFP fw	5'-GACCCAGATGTGTGCTGTTGTTTCATCTGCTCTGTTTCTCCGCAGTTGTGGACCATGGTGAGCAAGGGCGAGGAG-3'
<i>slc1a2b</i> HA2 KanR rv	5'-TCGATGGGCTCCAGGTGGCTTTTCGTGCATCCGTACCTCCACGTGCTTCGGTCAGAAGAACTCGTCAAGAAGGCG-3'
<i>slc1a2b</i> HA1 control fw	5'-CTCGACTGTGGTGACCTGTG-3'
<i>slc1a2b</i> HA2 control rv	5'-AGGTTCTTCCGCATCTTCTGG-3'

CRISPR-Cas9 genome editing in zebrafish

Hexb specific guideRNAs (gRNAs) were designed and synthesized by transcribing from PCR fragment containing a T7 promoter as described previously (80, 81). To target the *hexb* gene the online program CRISPRscan was used to design an 18 bp complementary gRNA targeting exon 1 (New Haven, Connecticut, USA) (80)(Table 2). PCR fragments containing a T7 promoter and gRNA sequence were generated by FastStart™ High Fidelity PCR System (Sigma, St. Louis, Missouri, USA) as described (80). To transcribe gRNAs from PCR fragments the mMMESSAGE mMACHINE™ T7 ULTRA Transcription Kit (Invitrogen, Carlsbad, California, USA) was used according to the manufacturer's instructions followed by RNA cleanup and determination of the quality and concentration by agarose gel electrophoresis and using NanoDrop™ (ThermoFisher, Waltham, Massachusetts, USA). *Hexb* specific gRNA 600-900 ng of the synthesized gRNA was mixed

with 4 ng of Cas9 nuclease (Sigma, St. Louis, Missouri, USA). The volume was adjusted with 300 mM KCl to a total volume of 6 μ l. Approximately 10 nl of the mix was injected in fertilized zebrafish oocytes. Genomic DNA surrounding the gRNA target site was sequenced using Sanger sequencing and indel efficiency was determined using the online tool TIDE (Table 2)(43). Founders were selected by sequencing DNA from the tails of adult zebrafish, fish containing mainly 14 bp deletions were selected for breeding. F1 fish were genotyped and selected for -14 bp deletions using sanger sequencing. Mutant fish containing -14 bp mutations in *hexb* are called *hexb^{re04}*, but referred to as *hexb⁻* throughout this report.

Table 2. Primers used for gRNA synthesis and sanger sequencing

Primer name	Primer sequence
<i>hexb</i> gRNA fw	taatacagactcactataGGGTCCGGCGGTGGACTGTTgttttagagctagaa
gRNA synthesis rev	GATCCGCACCGACTCGGTGCCACTTTTTCAAGTTGATAACGGACTAGCCTATTTTA ACTTGCTATTTCTAGCTCTAAAAC
<i>hexb</i> sequencing fw	GCTCAACACAACCATGCTCT
<i>hexb</i> sequencing rev	ATGTGATCCATACCTGCAGC

LysoTracker staining

Zebrafish larvae were incubated in 1.5 ml tubes with 10 μ l LysoTracker™ Red DND-99 (ThermoFisher, Waltham, Massachusetts, USA) in 100 μ l E3-PTU. The tube was kept at 28 °C for 40 minutes with the lid open and protected from light . The media was replaced by E3-PTU only and the fish were mounted after at least ten minutes to wash away excess dye.

Fluorescence microscopy imaging

Zebrafish were anesthetized using tricaine (0.016 %) and mounted in 1.8 % low melting point agarose. The imaging dish was covered with HEPES-buffered E3 containing tricaine during imaging. Larvae were imaged on a Leica SP5 intravital microscope with multiphoton laser using a 20x water dipping objective (Leica Plan-Apochromat, NA = 1.0) using 488 and 561 laser lines. Confocal z-stack images were acquired. Images were processed with ImageJ software.

β -Hexosaminidase activity assay

Heads were dissected from 4 dpf control larvae and *hexb* crispants or mutants after euthanizing them with ice water and an overdoses tricaine and analyzed for enzymatic activity. Pools of 2 or 3 dissected heads were grouped according to their genotype and homogenized using sonication in 100 μ l H₂O. Protein

concentration was measured using BCA reagent by spectrophotometry after 1-hour incubation at 37°C (Pierce). The substrate, 5 mM MU- β -GlcNAc in 0.2 M Na-phosphate/0.1 M citrate buffer, pH 4.4 + 0.02% (w/v) NaN₃, was added to each lysate pool, including one replicate per sample, and incubated for 1-hour at 37 °C in which β -Hexosaminidase will form 4-MU. After addition of 0.5 M Na₂CO₃ buffer, pH 10.7, 4-MU fluorescence was measured and normalized to the blank (substrate alone). The final read-out consisted of nmoles of 4-MU released per hour per mg of protein.

Locomotor activity assays

To assess the locomotor activity of zebrafish larvae from 3 to 5 dpf, locomotor activity assays were performed using an infrared camera system (DanioVision™ Observation chamber, Noldus) and using EthoVision® XT software (Noldus). Control (n = 24) and *hexb*^{-/-} (n = 24) zebrafish larvae, in 48 well plates, were subjected to two different light/dark routines. The White Light routine consisted of a 30 min habituation period, followed by 4 cycles of 15 min of light (100%)/ 15 min darkness 15 (2.5 h total). The Dawn routine 30 minutes habituation in the dark (0% light intensity), followed by the routine described in table 3 and comprised 3 h 12 min. Each experiment was performed twice for the three ages (3, 4 and 5 dpf) with n = 24 controls, and n = 24 mutants per experiment. Distance traveled (mm) per second was measured.

Table 3. Dusk-dawn routine

Light intensity (%)	1	5	10	20	30	40	50	40	30	20	10	5	0
Duration (min)	1	5	5	5	5	5	15	5	5	5	5	5	15

Statistical analysis

To measure *mpeg1*:GFP and LysoTracker (LT) volumes in confocal microscopic imaging data, images were analyzed using automatic thresholding in Fiji/ImageJ. The total area of the LT inside *mpeg1*⁺ microglia was measured and compared to the total *mpeg1*⁺ microglial area. For the radial glia LT area, images were automatically thresholded and the total LT⁺ area per imaged region was measured using the Analyze Particles plug-in (FIJI). For image processing and quantitative analysis, Excel (Microsoft), Prism (Graphpad) and ImageJ were used. Statistical significance was calculated using student's *t*-test and ANOVA with a bonferroni correction. Error bars indicate standard deviation (SD) and *p* < 0.05 was considered significant. Symbols in the graphs (*; **, ***) display levels

of significance ($p < 0.05$; $p < 0.01$; $p < 0.001$ respectively).

Acknowledgements

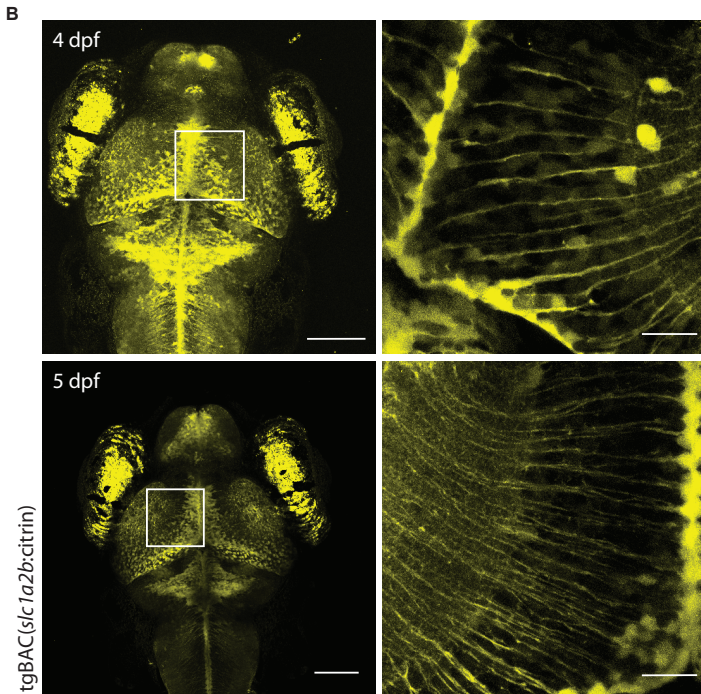
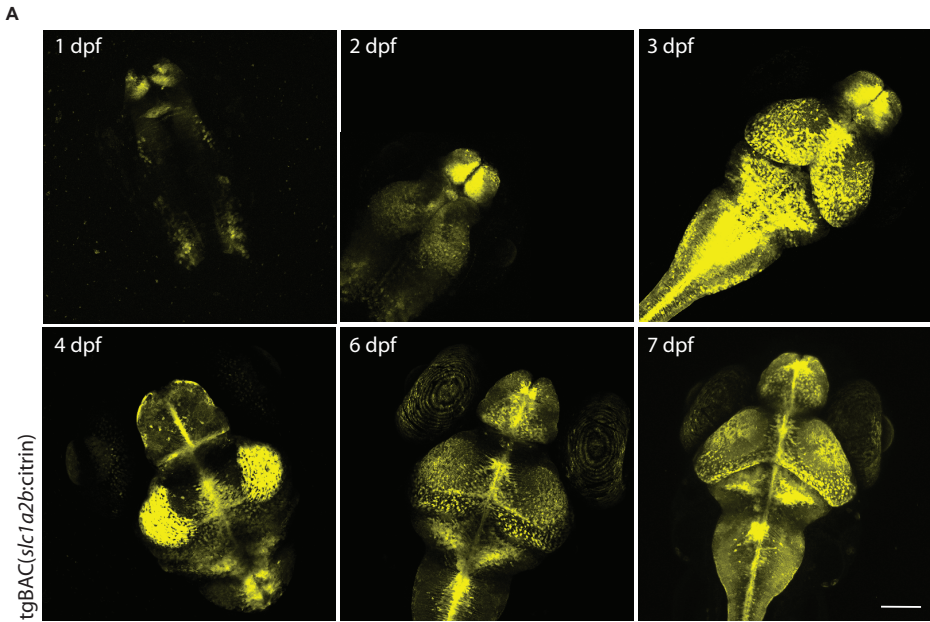
We thank dr. Gerben Schaaf for valuable feedback on the manuscript and Nynke Oosterhof for the help with the ImageJ macro for LT quantifications. The members of the Erasmus MC Optical Imaging Center (OIC) are acknowledged for assistance on microscopy. This work was sponsored by a ZonMW VENI grant and an Erasmus University Rotterdam fellowship to TJvH.

References

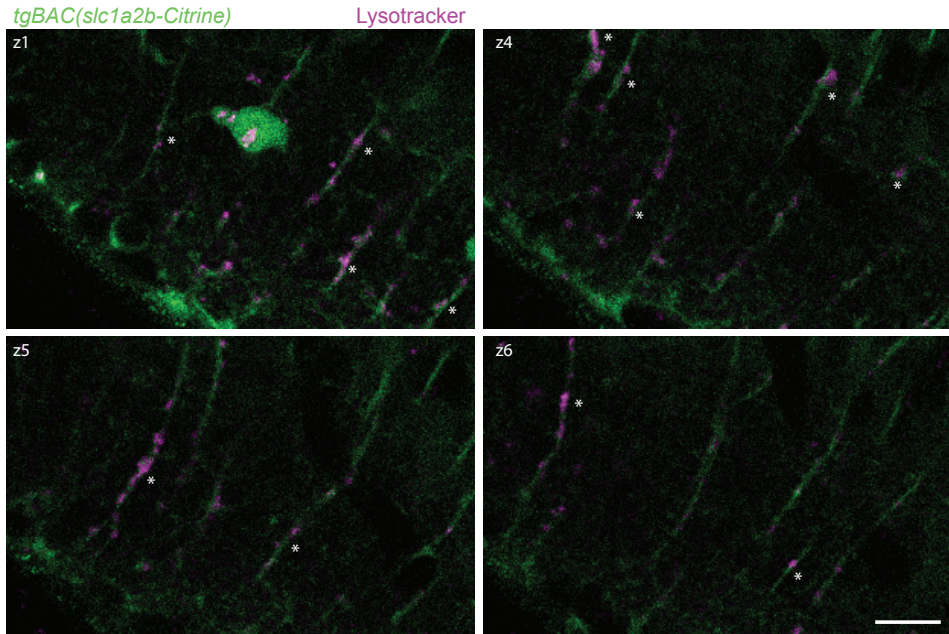
- Hendriksz, C.J., et al., Juvenile Sandhoff disease—nine new cases and a review of the literature. *J Inherit Metab Dis*, 2004. 27(2): p. 241-9.
- Jeyakumar, M., et al., Central nervous system inflammation is a hallmark of pathogenesis in mouse models of GM1 and GM2 gangliosidosis. *Brain*, 2003. 126(Pt 4): p. 974-87.
- Myerowitz, R., et al., Molecular pathophysiology in Tay-Sachs and Sandhoff diseases as revealed by gene expression profiling. *Hum Mol Genet*, 2002. 11(11): p. 1343-50.
- Sargeant, T.J., et al., Characterization of inducible models of Tay-Sachs and related disease. *PLoS Genet*, 2012. 8(9): p. e1002943.
- Fakhoury, M., Microglia and Astrocytes in Alzheimer's Disease: Implications for Therapy. *Curr Neuropharmacol*, 2018. 16(5): p. 508-518.
- Joe, E.H., et al., Astrocytes, Microglia, and Parkinson's Disease. *Exp Neurobiol*, 2018. 27(2): p. 77-87.
- Lee, J., et al., Astrocytes and Microglia as Non-cell Autonomous Players in the Pathogenesis of ALS. *Exp Neurobiol*, 2016. 25(5): p. 233-240.
- Geloso, M.C., et al., The Dual Role of Microglia in ALS: Mechanisms and Therapeutic Approaches. *Front Aging Neurosci*, 2017. 9: p. 242.
- Zhao, X., et al., Noninflammatory Changes of Microglia Are Sufficient to Cause Epilepsy. *Cell Rep*, 2018. 22(8): p. 2080-2093.
- Ponath, G., C. Park, and D. Pitt, The Role of Astrocytes in Multiple Sclerosis. *Front Immunol*, 2018. 9: p. 217.
- Oosterhof, N., et al., Colony-Stimulating Factor 1 Receptor (CSF1R) Regulates Microglia Density and Distribution, but Not Microglia Differentiation In Vivo. *Cell Rep*, 2018. 24(5): p. 1203-1217 e6.
- Tsuji, D., et al., Specific induction of macrophage inflammatory protein 1-alpha in glial cells of Sandhoff disease model mice associated with accumulation of N-acetylhexosaminyl glycoconjugates. *J Neurochem*, 2005. 92(6): p. 1497-507.
- Kawashima, N., et al., Mechanism of abnormal growth in astrocytes derived from a mouse model of GM2 gangliosidosis. *J Neurochem*, 2009. 111(4): p. 1031-41.
- Kyrkanides, S., et al., Conditional expression of human beta-hexosaminidase in the neurons of Sandhoff disease rescues mice from neurodegeneration but not neuroinflammation. *J Neuroinflammation*, 2012. 9: p. 186.
- Wada, R., C.J. Tiff, and R.L. Proia, Microglial activation precedes acute neurodegeneration in Sandhoff disease and is suppressed by bone marrow transplantation. *Proc Natl Acad Sci U S A*, 2000. 97(20): p. 10954-9.
- Bennett, F.C., et al., A Combination of Ontogeny and CNS Environment Establishes Microglial Identity. *Neuron*, 2018. 98(6): p. 1170-1183 e8.
- Oosterhof, N., et al., Identification of a conserved and acute neurodegeneration-specific microglial transcriptome in the zebrafish. *Glia*, 2017. 65(1): p. 138-149.
- Hickman, S.E., et al., The microglial sensome revealed by direct RNA sequencing. *Nat Neurosci*, 2013. 16(12): p. 1896-905.
- Gosselin, D., et al., An environment-dependent transcriptional network specifies human microglia identity. *Science*, 2017. 356(6344).
- Artegiani, B., et al., A Single-Cell RNA Sequencing Study Reveals Cellular and Molecular Dynamics of the Hippocampal Neurogenic Niche. *Cell Rep*, 2017. 21(11): p. 3271-3284.
- Butovsky, O., et al., Identification of a unique TGF-beta-dependent molecular and functional signature in microglia. *Nat Neurosci*, 2014. 17(1): p. 131-43.
- Wu, Y.P. and R.L. Proia, Deletion of macrophage-inflammatory protein 1 alpha retards neurodegeneration in Sandhoff disease mice. *Proc Natl Acad Sci U S A*, 2004. 101(22): p. 8425-30.
- Ogawa, Y., et al., Abnormal differentiation of Sandhoff disease model mouse-derived multipotent stem cells toward a neural lineage. *PLoS One*, 2017. 12(6): p. e0178978.
- Allende, M.L., et al., Cerebral organoids derived from Sandhoff disease-induced pluripotent stem cells exhibit impaired neurodifferentiation. *J Lipid Res*, 2018. 59(3): p. 550-563.
- Niemir, N., et al., Intravenous administration of scAAV9-Hexb normalizes lifespan and prevents pathology in Sandhoff disease mice. *Hum Mol Genet*, 2018. 27(6): p. 954-968.
- Wu, Y.P., et al., Sphingosine kinase 1/S1P receptor signaling axis controls glial proliferation in mice with Sandhoff disease. *Hum Mol Genet*, 2008. 17(15): p. 2257-64.
- Abo-Ouf, H., et al., Deletion of tumor necrosis factor-alpha ameliorates neurodegeneration in Sandhoff disease mice. *Hum Mol Genet*, 2013. 22(19): p. 3960-75.

28. Ogawa, Y., et al., FcRgamma-dependent immune activation initiates astrogliosis during the asymptomatic phase of Sandhoff disease model mice. *Sci Rep*, 2017. 7: p. 40518.
29. Ogawa, Y., et al., Inhibition of astrocytic adenosine receptor A2A attenuates microglial activation in a mouse model of Sandhoff disease. *Neurobiol Dis*, 2018. 118: p. 142-154.
30. Kolicheski, A., et al., GM2 Gangliosidosis in Shiba Inu Dogs with an In-Frame Deletion in HEXB. *J Vet Intern Med*, 2017. 31(5): p. 1520-1526.
31. Rahman, M.M., et al., A frameshift mutation in the canine HEXB gene in toy poodles with GM2 gangliosidosis variant 0 (Sandhoff disease). *Vet J*, 2012. 194(3): p. 412-6.
32. Martin, D.R., et al., An inversion of 25 base pairs causes feline GM2 gangliosidosis variant. *Exp Neurol*, 2004. 187(1): p. 30-7.
33. Kanae, Y., et al., Nonsense mutation of feline beta-hexosaminidase beta-subunit (HEXB) gene causing Sandhoff disease in a family of Japanese domestic cats. *Res Vet Sci*, 2007. 82(1): p. 54-60.
34. Cork, L.C., et al., GM2 ganglioside lysosomal storage disease in cats with beta-hexosaminidase deficiency. *Science*, 1977. 196(4293): p. 1014-7.
35. Zeng, B.J., et al., Spontaneous appearance of Tay-Sachs disease in an animal model. *Mol Genet Metab*, 2008. 95(1-2): p. 59-65.
36. Torres, P.A., et al., Tay-Sachs disease in Jacob sheep. *Mol Genet Metab*, 2010. 101(4): p. 357-63.
37. Shen, K., H. Sidik, and W.S. Talbot, The Rag-Ragulator Complex Regulates Lysosome Function and Phagocytic Flux in Microglia. *Cell Rep*, 2016. 14(3): p. 547-559.
38. Li, H., et al., Novel degenerative and developmental defects in a zebrafish model of mucopolipidosis type IV. *Hum Mol Genet*, 2017. 26(14): p. 2701-2718.
39. Berg, R.D., et al., Lysosomal Disorders Drive Susceptibility to Tuberculosis by Compromising Macrophage Migration. *Cell*, 2016. 165(1): p. 139-152.
40. Festa, B.P., et al., Impaired autophagy bridges lysosomal storage disease and epithelial dysfunction in the kidney. *Nat Commun*, 2018. 9(1): p. 161.
41. Louwette, S., et al., NPC1 defect results in abnormal platelet formation and function: studies in Niemann-Pick disease type C1 patients and zebrafish. *Hum Mol Genet*, 2013. 22(1): p. 61-73.
42. Keatinge, M., et al., Glucocerebrosidase 1 deficient *Danio rerio* mirror key pathological aspects of human Gaucher disease and provide evidence of early microglial activation preceding alpha-synuclein-independent neuronal cell death. *Hum Mol Genet*, 2015. 24(23): p. 6640-52.
43. Brinkman, E.K., et al., Easy quantitative assessment of genome editing by sequence trace decomposition. *Nucleic Acids Res*, 2014. 42(22): p. e168.
44. Keren-Shaul, H., et al., A Unique Microglia Type Associated with Restricting Development of Alzheimer's Disease. *Cell*, 2017. 169(7): p. 1276-1290 e17.
45. Ellett, F., et al., mpeg1 promoter transgenes direct macrophage-lineage expression in zebrafish. *Blood*, 2011. 117(4): p. e49-56.
46. Lyons, D.A. and W.S. Talbot, Glial cell development and function in zebrafish. *Cold Spring Harb Perspect Biol*, 2014. 7(2): p. a020586.
47. McKeown, K.A., et al., Disruption of *Eaat2b*, a glutamate transporter, results in abnormal motor behaviors in developing zebrafish. *Dev Biol*, 2012. 362(2): p. 162-71.
48. Marcus, R.C. and S.S. Easter, Jr., Expression of glial fibrillary acidic protein and its relation to tract formation in embryonic zebrafish (*Danio rerio*). *J Comp Neurol*, 1995. 359(3): p. 365-81.
49. Corbo, C.P., et al., Use of different morphological techniques to analyze the cellular composition of the adult zebrafish optic tectum. *Microsc Res Tech*, 2012. 75(3): p. 325-33.
50. Bussmann, J. and S. Schulte-Merker, Rapid BAC selection for *tol2*-mediated transgenesis in zebrafish. *Development*, 2011. 138(19): p. 4327-32.
51. Kokel, D., et al., Rapid behavior-based identification of neuroactive small molecules in the zebrafish. *Nat Chem Biol*, 2010. 6(3): p. 231-237.
52. Burgess, H.A. and M. Granato, Modulation of locomotor activity in larval zebrafish during light adaptation. *J Exp Biol*, 2007. 210(Pt 14): p. 2526-39.
53. MacPhail, R.C., et al., Locomotion in larval zebrafish: Influence of time of day, lighting and ethanol. *Neurotoxicology*, 2009. 30(1): p. 52-8.
54. van Ham, T.J., D. Kokel, and R.T. Peterson, Apoptotic cells are cleared by directional migration and *elmo1*-dependent macrophage engulfment. *Curr Biol*, 2012. 22(9): p. 830-6.
55. Xu, J., et al., Microglia Colonization of Developing Zebrafish Midbrain Is Promoted by Apoptotic Neuron and Lysophosphatidylcholine. *Dev Cell*, 2016. 38(2): p. 214-22.
56. Cole, L.K. and L.S. Ross, Apoptosis in the

- developing zebrafish embryo. *Dev Biol*, 2001. 240(1): p. 123-42.
57. Southwell, D.G., et al., Intrinsically determined cell death of developing cortical interneurons. *Nature*, 2012. 491(7422): p. 109-13.
 58. Sierra, A., et al., Microglia shape adult hippocampal neurogenesis through apoptosis-coupled phagocytosis. *Cell Stem Cell*, 2010. 7(4): p. 483-95.
 59. Doetsch, F., The glial identity of neural stem cells. *Nat Neurosci*, 2003. 6(11): p. 1127-34.
 60. Sild, M., et al., Neural Activity-Dependent Regulation of Radial Glial Filopodial Motility Is Mediated by Glial cGMP-Dependent Protein Kinase 1 and Contributes to Synapse Maturation in the Developing Visual System. *J Neurosci*, 2016. 36(19): p. 5279-88.
 61. Kolter, T. and K. Sandhoff, Lysosomal degradation of membrane lipids. *FEBS Lett*, 2010. 584(9): p. 1700-12.
 62. Jaishy, B. and E.D. Abel, Lipids, lysosomes, and autophagy. *J Lipid Res*, 2016. 57(9): p. 1619-35.
 63. Gressens, P., et al., The germinative zone produces the most cortical astrocytes after neuronal migration in the developing mammalian brain. *Biol Neonate*, 1992. 61(1): p. 4-24.
 64. Farias, G.G., et al., BORC/kinesin-1 ensemble drives polarized transport of lysosomes into the axon. *Proc Natl Acad Sci U S A*, 2017. 114(14): p. E2955-E2964.
 65. Ferguson, S.M., Axonal transport and maturation of lysosomes. *Curr Opin Neurobiol*, 2018. 51: p. 45-51.
 66. Gowrishankar, S., Y. Wu, and S.M. Ferguson, Impaired JIP3-dependent axonal lysosome transport promotes amyloid plaque pathology. *J Cell Biol*, 2017. 216(10): p. 3291-3305.
 67. Gowrishankar, S., et al., Massive accumulation of luminal protease-deficient axonal lysosomes at Alzheimer's disease amyloid plaques. *Proc Natl Acad Sci U S A*, 2015. 112(28): p. E3699-708.
 68. Paolicelli, R.C., et al., Synaptic pruning by microglia is necessary for normal brain development. *Science*, 2011. 333(6048): p. 1456-8.
 69. Reemst, K., et al., The Indispensable Roles of Microglia and Astrocytes during Brain Development. *Front Hum Neurosci*, 2016. 10: p. 566.
 70. Hagemeyer, N., et al., Microglia contribute to normal myelinogenesis and to oligodendrocyte progenitor maintenance during adulthood. *Acta Neuropathol*, 2017. 134(3): p. 441-458.
 71. Safaiyan, S., et al., Age-related myelin degradation burdens the clearance function of microglia during aging. *Nat Neurosci*, 2016. 19(8): p. 995-8.
 72. Wlodarczyk, A., et al., A novel microglial subset plays a key role in myelinogenesis in developing brain. *EMBO J*, 2017. 36(22): p. 3292-3308.
 73. Chong, M. and P. Drapeau, Interaction between hindbrain and spinal networks during the development of locomotion in zebrafish. *Dev Neurobiol*, 2007. 67(7): p. 933-47.
 74. Kimura, Y., et al., Hindbrain V2a neurons in the excitation of spinal locomotor circuits during zebrafish swimming. *Curr Biol*, 2013. 23(10): p. 843-9.
 75. Seyrantepe, V., et al., Murine Sialidase Neu3 facilitates GM2 degradation and bypass in mouse model of Tay-Sachs disease. *Exp Neurol*, 2018. 299(Pt A): p. 26-41.
 76. Kizil, C., et al., Adult neurogenesis and brain regeneration in zebrafish. *Dev Neurobiol*, 2012. 72(3): p. 429-61.
 77. Becker, C.G. and T. Becker, Adult zebrafish as a model for successful central nervous system regeneration. *Restor Neurol Neurosci*, 2008. 26(2-3): p. 71-80.
 78. Becker, T. and C.G. Becker, Axonal regeneration in zebrafish. *Curr Opin Neurobiol*, 2014. 27: p. 186-91.
 79. Caldwell, L.J., et al., Regeneration of dopaminergic neurons in adult zebrafish depends on immune system activation and differs for distinct populations. *bioRxiv*, 2018.
 80. Moreno-Mateos, M.A., et al., CRISPRscan: designing highly efficient sgRNAs for CRISPR-Cas9 targeting in vivo. *Nat Methods*, 2015. 12(10): p. 982-8.
 81. Kuil, L.E., et al., Reverse genetic screen reveals that I134 facilitates yolk sac macrophage distribution and seeding of the brain. *bioRxiv*, 2018.



Supplementary fig 1. Representative images of tgBAC(scl1a2b:Citrine) expression pattern in larvae of various development stages. Scale bar represents 100µm and 20µm.



Supplementary fig 2. Z-stack slices showing LT+ puncta (magenta) are inside the radial protrusions of tgBAC(slc1a2b:Citrine)+ cells (green) depicted by * (3 dpf).

Scale bar represents 10 μ m.

Supplementary movie 1. In vivo imaging of lysosomes and mpeg-GFP+ microglia in the optic tectum of a 4 dpf larva showing many LT+ speckles (magenta) outside microglia (green).

Supplementary movie 2. Z-stack showing all LT+ puncta (magenta) are inside the cell bodies or radial protrusions of tgBAC(slc1a2b:Citrine)+ cells (green)(4 dpf).

Chapter 7

General discussion

Macrophages are important for immunological defense and clearance, but in addition, they play a role in an extensive range of biological processes where they affect the development, repair and homeostasis in virtually all tissues. For example, tissue resident macrophages (TRMs) were found very recently to support intestinal homeostasis, intestinal stem cells, muscle satellite cells, arterial tone, and even to regulate cardiac electrical conduction (1-6). Since they have been implicated in a broad range of diseases, macrophages have emerged as important therapeutic targets in human disease, including atherosclerosis, cancer, rheumatoid arthritis, diabetes, and brain diseases (7-13). The receptor tyrosine kinase Colony stimulating factor 1 receptor (CSF1R), through signaling pathways including PI₃K/MEK/ERK, induces transcription of mRNAs encoding proteins that are important for macrophage biology, including their migration, proliferation, and differentiation (14). Therefore, CSF1R inhibitors and antibodies are currently tested to diminish tumor-associated macrophages in cancer and to deplete microglia in mouse models for ALS and Alzheimer's disease as potential therapeutic strategies (15-18). In fact, CSF1R inhibitors are currently tested in patients with acute myeloid leukemia (AML) and a rare type of cancer (19). Nevertheless, *CSF1R* mutations can cause severe disease, particularly affecting the brain, and the role of CSF1R in macrophage biology *in vivo* is still unclear. Similarly, other neurological disease related genes are particularly highly expressed in microglia, including genes associated with Alzheimer risk alleles, but also *HEXB*, an enzyme that is involved in lysosomal degradation of the ganglioside GM2 (20). It is unclear if the high expression level in microglia is indicative of an important role for microglia in the initiation of, and molecular processes underlying, the severe early onset neurological lysosomal storage disorder, caused by mutations in *HEXB*, called Sandhoff disease (SD).

Understanding macrophage development, diversity, and homeostatic functions is essential to understand the role of macrophages in disease, and explore their potential as therapeutic targets. In this thesis, focusing primarily on the CSF1R pathway and on microglia, we aimed to unravel molecular and cellular mechanisms of macrophage development and function *in vivo* and in human disease.

CRISPR/Cas9 reverse genetic screen to identify regulators of microglia

Our reverse genetic screening method, shows high targeting efficiency in F0/ injected zebrafish larvae enabling us to detect aberrant microglial phenotypes and thereby to discover new genes involved in microglia development using

direct mutagenesis by CRISPR/Cas9 (**chapter 2 and 6**). Parts of our screening methodology could also be applied to different research questions. For example, the automated brain detection could also be used as a readout for brain size and shape. Head size is used as a proxy for autism or micro- and macrocephaly in zebrafish and could be used to validate causality of new candidate disease genes (21-24). In addition, the automated microglia counting tool could be implemented in drug screening efforts to identify drugs that cause an expansion or decrease in the microglial population. This is of interest potentially also for other brain diseases, as reduced numbers or the absence of microglia may cause brain disease (**chapter 4 and 5**). Conversely, overactive, or inflammatory activated microglia could be damaging in other diseases, such as amyotrophic lateral sclerosis (ALS) and Alzheimer's disease, in which reducing microglia numbers could be beneficial (17, 18, 25, 26). Therefore, depending on the disease, both decreasing and increasing microglia numbers, or their activity, could be used therapeutically.

Csf1r regulates macrophage precursor migration and proliferation

In recent years, next generation transcriptome sequencing has led to the identification of unique transcriptomes of specific TRM subtypes. Hereby, many new genes that are likely important for TRM specific biology have been identified, but their role in TRM function and development often remains to be determined. Addressing this will increase our understanding of the part that TRMs play in health and disease. In **chapter 2**, we therefore developed a reverse genetic screening pipeline in zebrafish to identify genes important for development and function of microglia. We identified interleukin 34 (Il34) as a facilitator of macrophage precursor migration into the embryo and embryonic brain. IL34 was previously identified in the mouse to be necessary for microglia and Langerhans cells, but the requirement in early development and the underlying mechanism has remained unclear. In **chapter 3** we determined the role of the receptor for Il34, Csf1r, in macrophage development *in vivo*, using live imaging in the zebrafish. In 2010, it was shown for the first time, by lineage tracing, that microglia derive from yolk sac macrophages in mice (27). In this study, YSMs could not be detected at E12.5 and therefore were described to be absent. However, it remains to be elucidated whether YSMs develop in the absence of CSF1R preceding this time point. Surprisingly, we found in our zebrafish model that, both during embryonic and definitive -likely kidney marrow- myelopoiesis, macrophage precursors develop independently of Csf1r signaling. In zebrafish deficient in both *csf1ra*

and *csf1rb* (*csf1r^{DM}*), we observed reduced colonization of yolk sac macrophages (YSMs) into the embryo, reminiscent of our observations in *il34* mutants (**chapter 2**). In the following days and weeks of development, total macrophage numbers in *il34* mutants were similar to numbers in controls (**chapter 3**). In contrast, in *csf1r^{DM}* mutants we observed a halt in macrophage development, resulting in lower macrophages numbers. This revealed that, after two days of development, proliferation ceased in *csf1r^{DM}* mutant macrophages, showing that Csf1r signaling is needed for the self-renewal capacity of macrophages. Interestingly, in *il34* mutants, proliferation rates were normal (**chapter 2**; (28)). CSF1R stimulation by its other ligand, Csf1, directly induces the G1-S transition of the cell cycle (29, 30). Therefore, we speculate that Csf1 likely directly drives proliferation or Csf1 is able to compensate for the loss of Il34. Although CSF1R phosphorylation and ERK activation upon CSF1 or IL34 stimulation was similar both *in vivo* in mice, and *in vitro*, human IL34 was found less potent than human CSF1 in inducing proliferation *in vivo* in mice (31-33). In addition, both IL34 and CSF1 were found to induce migration of macrophages *in vitro* (33-35). Thus, in early development Csf1r signaling regulates the expansion of macrophages, and their tissue colonization, causing the lower macrophage numbers in *csf1r^{DM}* fish. Nevertheless, for generation of macrophages *in vivo*, Csf1r is dispensable.

Csf1r is an essential regulator of macrophage development *in vivo*

It is well known that loss of CSF1R expression affects microglia and osteoclasts, however the receptor is expressed on all macrophages (36-39). Therefore, it is likely that other TRM macrophage populations are also affected by the loss of Csf1r. For example, we showed that Il34 signaling does not only affect macrophage migration towards the brain, but also into other tissues, which could explain why specific macrophages are absent in *il34* mutant zebrafish or mice (**chapter 2**). In addition, *csf1r^{DM}* fish showed largely reduced macrophage numbers in all tissues during development (**chapter 3**). In **chapter 3** we showed the presence of two morphologically and behaviorally distinct macrophage populations in the zebrafish skin, one of which was absent in both *csf1r^{DM}* and *il34* mutant fish. In *Il34* knockout mice, macrophages fail to differentiate into Langerhans cells (LCs) (39, 40). Based on our *in vivo* imaging data, Il34-Csf1r signaling is facilitating both brain and epidermal colonization by macrophages, which would in the presence of Il34 and Csf1r differentiate into microglia and LCs.

Several studies, in which the regulation of LC expansion and dynamics in the epidermis is investigated, could explain the phenotype we observe in fish

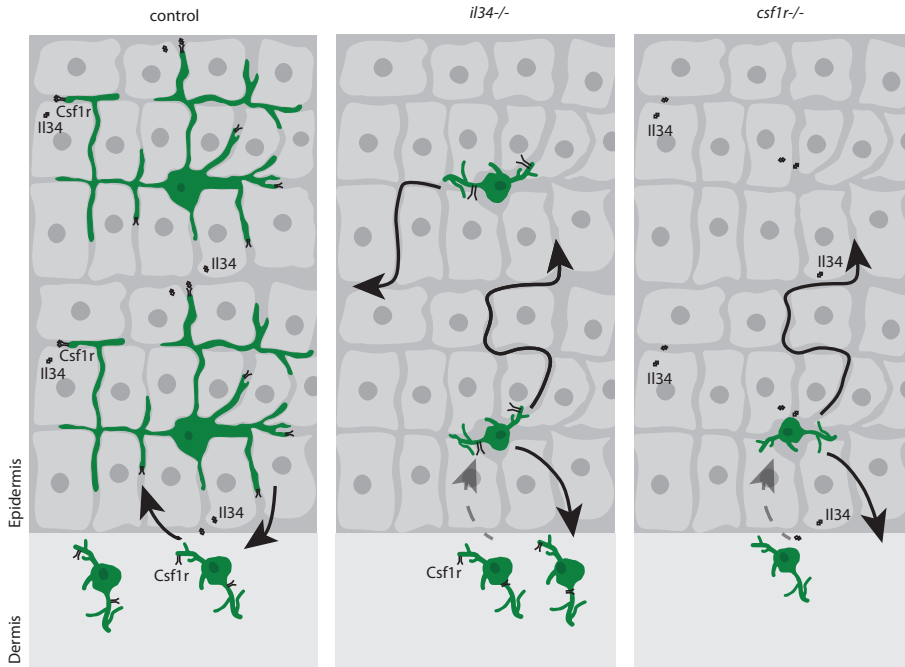


Fig. 1. Schematic representation of the proposed model of how LCs are regulated by IL34-Csf1r signaling in the epidermis. IL34 expressed by keratinocytes attract LC precursors towards the epidermis, where it acts as a beacon to keep them in place, long enough for the environmental factors to induce their typical branched LC morphology. In the absence of either IL34, or Csf1r, macrophage precursors may enter the epidermis but remain migratory and fail to remain at their position to induce TRM properties (Chapter 2 and 3).

(Fig. 1). Signaling pathways downstream of CSF1R have been studied quite well *in vitro* and include MAPK, PI₃Kinase and mTORC1-signaling (14, 41-49). In particular mTORC1 has been linked to cell migration, as for example loss of mTORC1 causes LCs to migrate away from the epidermis, resulting in their absence (50-53). In contrast, activating BRAF(V600E) mutations, activating MAPK-signaling, causes LCs to be retained in the epidermis (54). As both BRAF and mTORC1 are downstream targets of CSF1R, it seems likely that also in the zebrafish epidermis, IL34-Csf1r signaling (likely via Braf and mTorc1) is required to retain precursors within a cellular niche, followed by either direct induction, or enabling environmental factors for induction, of differentiation towards highly branched LCs (Fig. 1).

Csf1r knockout rats and mice lack microglia, LCs and osteoclasts, but in several other tissues macrophages are, although with lower numbers, still present (36, 38). This is in line with our findings that *csf1r* deficient macrophages,

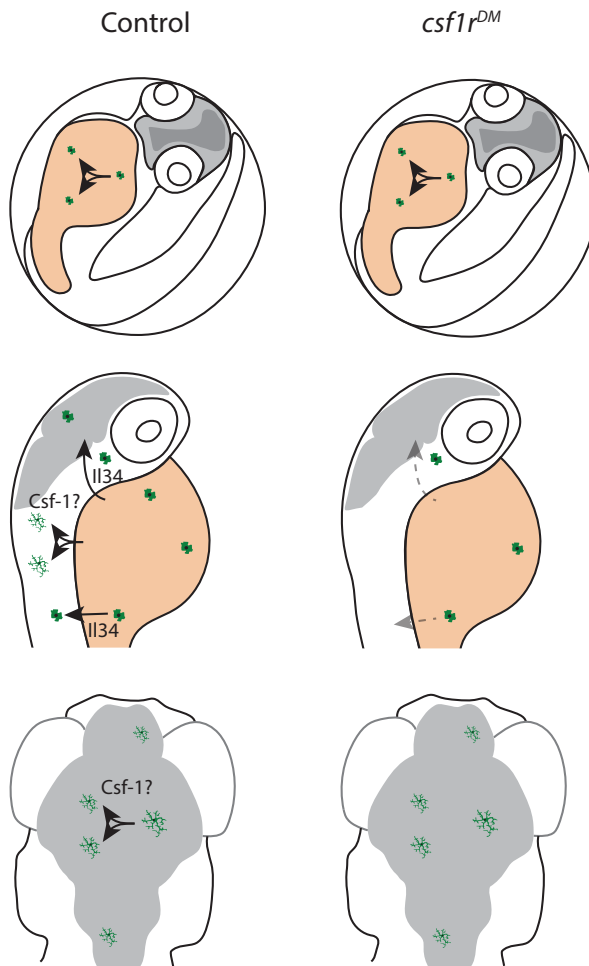


Fig. 2. Schematic representation of *Csf1r* signaling regulating microglia development.

YSMs proliferate in the presence and absence of *Csf1r*, however their proliferation and tissue colonization becomes impaired after 2 dpf. This leads to impaired colonization of the brain, and the failure of microglia to expand their population by proliferation (Chapter 2 & 3).

strikingly, had a normal macrophage transcriptome, showing that *Csf1r* is dispensable for initial generation of macrophages (**chapter 3**). Interestingly, macrophages in the spleen of *Csf1r* knockout rats are present, but lack a TRM specific gene expression profile (38). In addition to the absence of microglia and a branched population of macrophages in the skin, likely LCs, we also observed that branched macrophages in the adult liver were absent in *csf1r^{DM}* zebrafish. Together, this suggests that *Csf1r* signaling is not only important for the presence of microglia, LCs and osteoclasts, but also for inducing TRM-specific gene expression in at least one more subset of macrophages. A common mechanism might underlie these phenotypes, as we believe LC precursors are not attracted to the epidermis, or kept there long enough, for microenvironmental factors to induce their final differentiation into LCs. The aberrant microglial distribution, observed in

ALSP patients and *csf1ra*^{-/-}*b*^{+/-} zebrafish brains, could also be explained by altered migratory behavior due to reduced Csf1r signaling. In addition, in the absence of Csf1r signaling, microglia precursors are not attracted to the brain, which could also explain the lack of osteoclasts, since their attraction is likely also defective. Whether the TRM transcriptome is induced directly by Csf1r signaling rather than by factors from their environment remains unexplored. In all, these data suggests that CSF1R signaling may be involved in facilitating the migration macrophages to their target tissues, and, subsequently, to facilitate their final differentiation to specialized TRM populations.

Loss of microglia function as a pathogenic mechanism

In **chapter 4** we describe a patient lacking microglia, due to bi-allelic pathogenic variants in *CSF1R*. The post mortem brain pathology observed in this patient provides important clues regarding the potential roles of microglia in human brain development. Our findings described in **chapter 3**, provide multiple explanations for the absence of microglia in this patient. We showed that, in zebrafish, loss of functional Csf1r signaling affects microglia development in three ways: (1) it causes reduced numbers of YSMs due to reduced proliferation, (2) due to the absence of IL34-CSF1R signaling attracting precursors towards the brain, it causes reduced colonization of the brain, and (3) in the few precursors that do arrive in the brain, it causes a failure to expand and maintain their population by proliferation (Fig. 2). Together, based on the strong homology in CSF1R function between species, these events could also underlie the absence of microglia in the brain in patients with bi-allelic mutations in *CSF1R* as visualized in figure 2.

Importantly, heterozygous mutations in *CSF1R* cause a more prevalent neurodegenerative disease, adult-onset leukoencephalopathy with axonal spheroids (ALSP), hallmarked by the extensive degeneration of the white matter, axonal spheroids and brain calcifications, which are pathologies that also characterize the *CSF1R* homozygous patient (**chapter 4**). These two diseases appear distinct, since ALSP patients initially develop without symptoms or gross brain abnormalities, whereas the homozygous patient presents with major brain abnormalities before birth. In post mortem brains from ALSP patients and from *csf1ra*^{-/-}*b*^{+/-} zebrafish we found regions devoid of microglia (**chapter 5**). The observed similarities between human patients and our *csf1r* zebrafish models, e.g. reduced microglia, reduced *Cux1* expression, and the presence of osteopetrosis, suggests that underlying pathogenic mechanisms are conserved (Table 1). These results suggest that analysis in zebrafish can potentially be

used to gain insight into the consequences of loss of microglia also in the human brain. Therefore our analyses and model provide an opportunity to further study conserved but unexplored functions of microglia, relevant to brain development. In the homozygous patient mostly the generation of the white matter is affected, likely caused by the absence of microglia, whereas in ALS the white matter degenerates over time, perhaps by loss of homeostatic functions of microglia due to their regional absence. This is in line with adult onset microgliopathies, which also involve white matter degeneration (13, 55-58). Together with the selective expression of CSF1R on microglia in the brain, this makes it likely that microglia play a crucial role in myelin generation and homeostasis causing the myelin pathology in microgliopathies.

Table 1. Pathological findings upon loss of CSF1R alleles in human, mice, rat and zebrafish

	ALSP ¹	Human CSF1R_01 ²	fish <i>csf1ra</i> ^{-/-} <i>b</i> ^{+/-} ³	zebrafish <i>csf1r</i> ^{DM} ⁴	mouse <i>Csf1r</i> ^{+/-} ⁵	mouse <i>Csf1r</i> ^{-/-} ⁶	rat <i>Csf1r</i> ^{-/-} ⁷
Corpus callosum	Thinned	Agenesis	NA	NA	Thinned	Thinned	Minor thinning
Ventricles	Enlarged	Enlarged	NA	NA	Enlarged	Enlarged	Enlarged
Microglia	Reduced	Lacking	Reduced	Lacking	Increased	Lacking	Lacking
Osteopetrosis	NA	Present	Present	Present	NA	Present	Present

1 Adams et al., 2018(59); Chapter 5(37), 2 Chapter 4, 3 Chapter 4, 4 Chapter 4 and 5(37), 5 Chitu et al., 2015(60),

6 Erbllich et al., 2011(61), 7 Pridans et al., 2018(38)

Interestingly, a recent report provides a potential mechanism of white matter loss due to a lack of microglia, as they showed reduced numbers of myelin-producing oligodendrocytes and their precursors in the adult brain upon microglial depletion (62). How exactly microglia support myelinogenesis, and maintenance of myelin producing cells, remains elusive, although it seems likely microglia produce factors, for example insulin-like growth factor 1 (IGF1), that have beneficial effects on myelin production (63). Another way microglia could influence the white matter is related to myelin clearance. Microglia clear myelin debris and, since differentiation of oligodendrocyte progenitor cells (OPCs) is inhibited by the presence of myelin, could thereby indirectly facilitate OPC differentiation (64-69). In fact, during aging, undigested myelin accumulates in microglia and reduces their phagocytic capacity (70). Therefore, it seems likely that in the absence of microglia or upon impaired microglial function, myelin debris is not cleared, which could contribute to white matter impairment (64, 66, 70). We anticipate that in ALS a progressive depletion of microglia occurs,

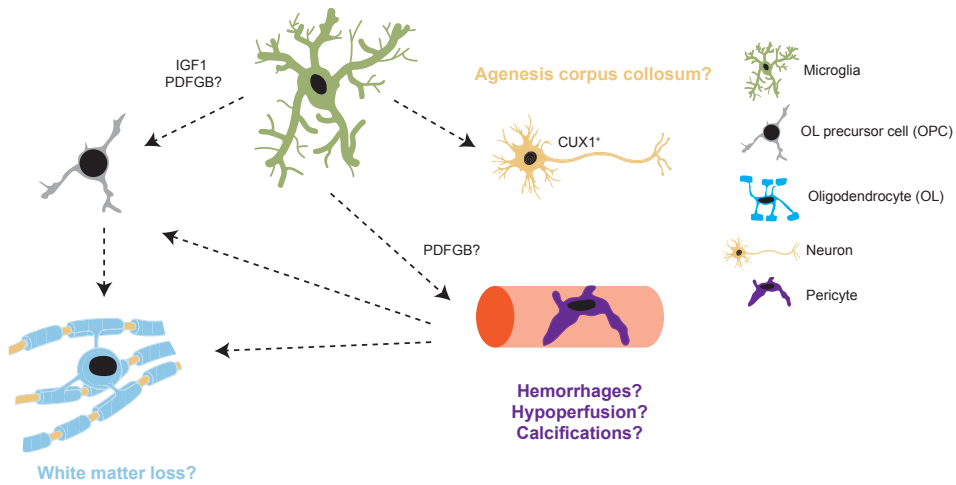


Fig. 3. Different ways microglia could affect the white matter. Loss of microglia has found to reduce the number of oligodendrocytes and OPCs, but also pericytes. The white matter is sensitive to changes in perfusion, which is regulated by pericytes. In addition, pericytes can directly influence the white matter. In microglia-less brains, fewer *Cux1*⁺ neurons were present, which could underlie the absence or thinning of the corpus callosum that is often observed in microgliopathies (Chapter 4).

leading to a defect in the maintenance of myelinating cells and impaired myelin clearance, resulting in progressive white matter loss (Fig. 3).

It would be of great interest to identify other factors produced by microglia that support myelinogenesis or the maintenance of myelin, also for other diseases involving myelin degeneration such as multiple sclerosis. We found *pdgfb*, encoding Platelet-derived growth factor b (*Pdgfb*), is highly expressed in wild type microglia, and strongly downregulated in *csf1ra*^{-/-}*b*^{+/-} microglia. This suggests that reduced *Csf1r* signaling leads to downregulation of *Pdgfb*. In adipose tissue, PDGFB from macrophages was found to cause pericytes, mural cells regulating blood vessel width, to detach from endothelial cells allowing angiogenesis to occur (71). This indicates that macrophages, and likely also microglia, can influence pericytes. Therefore, in the absence of microglia, pericytes might not be stimulated to detach from the blood vessels, causing aberrant angiogenesis, and possibly also leading to increased pericyte coverage. Pericyte coverage is inversely correlated to the permeability of the blood vessels, and increased pericyte coverage could result in reduced permeability and hypoperfusion of the brain (72, 73). Pericytes are dependent on platelet-derived growth factor receptor- β (PDGFRB) signaling for their

survival; therefore pericyte survival may be affected as an indirect consequence of *Csf1r* deficiency, and consequential lack microglia, and reduced production of *Pdgfb*. In line with this possibility, macrophage-less mice have diminished pericyte numbers in the skin and brain, supporting the idea that microglia-less brain areas could contain fewer pericytes (74, 75). Interestingly, loss of *PDGFRB*/pericytes was found to cause hypoperfusion of the brain, leading to hypoxia, metabolic stress and fibrin(ogen) accumulation, causing white matter loss and neurodegeneration in mice (76-81). The brain of patients with Fahr's disease, which can be caused by mutations in *PDGFRB* and its ligand *PDGFB*, show similar characteristics to the brain of ALSP patients, including particularly calcifications but also white matter loss (82-85). In another microgliopathy, Nasu-Hakola disease (NHD), the white matter is also affected and in patients and a mouse model reduced cerebral blood flow and brain glucose metabolism was found (86). This suggests microglia could, either directly or indirectly via pericytes, alter the vasculature and perfusion of the brain, possibly leading to the white matter degeneration observed in both ALSP and Fahr's disease patients brains (Fig. 3). Pericytes do not only regulate blood flow, but are often found in close proximity to the cerebral white matter, and upon de-myelinating lesions, they have been reported to enhance OPC differentiation (81, 87). Thus, pericytes can directly stimulate white matter generation by supporting oligodendrocyte differentiation, and absence of pericytes results in white matter loss via hypoperfusion of the brain (76, 78, 87, 88). We hypothesize that local depletion of microglia could lead to a failure to provide trophic factors, including *PDGFB*, which could contribute to ALSP pathogenesis by affecting pericyte function and coverage, which could lead to hypoperfusion and reduced oligodendrocyte differentiation (Fig. 3).

***hexb* deficient zebrafish mimic lysosomal storage disorder Sandhoff and show early pathology in glia**

Many genetic lysosomal storage disorders (LSDs) involve neurological symptoms, and many of the causative genes are strongly enriched in microglia in the brain. Therefore, we hypothesized that defective lysosomal processing in microglia plays a role in LSD onset and used CRISPR/Cas9-based reverse genetic screening to identify LSD genes that affect microglial lysosomes. In **chapter 6** we described our findings regarding loss of function mutants for *hexb*, an LSD gene related to Sandhoff disease (SD), which led to an abnormal phenotype in glia. We detected similar phenotypes in the directly mutagenized

F0 generation and in stable mutants, showing direct CRISPR/Cas9-based mutagenesis is an effective way to study phenotypes caused by defective LSD genes *in vivo*. Due to the transparency of the zebrafish brain we could detect subtle changes in lysosomal morphologies due to Hexb deficiency, real-time *in vivo*, enabling us to study lysosomal dynamics. It remains to be determined whether the aberrant lysosomal morphologies observed in microglia have consequences for microglial function. However, it has been reported that storage of undigested material in microglia could affect their function leading to for example accumulation of uncleared debris in the brain (70, 89). We observed lysosomes in the radial protrusions of radial glia, which were trafficking highly dynamically and bidirectionally. The function of these trafficking lysosomes, or the consequence of their persistence in Hexb deficient radial glia, remain unknown (Fig. 4). Even though we observed early lysosomal abnormalities in glia and reduced locomotor activity, reminiscent of muscle weakness observed in SD patients, adult Hexb deficient zebrafish do not show obvious pathology and are viable. Because *hexb* mutant fish do not show obvious problems in adulthood, it would be of great interest to determine potential alternative degradation routes that prevent GM2 accumulation, or mechanisms of resistance to GM2 accumulation. In addition, our *hexb* mutant larvae could be used to screen for small molecules that ameliorate or rescue the early abnormal glia and locomotor phenotypes, which could eventually contribute to developing targeted therapy for SD.

Mechanisms underlying neurodegenerative disease, including LSDs, have typically been studied via a neuron-centered approach. The increased presence of glia, which was often found in these diseases, was considered merely as a detrimental secondary process. Nowadays the role of abnormalities in other brain cells, including oligodendrocytes, astrocytes, microglia, and pericytes, as a primary event in brain disease is, however, beginning to be acknowledged (55, 90-92). In this thesis, we show that microglia likely play a primary role in the pathology of ALSP and patients with homozygous *CSF1R* mutations, leading to secondary defects in the formation or the degeneration of mainly the white matter (**chapter 3, 4 and 5**). In Hexb deficient fish both radial glia, and microglia are affected, likely preceding neurodegeneration (**chapter 6**). This suggests that perhaps Hexb deficiency also causes glia to be primarily affected, which is a mechanism that is now recognized for multiple LSDs (90). Since astrocytes and microglia function as a defense and support system, it is not surprising that dysfunction may, secondary to the loss of these homeostatic

functions, lead to neurodegeneration. These non-neuronal brain cells could be used as novel target for the much-needed strategies to contain or cure brain disease, which requires analysis with reduced bias for neurological defects, which in many cases are preceded by pathology in other non-neuronal cell types.

Future directions

In this thesis, we showed that, we could model human neurodevelopmental and neurodegenerative diseases that involve microglia in zebrafish, and discover genes regulating embryonic development of microglia and macrophages *in vivo*. Zebrafish microglia show extensive similarity to mammalian microglia, based on their ontogeny, developmental processes, functions, transcriptional profile and distribution in health and disease (**chapter 4** and **5**). Therefore, mechanistic insight gained in zebrafish in molecular and cellular processes *in vivo* is highly relevant to understand mammalian biology. We showed extensive parallels in the effect of an essential regulator of macrophage development, *csf1r*, on macrophage development between zebrafish and humans. Thereby we shed light on possible mechanisms underlying human pathology with respect to early microglia development and consequences of (partial) depletion of microglia. As microglia are involved in most brain disorders, further studies on understanding the consequences of not having microglia are warranted to understand their homeostatic functions, and develop interventions to prevent or ameliorate pathology. In this thesis we show, by using zebrafish to provide us with *in vivo* insight, how macrophage development and differentiation is regulated by *Csf1r*, which helps us to understand their role in human brain disease.

References

1. Naik S, Larsen SB, Gomez NC, Alaverdyan K, Sendoel A, Yuan S, et al. Inflammatory memory sensitizes skin epithelial stem cells to tissue damage. *Nature*. 2017;550(7677):475-80.
2. De Schepper S, Verheijden S, Aguilera-Lizarraga J, Viola MF, Boesmans W, Stakenborg N, et al. Self-Maintaining Gut Macrophages Are Essential for Intestinal Homeostasis. *Cell*. 2018;175(2):400-15 e13.
3. Du H, Shih CH, Wosczyzna MN, Mueller AA, Cho J, Aggarwal A, et al. Macrophage-released ADAMTS1 promotes muscle stem cell activation. *Nat Commun*. 2017;8(1):669.
4. Lim SY, Yuzhalin AE, Gordon-Weeks AN, Muschel RJ. Tumor-infiltrating monocytes/macrophages promote tumor invasion and migration by upregulating S100A8 and S100A9 expression in cancer cells. *Oncogene*. 2016;35(44):5735-45.
5. Sehgal A, Donaldson DS, Pridans C, Sauter KA, Hume DA, Mabbott NA. The role of CSF1R-dependent macrophages in control of the intestinal stem-cell niche. *Nat Commun*. 2018;9(1):1272.
6. Hulsmans M, Clauss S, Xiao L, Aguirre AD, King KR, Hanley A, et al. Macrophages Facilitate Electrical Conduction in the Heart. *Cell*. 2017;169(3):510-22 e20.
7. Honold L, Nahrendorf M. Resident and Monocyte-Derived Macrophages in Cardiovascular Disease. *Circ Res*. 2018;122(1):113-27.
8. Meshkani R, Vakili S. Tissue resident macrophages: Key players in the pathogenesis of type 2 diabetes and its complications. *Clin Chim Acta*. 2016;462:77-89.
9. Laria A, Lurati A, Marrazza M, Mazzocchi D, Re KA, Scarpellini M. The macrophages in rheumatic diseases. *J Inflamm Res*. 2016;9:1-11.
10. Bobryshev YV, Nikiforov NG, Elizova NV, Orekhov AN. Macrophages and Their Contribution to the Development of Atherosclerosis. *Results Probl Cell Differ*. 2017;62:273-98.
11. Nielsen SR, Schmid MC. Macrophages as Key Drivers of Cancer Progression and Metastasis. *Mediators Inflamm*. 2017;2017:9624760.
12. Colonna M, Butovsky O. Microglia Function in the Central Nervous System During Health and Neurodegeneration. *Annu Rev Immunol*. 2017;35:441-68.
13. Salter MW, Stevens B. Microglia emerge as central players in brain disease. *Nat Med*. 2017;23(9):1018-27.
14. Stanley ER, Chitu V. CSF-1 receptor signaling in myeloid cells. *Cold Spring Harb Perspect Biol*. 2014;6(6).
15. Pyonteck SM, Akkari L, Schuhmacher AJ, Bowman RL, Sevenich L, Quail DF, et al. CSF-1R inhibition alters macrophage polarization and blocks glioma progression. *Nat Med*. 2013;19(10):1264-72.
16. Stafford JH, Hirai T, Deng L, Chernikova SB, Urata K, West BL, et al. Colony stimulating factor 1 receptor inhibition delays recurrence of glioblastoma after radiation by altering myeloid cell recruitment and polarization. *Neuro Oncol*. 2016;18(6):797-806.
17. Olmos-Alonso A, Schettlers ST, Sri S, Askew K, Mancuso R, Vargas-Caballero M, et al. Pharmacological targeting of CSF1R inhibits microglial proliferation and prevents the progression of Alzheimer's-like pathology. *Brain*. 2016;139(Pt 3):891-907.
18. Martinez-Muriana A, Mancuso R, Francos-Quijorna I, Olmos-Alonso A, Osta R, Perry VH, et al. CSF1R blockade slows the progression of amyotrophic lateral sclerosis by reducing microgliosis and invasion of macrophages into peripheral nerves. *Sci Rep*. 2016;6:25663.
19. Edwards DK, Watanabe-Smith K, Rofelty A, Damernsawad A, Laderas T, Lamble A, et al. CSF1R inhibitors exhibit antitumor activity in acute myeloid leukemia by blocking paracrine signals from support cells. *Blood*. 2019;133(6):588-99.
20. Gosselin D, Skola D, Coufal NG, Holtman IR, Schlachetzki JCM, Sajti E, et al. An environment-dependent transcriptional network specifies human microglia identity. *Science*. 2017;356(6344).
21. Brooks SS, Wall AL, Golzio C, Reid DW, Kondyles A, Willer JR, et al. A novel ribosomopathy caused by dysfunction of RPL10 disrupts neurodevelopment and causes X-linked microcephaly in humans. *Genetics*. 2014;198(2):723-33.
22. Golzio C, Willer J, Talkowski ME, Oh EC, Taniguchi Y, Jacquemont S, et al. KCTD13 is a major driver of mirrored neuroanatomical phenotypes of the 16p11.2 copy number variant. *Nature*. 2012;485(7398):363-7.
23. Migliavacca E, Golzio C, Mannik K, Blumenthal I, Oh EC, Harewood L, et al. A Potential Contributory Role for Ciliary Dysfunction in the 16p11.2 600 kb BP4-BP5 Pathology. *Am J Hum Genet*. 2015;96(5):784-96.
24. Marin-Valencia I, Novarino G, Johansen A, Rosti B, Issa MY, Musaev D, et al. A homozygous

- founder mutation in TRAPPC6B associates with a neurodevelopmental disorder characterised by microcephaly, epilepsy and autistic features. *J Med Genet.* 2018;55(1):48-54.
25. Dagher NN, Najafi AR, Kayala KM, Elmore MR, White TE, Medeiros R, et al. Colony-stimulating factor 1 receptor inhibition prevents microglial plaque association and improves cognition in 3xTg-AD mice. *J Neuroinflammation.* 2015;12:139.
 26. Spangenberg EE, Lee RJ, Najafi AR, Rice RA, Elmore MR, Blurton-Jones M, et al. Eliminating microglia in Alzheimer's mice prevents neuronal loss without modulating amyloid-beta pathology. *Brain.* 2016;139(Pt 4):1265-81.
 27. Ginhoux F, Greter M, Leboeuf M, Nandi S, See P, Gokhan S, et al. Fate mapping analysis reveals that adult microglia derive from primitive macrophages. *Science.* 2010;330(6005):841-5.
 28. Wu S, Xue R, Hassan S, Nguyen TML, Wang T, Pan H, et al. IL34-Csf1r Pathway Regulates the Migration and Colonization of Microglial Precursors. *Dev Cell.* 2018;46(5):552-63 e4.
 29. Tushinski RJ, Stanley ER. The regulation of mononuclear phagocyte entry into S phase by the colony stimulating factor CSF-1. *J Cell Physiol.* 1985;122(2):221-8.
 30. Roussel MF. Regulation of cell cycle entry and G1 progression by CSF-1. *Mol Reprod Dev.* 1997;46(1):11-8.
 31. Wei S, Nandi S, Chitu V, Yeung YG, Yu W, Huang M, et al. Functional overlap but differential expression of CSF-1 and IL-34 in their CSF-1 receptor-mediated regulation of myeloid cells. *J Leukoc Biol.* 2010;88(3):495-505.
 32. Boulakirba S, Pfeifer A, Mhaidly R, Obba S, Goulard M, Schmitt T, et al. IL-34 and CSF-1 display an equivalent macrophage differentiation ability but a different polarization potential. *Sci Rep.* 2018;8(1):256.
 33. Segaliny AI, Brion R, Mortier E, Maillasson M, Chereil M, Jacques Y, et al. Syndecan-1 regulates the biological activities of interleukin-34. *Biochim Biophys Acta.* 2015;1853(5):1010-21.
 34. Webb SE, Pollard JW, Jones GE. Direct observation and quantification of macrophage chemoattraction to the growth factor CSF-1. *J Cell Sci.* 1996;109 (Pt 4):793-803.
 35. Chitu V, Pixley FJ, Macaluso F, Larson DR, Condeelis J, Yeung YG, et al. The PCH family member MAYP/PSTPIP2 directly regulates F-actin bundling and enhances filopodia formation and motility in macrophages. *Mol Biol Cell.* 2005;16(6):2947-59.
 36. Dai XM, Ryan GR, Hapel AJ, Dominguez MG, Russell RG, Kapp S, et al. Targeted disruption of the mouse colony-stimulating factor 1 receptor gene results in osteopetrosis, mononuclear phagocyte deficiency, increased primitive progenitor cell frequencies, and reproductive defects. *Blood.* 2002;99(1):111-20.
 37. Oosterhof N, Kuil LE, van der Linde HC, Burm SM, Berdowski W, van Ijcken WFJ, et al. Colony-Stimulating Factor 1 Receptor (CSF1R) Regulates Microglia Density and Distribution, but Not Microglia Differentiation In Vivo. *Cell Rep.* 2018;24(5):1203-+.
 38. Pridans C, Raper A, Davis GM, Alves J, Sauter KA, Lefevre L, et al. Pleiotropic Impacts of Macrophage and Microglial Deficiency on Development in Rats with Targeted Mutation of the Csf1r Locus. *J Immunol.* 2018;201(9):2683-99.
 39. Wang Y, Szretter KJ, Vermi W, Gilfillan S, Rossini C, Cella M, et al. IL-34 is a tissue-restricted ligand of CSF1R required for the development of Langerhans cells and microglia. *Nat Immunol.* 2012;13(8):753-60.
 40. Wang YM, Bugatti M, Ulland TK, Vermi W, Gilfillan S, Colonna M. Nonredundant roles of keratinocyte-derived IL-34 and neutrophil-derived CSF1 in Langerhans cell renewal in the steady state and during inflammation. *Eur J Immunol.* 2016;46(3):552-9.
 41. Kelley TW, Graham MM, Doseff AI, Pomerantz RW, Lau SM, Ostrowski MC, et al. Macrophage colony-stimulating factor promotes cell survival through Akt/protein kinase B. *J Biol Chem.* 1999;274(37):26393-8.
 42. Murray JT, Craggs G, Wilson L, Kellie S. Mechanism of phosphatidylinositol 3-kinase-dependent increases in BAC1.2F5 macrophage-like cell density in response to M-CSF: phosphatidylinositol 3-kinase inhibitors increase the rate of apoptosis rather than inhibit DNA synthesis. *Inflamm Res.* 2000;49(11):610-8.
 43. Golden LH, Insogna KL. The expanding role of PI3-kinase in bone. *Bone.* 2004;34(1):3-12.
 44. Chang M, Hamilton JA, Scholz GM, Masendycz P, Macaulay SL, Elsegood CL. Phosphatidylinositol-3 kinase and phospholipase C enhance CSF-1-dependent macrophage survival by controlling glucose uptake. *Cell Signal.* 2009;21(9):1361-9.
 45. Munugalavada V, Borneo J, Ingram DA, Kapur R. p85alpha subunit of class IA PI-3 kinase is crucial for macrophage growth and migration. *Blood.* 2005;106(1):103-9.

46. Bourette RP, Myles GM, Carlberg K, Chen AR, Rohrschneider LR. Uncoupling of the proliferation and differentiation signals mediated by the murine macrophage colony-stimulating factor receptor expressed in myeloid FDC-P1 cells. *Cell Growth Differ.* 1995;6(6):631-45.
47. Sampaio NG, Yu W, Cox D, Wyckoff J, Condeelis J, Stanley ER, et al. Phosphorylation of CSF-1R Y721 mediates its association with PI3K to regulate macrophage motility and enhancement of tumor cell invasion. *J Cell Sci.* 2011;124(Pt 12):2021-31.
48. Mouchemore KA, Sampaio NG, Murrey MW, Stanley ER, Lannutti BJ, Pixley FJ. Specific inhibition of PI3K p110delta inhibits CSF-1-induced macrophage spreading and invasive capacity. *FEBS J.* 2013;280(21):5228-36.
49. Cammer M, Gevrey JC, Lorenz M, Dovas A, Condeelis J, Cox D. The mechanism of CSF-1-induced Wiskott-Aldrich syndrome protein activation in vivo: a role for phosphatidylinositol 3-kinase and Cdc42. *J Biol Chem.* 2009;284(35):23302-11.
50. Kellersch B, Brocker T. Langerhans cell homeostasis in mice is dependent on mTORC1 but not mTORC2 function. *Blood.* 2013;121(2):298-307.
51. Glantschnig H, Fisher JE, Wesolowski G, Rodan GA, Reszka AA. M-CSF, TNFalpha and RANK ligand promote osteoclast survival by signaling through mTOR/S6 kinase. *Cell Death Differ.* 2003;10(10):1165-77.
52. Sparber F, Scheffler JM, Amberg N, Tripp CH, Heib V, Hermann M, et al. The late endosomal adaptor molecule p14 (LAMTOR2) represents a novel regulator of Langerhans cell homeostasis. *Blood.* 2014;123(2):217-27.
53. Weichhart T, Hengstschlager M, Linke M. Regulation of innate immune cell function by mTOR. *Nat Rev Immunol.* 2015;15(10):599-614.
54. Hogstad B, Berres ML, Chakraborty R, Tang J, Bigenwald C, Serasinghe M, et al. RAF/MEK/extracellular signal-related kinase pathway suppresses dendritic cell migration and traps dendritic cells in Langerhans cell histiocytosis lesions. *J Exp Med.* 2018;215(1):319-36.
55. van der Knaap MS, Bugiani M. Leukodystrophies: a proposed classification system based on pathological changes and pathogenetic mechanisms. *Acta Neuropathol.* 2017;134(3):351-82.
56. Satoh J, Tabunoki H, Ishida T, Yagishita S, Jinnai K, Futamura N, et al. Immunohistochemical characterization of microglia in Nasu-Hakola disease brains. *Neuropathology.* 2011;31(4):363-75.
57. Konno T, Kasanuki K, Ikeuchi T, Dickson DW, Wszolek ZK. CSF1R-related leukoencephalopathy: A major player in primary microgliopathies. *Neurology.* 2018.
58. Goldmann T, Zeller N, Raasch J, Kierdorf K, Frenzel K, Ketscher L, et al. USP18 lack in microglia causes destructive interferonopathy of the mouse brain. *EMBO J.* 2015;34(12):1612-29.
59. Adams SJ, Kirk A, Auer RN. Adult-onset leukoencephalopathy with axonal spheroids and pigmented glia (ALSP): Integrating the literature on hereditary diffuse leukoencephalopathy with spheroids (HDLs) and pigmentary orthochromatic leukodystrophy (POLD). *J Clin Neurosci.* 2018;48:42-9.
60. Chitu V, Gokhan S, Gulino M, Branch CA, Patil M, Basu R, et al. Phenotypic characterization of a Csf1r haploinsufficient mouse model of adult-onset leukodystrophy with axonal spheroids and pigmented glia (ALSP). *Neurobiol Dis.* 2015;74:219-28.
61. Erblich B, Zhu L, Etgen AM, Dobrenis K, Pollard JW. Absence of colony stimulation factor-1 receptor results in loss of microglia, disrupted brain development and olfactory deficits. *PLoS One.* 2011;6(10):e26317.
62. Hagemeyer N, Hanft KM, Akriditou MA, Unger N, Park ES, Stanley ER, et al. Microglia contribute to normal myelinogenesis and to oligodendrocyte progenitor maintenance during adulthood. *Acta Neuropathol.* 2017.
63. Lampron A, Laroche A, Laflamme N, Prefontaine P, Plante MM, Sanchez MG, et al. Inefficient clearance of myelin debris by microglia impairs remyelinating processes. *J Exp Med.* 2015;212(4):481-95.
64. Kotter MR, Li WW, Zhao C, Franklin RJ. Myelin impairs CNS remyelination by inhibiting oligodendrocyte precursor cell differentiation. *J Neurosci.* 2006;26(1):328-32.
65. Neumann H, Kotter MR, Franklin RJ. Debris clearance by microglia: an essential link between degeneration and regeneration. *Brain.* 2009;132(Pt 2):288-95.
66. Bauer NG, French-Constant C. Physical forces in myelination and repair: a question of balance? *J Biol.* 2009;8(8):78.
67. Plemel JR, Manesh SB, Sparling JS, Tetzlaff W. Myelin inhibits oligodendroglial maturation and regulates oligodendrocytic transcription factor expression. *Glia.* 2013;61(9):1471-87.
68. Syed YA, Zhao C, Mahad D, Mobius W, Altmann F, Foss F, et al. Antibody-mediated neutralization of myelin-associated EphrinB3 accelerates CNS remyelination. *Acta Neuropathol.* 2016;131(2):281-

- 98.
69. Safiain S, Kannaiyan N, Snaidero N, Brioschi S, Biber K, Yona S, et al. Age-related myelin degradation burdens the clearance function of microglia during aging. *Nat Neurosci.* 2016;19(8):995-8.
 70. Wlodarczyk A, Holtman IR, Krueger M, Yogev N, Bruttger J, Khorrooshi R, et al. A novel microglial subset plays a key role in myelinogenesis in developing brain. *EMBO J.* 2017;36(22):3292-308.
 71. Onogi Y, Wada T, Kamiya C, Inata K, Matsuzawa T, Inaba Y, et al. PDGFRbeta Regulates Adipose Tissue Expansion and Glucose Metabolism via Vascular Remodeling in Diet-Induced Obesity. *Diabetes.* 2017;66(4):1008-21.
 72. Winkler EA, Sengillo JD, Bell RD, Wang J, Zlokovic BV. Blood-spinal cord barrier pericyte reductions contribute to increased capillary permeability. *J Cereb Blood Flow Metab.* 2012;32(10):1841-52.
 73. Enge M, Bjarnegard M, Gerhardt H, Gustafsson E, Kalen M, Asker N, et al. Endothelium-specific platelet-derived growth factor-B ablation mimics diabetic retinopathy. *EMBO J.* 2002;21(16):4307-16.
 74. Yamazaki T, Nalbandian A, Uchida Y, Li W, Arnold TD, Kubota Y, et al. Tissue Myeloid Progenitors Differentiate into Pericytes through TGF-beta Signaling in Developing Skin Vasculature. *Cell Rep.* 2017;18(12):2991-3004.
 75. Arnold T, Betsholtz C. The importance of microglia in the development of the vasculature in the central nervous system. *Vasc Cell.* 2013;5(1):4.
 76. Uemura MT, Ihara M, Maki T, Nakagomi T, Kaji S, Uemura K, et al. Pericyte-derived bone morphogenetic protein 4 underlies white matter damage after chronic hypoperfusion. *Brain Pathol.* 2017.
 77. Lee ES, Yoon JH, Choi J, Andika FR, Lee T, Jeong Y. A mouse model of subcortical vascular dementia reflecting degeneration of cerebral white matter and microcirculation. *J Cereb Blood Flow Metab.* 2017;271678X17736963.
 78. Kisler K, Nelson AR, Rege SV, Ramanathan A, Wang Y, Ahuja A, et al. Pericyte degeneration leads to neurovascular uncoupling and limits oxygen supply to brain. *Nat Neurosci.* 2017;20(3):406-16.
 79. Kitamura A, Saito S, Maki T, Oishi N, Ayaki T, Hattori Y, et al. Gradual cerebral hypoperfusion in spontaneously hypertensive rats induces slowly evolving white matter abnormalities and impairs working memory. *J Cereb Blood Flow Metab.* 2016;36(9):1592-602.
 80. Miyamoto N, Maki T, Pham LD, Hayakawa K, Seo JH, Mandeville ET, et al. Oxidative stress interferes with white matter renewal after prolonged cerebral hypoperfusion in mice. *Stroke.* 2013;44(12):3516-21.
 81. Maki T, Maeda M, Uemura M, Lo EK, Terasaki Y, Liang AC, et al. Potential interactions between pericytes and oligodendrocyte precursor cells in perivascular regions of cerebral white matter. *Neurosci Lett.* 2015;597:164-9.
 82. Biancheri R, Severino M, Robbiano A, Iacomino M, Del Sette M, Minetti C, et al. White matter involvement in a family with a novel PDGFB mutation. *Neurol Genet.* 2016;2(3):e77.
 83. Keller A, Westenberger A, Sobrido MJ, Garcia-Murias M, Domingo A, Sears RL, et al. Mutations in the gene encoding PDGF-B cause brain calcifications in humans and mice. *Nat Genet.* 2013;45(9):1077-82.
 84. Nicolas G, Charbonnier C, de Lemos RR, Richard AC, Guillin O, Wallon D, et al. Brain calcification process and phenotypes according to age and sex: Lessons from SLC20A2, PDGFB, and PDGFRB mutation carriers. *Am J Med Genet B Neuropsychiatr Genet.* 2015;168(7):586-94.
 85. Nicolas G, Rovelet-Lecrux A, Pottier C, Martinaud O, Wallon D, Vernier L, et al. PDGFB partial deletion: a new, rare mechanism causing brain calcification with leukoencephalopathy. *J Mol Neurosci.* 2014;53(2):171-5.
 86. Kleinberger G, Brendel M, Mracsko E, Wefers B, Groeneweg L, Xiang X, et al. The FTD-like syndrome causing TREM2 T66M mutation impairs microglia function, brain perfusion, and glucose metabolism. *EMBO J.* 2017;36(13):1837-53.
 87. De La Fuente AG, Lange S, Silva ME, Gonzalez GA, Tempfer H, van Wijngaarden P, et al. Pericytes Stimulate Oligodendrocyte Progenitor Cell Differentiation during CNS Remyelination. *Cell Rep.* 2017;20(8):1755-64.
 88. Montagne A, Nikolakopoulou AM, Zhao Z, Sagare AP, Si G, Lazic D, et al. Pericyte degeneration causes white matter dysfunction in the mouse central nervous system. *Nat Med.* 2018;24(3):326-37.
 89. Shen K, Sidik H, Talbot WS. The Rag-Ragulator Complex Regulates Lysosome Function and Phagocytic Flux in Microglia. *Cell Rep.* 2016;14(3):547-59.
 90. Rama Rao KV, Kielian T. Astrocytes and lysosomal storage diseases. *Neuroscience.* 2016;323:195-206.
 91. Scuderi C, Noda M, Verkhatsky A. Editorial: Neuroglia Molecular Mechanisms in Psychiatric Disorders. *Front Mol Neurosci.* 2018;11:407.
 92. Verkhatsky A, Parpura V, Pekna M, Pekny M, Sofroniew M. Glia in the pathogenesis of neurodegenerative diseases. *Biochem Soc Trans.* 2014;42(5):1291-301.

Appendix

Summary

Macrophages are immune cells that are present in all parts of the human body and which clear dead or damaged cells, pathogens and foreign objects by phagocytosis. In addition to these characteristic functions, they play essential roles in the development, maintenance, and homeostasis of their resident tissue. However, their role differs among tissues and remains largely unknown, particularly for the brain's microglia. Macrophages are generated on the embryonic yolk sac during embryonic development, after which they differentiate into tissue resident macrophages. In some tissues these embryonically derived macrophages are later replaced by macrophages from other sources including the bone marrow. The microglia in the brain, however, are self-renewing and remain of embryonic origin. How yolk sac macrophages migrate to the brain and how they control their numbers remains largely undiscovered. We aimed to elucidate how this process is regulated genetically, and how changes in these processes may lead to disease. We made use of zebrafish, as their larvae are particularly well suited to trace processes at the cellular level in the living organism, due to their transparency and small size. Additionally, we aimed to translate findings from the zebrafish to human disease, involving defective macrophage development, by analysis of post-mortem human tissues.

Since activated microglia are often found in diseased brains, many studies on microglia have focused on their role in immune responses, and their functions in the healthy brain are only beginning to be discovered. Identification of genes important for microglia development or function could contribute to our understanding of microglial functions in the healthy and diseased brain. In **chapter 2** we developed a reverse genetic strategy to discover new genes important for microglial development and function. We used CRISPR/Cas9 mutagenesis to disrupt genes. Microglia were visualized in developing zebrafish, using a vital red dye. To quantify microglia numbers in the zebrafish brain we developed a software tool called 'SpotNGlia'. We validated our approach by disrupting genes known to affect microglia development. Using this strategy we targeted 20 candidate genes, and identified the conserved gene interleukin 34 (*il34*) as a regulator of microglia development. We showed that *il34* facilitates the migration of yolk sac macrophages into the embryonic tissues, including the brain. IL34 is one of two ligands for the colony stimulating 1 receptor (CSF1R), which is essential for microglia development in mice and rats.

In **chapters 3, 4** and **5** we studied the role of *Csf1r* in macrophage development and function in zebrafish and in human disease. Many studies on

regulation of macrophage development by CSF1R were performed *in vitro*, and indicated that CSF1R was essential, however it remains elusive how CSF1R regulates macrophage development *in vivo*. To investigate this, we generated zebrafish mutants for both *csf1r* genes, *csf1ra* and *csf1rb*, and studied the effects of reduced or absent Csf1r signaling on macrophage development. By *in vivo* microscopy we traced yolk sac macrophages and tissue resident macrophages, including microglia, during development, and showed that yolk sac macrophages, surprisingly, are formed independently of Csf1r. Transcriptome analysis revealed that Csf1r deficient macrophage contain a normal macrophage expression profile. However, the *csf1r* mutant macrophages, unlike control macrophages, fail to divide and show reduced migration into the embryonic tissue, including the brain. Together, these defects lead to a lack of microglia in the brain of *csf1r* mutants. The presence of macrophages in other tissues is also affected by the loss of Csf1r signaling. For example, skin macrophages that normally are highly branched, which are likely the Langerhans cells, are absent in Csf1r mutant fish, whereas several other macrophage populations remain present. In sum, we show that Csf1r signaling is dispensable for myelogenesis, but is required for proliferation and migration of macrophages, and likely for the acquisition of their tissue-specific properties.

To study the consequences of *CSF1R* mutations in humans, we collaborated with clinical geneticists who identified homozygous *CSF1R* mutations in patients. One patient presented with osteopetrosis and large developmental brain abnormalities, mainly in the white matter, including agenesis of the corpus callosum. Post mortem neuropathology showed that microglia were absent, and showed cortical abnormalities including heterotopia, calcifications and axonal spheroids. Zebrafish *csf1r* mutants also lack microglia and were osteopetrotic. To identify molecular changes due to a lack of microglia, we performed proteomics analysis of zebrafish brains and we found the transcription factor Cux1 was less abundant. By immunostaining for CUX1, which intriguingly is expressed in the majority of neurons that form the corpus callosum, showed that there were lower numbers of CUX1+ neurons in the patient. Thus, importantly, it appears that the identification of molecular changes in *csf1r* mutant zebrafish brain can assist in identifying changes that could underlie the pathogenic process also in patients and enable us to study the underlying molecular mechanisms.

Another neurological disorder, adult onset leuko-encephalopathy with axonal spheroids and pigmented glia (ALSP), is caused by heterozygous mutations in *CSF1R*. We discovered that the number of functional copies of *csf1r*

in zebrafish correlated with the number of microglia present in the embryonic and adult brain. To investigate whether fewer copies of *CSF1R* also leads to reduced numbers of microglia in humans, we analyzed post-mortem brain material from ALSP patients and controls. This showed that the number of microglia was reduced by approximately 50% in ALSP patients. Strikingly, the white matter abnormalities observed in the patient containing homozygous *CSF1R* mutations, were similar to those typically seen in ALSP patient brain tissue. In addition, in brain material from ALSP patients and from zebrafish with fewer functional *csf1r* copies we found regions that were devoid of microglia. As these regions included affected and non-affected areas, this suggests that the absence of microglia may precede the white matter loss observed in the brain from ALSP patients. The neuropathology of patients with homozygous or heterozygous *CSF1R* mutations shows resemblance, but is milder in heterozygous ALSP cases. Based on our data, the reduced presence or absence of microglia likely underlies respectively the white matter loss and defective myelin development, suggesting that in human microglia play an important role particularly in the white matter.

Many lysosomal genes, which when mutated cause lysosomal storage disorders that often affect the brain, are highly expressed in microglia. Therefore, we investigated the effect of disruption of several lysosomal genes on microglia by *in vivo* imaging. In **chapter 6** we generated zebrafish deficient for *hexb*, the homolog of *HEXB* which, when mutated, causes Sandhoff disease. The early pathogenic process in Sandhoff disease is poorly understood and it is unknown which cell types are precisely involved. Therefore, we analyzed lysosomes, the digestive organelles that show storage in LSDs, inside various brain cells of *hexb* deficient larvae by *in vivo* microscopy. Early in embryonic development we already detected alterations in the lysosomes of two glial cell types: microglia and radial glia. Radial glia are the neuronal and glial precursor cells in the developing brain. Lysosomal alterations coincided with cell death in the brain and reduced larval locomotion. By analyzing *hexb* mutant zebrafish we detected abnormalities in glia, which give important clues about processes that might be involved in the onset of Sandhoff disease. In addition, further studies on *hexb* mutant fish will increase understanding of cellular processes in Sandhoff disease and can assist in the discovery of small molecules that could suppress lysosomal alterations.

In this thesis, we demonstrate that zebrafish macrophages, in particular the microglia, share high genetic and functional homology with their human counterparts. This enabled us to gain basic scientific insight in processes related

to rare genetic disease, which also likely is valuable to understand other diseases involving macrophages or microglia. Based on our data and that of others it seems likely that microglia could affect the onset and course of brain diseases. In addition, macrophages play a role in disease progression of amongst others various types of cancer and the autoimmune disorder rheumatoid arthritis. In fact, the therapeutic potential of macrophage or microglia depletion in diseases where they are thought to be detrimental, for example in Alzheimer's disease and some types of cancer, is currently studied and bone marrow transplantations are applied to treat patients with the severe white matter disorder Krabbe disease. However, to predict when and how macrophage numbers should be enhanced or reduced as a therapeutic strategy, their normal functions and their role in disease, whether this is detrimental or beneficial, should be understood. Our findings indicate that the absence of microglia, particularly in human disease, primarily has negative consequences for myelinated white matter tracts, and therefore it is important to study how microglia normally affect the myelinating cells. Similarly, as many tissues are affected by a lack of macrophages, zebrafish *csf1r* mutants provide an interesting genetic background to study thoroughly how diverse macrophage subsets affect their host tissues. Many aspects of myelopoiesis and tissue resident macrophage properties described in this thesis were not yet studied in zebrafish. The datasets we generated –both transcriptomics and proteomics- could be of use to understand the consequences of CSF1R inhibition on macrophages, microglia and the brain. Our results imply that fundamental and pioneering research in zebrafish can give direct insight in human diseases, which are currently not understood. This type of research will increase our knowledge about the function, development and genetics of macrophages, leading to an understanding of how macrophages play a role in disease processes and how they could possibly be used for therapeutic purposes in disease.

A

Samenvatting

Macrofagen zijn immuuncellen die aanwezig zijn in alle weefsels van het menselijk lichaam. Ze verwijderen, door middel van fagocytose, dode of beschadigde cellen, micro-organismen en lichaamsvreemd materiaal. Naast deze bekende functies, spelen macrofagen een belangrijke rol in de ontwikkeling en homeostase van het weefsel waarin zij zich bevinden. Echter wat die rol precies is verschilt per orgaan en is vooral in het menselijke brein nog grotendeels onbekend. Tijdens de hele vroege embryonale ontwikkeling ontstaan op de embryonale dooierzak de eerste macrofagen (dooierzakmacrofagen). Deze migreren naar alle zich ontwikkelende weefsels en differentiëren daar tot weefsel- of orgaanspecifieke macrofagen met specifieke functies. Dooierzakmacrofagen worden in veel weefsels na de geboorte deels of geheel vervangen door nieuwe macrofagen die vanuit het beenmerg komen. De microglia in het brein daarentegen worden niet vervangen en vernieuwen zichzelf door middel van celdeling. Hoe dooierzakmacrofagen naar het brein migreren en hoe ze, als uitgedifferentieerde cellen, zichzelf vernieuwen is nog grotendeels onduidelijk. Het doel van ons onderzoek was om te achterhalen welke genen betrokken zijn bij deze processen en hoe veranderingen in deze processen kunnen leiden tot ziekte. Hiervoor hebben we gebruik gemaakt van zebrafislarven, die klein en doorzichtig zijn, waardoor ze geschikt zijn om dynamische cellulaire processen op microscopisch niveau te volgen in het levende organisme met zogenaamde *in vivo* imaging. We hebben het effect van het verlies van bepaalde genen op de functie en ontwikkeling van microglia bestudeerd. Daarnaast hebben we deze bevindingen in zebrafissen gebruikt om meer inzicht te krijgen in de humane situatie.

Doordat microglia worden aangetroffen in ziek hersenweefsel bij bijvoorbeeld multiple sclerose en Alzheimer, wordt er al heel lang vooral onderzoek gedaan naar de rol van microglia in ontstekingsreacties in het brein. Vreemd genoeg begint er nu pas aandacht te komen voor de rol van microglia in het gezonde brein en worden de essentiële functies van deze cellen ontdekt. Wanneer we begrijpen welke genen de ontwikkeling en functie van microglia beïnvloeden, kan dit bijdragen aan ons begrip van de rol die microglia spelen in het zieke en gezonde brein. In **hoofdstuk 2** hebben we een strategie ontwikkeld om zulke nieuwe genen te identificeren. We hebben in zebrafis embryo's genen uitgeschakeld met behulp van CRISPR/Cas9 genetische modificatie. Vervolgens hebben we met een rode kleurstof de microglia gevisualiseerd en het aantal microglia per brein automatisch gekwantificeerd met de zelf ontwikkelde beeldanalyse software 'SpotNGlia'. Om deze opzet te valideren hebben we eerst

genen uitgeschakeld waarvan bekend is dat ze nodig zijn voor de ontwikkeling van microglia. Vervolgens hebben we 20 kandidaatgenen geselecteerd en uitgeschakeld, en hebben we het geconserveerde gen *interleukine 34 (il34)* geïdentificeerd als een belangrijke regulator van de ontwikkeling van microglia. We hebben aangetoond dat *il34* werkt als een signaalstof om macrofagen van de dooierzak aan te trekken naar specifieke organen waaronder het brein. Het eiwit IL34 bindt aan de colony stimulating 1 receptor (CSF1R), een receptor die essentieel is voor de ontwikkeling van microglia in zoogdieren.

In **hoofdstukken 3, 4 en 5** hebben we de functie van Csf1r in macrofagen verder onderzocht in de zebrafish en in zeldzame genetische hersenaandoeningen bij mensen. Op basis van celweekonderzoek leek CSF1R essentieel te zijn voor macrofaagontwikkeling, maar het is nog onduidelijk hoe dit precies in het levende organisme werkt. Om dit te onderzoeken hebben we zebrafishmutanten voor beide *csf1r* genen, *csf1ra* en *csf1rb* gemaakt en hebben we de gevolgen van een verminderde, dan wel volledige afwezige, Csf1r signalering op macrofaagontwikkeling bestudeerd. Met behulp van microscopische beeldvormingstechnieken waarbij cellen over de tijd in het levende organisme zijn te volgen hebben we dooierzakmacrofagen en weefselmacrofagen, waaronder de microglia, onderzocht. We ontdekten verassend genoeg dat dooierzakmacrofagen ondanks de afwezigheid van Csf1r signalering toch gevormd werden. Door middel van RNA sequencing, waarmee de expressie van bijna alle genen in één keer gemeten kan worden, hebben we de gen expressie onderzocht en vonden een vergelijkbaar macrofaag expressiepatroon in controle en mutante macrofagen. In tegenstelling tot controle macrofagen, delen *csf1r* mutante macrofagen echter niet én migreren ze minder naar de embryonale weefsels (waaronder het brein). Tezamen leiden deze defecten tot de afwezigheid van microglia in het brein van *csf1r* mutanten. Ook in andere weefsels zijn door het verlies van Csf1r de aantallen macrofagen verminderd. Zo ontbreken in de huid van *csf1r* mutanten de weefsel-specifieke macrofagen die in gezonde larven lange vertakte uitlopers vormen. Samenvattend kunnen macrofagen blijkbaar onafhankelijk van Csf1r gevormd worden, maar lijkt de delingscapaciteit, migratie en het verkrijgen van weefsel-specifieke eigenschappen van macrofagen wel afhankelijk van Csf1r.

Om de gevolgen van het verlies van CSF1R functie, en daarmee ook de microglia, voor het brein te onderzoeken hebben we, in samenwerking, een patiënt met een homozygote frameshift mutatie in *CSF1R* onderzocht. Deze patiënt liet osteopetrose zien, een botafwijking vermoedelijk veroorzaakt door het gebrek aan osteoclasten, de macrofagen in het bot. Daarnaast presenteerde de

patiënt zich met een sterk afwijkende hersenontwikkeling met name in de witte stof en agenese van het corpus callosum. Post-mortem werden de afwezigheid van microglia en corticale afwijkingen aangetoond waaronder heterotopie, maar ook calcificaties en axonale sferoïden. Zebravis *csf1r* mutanten zijn ook osteopetrotisch en hebben ook geen microglia. Om moleculaire veranderingen veroorzaakt door de afwezigheid van microglia te achterhalen hebben we daarom proteomics experimenten (grootschalige analyse van eiwitten) uitgevoerd op zebravishersenen en vonden we o.a. een sterk verlaagde hoeveelheid van het Cux1a eiwit. CUX1 positieve neuronen vormen o.a. het corpus callosum. Met antilichaamkleuringen hebben we daarom CUX1 expressie onderzocht in post-mortem brein weefsel van deze patiënt. We hebben aangetoond dat er minder cellen met CUX1 expressie waren, consistent met de afwezigheid van het corpus callosum. Hierdoor lijkt het erop dat er overeenkomsten zijn wat betreft de gevolgen van de afwezigheid van microglia voor het humane en zebravissen brein. De identificatie van andere cellulaire en moleculaire veranderingen in *csf1r* mutante zebravissen zou daardoor kunnen helpen om het pathogene proces in patiënten en de onderliggende mechanismen met name de rol van microglia bij humane breinontwikkeling beter te begrijpen.

Heterozygote mutaties in *CSF1R* veroorzaken een andere hersenaandoening genaamd leukoencefalopathie met axonale sferoïden en gepigmenteerde glia in volwassenen (ALSP). We hebben aangetoond dat het aantal functionele kopieën van *csf1r* correleert met het aantal microglia dat aanwezig is in het embryonale en volwassen zebravisbrein. Om te onderzoeken of minder *CSF1R* ook in mensen leidt tot lagere aantallen microglia, hebben we post-mortem hersenmateriaal van ALSP patiënten met bekende *CSF1R* mutaties en controles bestudeerd. Kwantificatie van de microglia in corticale gebieden liet zien dat er een ongeveer 50% lagere microglia dichtheid was in het brein van de patiënten. Daarnaast vonden we in hersenweefsel van zowel ALSP patiënten als in *Csf1r*-deficiënte zebravissen dat er in gedeeltes van het brein helemaal geen microglia meer waren. De neuropathologische bevindingen in ALSP patiënten lijken ook op die in de patiënt met homozygote *CSF1R* mutatie, maar zijn milder. Op basis van onze data lijkt de afwezigheid van microglia ten grondslag te liggen aan het verlies van witte stof in volwassenen bij ALSP en aan de defectieve aanmaak van de witte stof in embryonale ontwikkeling bij homozygote mutaties. Dit duidt erop dat microglia in mensen een heel belangrijke rol hebben vooral in de witte stof.

Genen die betrokken zijn bij de ziekte van Alzheimer komen hoog tot

expressie in microglia en daarnaast veroorzaken mutaties in microgliagenen ernstige neurodegeneratieve aandoeningen. Veel lysosomale genen, waarin mutaties lysosomale stapelingsziekten met neuronale afwijkingen veroorzaken, komen ook vooral hoog tot expressie in microglia. Daarom hebben we onderzocht hoe de lysosomen van microglia worden beïnvloed door het uitschakelen van deze genen. In **hoofdstuk 6** hebben we het gen *HEXB*, waarin mutaties de ziekte van Sandhoff veroorzaken, uitgeschakeld in zebravissen. Het is nog onbekend welke gliacellen precies een rol spelen in de vroege pathologie in de ziekte van Sandhoff, en daarom hebben we de lysosomen in verschillende hersencellen van *hexb* mutanten onderzocht met behulp van microscopie in het levende brein (intravitaal imaging). Al tijdens de vroege embryonale ontwikkeling ontdekten we verschillen in de morfologie en de aanwezigheid van lysosomen in twee gliaceltypes: microglia en radiale glia. Radiale glia omvatten de neuronale stamcellen, maar produceren ook verschillende typen gliacellen. In *hexb* deficiënte zebravisslarven gingen lysosomale veranderingen in glia gepaard met celdood in het brein en een verminderde zwemactiviteit. Door *hexb* mutanten verder te onderzoeken hebben we afwijkingen in glia ontdekt die ons belangrijke aanwijzingen geven over de processen die betrokken zijn bij de ontwikkeling van de ziekte van Sandhoff. Toekomstig onderzoek in deze vissen kan ons helpen om het ziekte proces beter te begrijpen en kan het zoeken naar medicijnen die deze lysosomale veranderingen tegen gaan faciliteren.

In dit proefschrift laten we zien dat macrofagen in mensen en zebravissen, in het bijzonder microglia, grote overeenkomsten vertonen zowel op het vlak van genetica, functie en ontogenie (hun ontwikkeling). Hierdoor hebben we inzicht verkregen in fundamentele processen, relevant voor het begrip van zeldzame genetische ziekten, die we kunnen gebruiken om de rol van macrofagen en microglia bij meer prevalentie ziektes te begrijpen. Op basis van onze data en die van andere groepen lijkt het er sterk op dat microglia betrokken zijn bij het ontstaan van hersenaandoeningen en dat ze het verloop van het ziekteproces sterk kunnen beïnvloeden. Daarnaast beïnvloeden macrofagen het ziekteproces van uiteenlopende aandoeningen waaronder vele vormen van kanker en bijvoorbeeld auto-immuunziekten als reumatoïde artritis. Vandaag de dag wordt er gekeken naar de therapeutische mogelijkheden van depletie van microglia of macrofagen bij onder andere de ziekte van Alzheimer en bij bepaalde vormen van kanker, en beenmerg transplantaties worden toegepast in de behandeling van patiënten met een ernstige wittestofziekte, de ziekte van Krabbe. Om te kunnen voorspellen

in welke gevallen macrofagen het beste kunnen worden geëlimineerd of juist worden toegediend is het van belang om de normale functies van macrofagen beter te begrijpen en te achterhalen wanneer macrofagen in de patiënt schade toebrengen of juist de schade beperken en herstel bevorderen. Ons onderzoek laat zien dat de afwezigheid van microglia met name in de mens voornamelijk schadelijk is voor de witte stof, en daarom is het belangrijk om te onderzoeken hoe microglia normaal gesproken de witte stof beïnvloeden. Veel van het hier beschreven werk omvat aspecten van myelopoïese (de aanmaak van macrofagen) en macrofaag functies die nog niet eerder onderzocht zijn in zebrevissen. De beschreven datasets (zowel op cellulair niveau als moleculair eiwit en RNA expressieniveau) kunnen bijvoorbeeld van nut zijn om beter te voorspellen wat de effecten van CSF1R remmers zijn op macrofagen. Doordat macrofagen afwezig zijn in verschillende weefsels in *csf1r* mutante zebrevissen, kunnen deze vissen gebruikt worden om te onderzoeken hoe verschillende macrofaagpopulaties het weefsel waarin zij zich bevinden beïnvloeden. De resultaten tonen aan dat dergelijk basaal en pionierend onderzoek in de zebrevis direct inzicht kan leveren in humane onbegrepen aandoeningen. Dit type onderzoek zal onze kennis over de functie, ontwikkeling en genetica van macrofagen doen toenemen, waardoor we beter zullen begrijpen welke rol macrofagen spelen in ziekteprocessen en hoe ze mogelijk ingezet kunnen worden voor de behandeling van ziektes.

A

Curriculum vitae

Personal information

Name: Laura Esmee Kuil

Date of birth: 04-08-1990

Place of birth: Amsterdam

Professional experience

2014 – 2019 PhD student in the group of Dr. T.J. van Ham at the Clinical genetics department of the Erasmus MC, Rotterdam.

Education

2014 - 2019 PhD, Erasmus Medical Center, Rotterdam.

2012 - 2014 Master of Science, Biomedical Sciences: Psychopharmacology and Pathophysiology, University of Amsterdam, Amsterdam
Certificate: Laboratory animal science (Art. 9)

2009 - 2012 Bachelor of Science, Psychobiology, University of Amsterdam, Amsterdam.

Internships

2013 – 2014 Master internship, Leiden University (IBL), Leiden: The role of pituitary Wnt signaling in the regulation of stress axis activity in zebrafish.

Dr. M.J.M. Schaaf.

2013 Master internship, University of Amsterdam (SILS-CNS), Amsterdam: Hippocampal neurogenesis in relation to chronic stress in mice overexpressing the mineralocorticoid receptor.

Dr. H.J. Krugers

2012 Bachelor internship, Academic Medical Center (AMC), Amsterdam: Reconstructing the 3D embryo atlas of human development.

Prof. Dr. R.J. Oostra & Prof. Dr. A.F. Moorman

List of publications

Oosterhof N,*Chang IJ,* Karimini EG,* **Kuil LE**, Jensen DM, Daza R, Young E, Astle L, van der Linde HC, Demmers J, Latimer CS, Keene CD, Loter E, Maroofian R, van Ham TJ,* Hevner RF,* Bennett JT* (2019) Homozygous mutations in CSF1R cause a pediatric onset leukoencephalopathy and can result in congenital absence of microglia. *American Journal of Human Genetics*

Kuil LE*, Oosterhof N*, Geurts SN, van der Linde HC, Meijering E & van Ham TJ. (2019) Reverse genetic screen reveals that Il34 facilitates yolk sac macrophage distribution and seeding of the brain. *Disease Models and Mechanisms*.

Oosterhof N, **Kuil LE**, van der Linde HC, Burm SM, Berdowski W, van Ijcken WFJ, J.C. van Swieten, E.M. Hol, M.H.G. Verheijen & T.J. van Ham (2018). Colony-Stimulating Factor 1 Receptor (CSF1R) Regulates Microglia Density and Distribution, but Not Microglia Differentiation In Vivo. *Cell Reports*. 24(5).

Oosterhof N, Holtman IR*, **Kuil LE***, van der Linde HC, Boddeke EW, Eggen BJ, & van Ham TJ. (2017) Identification of a conserved and acute neurodegeneration-specific microglial transcriptome in the zebrafish. *Glia*. 65(1):138-49.

Oosterhof N, **Kuil LE**, & van Ham TJ (2017). Microglial Activation by Genetically Targeted Conditional Neuronal Ablation in the Zebrafish. *Inflammation*. Volume 1559 of the series Methods in Molecular Biology pp 377-390

Kanatsou S, Feary BC, **Kuil LE**, Lucassen PJ, Harris AP, Seckl JR, Krugers HJ & Joels M (2015). Overexpression of Mineralocorticoid Receptors Partially Prevents Chronic Stress-Induced Reductions in Hippocampal Memory and Structural Plasticity. *PLoS ONE* 10(11)

Kanatsou S, **Kuil LE**, Arp M, Oitzl MS, Harris AP, Seckl JR, Krugers HJ & Joels M (2015). Overexpression of mineralocorticoid receptors does not affect memory and anxiety-like behavior in female mice. *Frontiers in Behavioral Neuroscience* 9(182)

PHD portfolio

Courses		
Zebrafish genome browsing, Oslo	2014	0,3
Biochemistry and Biophysics	2014	3
Advanced immunology	2014	1
Safely working in the laboratory	2015	0,3
Genetics course	2015	3
OIC Functional imaging & Super resolution	2015	1,5
Special topic course	2016	3
Microscopic image analysis: from theory to practice	2016	0,8
Biomedical writing in English	2017	2
Microglia in development and disease, Hasselt	2017	0,3
Research integrity	2018	0,3
Seminars and workshops		
MGC PhD workshop, Maastricht	2015	1
MGC PhD workshop, Dortmund	2016	1
Sophia research days	2014 - 2018	1
Immunology lectures	2014 - 2019	1
Hematology lectures	2014 - 2019	1
Clinical genetics lectures	2014 - 2019	2
(Inter)national conferences		
European zebrafish meeting, Oslo	2014	2
GliaNED meeting, Groningen	2015	0,5
Dutch neuroscience meeting, Lunteren	2016	1
GliaNED meeting, Rijswijk	2017	1
Microglia symposium, Rijswijk	2017	0,5
Microglia meeting, Groningen	2017	1
Microglia in health and disease, Hasselt	2017	1
European glia meeting, Edinburgh	2017	2
GliaNED meeting, Amsterdam	2018	1
Zebrafish disease models meeting, Leiden	2018	2
MGC symposia	2014 - 2019	2

GliaNED meeting, Rotterdam	2019	1
----------------------------	------	---

Teaching

Supervision Master student Molecular medicine	2015 - 2016	2
Supervision Master student Molecular medicine	2016 - 2017	2
Supervision Master thesis	2017	1
Supervision Master thesis	2018	1
Supervision Master student Molecular medicine	2017 - 2018	2
Lecture minor Genetica in de maatschappij	2018	0,5

Total		46
--------------	--	-----------

